2019 IEEE Radar Conference Tutorial

Signal Processing for Passive Radar

Hongbin Li[†], Yimin D. Zhang[‡], Braham Himed[⋆]

[†]ECE Department, Stevens Institute of Technology, Hoboken, NJ

[‡]ECE Department, Temple University, Philadelphia, PA

[⋆]RF Technology Branch, Air Force Research Laboratory, WPAFB, OH

April 22, 2019

Agenda

Time	Topic	Lecturer
16:00 – 16:50	Passive Radar Fundamentals	Braham Himed
16:50 – 17:00	Break	
17:00 – 18:20	Signal Detection and Estimation for Passive Radar	Hongbin Li
18:20 – 18:40	Break	
18:40 – 20:00	SAR Imaging and STAP for Passive Radar	Yimin Zhang
20:00	Adjourn	

Part I
Fundamentals of Passive Radar

Outline

- Motivation
- Bistatic Radar
- Passive Radar
- Experimental Systems
- Unifying Theory
- Conclusions

Global RF Sensing

- Long Range Wide Area Surveillance
- Distributed Sensing
- Fast In/Fast Out Sensing

Approved for Public Release - PA#: 88ABW-2018-1622

RF Sensing Tech Areas

	•Problems	•Technology Challenges	•Potential Solutions
	• Long Stand-Off Sensing Against • Layered IADS	• Power / Aperture • Area Coverage/Resolution • Reduced SINR	• Wideband Agile Radars on smaller Air Vehicles • Space Based Radar
	• Persistent Sensing Within Layered IADS Airspace	• Silent EM operation • Precision Time Reference • On-board Processing	• Passive Multimode • Netted UAV Sensors • Conformal AESAs
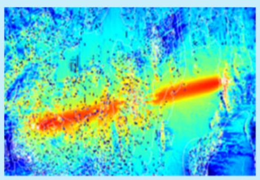	• SOA Jammers • Self-interference • Multistatic Clutter	• Wideband Algorithms • On-board Processing • Clutter Characterization	• Waveform Diversity • MIMO (close-in) • Knowledge Aided Algos
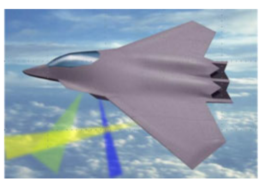	• Reduced Spectrum • Overlapping Need for Spectrum	• Interference Tolerance • Simultaneous Tx/Rx • Silent EM operation	• Multi-Diversity Systems • Wideband LPI Waveforms • Passive Multimode
	• Rapidly Flexible • Mission-Tailored • RF Modes	• Simultaneous Tx/Rx • Cooperative Radar / EW • Modular Subsystems	• SW Defined Radar / EW • Modular Open Systems • Modular Software
	• Geolocation of Frequency-agile RF Emitters	• Short on-time Transmit • LPI, LPD Waveforms	• Wideband Compressive Receiver Techniques • Improved Algorithms

Outline

- Motivation
- Bistatic Radar
- Passive Radar
- Experimental Systems
- Unifying Theory
- Conclusions

Bistatic Radar Concept

- Improved surveillance
- Extended detection and tracking ranges
- Detect more targets
- Safeguard and reduce number of high value assets

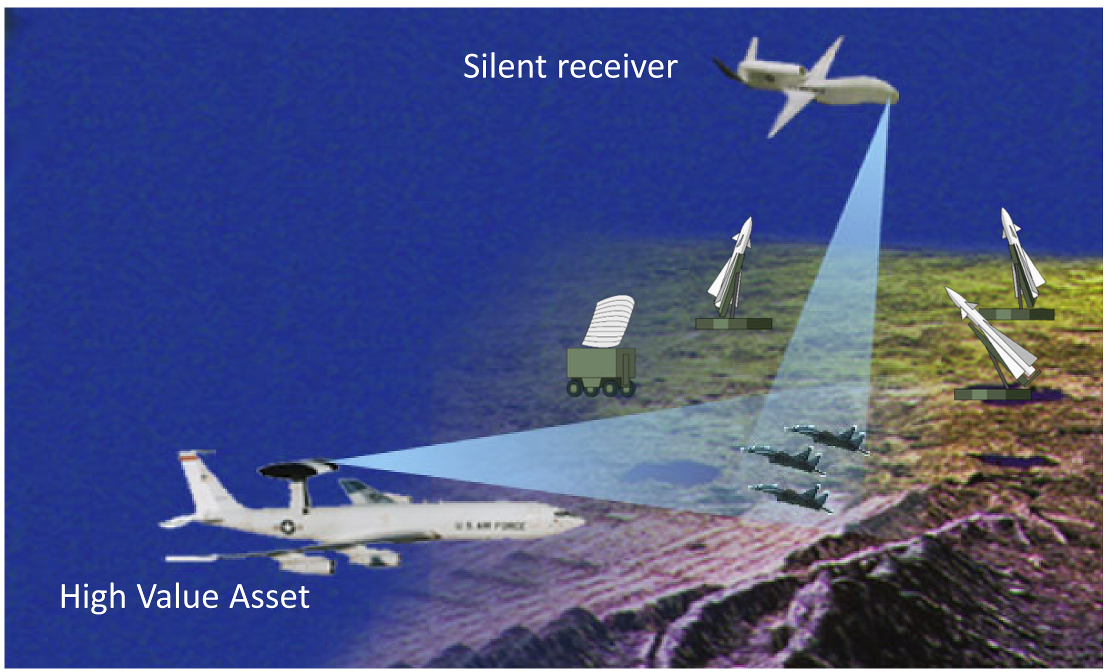

Bistatic Radar Range Equation

$$\left(\frac{S}{N}\right)_{min} = \frac{P_T G_T G_R \lambda^2 \sigma}{(4\pi)^3 k T_s B_n L_T L_{R(RF)} L_{R(Proc)} R_T^2 R_R^2}$$

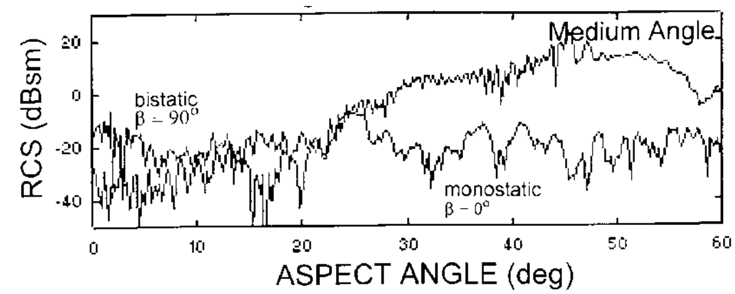

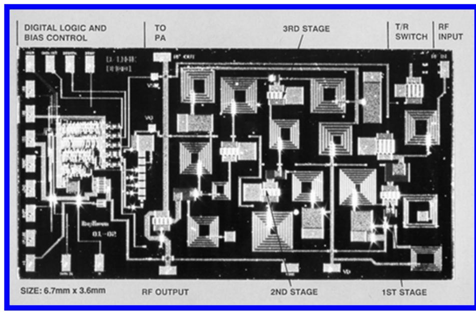

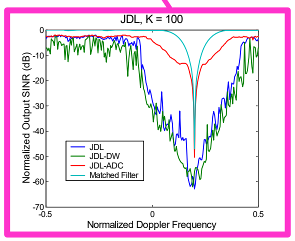

Normalized Ranges

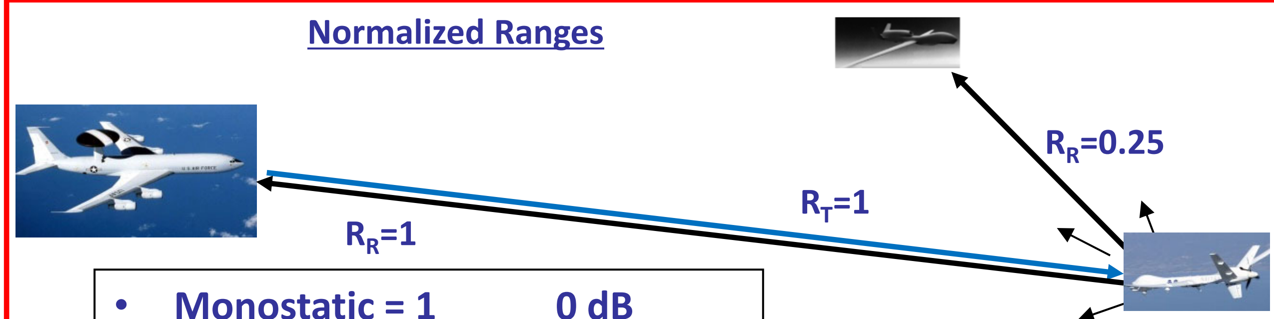

- Monostatic = 1 0 dB
- Bistatic = 0.0625 -11.5 dB

Bistatic Geometry

- Determines many of the operating characteristics
  - Radar range equation
  - Doppler velocity equation
  - Radar Cross Section
  - Coverage area

- Bistatic angle: Angle between the illumination and target paths

- Bistatic angle vs. radar mode
  - $\beta<20^\circ$ – Pseudo-monostatic
  - $20^\circ<\beta<145^\circ$ – Bistatic
  - $145^\circ<\beta<180^\circ$ – Forward

Bistatic Ambiguity Functions

- Geometry-dependent

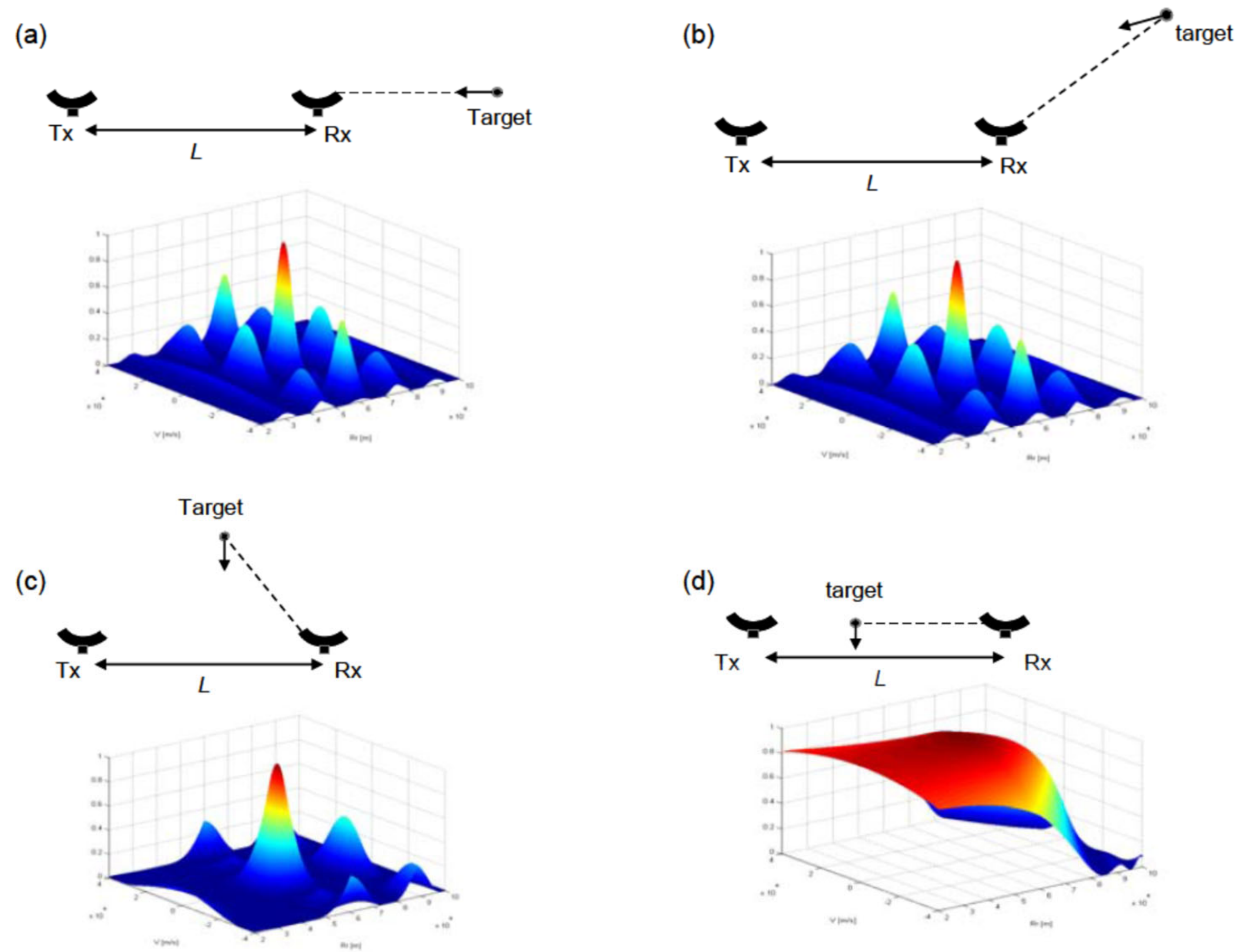

- H.D. Griffitths, “Passive Bistatic Radar and Waveform Diversity,” NATO RTO-EN-SET 119, 2009
- Tsao, et al, “Ambiguity function for bistatic radar,” I*EEE Trans. AES*, Vol.AES-33, pp1041-1051,1997

Bistatic Airborne Radar Challenges

$R_B \equiv$ Bistatic range

$\theta_R \equiv$ Rcvr cone angle

$\theta_R \equiv$ Xmtr cone angle

$R_R \equiv$ Range to rcvr

$R_T \equiv$ Range to xmtr

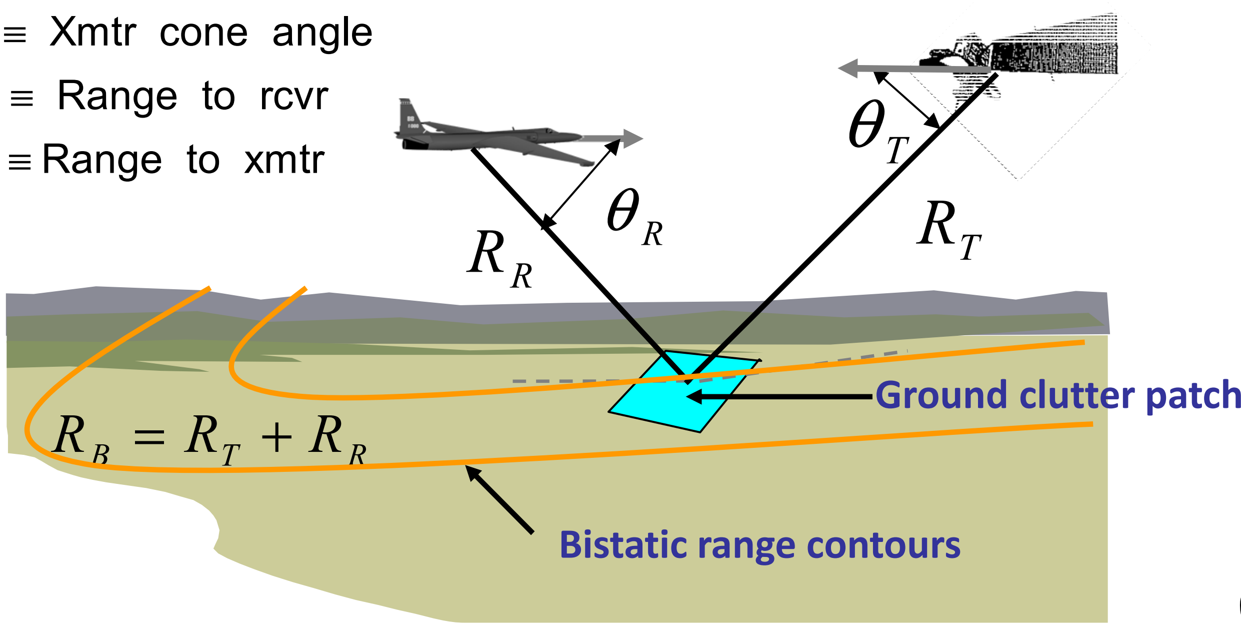

Doppler frequency equations:

•Monostatic radar:

$$f_d = \frac{2V_R}{\lambda}\cos\theta_R$$

- **straight line**
- **clutter ridge**

•Bistatic radar:

$$f_d = \frac{V_R}{\lambda}\cos\theta_R + \frac{V_T}{\lambda}\cos\theta_T$$

θ_T varies with θ_R

- **Non-linear**
- **clutter ridge**

θ_T varies with R_B

- **range-varying**
- **clutter ridge**

- Bistatic geometry produces a non-linear, range-varying clutter ridge
  - Standard STAP using a range-averaged estimated covariance matrix suffers a severe degradation
  - Advanced techniques are required to mitigate clutter non-stationarities

Bistatic Clutter Paths

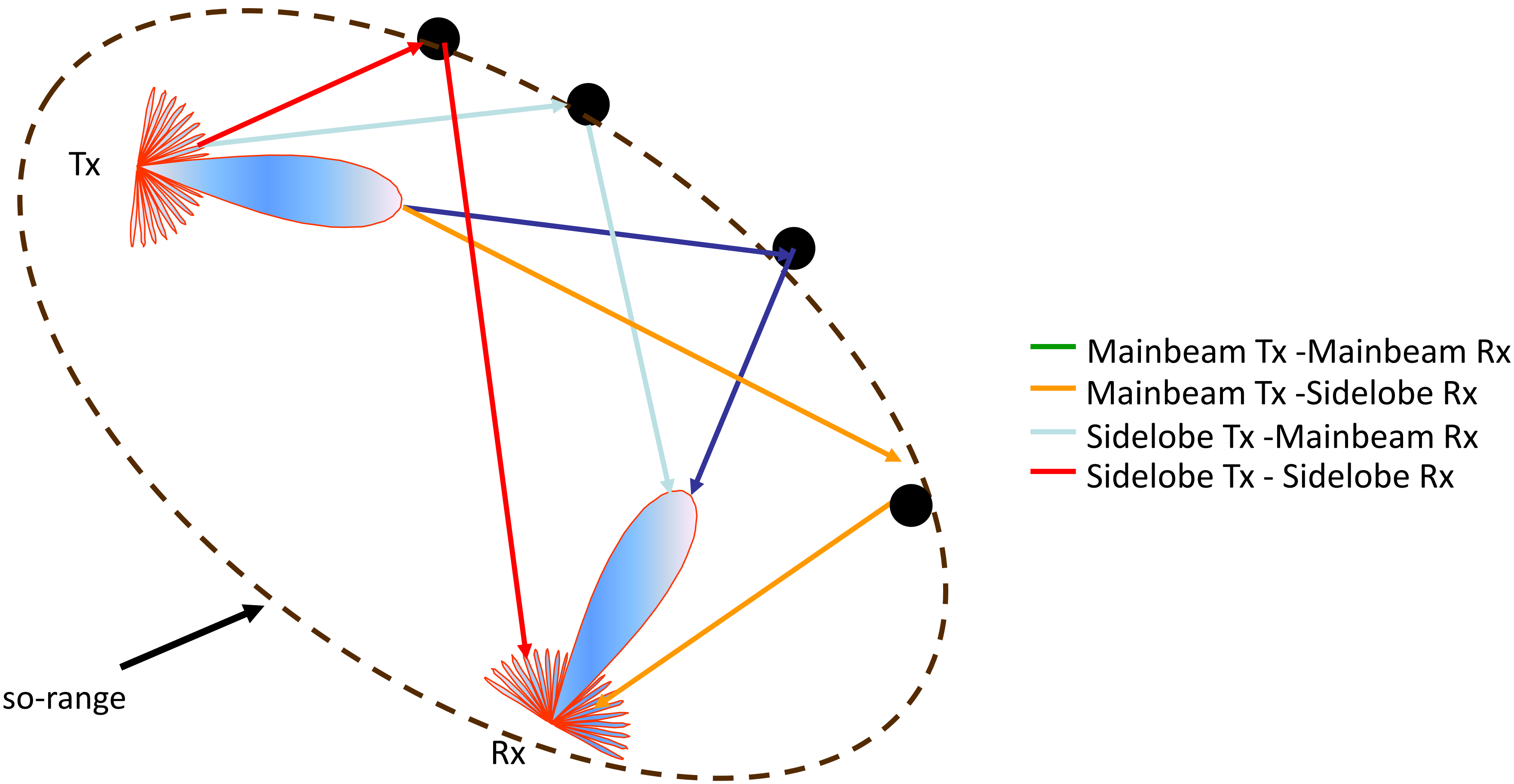

- Bistatic Clutter Spectrum is Range-Dependent and Geometry-Dependent.
- Clutter Spectral Misalignment Main Source of Clutter Dispersion
- Align spectral centers: Angle-Doppler compensation, increased degrees of freedom (less training data), data efficient approaches, waveform diversity

AFRL Bistatic MCARM

Horseshoe Beach
TARS Aerostat

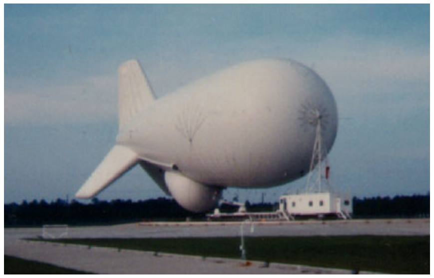

Bistatic Transmitter

AFRL/Northrop Grumman
BAC1-11 MCARM

Bistatic Receiver

- Multi-channel bistatic radar data has been collected to support STAP algorithm development
  - USAF tethered aerostat radar system (TARS) was transmitter
  - AFRL / Northrop Grumman multi-channel airborne radar measurements (MCARM) system was receiver
- Bistatic collection experiment used:
  - Horseshoe beach, Florida aerostat site
  - Gainesville, Florida BAC1-11 basing and flight routes
- Data collection performed from 13 May to 21 May, 1995

MCARM Bistatic System

Northrop Grumman Airborne Surveillance Technology Testbed (BAC1-11)

MCARM Array at Antenna Test Range

- Antenna
  - L-band phased array
  - 6 feet x 4 feet
  - 16 columns
  - 8 rows (4 upper + 4 lower)
  - 16 columns x 2 elevation ports
- Receiver
  - 24 digital receivers
  - 11 columns by 2 rows used for bistatic data collection
  - Operated in passive mode
- Data collection
  - DCRSI Recorded
  - 24 channels
  - ~0.1 sec of data every 12 seconds
  - Cued to record as tars beam passed over multi-target simulator

Bistatic Flight # 9 Flight Path

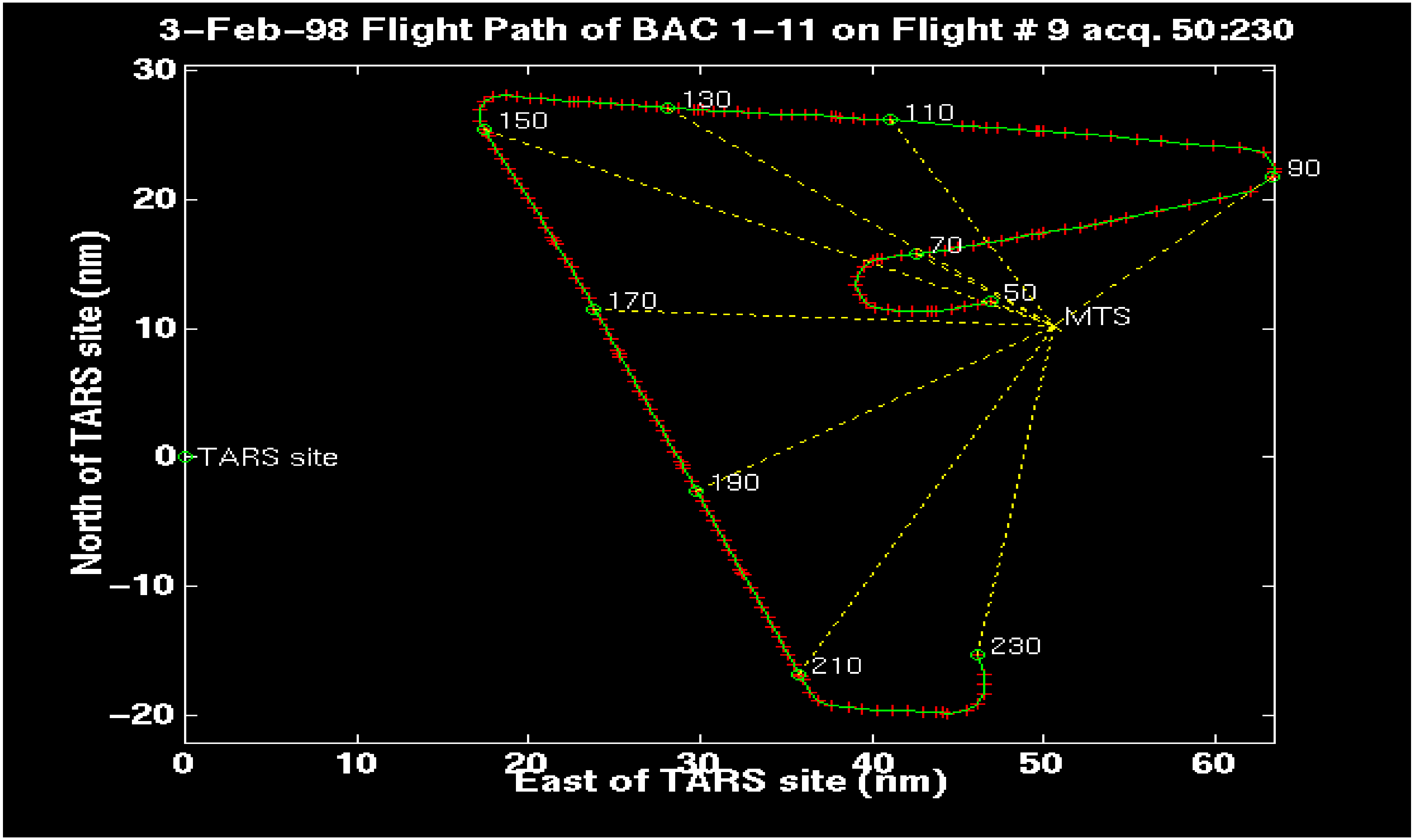

Approved for Public Release - PA#: 88ABW-2018-1622

Clutter Range-Doppler Intensity

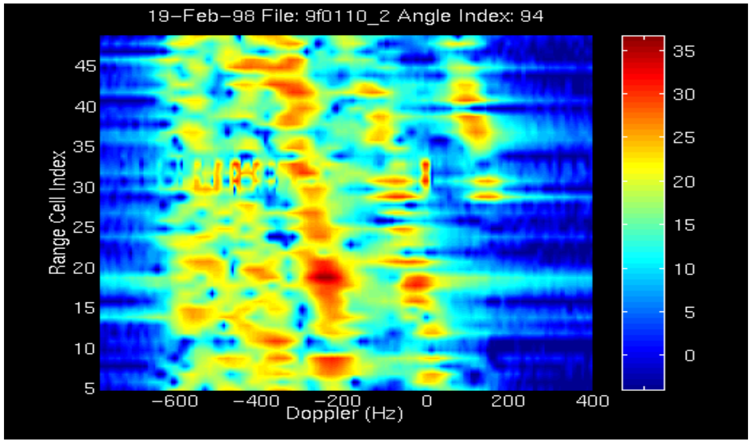

(a) Angle Index = 94

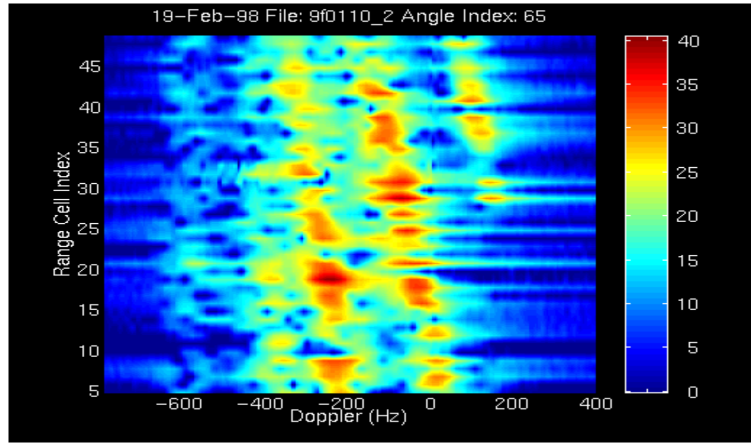

(b) 65

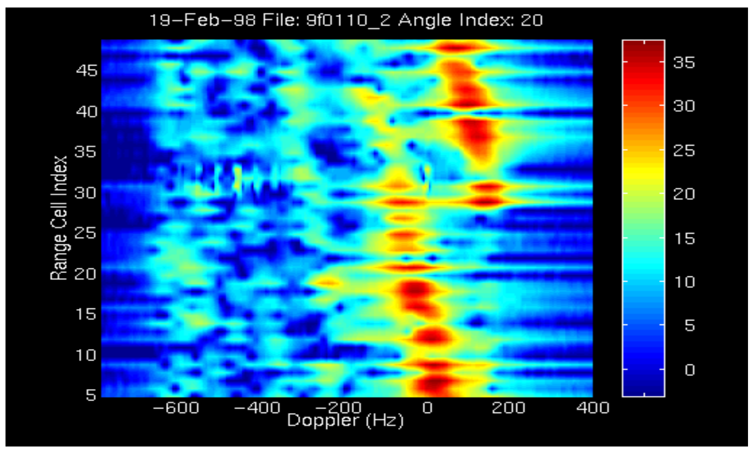

(c) 20

STAP Processing

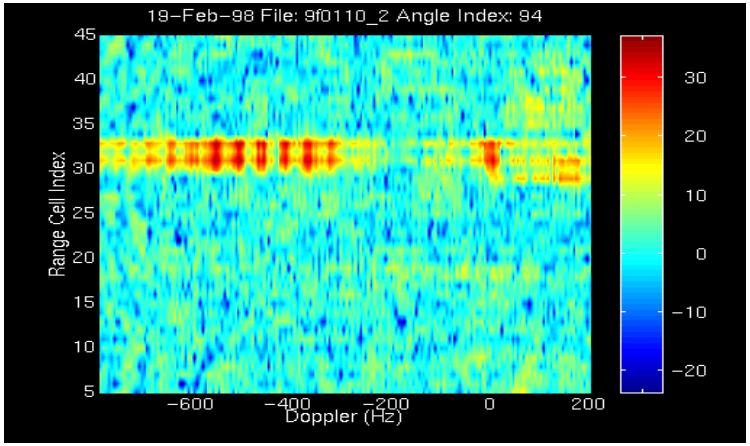

(a) All Pulses, Ang. Ind. 94, CSR = 14.3 dB

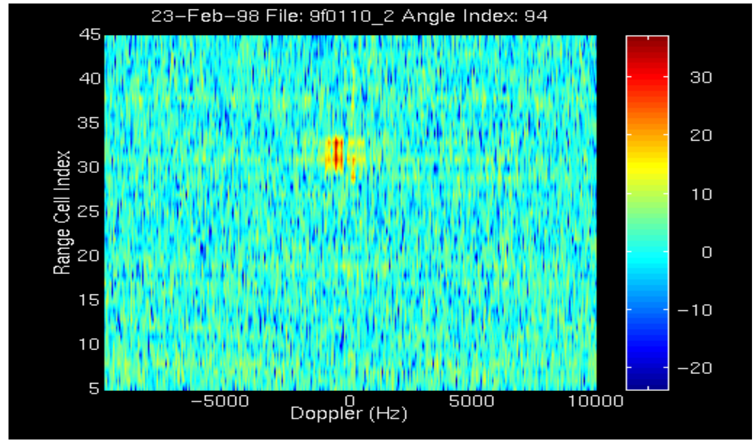

(b) Same as (a), Full Doppler Window

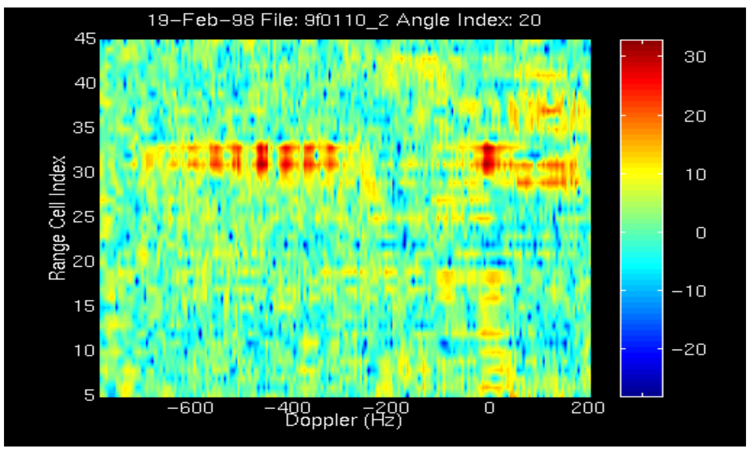

(c) All Pulses, Ang. Ind. 20, CSR = 14.3 dB

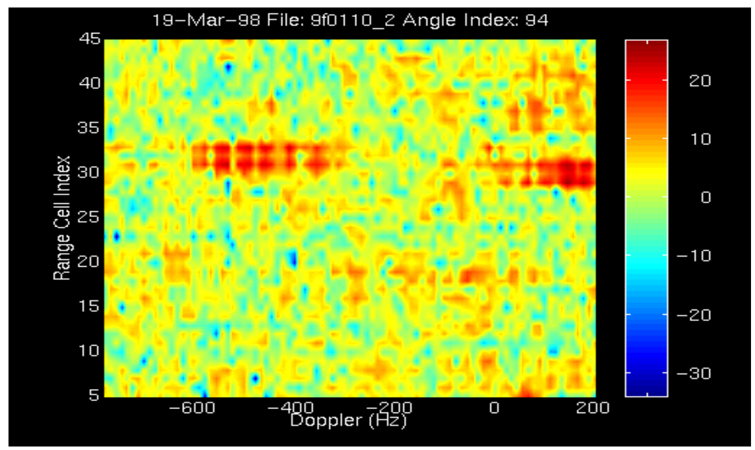

(d) Pulses = #1600, Ang. Ind. 94, CSR=16dB

Outline

- Motivation
- Bistatic Radar
- **Passive Radar**
- Experimental Systems
- Unifying Theory
- Conclusions

Passive Radar

- Strengths
  - Lower cost, no dedicated transmitter and moving parts
  - Physically small and hence, easily deployed in places where conventional radars cannot be
  - Many IOs are available: HF broadcast, VHF/UHF, FM, DAB/DVB, satellite, cellular, WIFI, WiMAX, …
  - Spatial diversity available for enhanced detection/classification capability by multi-static configurations

- Weaknesses
  - Rely on third-party illuminators
  - Probing waveforms not optimized for sensing

History – Daventry Experiment

- Earliest passive bistatic radar experiment, performed in February 1935 by Sir Robert Watson-Watt and Arnold Wilkins
  - Detected a Hayford bomber using a shortwave BBC Empire broadcast as the signal of opportunity

History – Klein Heidelberg

- First operational bistatic radar developed by Germany during WWII (by Dr. Wachter in 1942)
- System hitchhiked on the British Chain Home transmissions, which were located in South-East England

•www.doramusic.com/Chain%2520Home.jpg

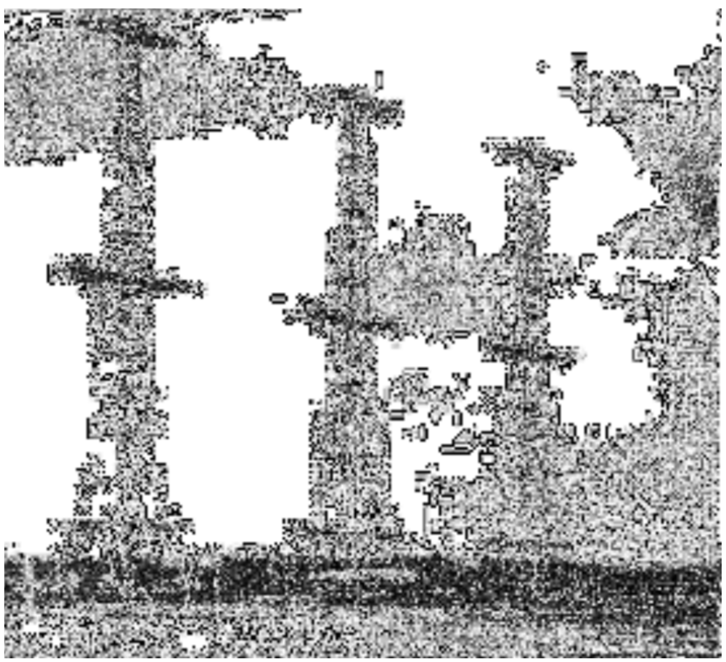

- P= 350 kW (later 750 kW)
- f= 20–30 MHz

- 40 m Wasserman S tower
- 18 dipole elements in front of reflector plane
- 3 column x 6 element array
- beam-width of 45°
- angular accuracy 5°

Additional dipole antenna at 15 m height to receive direct transmitted signal

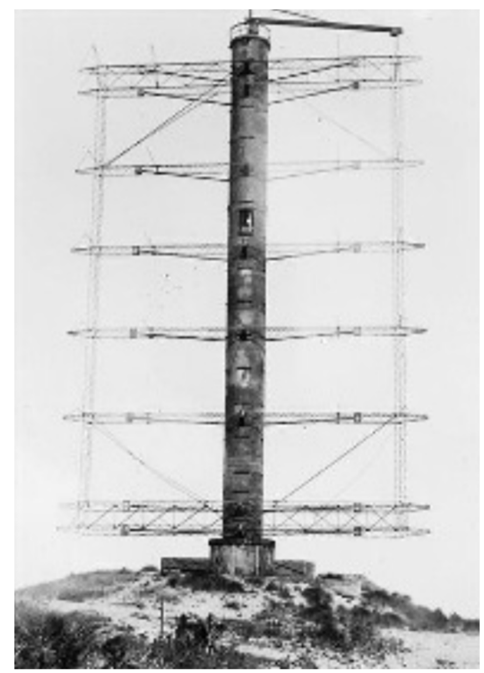

New Resurgence

- With the advent of high speed A/D converters, with superior dynamic range, faster digital processing and GPS, research into bistatic radar has been reignited
  - Several NATO Panels
  - Over 400 papers published in last 20 years
  - Several experimental and demonstration systems

Classification of Passive Sensors

- Hitchhiker or Hitchhiking Bistatic Radar
  - Non-cooperative transmitter is from another radar
- Passive coherent location
- Passive covert radar
- Parasitic radar
- Piggy-back radar

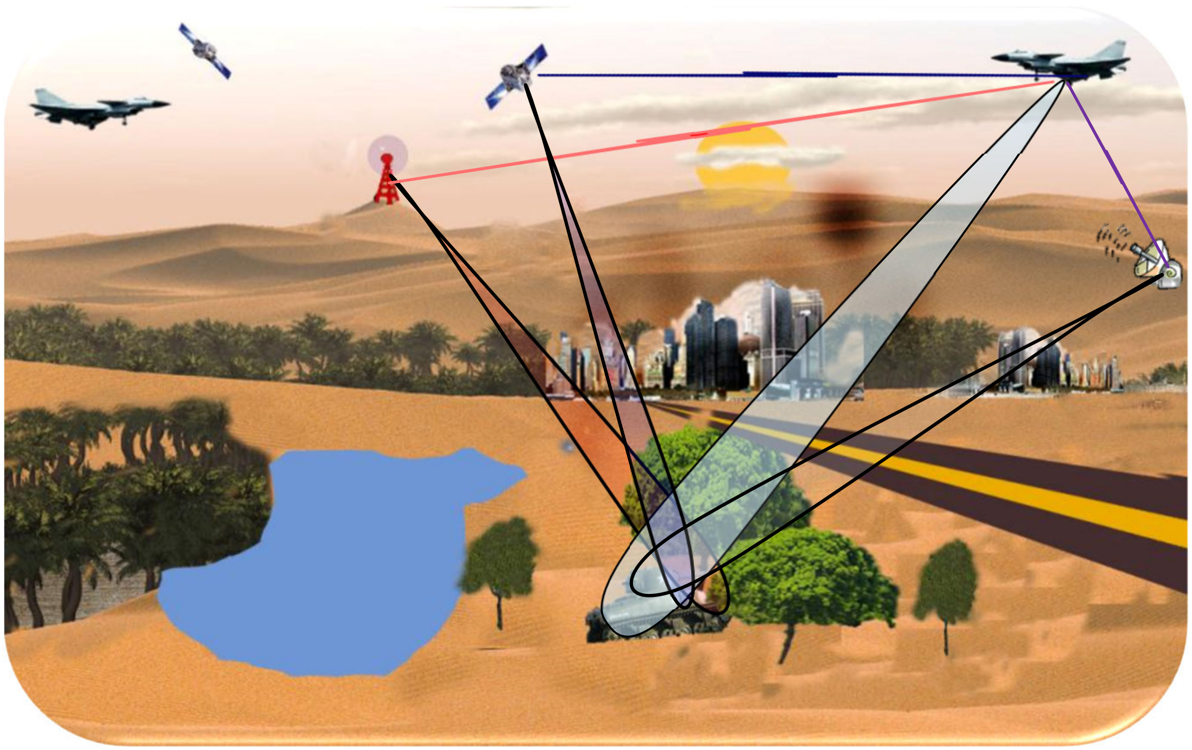

Typical Illumination Sources

Illuminators	Frequency, Bandwidth	Modulation, bandwidth	Typical EIRP
Analog FM Radio	~ 100 MHz	FM, 50 kHz (Composite signal)	Up to 250 kW (UK) 4500 FM Transmitters≥5kW (US)
Digital Audio Broadcast	~220 MHz	COFDM, 220 kHz	10kW
Cellular Phone (GSM)	900 MHz, 1.8 GHz	GMSK, FDM/TDMA/FDD, 200 kHz	100W
Cellular Phone (3G)	~2 GHz	TD-CDMA , 3.84 MHz TD-SCDMA, 1.28 MHz	100W
Analog UHF TV	~550 MHz	VSB AM (vision), 64μs Repetition Rate; FM (sound), 5.5 MHz	1 MW (UK)
Digital TV	~750 MHz	DVB-T(C-OFDM),Europe/Australia ISDB-T (OFDM, 2D Interleaving), Japan, S. America ATSC(8VSB), USA DTMB(TDF-OFDM), China 6MHz	8 kW, (WKTV-DT 29 : ERP=708kW)
DBS TV, Satellite Radio	~11-12GHz ~2.33 GHz		52dBW

Bistatic Passive Ambiguity Functions

- Illumination-dependent,

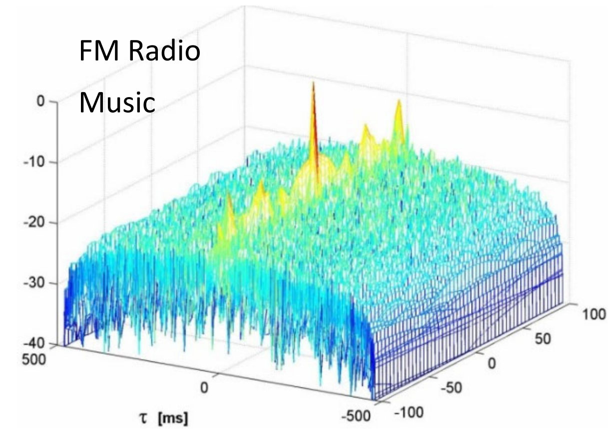

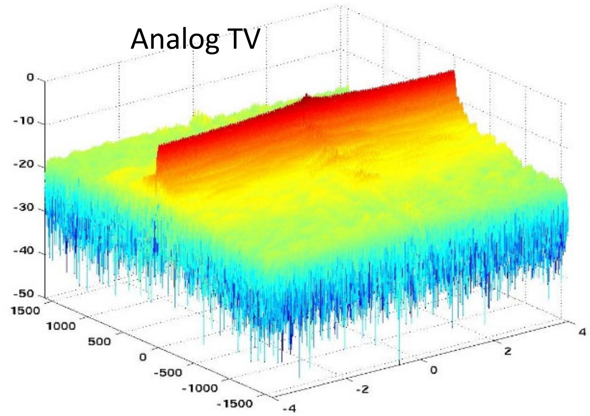

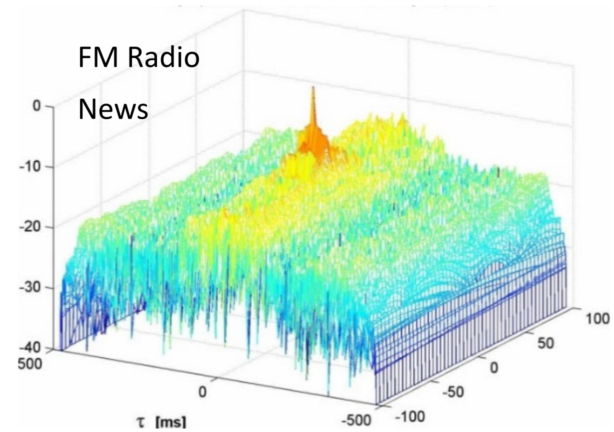

- But also content-dependen

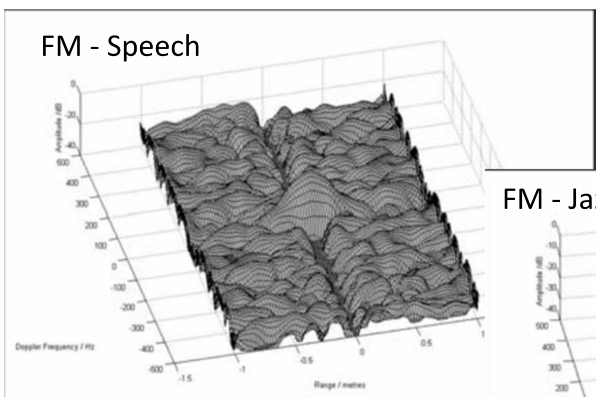

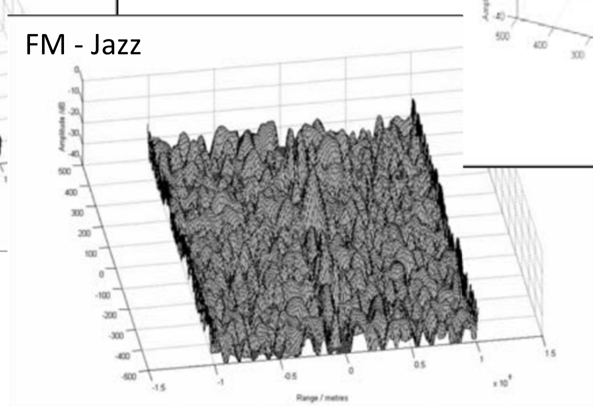

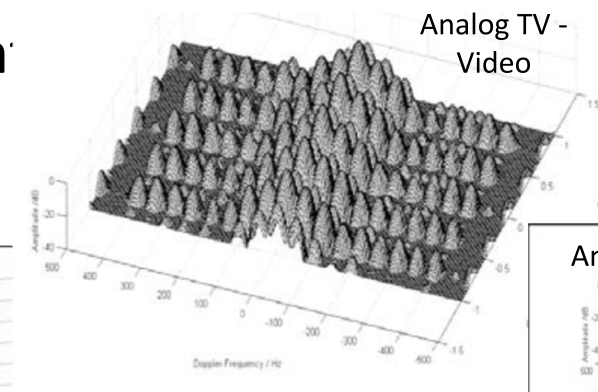

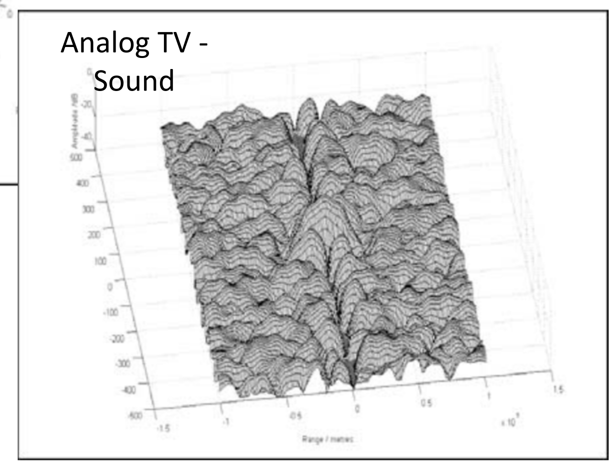

Bistatic Clutter

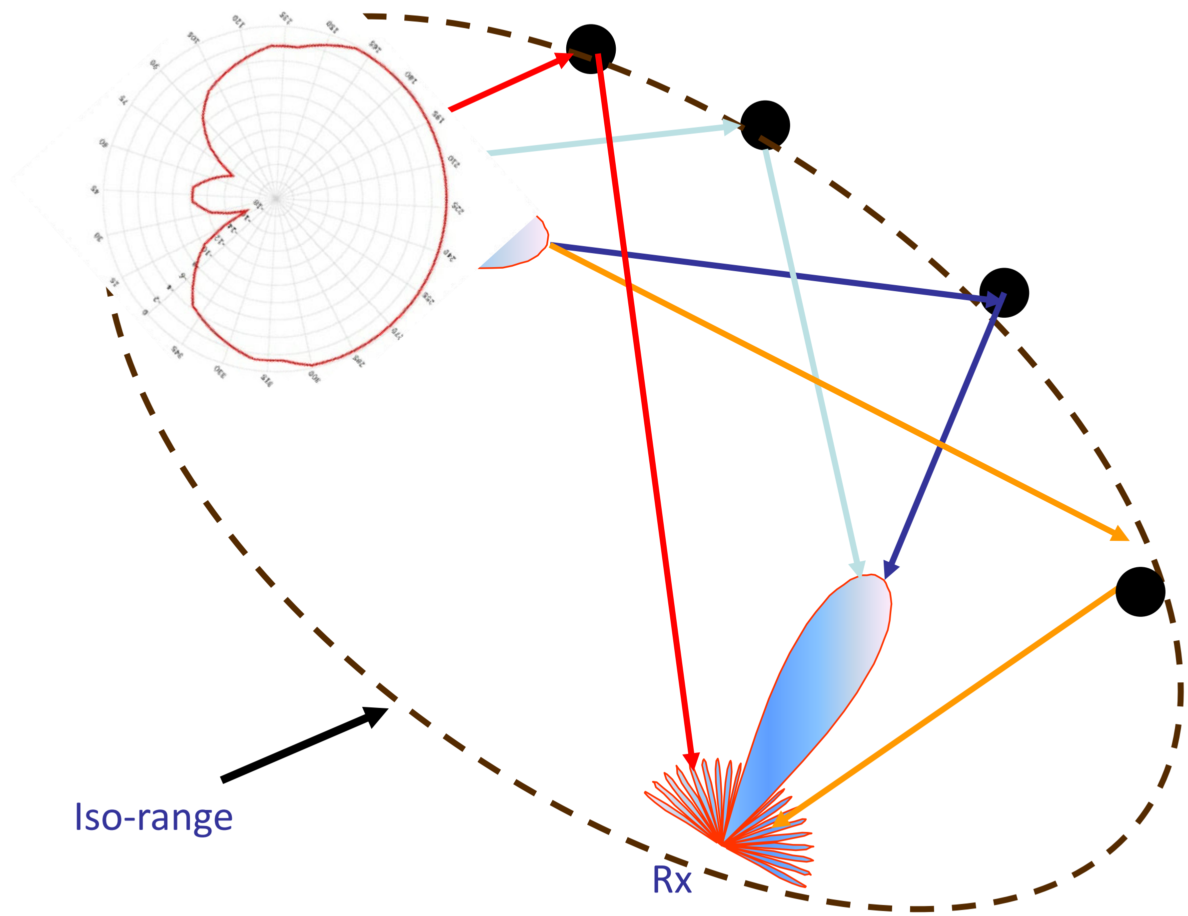

Outline

- Motivation
- Bistatic Radar
- Passive Radar
- Experimental Systems
- Unifying Theory
- Conclusions

Early Developments

- NATO-DRG - Study on Passive and Noise Radar (Symposium in 1994)

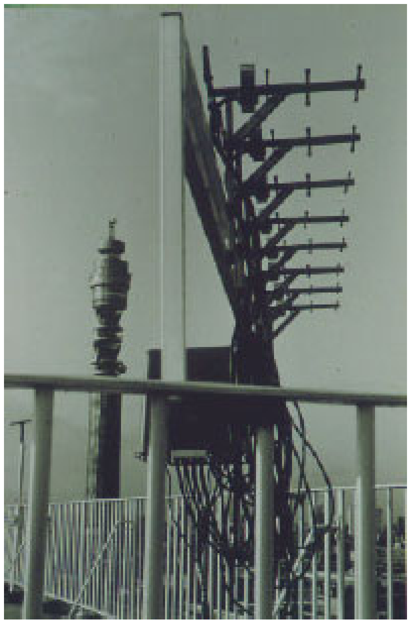

TV-radar with Video carrier of Crystal Palace Tx, UCL

TV-radar with Video carrier and line sync. Pulses, Thales patent

Silent sentry - SS1, Lockheed-Martin

Silent sentry – SS3, Lockheed-Martin

http://servv89pn0aj.sn.sourcedns.com/~gbpprorg/mil/radar/sentry.pdf

PAssive RAdar DEmonstrator (PARADE) Cassidian, Germany

- Mercedes Sprinter
- Loading space: 3265mm x 1780mm x 1940mm
- Gross vehicle weight: 5000kg
- Motor power: 160PS

- Lifting height: 12m
- Allowable load: 200 kg
- Integrated antenna mast

A. Schroeder, et al., “CASSIDIAN multiband mobile passive radar system ” Proc. IRS 2011, Sep 2011

Passive Radar At FHR, Germany

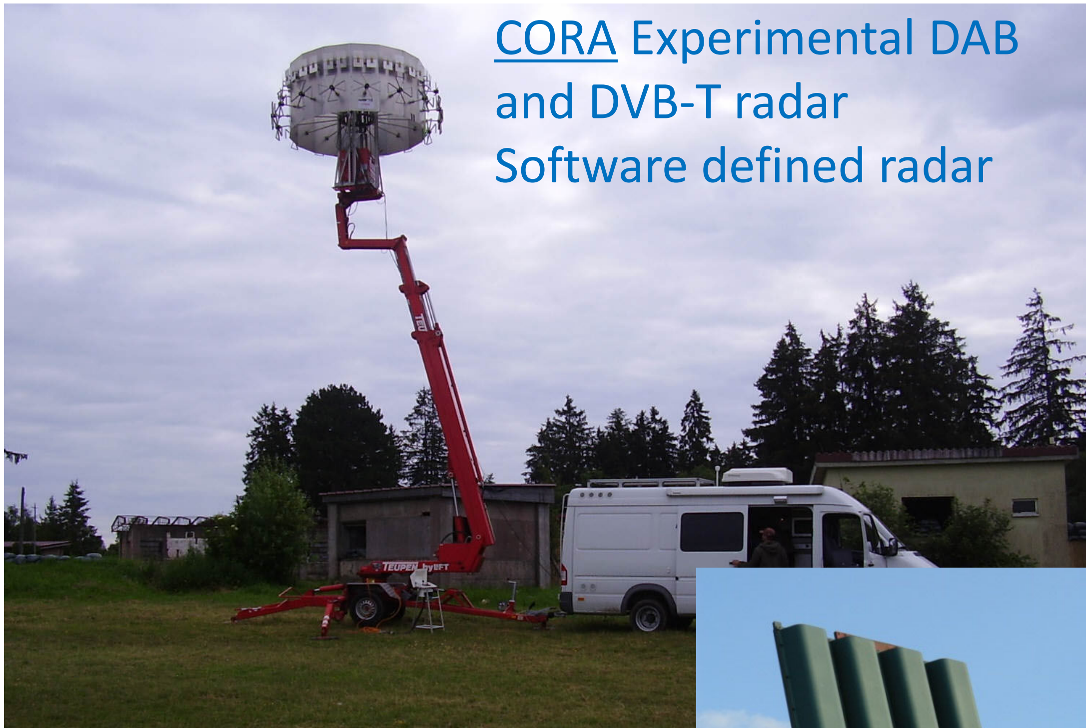

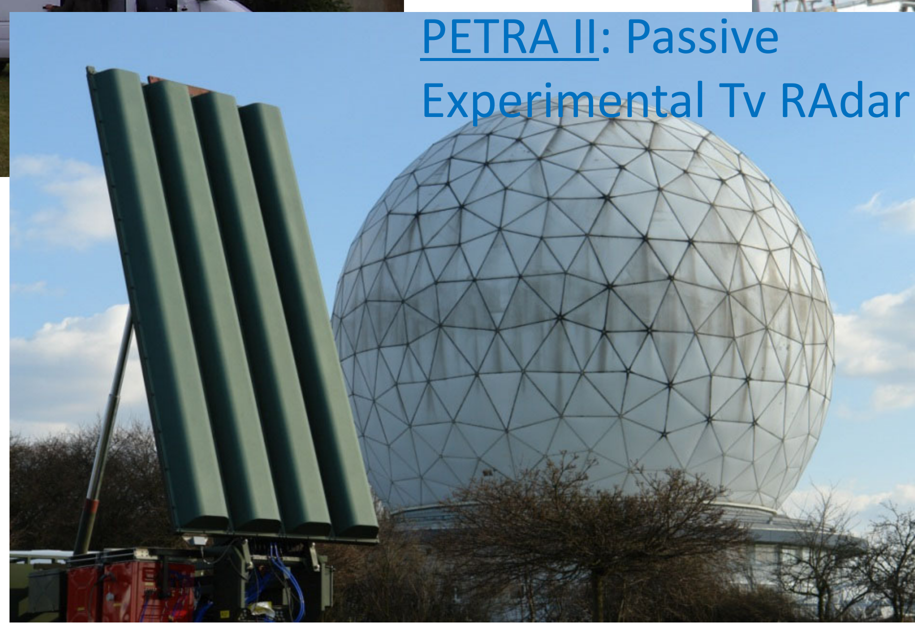

Use of digital illuminators

http://www.fhr.fraunhofer.de/en.html

Homeland Alerter (HA)-100
Thales, France

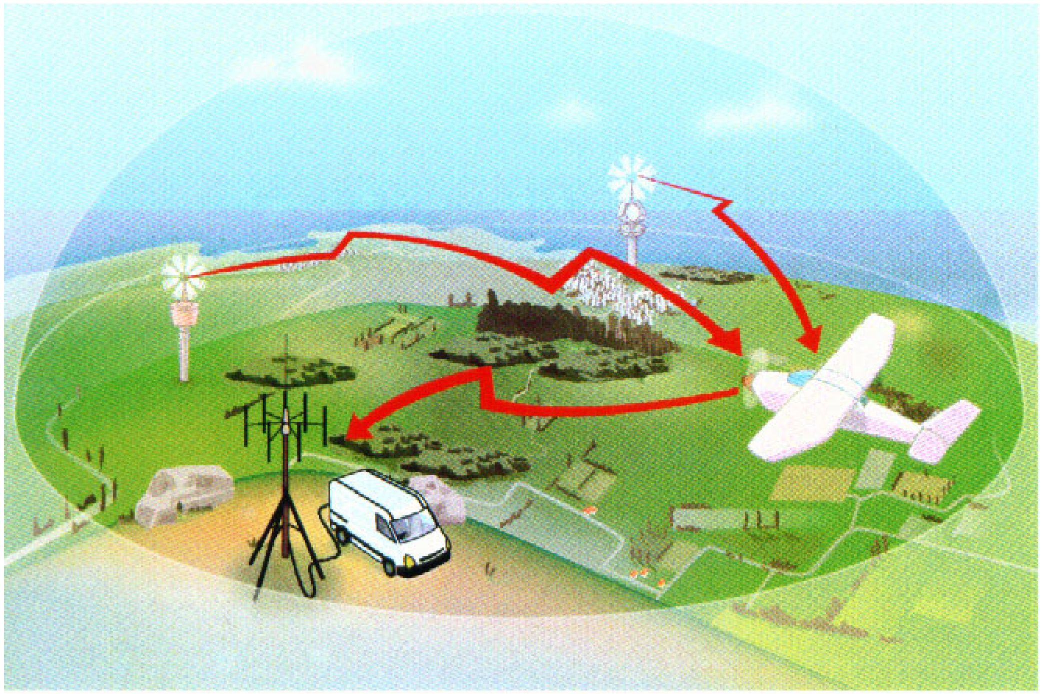

- Passive radar target location
- Uses up to 8 FM-Radio Stations
- Vertical polarisation

www.thalesgroup.com/en/homeland-alerter-100

PaRaDe - Warsaw University of Technology, Poland

- Transportable system
- FM radio signals
- 8 element circular array
- Ground and Airborne

- M. Malanowski, et al., “Experimental results of the PaRaDe passive radar field trials”, Proc. IRS 2012, Warsaw, Poland, 2012
- B. Dawidowicz, et al., “Detection of Moving Targets with Multichannel Airborne Passive Radar” IEEE AESS Mag., Vol. 1, Issue 11, 2012

Aulos – SELEX SI

Aulos FM PCL System by SELEX Sistemi Integrati

- Mobile experimental system
- 8-Element circular array
- Signal processing on CPU and GPU

- http://www.microwavejournal.com/articles/18896-aulos-a-passive-covert-radar-system
- http://www.selex-si-uk.com/pdf/Aulos.pdf

Example Results – CORA System

- Two target resolution performance

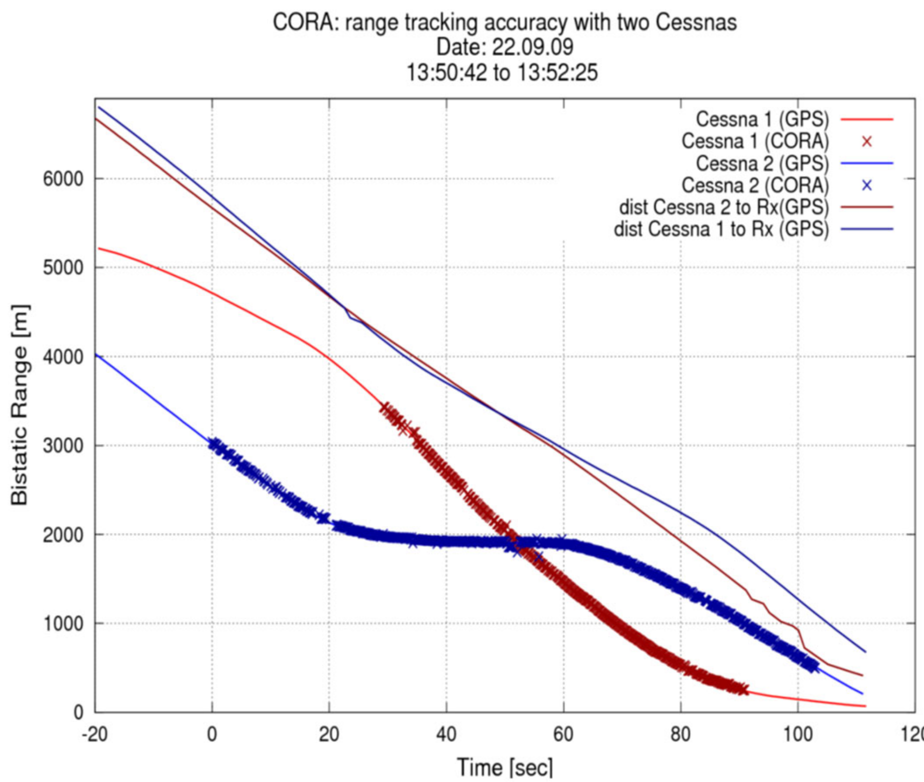

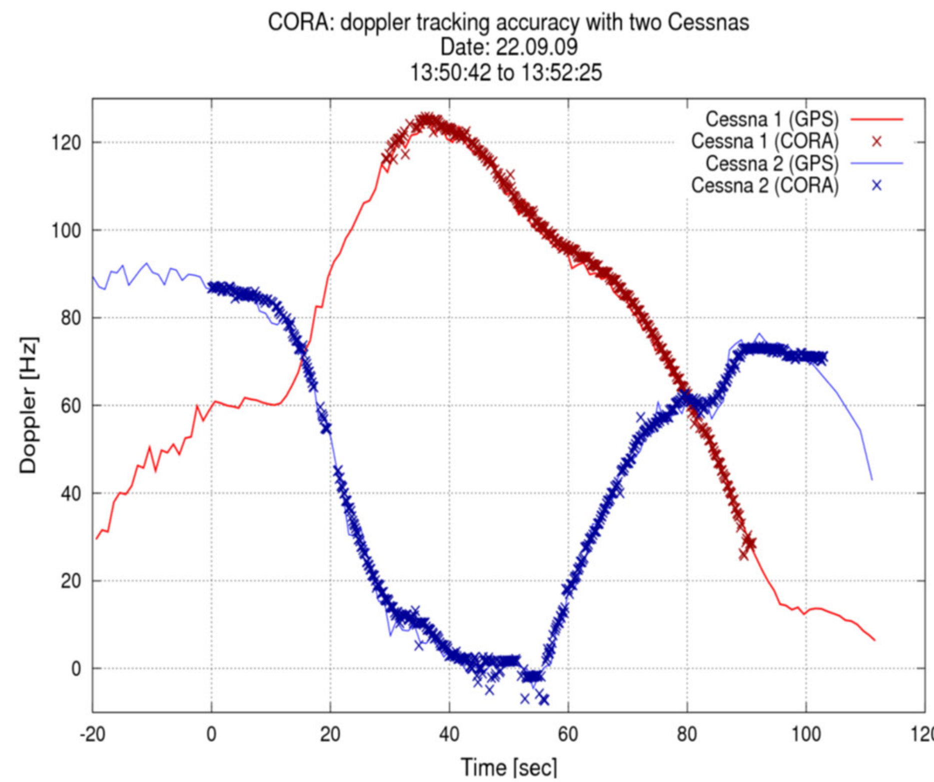

Courtesy Dr. Heiner Kushel, FHR, Germany

Outline

- Motivation
- Bistatic Radar
- Passive Radar
- Experimental Systems
- **Unifying Theory**
- Conclusions

Unified Framework

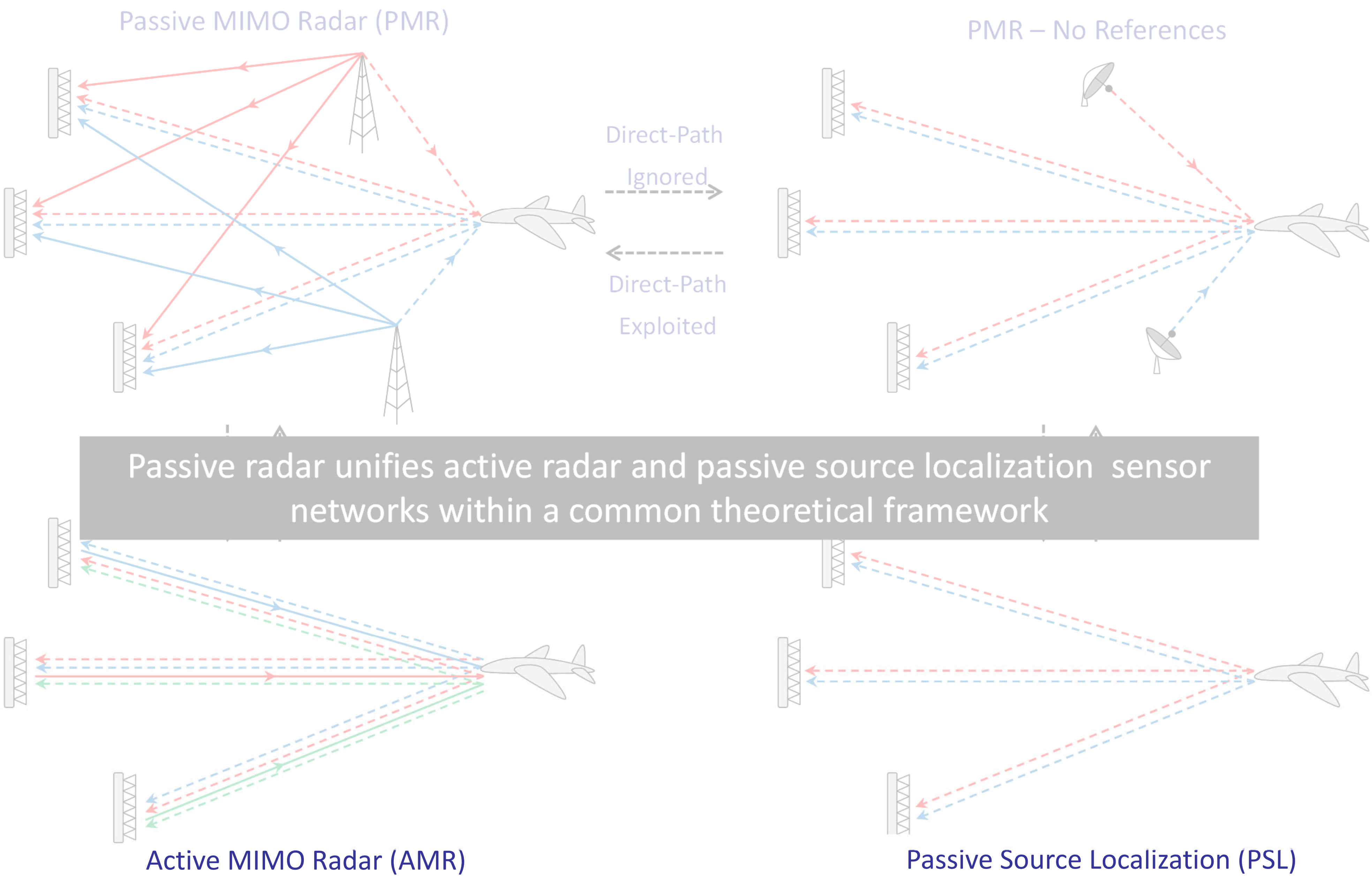

Unified Framework

Sensor Networks:

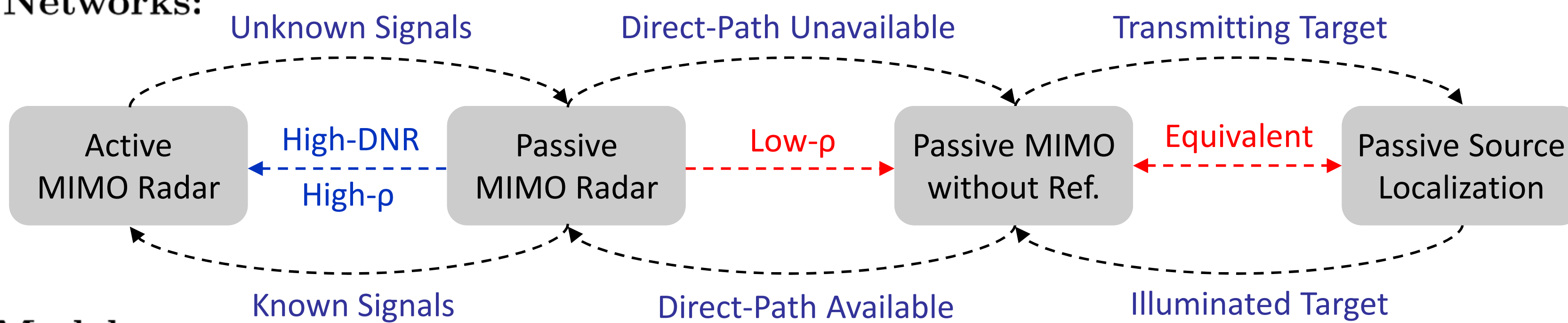

Signal Models:

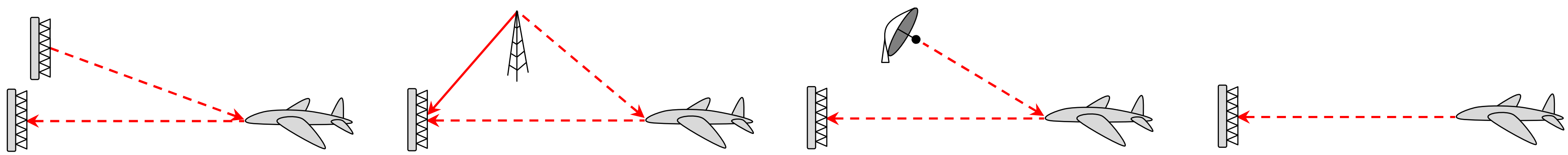

$$\mathbf{s}_s^{ij} = \mu_s^{ij}\mathcal{D}_s^{ij}\mathbf{u}^i + \mathbf{n}_s^{ij}$$

$\mathbf{u}^i$ known

$$\mathbf{s}_s^{ij} = \mu_s^{ij}\mathcal{D}_s^{ij}\mathbf{u}^i + \mathbf{n}_s^{ij}$$
$$\mathbf{s}_r^{ij} = \mu_r^{ij}\mathcal{D}_r^{ij}\mathbf{u}^i + \mathbf{n}_r^{ij}$$

$\mathbf{u}^i$ unknown

$$\mathbf{s}_s^{ij} = \mu_s^{ij}\mathcal{D}_s^{ij}\mathbf{u}^i + \mathbf{n}_s^{ij}$$

$\mathbf{u}^i$ unknown

$$\mathbf{s}_s^{ij} = \mu_{s,2}^{ij}\mathcal{D}_{s,2}^{ij}\mathbf{u}^i + \mathbf{n}_s^{ij}$$

$\mathbf{u}^i$ unknown

Detectors:

$$\frac{1}{\sigma^2}\sum_{i=1}^{N_t}\sum_{j=1}^{N_r}\left|(\mathbf{u}^i)^H\tilde{\mathbf{s}}_s^{ij}\right|^2$$

(MF-GLRT)

Matched Filtering

$$\frac{1}{\sigma^2}\sum_{i=1}^{N_t}\Big(\lambda_{\max}(\mathbf{G}_1^i) - \lambda_{\max}(\mathbf{G}_{rr}^i)\Big)$$

(RS-GLRT)

Reference-Surveillance

Surveillance-Surveillance

$$\frac{1}{\sigma^2}\sum_{i=1}^{N_t}\lambda_{\max}(\mathbf{G}_{ss}^i)$$

(SS-GLRT)

Surveillance-Surveillance

$$\frac{1}{\sigma^2}\sum_{i=1}^{N_t}\lambda_{\max}(\mathbf{G}_{ss}^i)$$

(SS-GLRT)

Surveillance-Surveillance

Detection Comparison

Scenario: $N_t = 2$ transmitters $L = 0$ to $+40$ dB in 5 dB steps

$N_r = 3$ receivers

$P_d = 0.90$ iso-contours for MF-GLRT (blue), SS-GLRT (red), and RS-GLRT

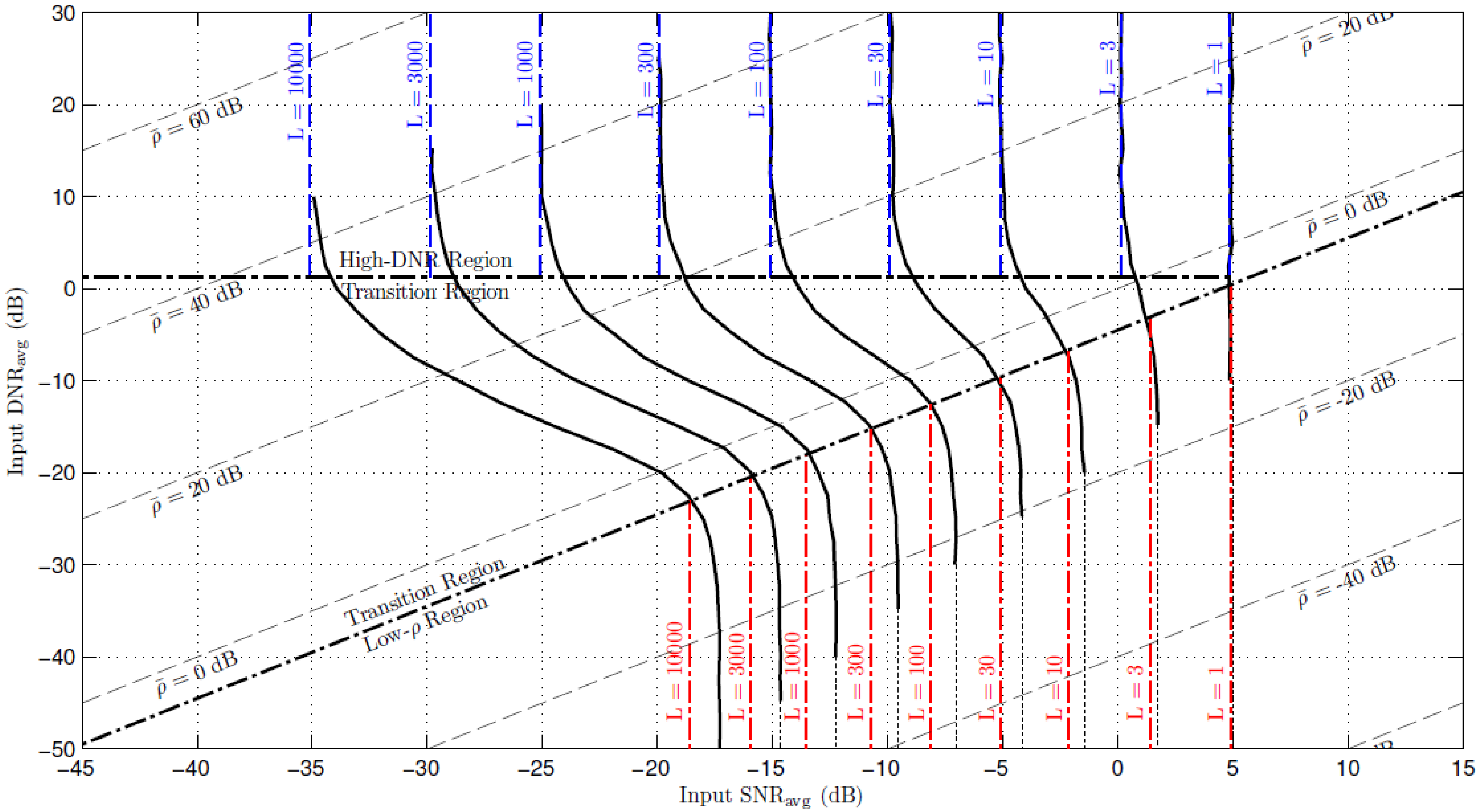

Outline

- Introduction/Motivation
- Bistatic Radar
- Bistatic & Multistatic Passive Radar
- Experimental Systems
- Unifying Theory
- Conclusions

Conclusions

- Reviewed the bistatic radar concept
- Extended concept to passive radar, to include illuminators of opportunity
- Addressed issues of geometry and waveforms
- Reviewed some experimental systems
- Introduced a theory that unifies Passive and Active MIMO radar
- Passive radar will play a major role in future systems

Part 2
Signal Detection and Estimation for Passive Radar

Outline

- Cross-correlator in the presence of noisy reference and DPI
- Passive detection with noisy reference
- Passive detection with multiple receivers
  - Part I: No DPI
  - Part II: With DPI
- Exploit waveform correlation for passive detection and estimation
  - Part I: Joint delay-Doppler estimation
  - Part II: Multi-static detection with DPI
  - Part III: A parametric approach
- Summary

Data Model

- We examine the impact of noise and direct path interference (DPI) on conventional passive detection
  - Reference is distorted by noise
  - DPI is much stronger (by up to 100 dB) than target signal
  - DPI may not be fully cancelled: small array aperture, mismatch between array null and DPI direction…

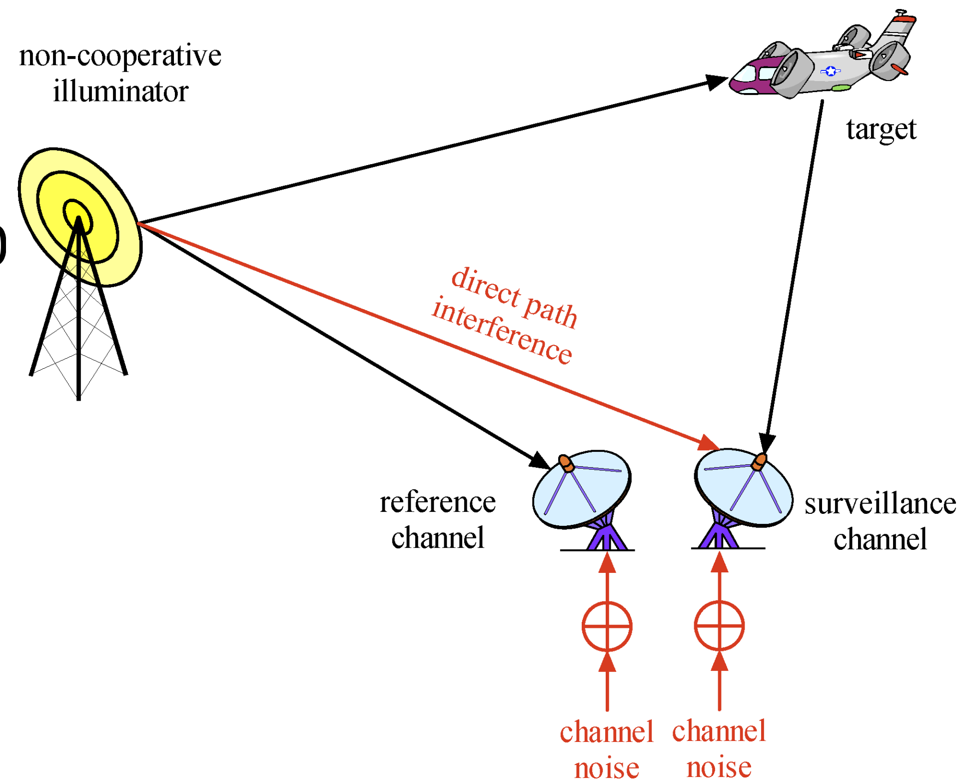

- Signal model:

IO waveform

$$\text{RC:} \quad x_{\mathrm{r}}(n) = \beta p(n) + v(n)$$

$$\text{SC:} \quad x_{\mathrm{s}}(n) = \boxed{\gamma p(n)} + \boxed{\alpha p(n-\tau)\exp(j\Omega_d n)} + w(n)$$

DPI

target echo w/ delay & Doppler

The Problem

- Cross-correlation (CC) detector:

$$T_{\mathsf{CC}} = |\bar{T}|^2 = \left| \sum_{n=0}^{N-1} x_{\mathsf{s}}^*(n) x_{\mathsf{r}}(n-\tau) \exp(j\Omega_d n) \right|^2 \underset{H_0}{\overset{H_1}{\gtrless}} \lambda$$

  – Simple, no need for prior knowledge of IO waveform
  – Equivalent to the optimum matched filter (MF) (used in active radar) if the RC is noiseless
  – Performance degrade in the presence of noise and DPI
- **Question**: To what extent can the CC cope with noise and DPI?
  – Given a targeted performance, compute upper bounds for the noise level (in RC) and DPI level that can be tolerated by CC
  – Using the MF as a benchmark, the targeted performance is measured by a SNR loss δ dB from the MF (in terms of the extra SNR needed for the CC to achieve the same P_D)

Performance of CC with Noisy Reference and DPI

- Define SNR in both channels and interference-to-noise ratio (INR) in SC

$$\mathsf{SNR_s} = 10\log_{10}\frac{|\alpha|^2}{\sigma_w^2}, \quad \mathsf{SNR_r} = 10\log_{10}\frac{|\beta|^2}{\sigma_v^2}, \quad \mathsf{INR_s} = 10\log_{10}\frac{|\gamma|^2}{\sigma_w^2}$$

- **Main Result:** To ensure a performance loss of no more than δ dB relative to the MF for a given $\mathrm{SNR_s}$, the $\mathrm{INR_s}$ and $\mathrm{SNR_r}$ for the CC detector must satisfy (in dB)

$$\boxed{\begin{aligned} \mathsf{INR_s} &\le 10\log_{10}\left[\frac{10^{\frac{\delta+\mathsf{SNR_r}}{10}} - 10^{\frac{\delta+\mathsf{SNR_s}}{10}} - 10^{\frac{\mathsf{SNR_r}}{10}} - 1}{1+10^{\frac{\mathsf{SNR_r}}{10}}}\right] \\ \mathsf{SNR_r} &\ge 10\log_{10}\left[\frac{10^{\frac{\mathsf{INR_s}}{10}} + 10^{\frac{\delta+\mathsf{SNR_s}}{10}} + 1}{10^{\frac{\delta}{10}} - 10^{\frac{\mathsf{INR_s}}{10}} - 1}\right] \end{aligned}}$$

J. Liu, H. Li, and B. Himed, "On the performance of the cross-correlation detector for passive radar applications," *Signal Processing*, vol.113, pp.32-37, Aug. 2015

Discussions

- Previous bounds are necessary/sufficient, but coupled between noise and DPI. Decoupled bounds can be found which are only necessary
- **Corollary:** To ensure a performance loss of no more than δ dB relative to the MF for a given $\mathrm{SNR_s}$, the following conditions are necessary

$$\boxed{\begin{aligned} \mathrm{INR_s} &< 10\log_{10}\left(10^{\frac{\delta}{10}} - 1\right) \\ \mathrm{SNR_r} &> 10\log_{10}\left(\frac{10^{\frac{\delta+\mathrm{SNR_s}}{10}} + 1}{10^{\frac{\delta}{10}} - 1}\right) \end{aligned}}$$

- 1^{st} bound specifies the highest tolerable DPI. If not met, CC cannot achieve the targeted performance, irrespective of the noise level of the reference. Note the bound only depends on δ
- 2^{nd} bound denotes the highest tolerable noise level in the reference, irrespective of the level of the DPI. In this case, the bound depends on both δ and the $\mathrm{SNR_s}$

Numerical Results

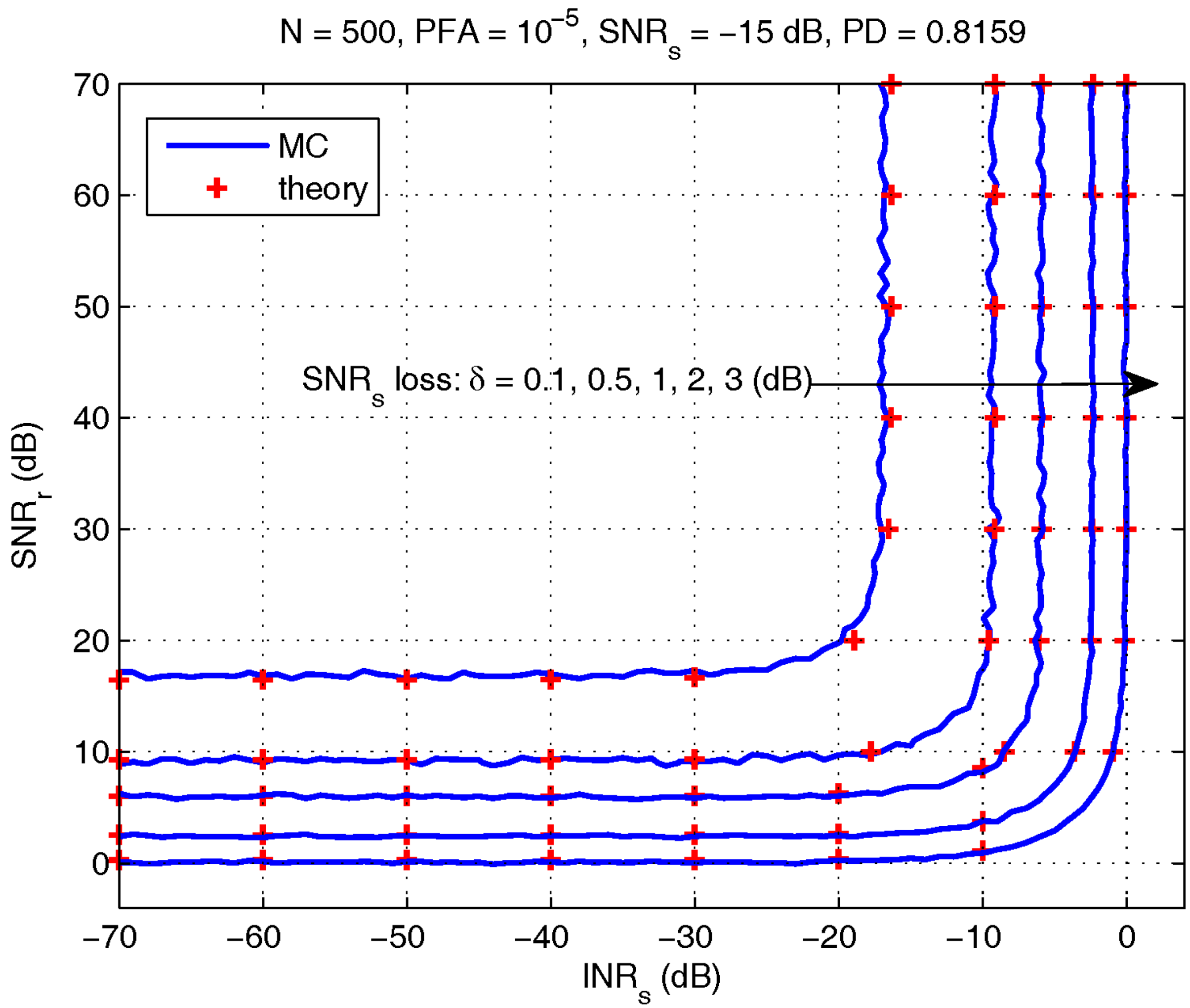

Contour of P_D of the CC detector with different $\mathrm{SNR_s}$ loss relative to the MF detector. The lines denote simulation results, and the symbols '+' are the results obtained from analysis

Numerical Results

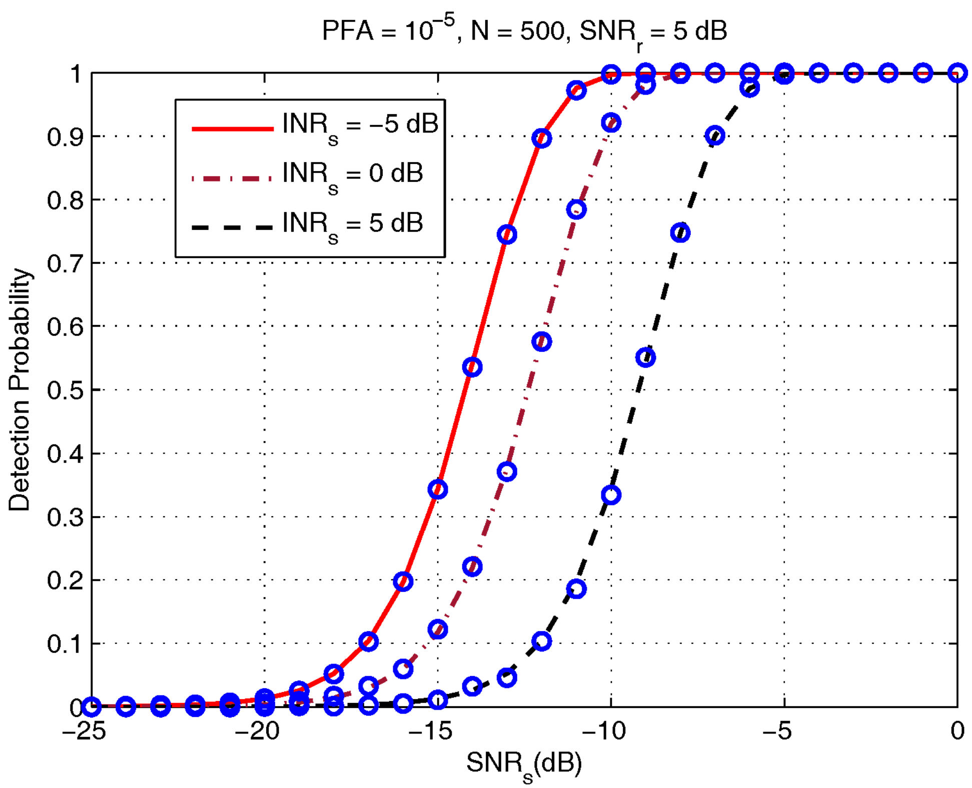

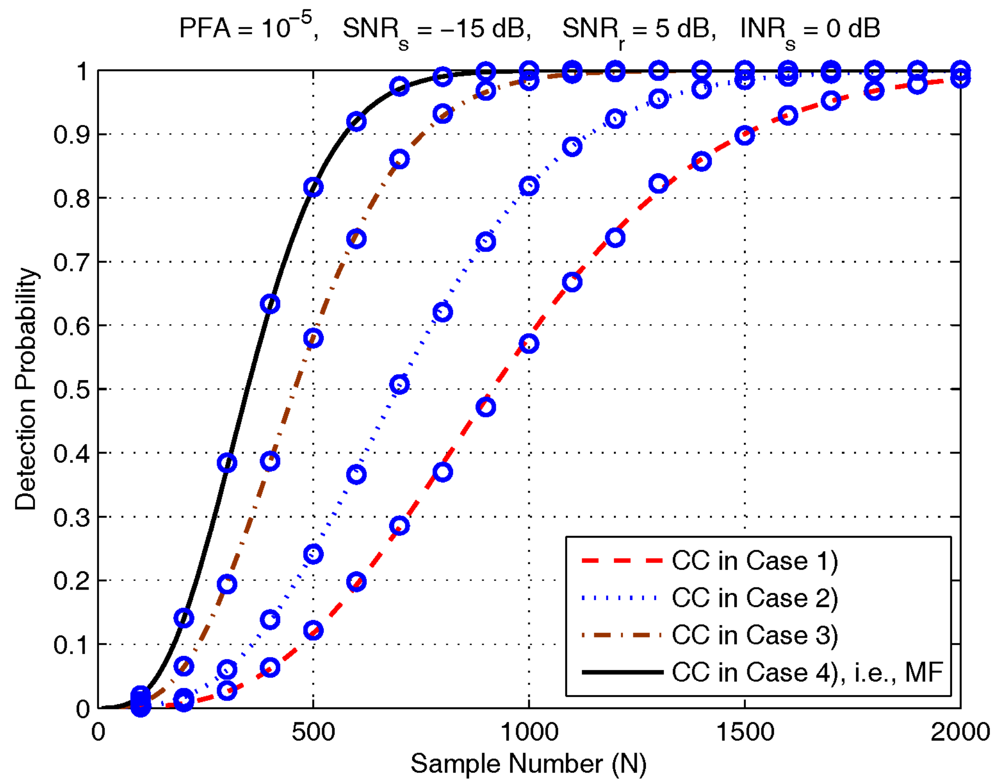

P_D of the CC detector with different values of SNR$_s$ The symbols 'o' denote the simulation results, and the lines denote the results obtained from analysis

Case 1) with noise in RC and DPI in SC;
Case 2) with no noise in RC but with DPI in SC;
Case 3) with noise in RC but no DPI in SC;
Case 4) with no noise in RC and no DPI in SC

Remarks

- Derived approximate expressions for the P_{FA} and P_D of the CC detector in the presence of noise in the reference and the direct-path interference (DPI) in the surveillance channel
- Obtained analytical expressions showing to what extent the noise in the RC and the DPI in the SC must be mitigated in order to achieve a targeted performance loss of the CC detector, relative to the optimal MF detector
- Our result shows that the CC detector, albeit simple to implement, is quite sensitive to the presence of noise in the RC and DPI $\Rightarrow$ There is a clear need for more sophisticated passive techniques that explicitly account for the noise in reference and DPI

Outline

- Cross-correlator in the presence of noisy reference and DPI
- Passive detection with noisy reference
- Passive detection with multiple receivers
  - Part I: No DPI
  - Part II: With DPI
- Exploit waveform correlation for passive detection and estimation
  - Part I: Joint delay-Doppler estimation
  - Part II: Multi-static detection with DPI
  - Part III: A parametric approach
- Summary

Problem Statement

- Reference channel (RC): $x_r(n) = \beta s(n - n_r) + v(n)$
- Surveillance channel (SC): $x_t(n) = \alpha s(n - n_t)\,\exp(j\Omega_d n) + w(n)$
  - $s(n)$ is the unknown transmitted signal, n_r and n_t are time delays
  - Ω_d is a Doppler shift, α and β are channel coefficients
  - v and w are Gaussian noise
- After delay/Doppler compensation and collecting multiple samples in vectors:

$$H_0 : \begin{cases} \mathbf{x}_r = \beta \mathbf{s} + \mathbf{v} \\ \mathbf{x}_t = \mathbf{w} \end{cases} \qquad H_1 : \begin{cases} \mathbf{x}_r = \beta \mathbf{s} + \mathbf{v} \\ \mathbf{x}_t = \alpha \mathbf{s} + \mathbf{w} \end{cases}$$

- The problem of interest is to solve the hypothesis testing using observations $\mathbf{x}_r$ and $\mathbf{x}_t$, with unknown IO waveform $\mathbf{s}$, amplitude α and β
- We consider generalized likelihood ratio test (GLRT) based detectors in 4 different cases with $\mathbf{s}$ being modeled as deterministic or stochastic and the noise power η being known or unknown

G. Cui, J. Liu, H. Li, and B. Himed, "Signal detection with noisy reference for passive sensing," *Signal Processing*, vol.108, pp.389-399, Mar. 2015

Summary of 4 GLRTs with Noisy Reference

- Deterministic IO waveform $\mathbf{s}$, unknown noise power η:

$$T_1 = \frac{\hat{\eta}_0}{\hat{\eta}_1} = \frac{\|\mathbf{x}_t\|^2}{\|\mathbf{x}_t\|^2 + \|\mathbf{x}_r\|^2 - \sqrt{(\|\mathbf{x}_t\|^2 - \|\mathbf{x}_r\|^2)^2 + 4|\mathbf{x}_t^\dagger \mathbf{x}_r|^2}} \underset{H_0}{\overset{H_1}{\gtrless}} \gamma_1$$

- Deterministic $\mathbf{s}$, known η:

$$T_2 = \frac{1}{\eta}\left(\|\mathbf{x}_t\|^2 - \|\mathbf{x}_r\|^2 + \sqrt{(\|\mathbf{x}_t\|^2 - \|\mathbf{x}_r\|^2)^2 + 4|\mathbf{x}_t^\dagger \mathbf{x}_r|^2}\right) \underset{H_0}{\overset{H_1}{\gtrless}} \gamma_2$$

- Stochastic $\mathbf{s}$, known η:

$$\frac{\|\mathbf{x}_r\|^{2N}}{(\hat{a}^2 + \hat{b}^2 + \eta)^N} \exp\left(\frac{\|\mathbf{x}_t\|^2 \hat{a}^2 - (\hat{a}^2 + \eta)\|\mathbf{x}_r\|^2 + 2\hat{a}\hat{b}|\mathbf{x}_t^\dagger \mathbf{x}_r|}{\eta(\hat{a}^2 + \hat{b}^2 + \eta)}\right) \underset{H_0}{\overset{H_1}{\gtrless}} \gamma_3$$

$$a = |\alpha| \quad \text{and} \quad b = |\beta|$$

- Stochastic $\mathbf{s}$, known η:

$$\frac{\|\mathbf{x}_r\|^{2N}\|\mathbf{x}_t\|^{2N}}{\hat{\eta}^N(\hat{a}^2 + \hat{b}^2 + \hat{\eta})^N} \exp\left(-\frac{(\hat{b}^2 + \hat{\eta})\|\mathbf{x}_t\|^2 + (\hat{a}^2 + \hat{\eta})\|\mathbf{x}_r\|^2 - 2\hat{a}\hat{b}|\mathbf{x}_t^\dagger \mathbf{x}_r|}{\hat{\eta}(\hat{a}^2 + \hat{b}^2 + \hat{\eta})}\right) \underset{H_0}{\overset{H_1}{\gtrless}} \gamma_4$$

Numerical Results

- For comparison, we consider two detectors
  - cross-correlation (CC) detector: $$\boxed{T_{\mathsf{CC}} = \left|\mathbf{x}_t^\dagger \mathbf{x}_r\right|^2 \underset{H_0}{\overset{H_1}{\gtrless}} \gamma}$$
  - matched filter (MF) detector: $$\boxed{T_{\mathsf{MF}} = \left|\mathbf{x}_t^\dagger \mathbf{s}\right|^2 \underset{H_0}{\overset{H_1}{\gtrless}} \gamma}$$
- SNR in the surveillance and reference channels:

$$\mathsf{SNR} = 10 \log_{10} \frac{a^2}{\eta}$$

$$\mathsf{SNR}_r = 10 \log_{10} \frac{b^2}{\eta}$$

Numerical Results

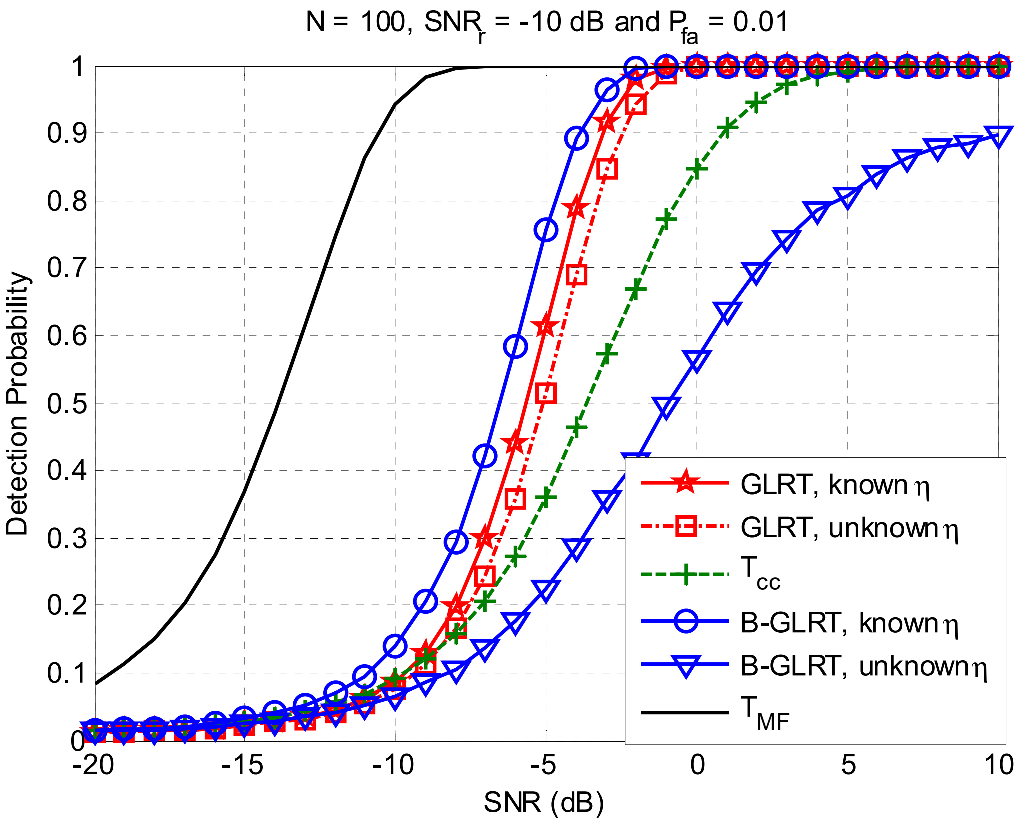

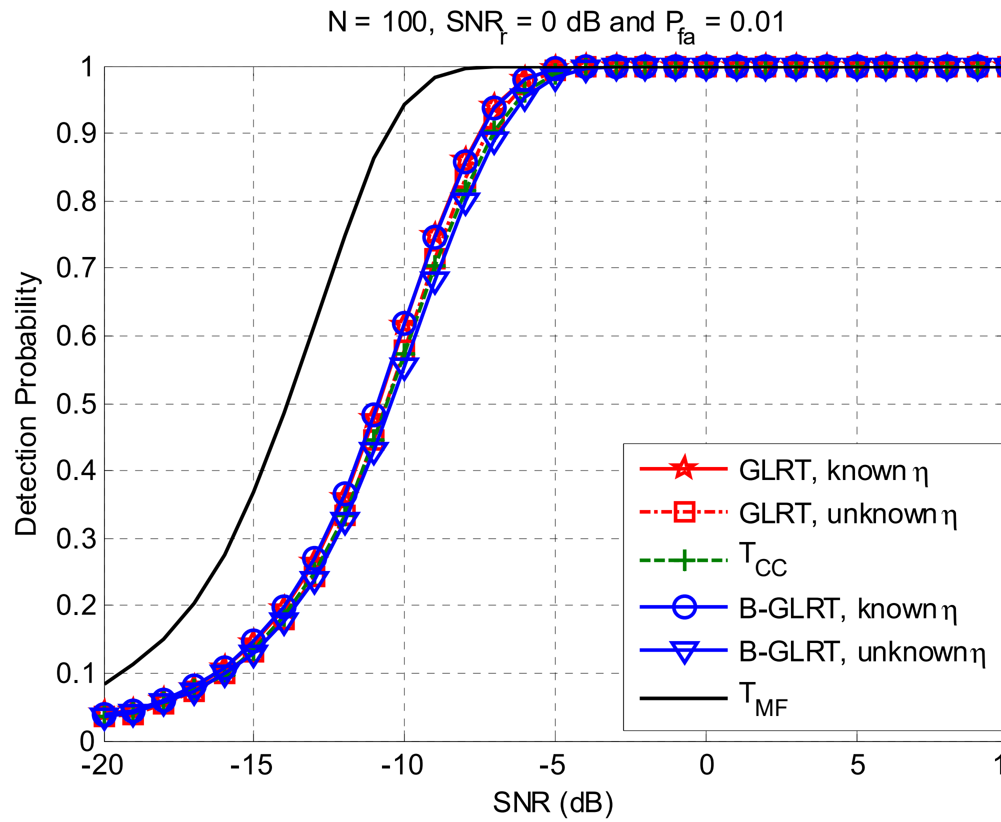

Remarks

- Examined detection for passive radar equipped with a reference channel and a surveillance channel
- Four GLRT detectors with noisy reference
  - Deterministic signal model, known noise power
  - Deterministic signal model, unknown noise power
  - Stochastic signal model, known noise power
  - Stochastic signal model, unknown noise power
- The four GLRT except the one developed with unknown noise power in the stochastic model outperform the CC detector, especially at low SNR_r
- Detection performance of the four detectors depends on the SNR_r in the reference channel

An SVD Detector

- Stack the measurement vectors corresponding to different pulses to obtain $M \times N$ data matrices $\boldsymbol{Y}_s$ and $\boldsymbol{Y}_r$
- Similarly, define the $1 \times N$ vectors $\boldsymbol{\mu}_s = [\mu_{s1}, \dots, \mu_{sN}]$ and $\boldsymbol{\mu}_r = [\mu_{r1}, \dots, \mu_{rN}]$. Therefore, we have

$$H_0 : \begin{cases} \boldsymbol{Y}_s = \boldsymbol{N}_s, \\ \boldsymbol{Y}_r = \boldsymbol{u}\boldsymbol{\mu}_r + \boldsymbol{N}_r, \end{cases}$$

$$H_1 : \begin{cases} \boldsymbol{Y}_s = \boldsymbol{u}\boldsymbol{\mu}_s + \boldsymbol{N}_s, \\ \boldsymbol{Y}_r = \boldsymbol{u}\boldsymbol{\mu}_r + \boldsymbol{N}_r. \end{cases}$$

- By exploiting the rank-1 structure of the data matrices, the SVD detector is given by

$$T_{\mathrm{SVD}} = \left| \widetilde{\boldsymbol{u}}_s^H \widetilde{\boldsymbol{u}}_r \right|^2$$

where $\widetilde{\boldsymbol{\mu}}_s$ and $\widetilde{\boldsymbol{\mu}}_r$ denote the denote the dominant left singular vectors of matrices $\boldsymbol{Y}_s$ and $\boldsymbol{Y}_r$

S. Gogineni, P. Setlur, M. Rangaswamy, and R.R. Nadakuditi. "Passive Radar Detection With Noisy Reference Channel Using Principal Subspace Similarity." *IEEE Trans. Aerospace and Electronic Systems*, vol.54, no.1, pp. 18-36, Jan. 2018

An SVD Detector

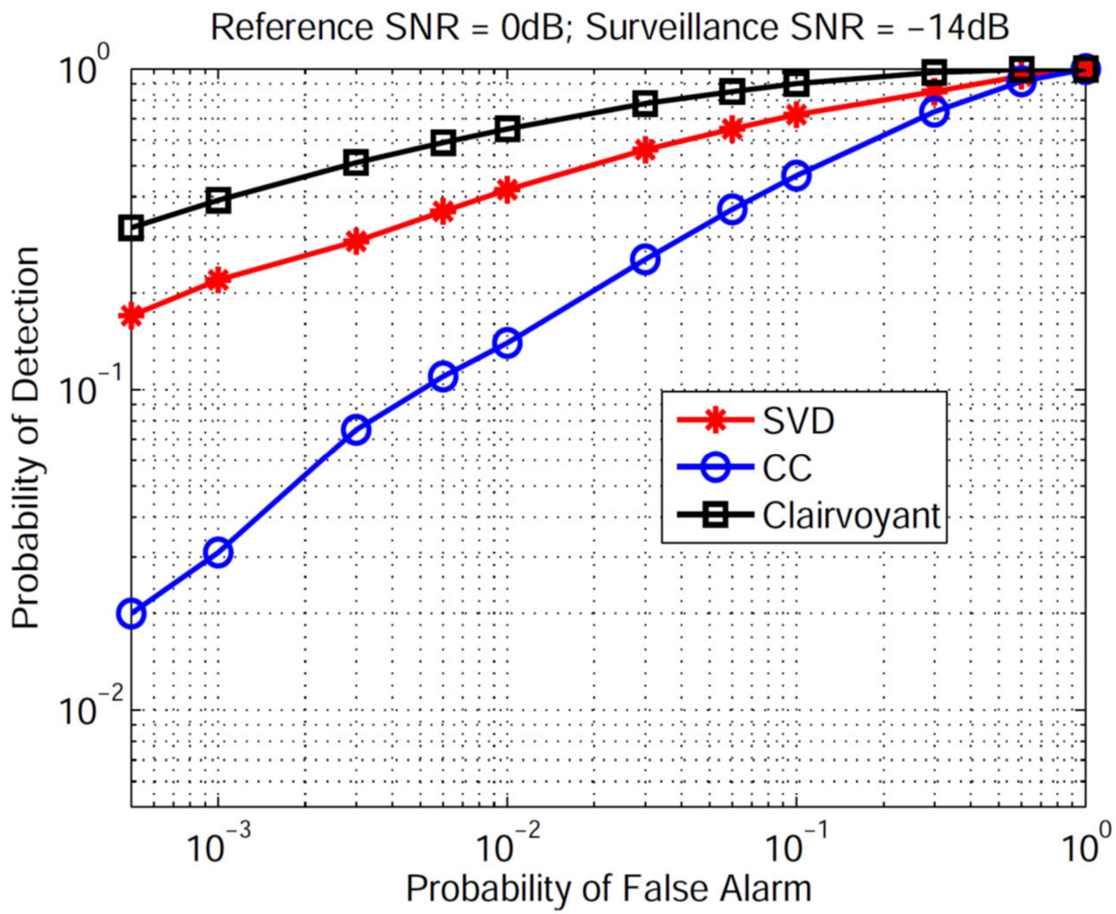

$M = 11$ and $N = 50$

The SVD detector performs better than the cross correlation detector because the left singular vector acts like a joint estimate of the unit-norm transmit pulse

Outline

- Cross-correlator in the presence of noisy reference and DPI
- Passive detection with noisy reference
- Passive detection with multiple receivers
  - Part I: No DPI
  - Part II: With DPI
- Exploit waveform correlation for passive detection and estimation
  - Part I: Joint delay-Doppler estimation
  - Part II: Multi-static detection with DPI
  - Part III: A parametric approach
- Summary

Signal Model

- Consider a distributed passive radar with K RX's. Signal received at k-th RX under H_1 is given by

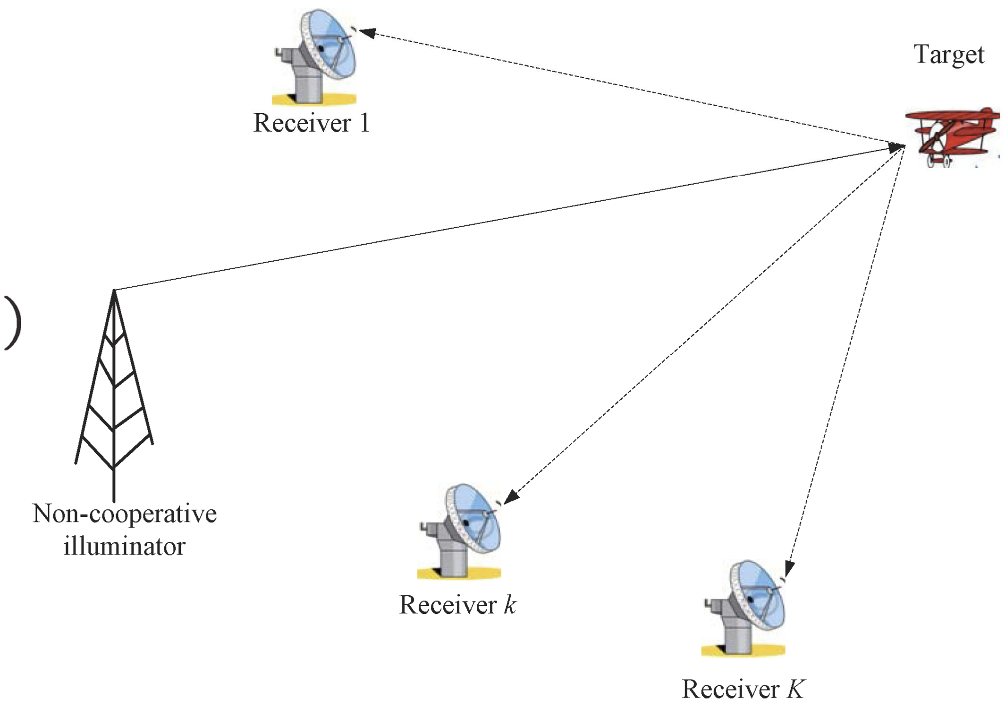

channel/target RCS

IO waveform

$$x_k(n) = \alpha_k s(n - n_k) \exp(\jmath \Omega_k n) + w_k(n)$$

n_k :propagation delay

Ω_k,normalized Doppler frequency

- After delay and Doppler compensation for a specific hypothesized parameter set, the problem is

$N \times 1$ test signal

$N \times 1$ unknown waveform vector

$$\begin{cases} H_0 : \mathbf{x}_k = \mathbf{w}_k \\ H_1 : \mathbf{x}_k = \alpha_k \mathbf{s} + \mathbf{w}_k \end{cases} \qquad k = 1, 2, \ldots, K$$

$N \times 1$ noise vector $\mathcal{N}(0, \sigma^2 \mathbf{I})$

- Two cases are examined:
  - (1) noise variance σ^2 known; (2) σ^2 unknown

GCC with Known σ^2

- This case was considered in [Bialkowski et al.'11]. The detector is called generalized canonical correlation (GCC) detector

$$\Delta = \lambda_1(\boldsymbol{\Phi}) \underset{H_0}{\overset{H_1}{\gtrless}} \delta, \quad \text{equivalently,} \quad \Delta_1 = \frac{1}{\sigma^2}\lambda_1(\boldsymbol{\Phi}) \underset{H_0}{\overset{H_1}{\gtrless}} \delta_1$$

- Gram matrix $\boldsymbol{\Phi} = \mathbf{X}^H\mathbf{X}$ has a complex central Wishart distribution under H_0. The distribution of the principal eigenvalue λ_1 of a complex central Wishart distribution was studied in [Khatri'64], from which the probability of false alarm of GCC can be determined in closed form
- Under H_1, $\boldsymbol{\Phi}$ is a complex non-central Wishart random matrix. The distribution of λ_1 was examined in in [Kang-Alouini'03]. Using the result, we can determine the probability of detection of GCC

K.S. Bialkowski, I.V.L. Clarkson, and S.D. Howard, "Generalized canonical correlation for passive multistatic radar detection," in *Proc. IEEE Statistical Signal Process. Workshop*, Jun. 2011

C. G. Khatri, "Distribution of the largest or the smallest characteristic root under null hypothesis concerning complex multivariate normal populations," *Ann. Math. Statist*., vol. 35, Dec. 1964

M. Kang and M.-S. Alouini, "Largest eigenvalue of complex Wishart matrices and performance analysis of MIMO MRC systems," IEEE J. Sel. Areas Commun., vol. 21, no. 3, pp. 418–426, Apr. 2003

GLRT with Unknown σ^2

- GCC is sensitive to the accuracy of the noise variance. When σ^2 is unknown, an alternative is the GLRT given by

$$\frac{\max_{\{\alpha_k,\mathbf{s},\sigma^2\}} f(\mathbf{X}|H_1)}{\max_{\{\sigma^2\}} f(\mathbf{X}|H_0)} \Longrightarrow \boxed{\Xi = \frac{\lambda_1(\mathbf{\Phi})}{\sum_{k=1}^{K} \lambda_k(\mathbf{\Phi})} \underset{H_0}{\overset{H_1}{\gtrless}} \xi}$$

$$f(\mathbf{X}|H_i) = \frac{1}{\pi^{KN}\sigma^{2KN}} \exp\left(-\frac{1}{\sigma^2}\sum_{k=1}^{K} \|\mathbf{x}_k - \alpha_k b_i \mathbf{s}\|^2\right), \quad b_0 = 0 \quad \text{and} \quad b_1 = 1$$

- The test statistic can be written in a form similar to GCC by using an estimate of the noise variance

$$\frac{\lambda_1(\mathbf{\Phi})}{\hat{\sigma}^2} \underset{H_0}{\overset{H_1}{\gtrless}} \xi', \quad \text{where } \hat{\sigma}^2 \triangleq \frac{1}{KN}\sum_{k=2}^{K} \lambda_k(\mathbf{\Phi})$$

- The probability of false alarm can be determined, which indicates GLRT is CFAR, but a closed-form expression of the probability of detection is unavailable

J. Liu, H. Li, and B. Himed, “Two target detection algorithms for passive multistatic radar," *IEEE Trans. Signal Processing*, vol.62, no.22, pp.5930-5939, Nov. 2014

Numerical Results

- The following detectors are considered
  - GLRT (unknown σ^2): $$\frac{\lambda_1(\mathbf{\Phi})}{\sum_{k=1}^{K} \lambda_k(\mathbf{\Phi})} \overset{H_1}{\underset{H_0}{\gtrless}} \xi_{\text{GLRT}}$$
  - Generalized coherence (GC) detector (unknown σ^2) [Cochran et al.'95, Sirianunpiboon et al.'12] $$1 - \frac{\det\{\mathbf{\Phi}\}}{\prod_{k=1}^{K} \|\mathbf{x}_k\|^2} \overset{H_1}{\underset{H_0}{\gtrless}} \zeta_{\text{GC}}$$
  - GCC (known σ^2): $\lambda_1(\mathbf{\Phi}) \overset{H_1}{\underset{H_0}{\gtrless}} \delta_{\text{GCC}}$
  - Energy detector (known σ^2): $\sum_{k=1}^{K} \|\mathbf{x}_k\|^2 \overset{H_1}{\underset{H_0}{\gtrless}} \zeta_{\text{ED}}$

D. Cochran, H. Gish, and D. Sinno, "A geometric approach to multichannel signal detection," *IEEE Transactions on Signal Processing*, vol. 43, no. 9, Sep. 1995

S. Sirianunpiboon, S. D. Howard, and D. Cochran, "A Bayesian derivation of generalized coherence detectors," in *Proc. Int. Conf. Acoust., Speech, Signal Process.*, Kyoto, Japan, Mar. 2012

Threshold Setting

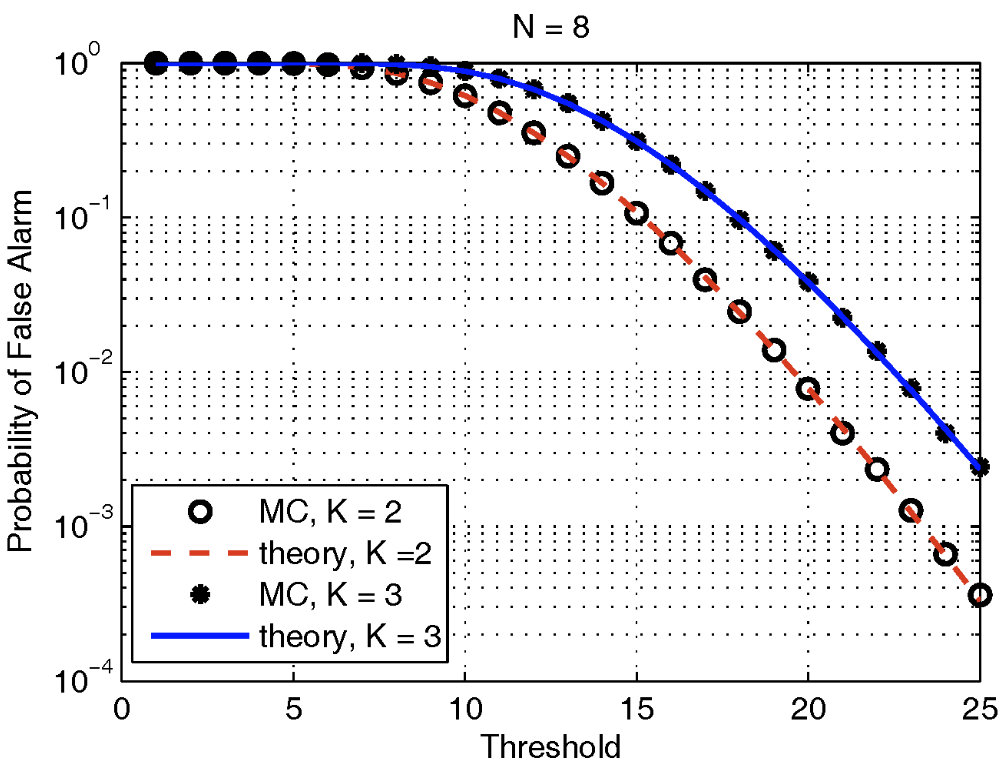

GCC

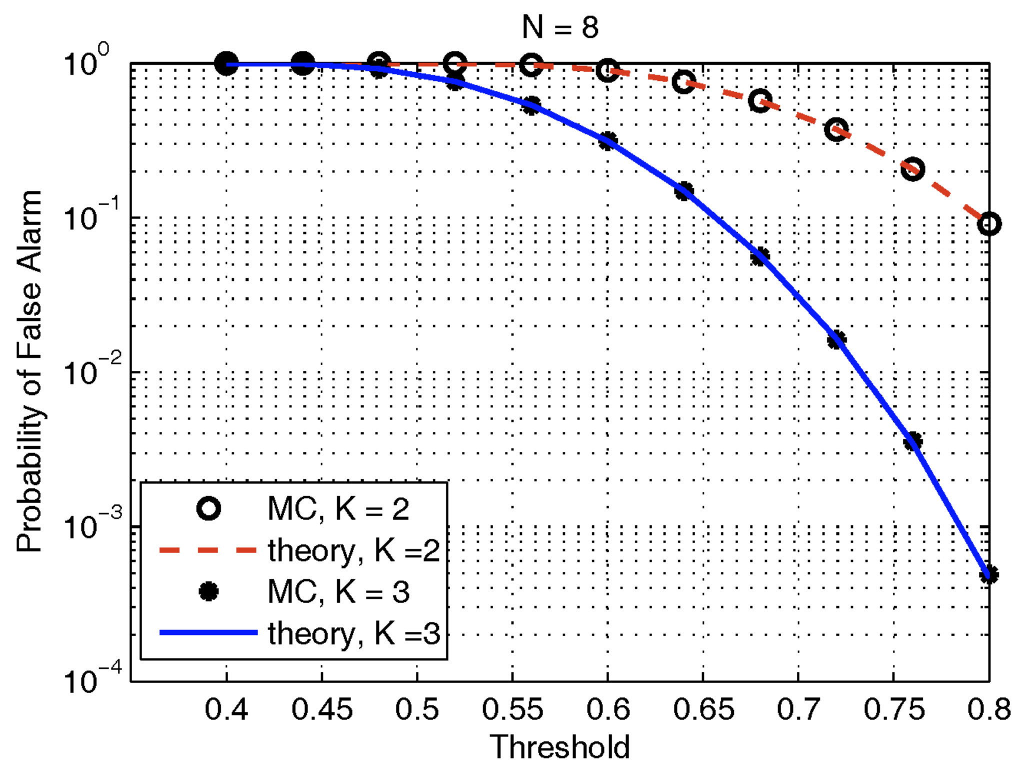

GLRT

Effect of K (Channel #)

GLRT outperforms ED with $K \geq 6$

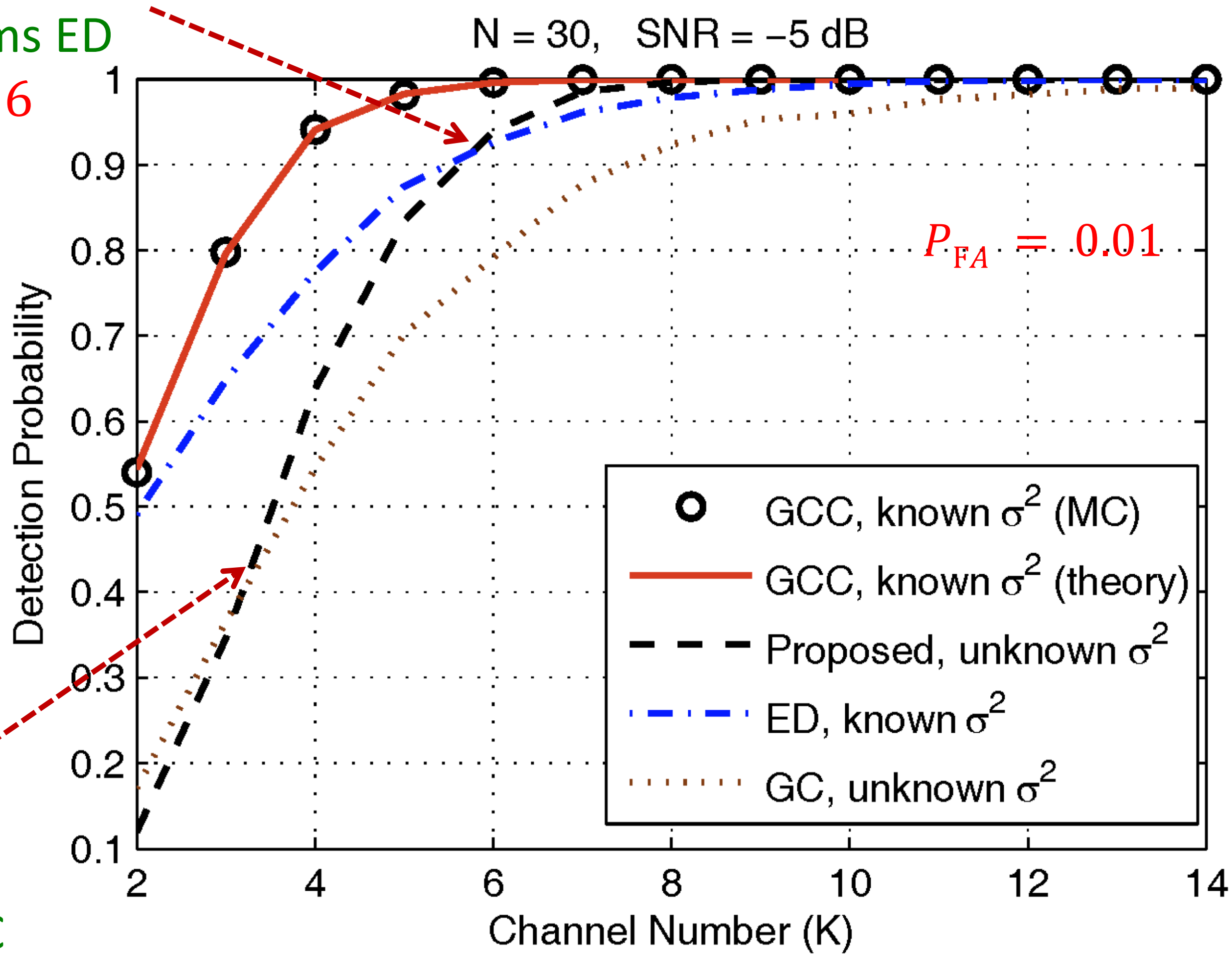

GLRT outperforms GC with $K \geq 4$

Accurate Knowledge of σ^2

$P_{\text{FA}} = 0.01$

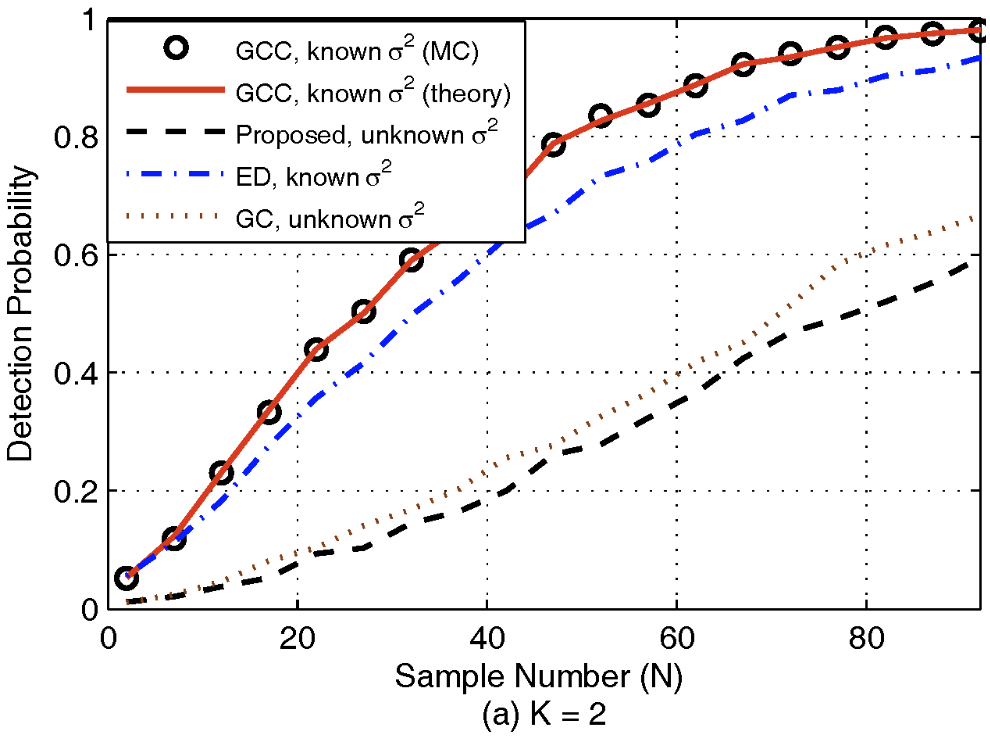

$K = 2$, $\text{SNR} = -5$ dB

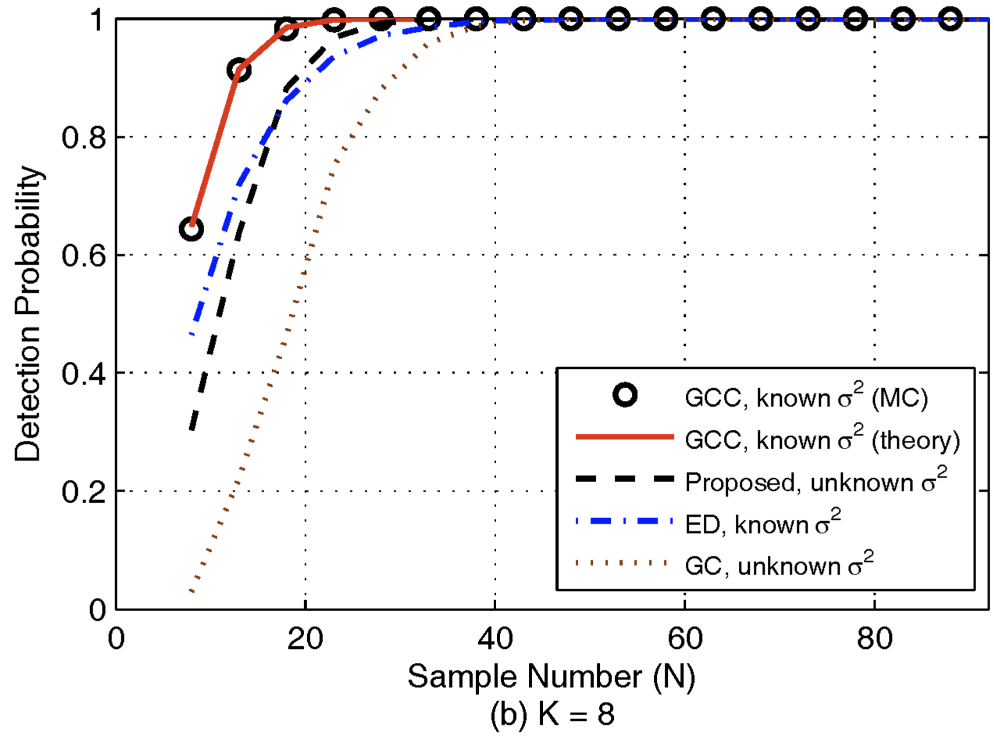

$K = 8$, $\text{SNR} = -5$ dB

Inaccurate Knowledge of σ^2

$P_{FA} = 0.01$

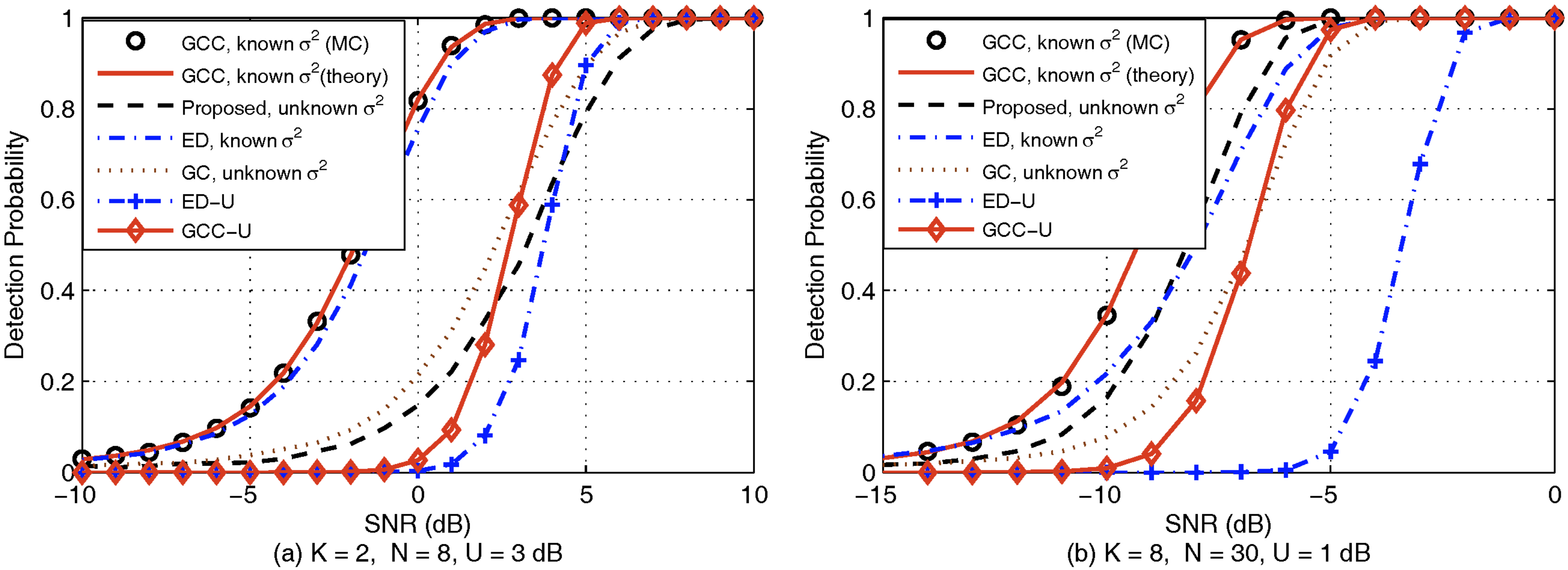

$K = 2,\ U = 3$ dB

$K = 8,\ U = 1$ dB

An estimated noise variance $U\sigma^2$ is used to set threshold: U stands for the amount of uncertainty in the estimate

Remarks

- Introduced a GLRT detector for passive radar with multiple receivers
  - No need for noise variance, CFAR, closed-form P_{FA}
- Studied the GCC (generalized canonical correlation) detector and obtained expressions for P_{FA} and P_{D}
- Numerical results indicate
  - GLRT outperforms the generalized coherence (GC) detector, which also does not need σ^2, and the energy detector, which does require σ^2 , when K (# of channels) is sufficiently large
  - GCC is the best detector when σ^2 is accurately known, but is sensitive to the accuracy of the knowledge

Outline

- Cross-correlator in the presence of noisy reference and DPI
- Passive detection with noisy reference
- Passive detection with multiple receivers
  - Part I: No DPI
  - Part II: With DPI
- Exploit waveform correlation for passive detection and estimation
  - Part I: Joint delay-Doppler estimation
  - Part II: Multi-static detection with DPI
  - Part III: A parametric approach
- Summary

Signal Model

- Consider a multistatic passive radar with one IO and K receivers
- The signal received at k-th receiver in the presence of direct-path interference (DPI):

$$y'_k(t) = \beta_k x(t - d_k) + \alpha'_k x(t - t_k) e^{\jmath 2\pi f_k t} + n'_k(t), \qquad k = 1, \ldots, K$$

d_k : propagation delay of DPI

t_k : progation delay of target

- To simplify, apply delay compensation

$$\begin{aligned} y_k(t) &\triangleq y_k(t + d_k) \\ &= \beta_k x(t) + \alpha_k x(t - \tau_k) e^{\jmath 2\pi f_k t} \\ &\quad + n_k(t) \end{aligned}$$

$$\alpha_k \triangleq \alpha'_k e^{\jmath 2\pi f_k d_k}$$

$$\tau_k \triangleq t_k - d_k \text{ (bistatic delay)}$$

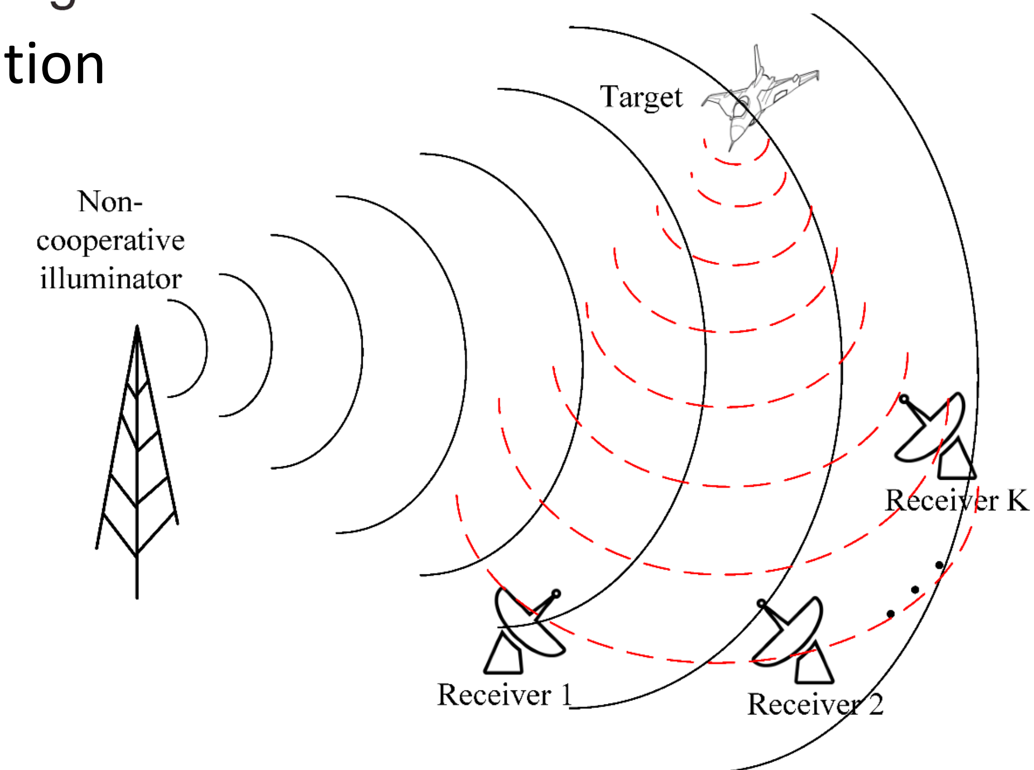

Signal Model

- Take M samples at Nyquist rate and write the signal in vector form

$$\mathbf{y}_k = \beta_k \mathbf{x} + \alpha_k \mathcal{D}(\tau_k, f_k)\mathbf{x} + \mathbf{n}_k, \; k = 1, \ldots, K$$

where $\mathcal{D}(\tau_k, f_k)$ denotes the delay-Doppler shifting operator:

$$\mathcal{D}(\tau_k, f_k) = \mathbf{W}(f_k T_s)\mathbf{T}^H \mathbf{W}(-\tau_k \Delta f)\mathbf{T}$$

$$[\mathbf{W}(x)]_{p,p} = e^{\jmath 2\pi (p-1)x} M \times M \text{ (diagaonl matrix)}$$

$$\mathbf{T} : M \times M \text{ DFT matrix}$$

$$T_s = 1/f_s \text{ sampling interval} \qquad \Delta f = f_s/M \text{ FFT stepsize}$$

- The target detection problem is a composite hypothesis testing

$$\mathcal{H}_1 : \mathbf{y}_k = \beta_k \mathbf{x} + \alpha_k \mathcal{D}(\tau_k, f_k)\mathbf{x} + \mathbf{n}_k, \qquad k = 1, \ldots, K$$

$$\mathcal{H}_0 : \mathbf{y}_k = \beta_k \mathbf{x} + \mathbf{n}_k \qquad k = 1, \ldots, K$$

- Unknown parameters: $\mathbf{x}$, $\boldsymbol{\beta} = [\beta_1, \ldots, \beta_K]^T, \boldsymbol{\alpha} = [\alpha_1, \ldots, \alpha_K]^T$, and channel noise η (detection is performed on each delay-Doppler bin one by one with known delay and Doppler)

GLRT

- Consider the GLRT for the detection problem:

$$\frac{\max_{\{\boldsymbol{\alpha},\boldsymbol{\beta},\mathbf{x},\eta\}} p(\mathbf{Y}|\boldsymbol{\alpha},\boldsymbol{\beta},\mathbf{x},\eta)}{\max_{\{\boldsymbol{\beta},\mathbf{x},\eta\}} p(\mathbf{Y}|\boldsymbol{\beta},\mathbf{x},\eta)} \underset{\mathcal{H}_0}{\overset{\mathcal{H}_1}{\gtrless}} \zeta$$

$$p(\mathbf{Y}|\boldsymbol{\alpha},\boldsymbol{\beta},\mathbf{x},\eta) = \frac{1}{(\pi\eta)^{KM}} \exp\left\{ -\frac{1}{\eta} \sum_{k=1}^{K} \|\mathbf{y}_k - \beta_k \mathbf{x} - \alpha_k \mathcal{D}_k \mathbf{x}\|^2 \right\}$$

$$p(\mathbf{Y}|\boldsymbol{\beta},\mathbf{x},\eta) = p(\mathbf{Y}|\boldsymbol{\alpha}=\mathbf{0},\boldsymbol{\beta},\mathbf{x},\eta)$$

- GLRT requires the maximum likelihood estimates (MLEs) of the unknown parameters
- The estimation of the IO waveform $\mathbf{x}$ under $\mathcal{H}_1$ and $\mathcal{H}_0$ hypotheses is most critical
  - There is a multiplicative ambiguity among the amplitudes parameters $\{\boldsymbol{\alpha},\boldsymbol{\beta}\}$ and the IO waveform $\mathbf{x}$
  - To resolve the ambiguity, we can impose a constraint $\|\mathbf{x}\| = 1$, which does not affect the GLRT

X. Zhang, H. Li, and B. Himed, "A direct-path interference resistant passive detector," *IEEE Signal Processing Letters*, vol.24, no.6, pp.818-822, Jun. 2017

Iterative Algorithm for IO Waveform Estimation

- It can be shown under under $\mathcal{H}_1$,

$$\boxed{\hat{\mathbf{x}} = \arg\max_{\|\mathbf{x}\|=1} \mathbf{x}^H \boldsymbol{\Theta}(\mathbf{x})\mathbf{x}}$$

$$\boldsymbol{\Theta}(\mathbf{x}) = \sum_{k=1}^{K} \left(\omega_{1,k}\mathcal{D}_k^H \mathbf{y}_k \mathbf{y}_k^H \mathcal{D}_k + \omega_{1,k}\mathbf{y}_k\mathbf{y}_k^H + \omega_{2,k}^* \mathcal{D}_k^H \mathbf{y}_k \mathbf{y}_k^H + \omega_{2,k}\mathbf{y}_k\mathbf{y}_k^H \mathcal{D}_k\right)$$

$$\omega_{1,k}(\mathbf{x}) = \frac{1}{1 - |\mathbf{x}^H \mathcal{D}_k \mathbf{x}|^2}, \quad \omega_{2,k}(\mathbf{x}) = \frac{-\mathbf{x}^H \mathcal{D}_k^H \mathbf{x}}{1 - |\mathbf{x}^H \mathcal{D}_k \mathbf{x}|^2}$$

- If the dependence of $\boldsymbol{\Theta}(\mathbf{x})$ on $\mathbf{x}$ is neglected, the cost function is maximized by the principal eigenvector. This leads to an iterative algorithm

Algorithm 1 Proposed Approach

Initialization: $l = 0$ and $\mathbf{x}^{(0)} = \sum_{k=1}^{K} \mathbf{y}_k / \| \sum_{k=1}^{K} \mathbf{y}_k \|$.

for $l = 0, 1, 2, \ldots$ **do**

1) Compute $\boldsymbol{\Theta}^{(l)}$ by substituting $\mathbf{x}^{(l)}$ into $\boldsymbol{\Theta}(\mathbf{x})$.
2) $\mathbf{x}^{(l+1)} = \arg\max_{\|\mathbf{x}\|=1} \mathbf{x}^H \boldsymbol{\Theta}^{(l)} \mathbf{x}$, i.e., the principal eigenvector of $\boldsymbol{\Theta}^{(l)}$, and $\gamma^{(l+1)}$ is the corresponding principal eigenvalue.
3) Check convergence.

end for

GLRT

- Let γ denote the final update of the principal eigenvector. The noise power estimate under $\mathcal{H}_1$ is given by

$$\hat{\eta}_1 = \frac{1}{MK}\sum_{k=1}^{K}(\|\mathbf{y}_k\|^2 - \gamma)$$

- Under $\mathcal{H}_0$, the MLEs of the IO waveform and noise power are

$$\hat{\mathbf{x}} = \arg\max_{\|\mathbf{x}\|=1} \mathbf{x}^H\mathbf{Y}\mathbf{Y}^H\mathbf{x} = \text{princpal e-vector}\{\mathbf{Y}\mathbf{Y}^H\}$$

$$\hat{\eta}_0 = \frac{1}{MK}\sum_{k=1}^{K}(\|\mathbf{y}_k\|^2 - \lambda_1)$$

- GLRT test statistic is given by $\hat{\eta}_0/\hat{\eta}_1$, which can be equivalently written as

$$\boxed{\frac{1}{\frac{1}{MK}\sum_{k=2}^{K}\lambda_k}\left(\gamma - \lambda_1\right) \underset{\mathcal{H}_0}{\overset{\mathcal{H}_1}{\gtrless}} \bar{\xi}}$$

  - Denominator is the MLE of the noise power under $\mathcal{H}_0$
  - Numerator is the difference of two principal eigenvalues obtained under $\mathcal{H}_1$ and $\mathcal{H}_0$, respectively

Clairvoyant MF Detector

- For comparison, consider a clairvoyant matched filter (MF) in the presence of DPI, which assumes knowledge of the IO waveform $\mathbf{x}$
- Derivation of clairvoyant MF follows similar steps in GLRT except that the estimation of $\mathbf{x}$ is no longer needed
- The MLE of the noise power under $\mathcal{H}_1$ is

$$\widehat{\eta}_{\text{MF},1} = \frac{1}{MK}\Big(\sum_{k=1}^{K} \|\mathbf{y}_k\|^2 - \sum_{k=1}^{K} \mathbf{y}_k^H \mathbf{P}_k \mathbf{y}_k\Big)$$

- The MLE of the noise power under $\mathcal{H}_0$ is

$$\widehat{\eta}_{\text{MF},0} = \frac{1}{MK}\Big(\sum_{k=1}^{K} \|\mathbf{y}_k\|^2 - \frac{\mathbf{x}^H \mathbf{Y}\mathbf{Y}^H \mathbf{x}}{\mathbf{x}^H \mathbf{x}}\Big)$$

- The test variable of the clairvoyant MF is the ratio of the two noise power estimates:

$$\mathcal{L}_{\text{MF}} = \frac{\widehat{\eta}_{\text{MF},0}}{\widehat{\eta}_{\text{MF},1}}$$

Numerical Results

- The GLRT detector is compared with the clairvoyant MF and two other detectors
- LAM (Largest-to-Arithmetic mean) detector [Liu et al.'14] which neglects the presence of DPI. The test variable is given by

$$\mathcal{L}_{\mathrm{LAM}} = \frac{K\lambda_1}{\sum_{k=1}^{K} \lambda_k}$$

- Modified generalized canonical correlation (mGCC)
  - Extends the original GCC [Bialkowski et al.'11] with DPI cancellation
  - It first obtains an estimate of the DPI, which is subtracted from the observed signal
  - The residual is then input into the original GCC detector, which computes the principal eigenvalue of the Gram matrix as test variable

J. Liu, H. Li, and B. Himed, "Two target detection algorithms for passive multistatic radar," *IEEE Trans. Signal Processing*, vol.62, no.22, pp.5930-5939, Nov. 2014

K.S. Bialkowski, I.V.L. Clarkson, and S.D. Howard, "Generalized canonical correlation for passive multistatic radar detection," in *Proc. IEEE Statist. Signal Process. Workshop*, Jun. 2011

P_d versus SNR

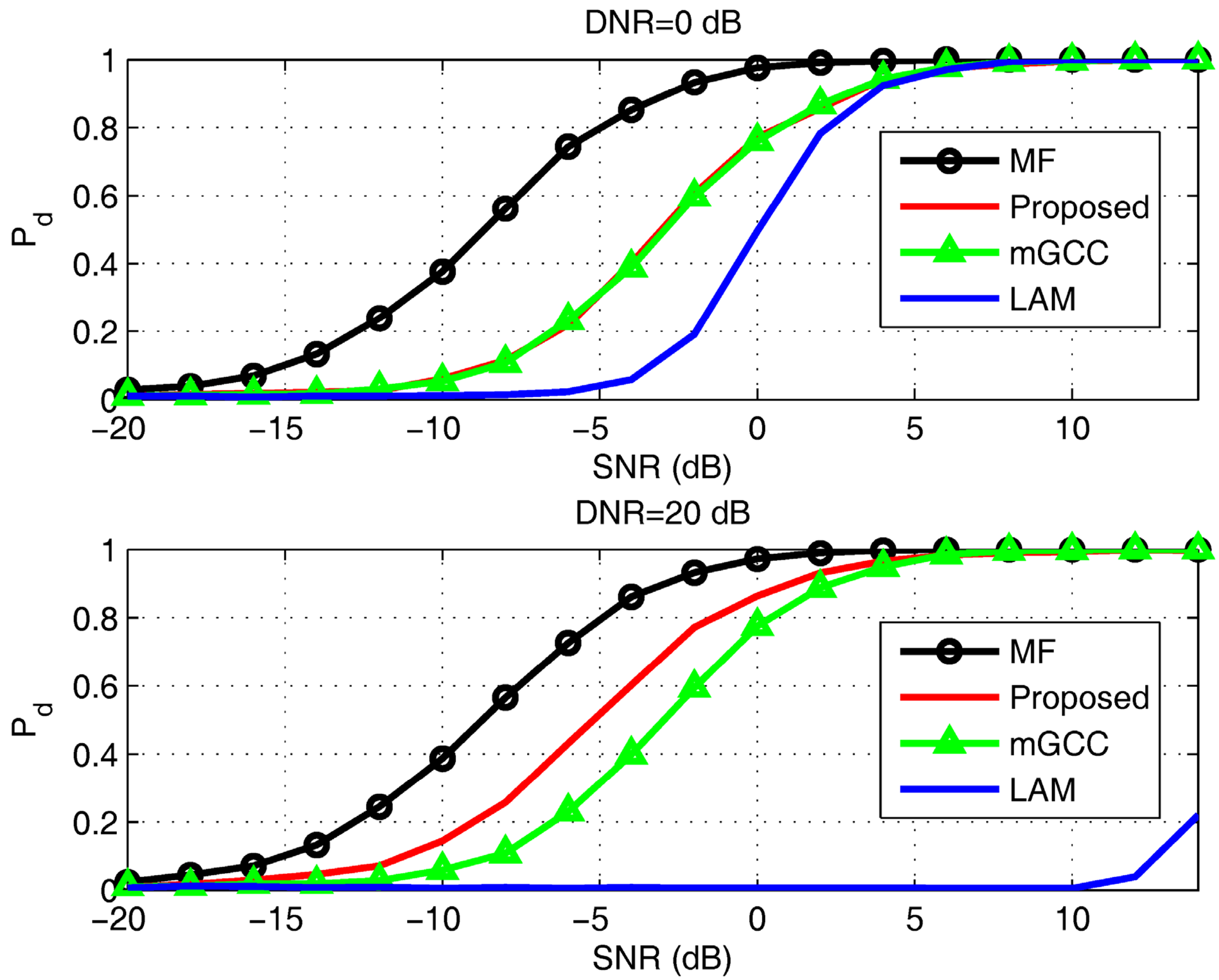

$$\mathrm{SNR} = \sum_{k=1}^{K} |\alpha_k|^2 / K\eta$$

$$\mathrm{DNR} = \sum_{k=1}^{K} |\alpha_k|^2 / K\eta$$

$M = 20, K = 3, P_f = 10^{-2}$

P_d versus DNR

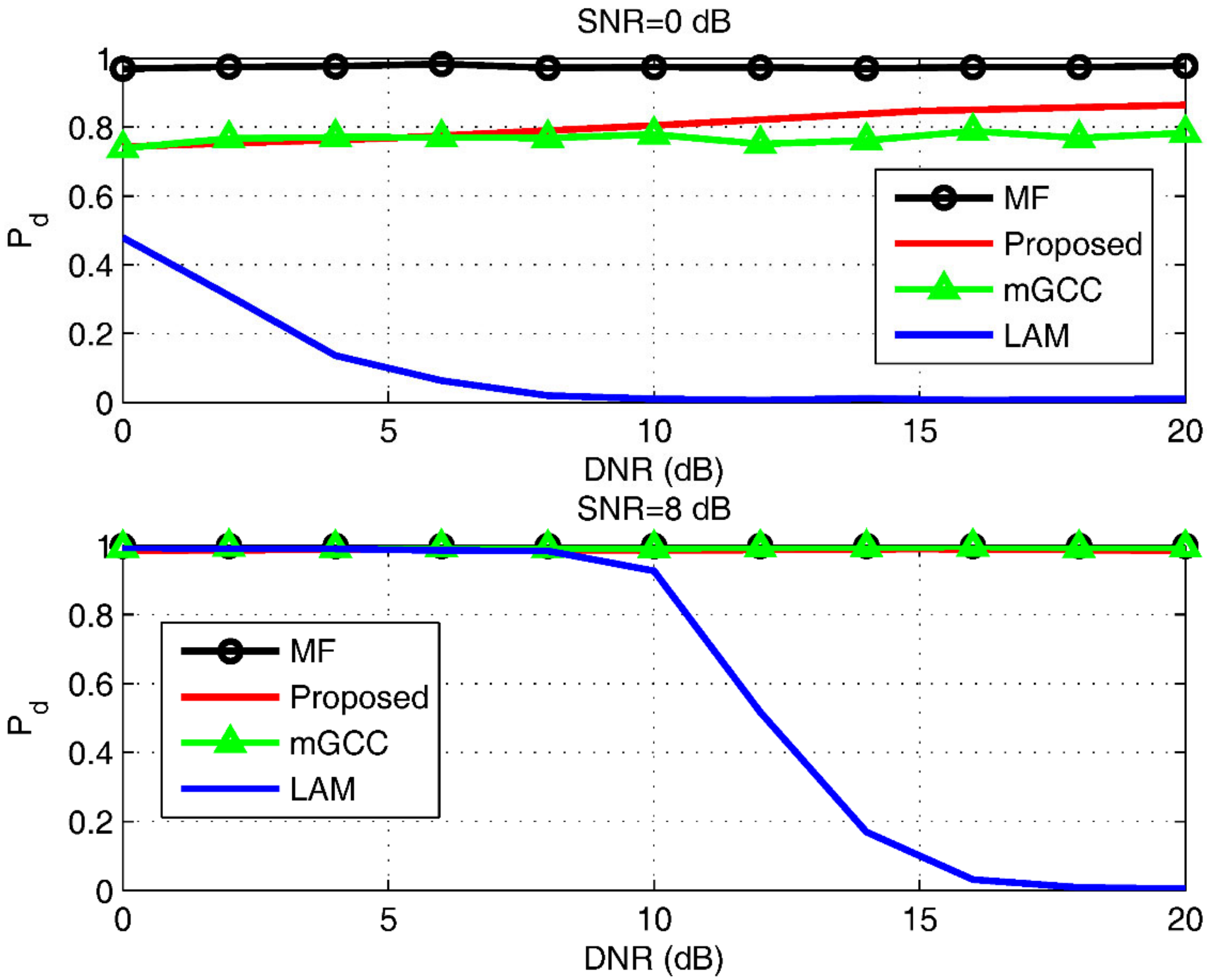

$$\text{SNR} = \sum_{k=1}^{K} |\alpha_k|^2 / K\eta$$

$$\text{DNR} = \sum_{k=1}^{K} |\alpha_k|^2 / K\eta$$

$M = 20, K = 3, P_f = 10^{-2}$

Remarks

- Examined the target detection problem for a multistatic passive radar in the presence of DPI
- Presented a GLRT detector by treating the IO waveform as a deterministic process
  - Utilized an iterative method for IO waveform estimation and DPI cancellation
- Also introduced a clairvoyant MF method as a benchmark
- Numerical results show the GLRT outperforms the mGCC and LAM detectors

Outline

- Cross-correlator in the presence of noisy reference and DPI
- Passive detection with noisy reference
- Passive detection with multiple receivers
  - Part I: No DPI
  - Part II: With DPI
- Exploit waveform correlation for passive detection and estimation
  - Part I: Joint delay-Doppler estimation
  - Part II: Multi-static detection with DPI
  - Part III: A parametric approach
- Summary

Motivation

- Limitations of prior art:
  - Conventional passive detection employs a two-step process: (1) interference cancellation; (2) detection assuming no interference
    - ✓ In practice, non-negligible residual DPI may still exist since DPI is much stronger than target echo (by many 10s to even over 100 dB)
  - Most existing methods treat the IO signal as an unknown deterministic or stochastic process with uncorrelated samples
    - ✓ It is more challenging to obtain accurate IO waveform estimate under above assumption
    - ✓ In practice, IO waveform often exhibits some temporal correlation
- Main contributions:
  - New passive esitmators and detectors in the presence of non-negligible residual DPI
  - Exploiting waveform correlation to improve sensing performance

Problem Formulation

- RC observation: $y_r'(t) = \gamma x'(t - t_r) + n_r'(t)$
- SC observation:

$$y_s'(t) = \beta' x'(t - t_r) + \alpha' x'(t - t_s) e^{j2\pi f_d t} + n_s'(t)$$

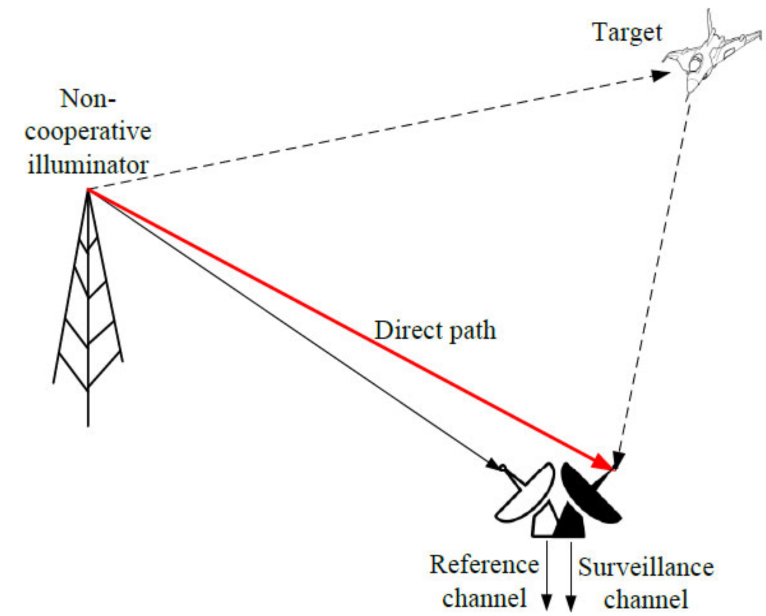

- Above equations can be written as

$$y_r(t) = x(t) + n_r(t)$$
$$y_s(t) = \beta x(t) + \alpha x(t - \tau) e^{j2\pi f_d t} + n_s(t)$$
$$x(t) = \gamma x'(t), \quad \beta = \beta'/\gamma, \quad \alpha = \alpha' e^{j2\pi f_d t_r}/\gamma$$
$$\tau = t_s - t_r \quad \text{(bistatic delay)}$$

- Suppose $x(t)$ has a duration of T seconds, observation interval $T_o \geq T + \tau_{\max}$, sampling frequency $f_s \geq 2(B + f_{D_{\max}})$, and M samples are collected for each channel
- Discrete-time model of received signals (in time domain):

$$\begin{cases} \bar{\mathbf{y}}_r = \bar{\mathbf{x}} + \bar{\mathbf{n}}_r \\ \bar{\mathbf{y}}_s = \beta \bar{\mathbf{x}} + \alpha \bar{\mathbf{x}}_d(\tau) \odot \bar{\mathbf{a}}(f_d) + \bar{\mathbf{n}}_s \end{cases}$$

Problem Formulation

- After M-point discrete Fourier transform (DFT), we have

$$\begin{cases} \mathbf{y}_r = \mathbf{x} + \mathbf{n}_r \\ \mathbf{y}_s = \beta\mathbf{x} + \alpha\mathbf{A}(f_d)\mathbf{W}(\tau)\mathbf{x} + \mathbf{n}_s \end{cases}$$

where $\mathbf{x} \sim \mathcal{CN}(\mathbf{0}, \mathbf{C}_x),\ \mathbf{n}_r \sim \mathcal{CN}(\mathbf{0}, \mathbf{C}_{nr}),\ \mathbf{n}_s \sim \mathcal{CN}(\mathbf{0}, \mathbf{C}_{ns})$

$$[\mathbf{A}(f_d)]_{p,q} = \frac{1}{\sqrt{M}} A((p-q)\Delta f),\ p, q = 1, 2, \ldots, M$$

$$A(m\Delta f) = \begin{cases} \sqrt{M}, & \text{if } m = \frac{f_d}{\Delta f} \\ \frac{1 - e^{j2\pi\left(\frac{f_d}{\Delta f} - m\right)}}{\sqrt{M}\left[1 - e^{j\frac{2\pi}{M}\left(\frac{f_d}{\Delta f} - m\right)}\right]}, & \text{otherwise} \end{cases}$$

circulant matrix containing Doppler information

$$[\mathbf{W}(\tau)]_{p,p} = e^{-j2\pi\Delta f(p-1)\tau},\ p = 1, 2, \ldots, M$$

diagonal matrix containing delay information

- The problem of interest is to jointly estimate the unknown parameters β, α, τ, and f_d from the observations

$$\mathbf{y} = [\mathbf{y}_r^T, \mathbf{y}_s^T]^T \sim \mathcal{CN}(\mathbf{0}, \mathbf{C}_y)$$

Maximum Likelihood Estimator

- Direct maximum likelihood estimation is computationally involved

$$\min_{\boldsymbol{\theta} \triangleq [\beta, \alpha, \tau, f_d]^T} \left[\mathbf{y}^H (\mathbf{C}_y)^{-1} \mathbf{y} + \ln \det(\mathbf{C}_y) \right]$$

where

$$\mathbf{C}_y = E\{\mathbf{y}\mathbf{y}^H\} = \begin{bmatrix} \mathbf{G} & \mathbf{B} \\ \mathbf{B}^H & \mathbf{D} \end{bmatrix}$$

$$\mathbf{G} = \mathbf{C}_x + \mathbf{C}_{nr}$$

$$\mathbf{B} = \beta^* \mathbf{C}_x + \alpha^* \mathbf{C}_x \mathbf{W}^H \mathbf{A}^H$$

$$\mathbf{D} = |\beta|^2 \mathbf{C}_x + \mathbf{C}_{ns} + |\alpha|^2 \mathbf{A}\mathbf{W}\mathbf{C}_x \mathbf{W}^H \mathbf{A}^H + \alpha^* \beta \mathbf{C}_x \mathbf{W}^H \mathbf{A}^H + \alpha \beta^* \mathbf{A}\mathbf{W}\mathbf{C}_x$$

- The cost function is highly non-linear. A brute force search over the multi-dimensional parameter space is computationally difficult
- We consider the expectation-maximization (EM) algorithm

EM Algorithm

- The hidden variables are the IO waveform samples $\mathbf{x}$
- "Complete" data: hidden variables + observed signals

$$\mathbf{z} = [\mathbf{x}^T, \mathbf{y}^T]^T$$

- In $(l+1)$-st iteration: $l = 0,1,2, \ldots$
  - E-step: $$Q\left(\boldsymbol{\theta}; \widehat{\boldsymbol{\theta}}^{(l)}\right) = E_{\mathbf{x}|\mathbf{y}, \widehat{\boldsymbol{\theta}}^{(l)}} \{\log p(\mathbf{z}|\boldsymbol{\theta})\}$$
  - M-step: $$\widehat{\boldsymbol{\theta}}^{(l+1)} = \arg\max_{\boldsymbol{\theta}} Q\left(\boldsymbol{\theta}; \widehat{\boldsymbol{\theta}}^{(l)}\right)$$

- E-step: computes the expectation of the log-likelihood function (LLF) of the "complete" data $\mathbf{z}$, taken with respect to the hidden variable $\mathbf{x}$
- M-step: maximize the expectation with respect to the unknown parameters
- Algorithm iterates between above E- and M-step until convergence

EM Estimator: E-Step

- Compute the MMSE estimate of the IO waveform and its associated covariance matrix

$$\hat{\mathbf{x}}^{(l)} = \mathbf{C}_{nr}\mathbf{G}^{-1}\mathbf{B}^{(l)}\mathbf{S}_G^{-1}\mathbf{y}_s + \mathbf{y}_r - \mathbf{C}_{nr}\mathbf{S}_D^{-1}\mathbf{y}_r$$

$$\mathbf{C}_{xx|y}^{(l)} = \hat{\mathbf{x}}^{(l)}\left(\hat{\mathbf{x}}^{(l)}\right)^H + \mathbf{C}_{nr} - \mathbf{C}_{nr}\mathbf{S}_D^{-1}\mathbf{C}_{nr}$$

where the *Schur complements* are

$$\mathbf{S}_G = \mathbf{D}^{(l)} - \left(\mathbf{B}^{(l)}\right)^H \mathbf{G}^{-1}\mathbf{B}^{(l)}, \quad \mathbf{S}_D = \mathbf{G} - \mathbf{B}^{(l)}\left(\mathbf{D}^{(l)}\right)^{-1}\left(\mathbf{B}^{(l)}\right)^H$$

- Update coefficients of the cost function used in M-step:

$$\boxed{Q_1\left(\boldsymbol{\theta}; \hat{\boldsymbol{\theta}}^{(l)}\right) = |\beta|^2 c_1^{(l)} + |\alpha|^2 c_2^{(l)}(\tau, f_d) + 2\Re\left\{\alpha\beta^* c_3^{(l)}(\tau, f_d) - \beta c_4^{(l)} - \alpha c_5^{(l)}(\tau, f_d)\right\}}$$

where

$$c_1^{(l)} = \mathrm{tr}\left\{\mathbf{C}_{ns}^{-1}\mathbf{C}_{xx|y}^{(l)}\right\}, \quad c_2^{(l)}(\tau, f_d) = \mathrm{tr}\left\{\mathbf{W}\mathbf{C}_{xx|y}^{(l)}\mathbf{W}^H\mathbf{A}^H\mathbf{C}_{ns}^{-1}\mathbf{A}\right\}$$

$$c_3^{(l)}(\tau, f_d) = \mathrm{tr}\left\{\mathbf{C}_{ns}^{-1}\mathbf{A}\mathbf{W}\mathbf{C}_{xx|y}^{(l)}\right\}, \quad c_4^{(l)} = \mathbf{y}_s^H\mathbf{C}_{ns}^{-1}\hat{\mathbf{x}}^{(l)}, \quad c_5^{(l)}(\tau, f_d) = \mathbf{y}_s^H\mathbf{C}_{ns}^{-1}\mathbf{A}\mathbf{W}\hat{\mathbf{x}}^{(l)}$$

X. Zhang, H. Li, J. Liu, and B. Himed, "Joint delay and Doppler estimation for passive sensing with direct-path interference," *IEEE Trans. Signal Processing*, vol.64, no.3, pp.630-640, Feb. 2016

EM Estimator: M-Step

- In M-step, we need to solve the following optimization problem

$$\widehat{\boldsymbol{\theta}}^{(l+1)} = \arg\min_{\boldsymbol{\theta}} Q_1\left(\boldsymbol{\theta}; \widehat{\boldsymbol{\theta}}^{(l)}\right)$$

- Using person-by-person optimization,

$$\widehat{\tau}^{(l+1)} = \arg\min_{\tau} Q_1\left(\tau, \widehat{f}_d^{(l)}, \widehat{\alpha}^{(l)}, \widehat{\beta}^{(l)}; \widehat{\boldsymbol{\theta}}^{(l)}\right)$$

$$\widehat{f}_d^{(l+1)} = \arg\min_{f_d} Q_1\left(\widehat{\tau}^{(l+1)}, f_d, \widehat{\alpha}^{(l)}, \widehat{\beta}^{(l)}; \widehat{\boldsymbol{\theta}}^{(l)}\right)$$

$$\left\{\widehat{\alpha}^{(l+1)}, \widehat{\beta}^{(l+1)}\right\} = \arg\min_{\alpha,\beta} Q_1\left(\widehat{\tau}^{(l+1)}, \widehat{f}_d^{(l+1)}, \alpha, \beta; \widehat{\boldsymbol{\theta}}^{(l)}\right)$$

- For the first two problems, the estimates can be obtained by using Newton's method. The 3rd problem has a closed-form solution

$$\widehat{\alpha}^{(l+1)} = \frac{\left(\left(c_1^{(l)}\right)^* c_5^{(l)} - c_3^{(l)} c_4^{(l)}\right)^*}{c_1^{(l)} c_2^{(l)} - \left|c_3^{(l)}\right|^2}, \quad \widehat{\beta}^{(l+1)} = \frac{c_2^{(l)}\left(c_4^{(l)}\right)^* - c_3^{(l)}\left(c_5^{(l)}\right)^*}{c_1^{(l)} c_2^{(l)} - \left|c_3^{(l)}\right|^2}$$

Numerical Results

- We compare the following estimators:
  - EM estimator
  - Cross-correlation (CC) method
  - Modified CC (MCC) method: coarse DPI cancellation + CC
- Cramér–Rao lower bound (CRLB) is employed to benchmark the performance of the estimators
- For delay and Doppler frequency estimation, we use Monte Carlo simulations to measure the mean-square errors (MSEs); for amplitude estimation, we use the normalized standard deviation (NSD)

$$\mathrm{MSE}_{\tau} = E\{|\hat{\tau} - \tau|^2\}$$

$$\mathrm{MSE}_{f} = M^2 E\{|\hat{f}_d - f_d|^2\}$$

$$\mathrm{NSD}_{\alpha} = \left(\sqrt{E\left\{|\hat{\alpha} - \alpha|^2\right\}} / |\alpha|\right) \times 100\%$$

$SNR_r = 0$ dB, $DNR_s = 10$ dB

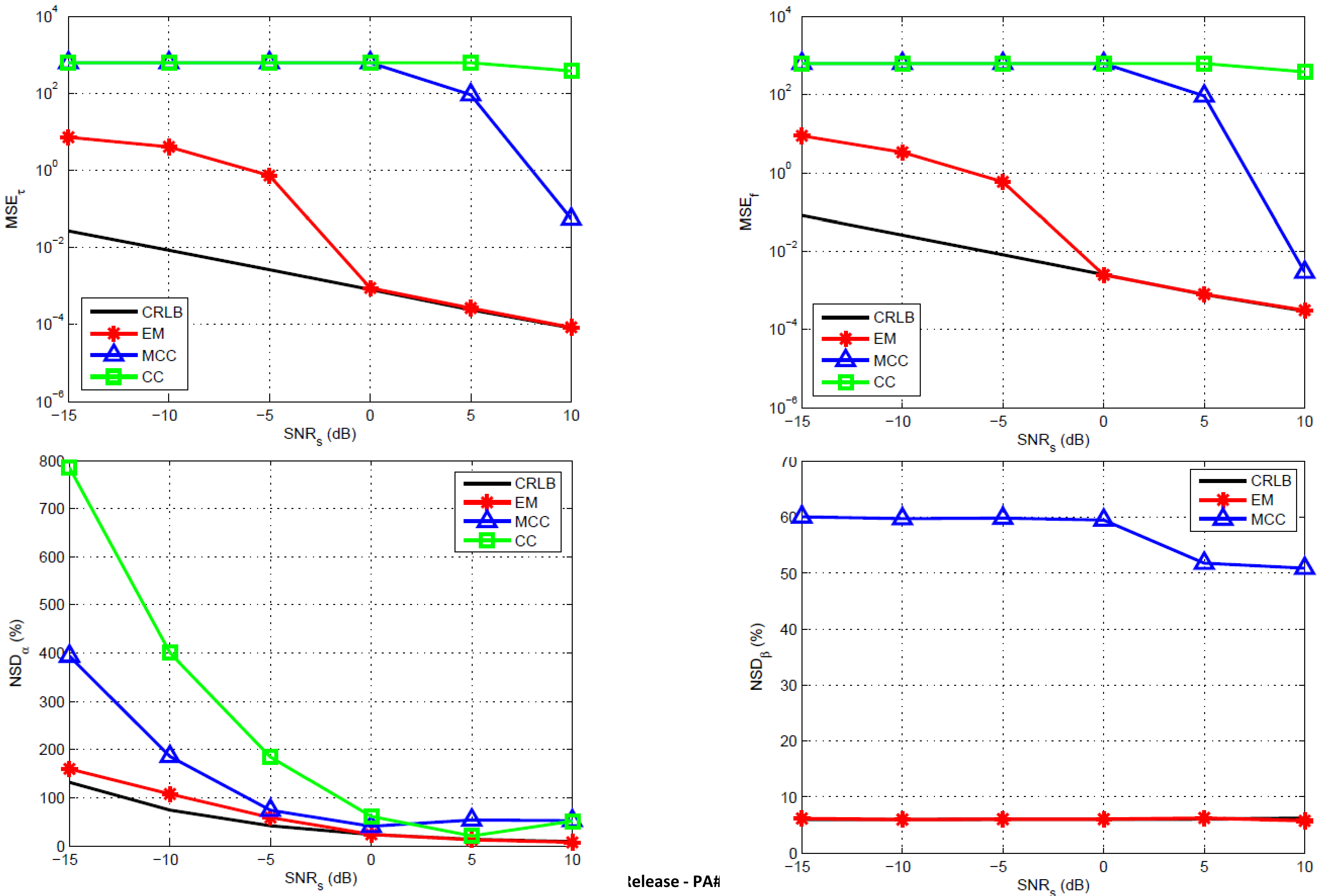

$SNR_r = 30$ dB, $DNR_s = -20$ dB

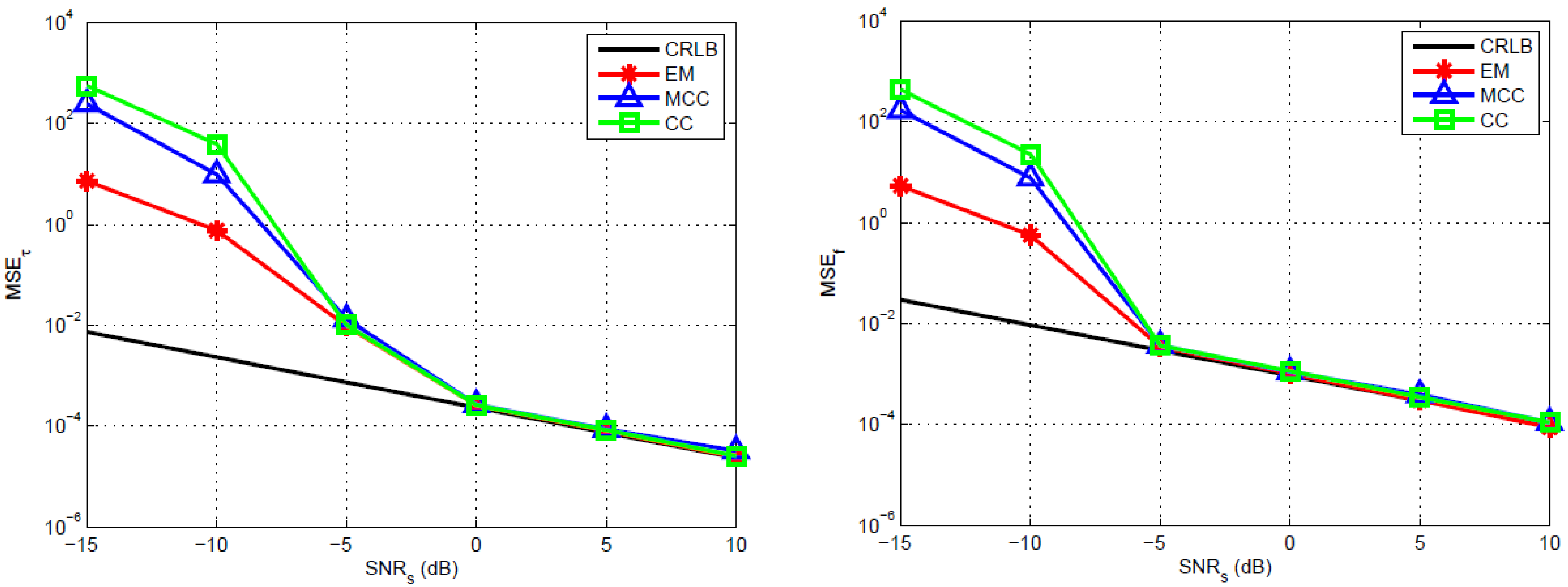

$SNR_s = 0$ dB, $DNR_s = 10$ dB

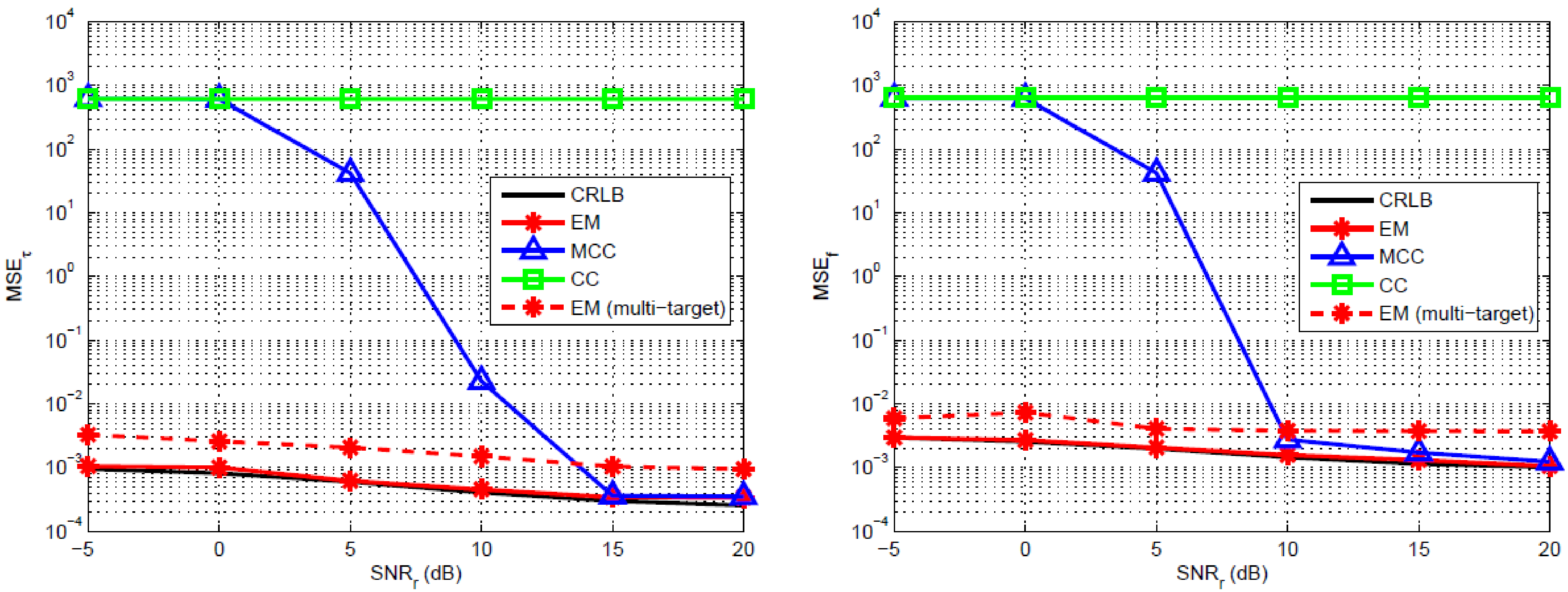

$SNR_r = 5$ dB, $SNR_s = 0$ dB

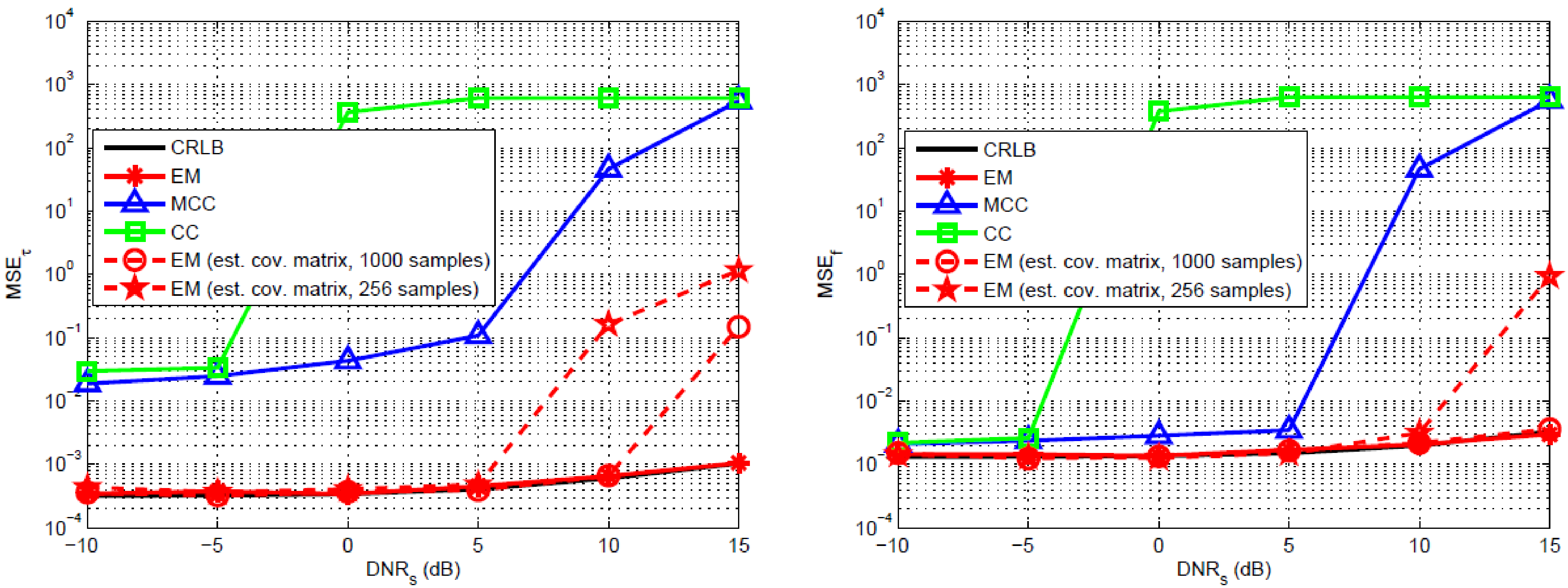

Remarks

- Examined the joint delay-Doppler estimation problem for passive radar with noisy reference and direct-path interference (DPI)
- Delay and Doppler were treated as continuous parameters with no discretization
- Proposed an expectation maximization (EM) based and a modified cross-correlation (MCC) estimators by exploiting the correlation of the IO waveform
  - EM significantly outperforms MCC and CC
  - MCC is computationally more efficient than EM and outperforms CC, due to DPI cancellation
  - EM achieves the CRLB as SNR_s increases
  - MCC and CC are more sensitive to the noise in the RC and DPI

Outline

- Cross-correlator in the presence of noisy reference and DPI
- Passive detection with noisy reference
- Passive detection with multiple receivers
  - Part I: No DPI
  - Part II: With DPI
- Exploit waveform correlation for passive detection and estimation
  - Part I: Joint delay-Doppler estimation
  - Part II: Multi-static detection with DPI
  - Part III: A parametric approach
- Summary

Signal Model

- The k-th channel observation is

$$y_k(t) = \beta_k x(t) + \alpha_k x(t-\tau_k) e^{\jmath 2\pi f_k t} + n_k(t)$$
$$k = 1, \ldots, K$$

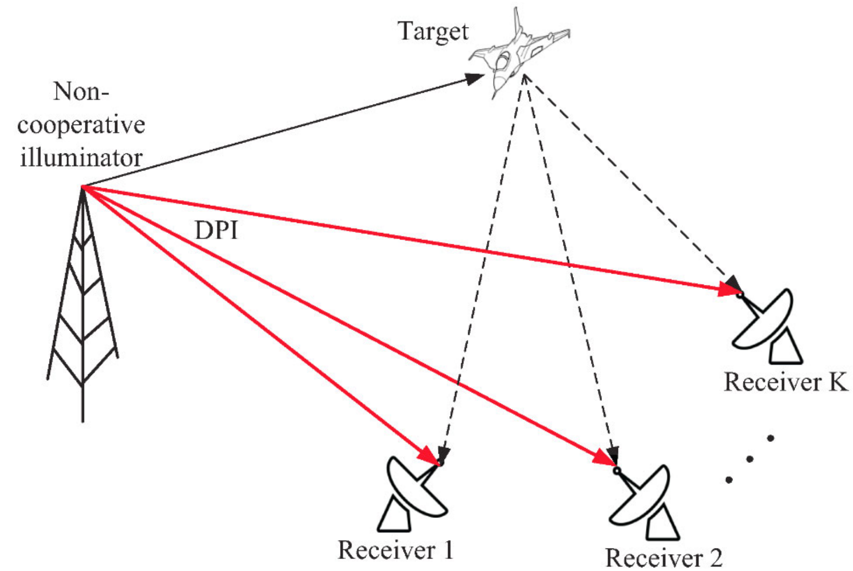

- The discrete-time model is

$$\bar{\mathbf{y}}_k = \beta_k \bar{\mathbf{x}} + \alpha_k \bar{\mathbf{x}}_d(\tau_k) \odot \bar{\mathbf{a}}(f_k) + \bar{\mathbf{n}}_k$$

where

$$\bar{\mathbf{x}} \sim \mathcal{CN}(\mathbf{0}, \mathbf{R}_x), \quad \bar{\mathbf{n}}_k \sim \mathcal{CN}(\mathbf{0}, \eta_k \mathbf{I}_M)$$
$$\bar{\mathbf{x}}_d(\tau_k) = [x(0-\tau_k), x(T_s-\tau_k), \ldots, x((M-1)T_s-\tau_k)]^T$$
$$\bar{\mathbf{a}}(f_k) = [1, e^{\jmath 2\pi f_k T_s}, \ldots, e^{\jmath 2\pi f_k (M-1) T_s}]^T$$

- After M-point DFT, the frequency-domain signals are

$$\mathbf{y}_k = \beta_k \mathbf{x} + \alpha_k \mathbf{A}(f_k)\mathbf{W}(\tau_k)\mathbf{x} + \mathbf{n}_k$$
$$\mathbf{x} \sim \mathcal{CN}(\mathbf{0}, \mathbf{C}_x) \text{ and } \mathbf{n}_k \sim \mathcal{CN}(\mathbf{0}, \eta_k \mathbf{I}_M)$$

The Problem

- The composite binary hypothesis test is given by

$$\begin{aligned} \mathcal{H}_1 : \mathbf{y}_k &= \beta_k \mathbf{x} + \alpha_k \mathcal{D}_k \mathbf{x} + \mathbf{n}_k \\ \mathcal{H}_0 : \mathbf{y}_k &= \beta_k \mathbf{x} + \mathbf{n}_k, \qquad\qquad k = 1, 2, \ldots, K, \end{aligned}$$

where the delay-Doppler operator (unitary matrix) associated with the k-th channel

$$\mathcal{D}_k = \mathbf{A}(f_k)\mathbf{W}(\tau_k)$$

- Two algorithms are developed in the following, depending on whether the noise powers η_k are known or unknown
  - Delay and Doppler are assumed known, as detection is performed in each range/Doppler cell
  - Joint delay/Doppler estimation was examined

X. Zhang, H. Li, and B. Himed, "Multistatic detection for passive radar with direct-path interference," *IEEE Trans. Aerospace and Electronic Systems*, vol.53, no.2, pp.915-925, Apr. 2017

GLRT with Known Noise Power

- In this case, the problem becomes

$$\mathcal{H}_1 : \mathbf{y} \sim \mathcal{CN}(\mathbf{0}_{MK\times 1}, \mathbf{C}_y(\boldsymbol{\alpha}, \boldsymbol{\beta}))$$
$$\mathcal{H}_0 : \mathbf{y} \sim \mathcal{CN}(\mathbf{0}_{MK\times 1}, \mathbf{C}_y(\boldsymbol{\alpha} = \mathbf{0}, \boldsymbol{\beta}))$$

$$\mathbf{y} = [\mathbf{y}_1^T, \mathbf{y}_2^T, \ldots, \mathbf{y}_K^T]^T, \quad \boldsymbol{\beta} = [\beta_1, \beta_2, \ldots, \beta_K]^T, \quad \boldsymbol{\alpha} = [\alpha_1, \alpha_2, \ldots, \alpha_K]^T$$
$$\mathbf{C}_y(\boldsymbol{\alpha}, \boldsymbol{\beta}) = [(\boldsymbol{\beta}\boldsymbol{\alpha}^H) \otimes \mathbf{C}_x]\mathbf{D}^H + \mathbf{D}[(\boldsymbol{\alpha}\boldsymbol{\beta}^H) \otimes \mathbf{C}_x] + \mathbf{D}[(\boldsymbol{\alpha}\boldsymbol{\alpha}^H) \otimes \mathbf{C}_x]\mathbf{D}^H + (\boldsymbol{\beta}\boldsymbol{\beta}^H) \otimes \mathbf{C}_x + \mathbf{C}_n$$
$$\mathbf{C}_n = \text{diag}\{\boldsymbol{\eta}\} \otimes \mathbf{I}_M, \quad \boldsymbol{\eta} = [\eta_1, \eta_2, \ldots, \eta_K]^T, \quad \mathbf{D} = \text{diag}\{\mathcal{D}_1, \mathcal{D}_2 \ldots, \mathcal{D}_K\}$$

- The GLRT is given by

$$\frac{\max_{\{\boldsymbol{\alpha},\boldsymbol{\beta}\}} p_1(\mathbf{y}|\boldsymbol{\alpha}, \boldsymbol{\beta})}{\max_{\{\boldsymbol{\beta}\}} p_0(\mathbf{y}|\boldsymbol{\beta})} \underset{\mathcal{H}_0}{\overset{\mathcal{H}_1}{\gtrless}} \gamma$$

- Directly maximizing the likelihood functions is computationally difficult. The EM estimator is employed instead for parameter estimation

GLRT with Known Noise Power

- Consider the expectation-maximization (EM) algorithm to obtain parameter estimates
- "Complete" data: $\mathbf{z} = [\mathbf{x}^T, \mathbf{y}^T]^T$
- Expectation Step (E-step):

$$Q\left(\boldsymbol{\theta}; \hat{\boldsymbol{\theta}}^{(l)}\right) = E_{\mathbf{x}|\mathbf{y},\hat{\boldsymbol{\theta}}^{(l)}}\{\log p(\mathbf{z}|\boldsymbol{\theta})\}$$

$$\log p(\mathbf{z}|\boldsymbol{\theta}) = \log p(\mathbf{y}|\mathbf{x}, \boldsymbol{\theta}) p(\mathbf{x}|\boldsymbol{\theta})$$

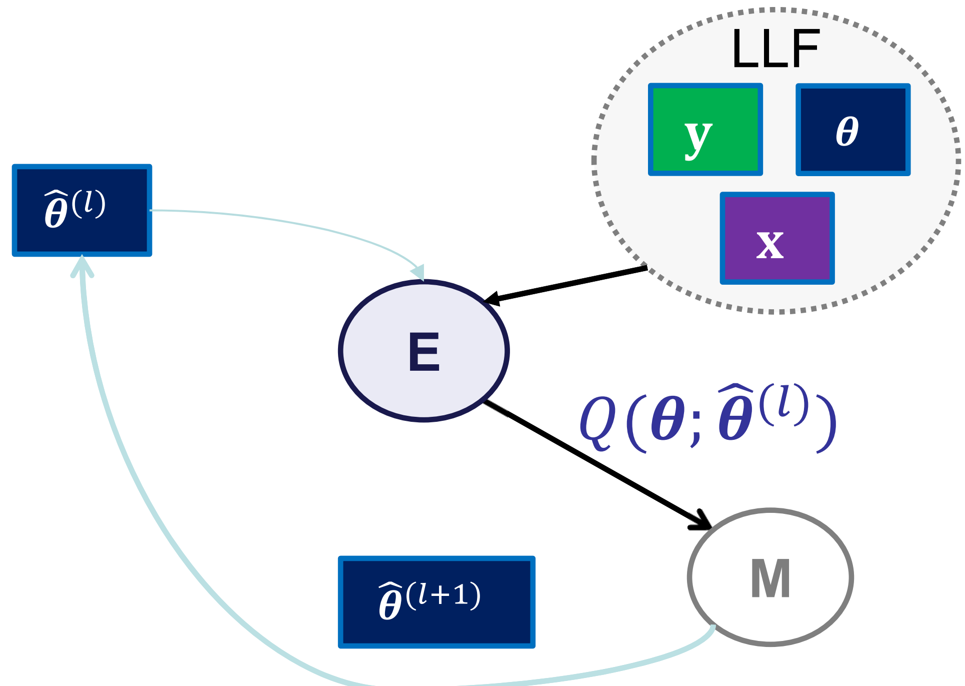

- Maximization Step (M-step):

$$\hat{\boldsymbol{\theta}}^{(l+1)} = \arg\max_{\boldsymbol{\theta}} Q\left(\boldsymbol{\theta}; \hat{\boldsymbol{\theta}}^{(l)}\right)$$

- The unknown parameters $\boldsymbol{\theta} = \{\boldsymbol{\alpha}, \boldsymbol{\beta}\}$ under H_1, and $\boldsymbol{\theta} = \boldsymbol{\beta}$ under H_0
- The EM algorithm starts with an initial "guess" of the unknown parameters $\hat{\boldsymbol{\theta}}^{(0)}$ and stops until the convergence is achieved

GLRT with Known Noise Power

- Test variable (GLRT$_1$)

$$\mathcal{L}_1 = \mathbf{y}^H\left[\mathbf{C}_y^{-1}(0,\widehat{\beta}_0) - \mathbf{C}_y^{-1}(\widehat{\alpha}_1,\widehat{\beta}_1)\right]\mathbf{y} + \ln \frac{\det\left\{\mathbf{C}_y(0,\widehat{\beta}_0)\right\}}{\det\left\{\mathbf{C}_y(\widehat{\alpha}_1,\widehat{\beta}_1)\right\}} \underset{\mathcal{H}_0}{\overset{\mathcal{H}_1}{\gtrless}} \xi$$

parameter estimation under H_0

$$\widehat{\beta}_k^{(l+1)} = \frac{1}{c_1^{(l)}}\left(c_{3,k}^{(l)}\right)^*$$

M

parameter estimation under H_1

$$\widehat{\alpha}_k^{(l+1)} = \frac{\left(c_1^{(l)}c_{4,k}^{(l)} - c_{2,k}^{(l)}c_{3,k}^{(l)}\right)^*}{\left(c_1^{(l)}\right)^2 - \left|c_{2,k}^{(l)}\right|^2} \quad \widehat{\beta}_k^{(l+1)} = \frac{c_1^{(l)}\left(c_{3,k}^{(l)}\right)^* - c_{2,k}^{(l)}\left(c_{4,k}^{(l)}\right)^*}{\left(c_1^{(l)}\right)^2 - \left|c_{2,k}^{(l)}\right|^2}$$

$$c_1^{(l)} = \mathrm{tr}\left\{\mathbf{C}_{xx|y}^{(l)}\right\}, \quad c_{2,k}^{(l)} = \mathrm{tr}\left\{\mathcal{D}_k\mathbf{C}_{xx|y}^{(l)}\right\}, \quad c_{3,k}^{(l)} = \mathbf{y}_k^H\widehat{\mathbf{x}}^{(l)}, \quad c_{4,k}^{(l)} = \mathbf{y}_k^H\mathcal{D}_k\widehat{\mathbf{x}}^{(l)}$$

E

$$\widehat{\mathbf{x}}^{(l)} = \mathbf{C}_{xy}^{(l)}\left(\mathbf{C}_{yy}^{(l)}\right)^{-1}\mathbf{y}, \quad \mathbf{C}_{xx|y}^{(l)} = \widehat{\mathbf{x}}^{(l)}\left(\widehat{\mathbf{x}}^{(l)}\right)^H + \mathbf{C}_x - \mathbf{C}_{xy}^{(l)}\left(\mathbf{C}_{yy}^{(l)}\right)^{-1}\left(\mathbf{C}_{xy}^{(l)}\right)^H$$

$$\mathbf{C}_{xy}^{(l)} = \left(\widehat{\beta}^{(l)}\right)^H \otimes \mathbf{C}_x + \mathbf{C}_x\left(\widehat{\alpha}^{(l)} \otimes \mathbf{I}_M\right)^H\mathbf{D}^H, \quad \mathbf{C}_{yy}^{(l)} = \mathbf{C}_y(\widehat{\alpha}^{(l)},\widehat{\beta}^{(l)})$$

= 0 under H_0 = 0 under H_0

GLRT with Unknown Noise Power

- In this case, the channel noise powers are unknown and may be different from one channel to another:

$$\mathcal{H}_1 : \mathbf{y} \sim \mathcal{CN}(\mathbf{0}_{MK\times 1}, \mathbf{C}_y(\boldsymbol{\alpha}, \boldsymbol{\beta}, \boldsymbol{\eta}))$$
$$\mathcal{H}_0 : \mathbf{y} \sim \mathcal{CN}(\mathbf{0}_{MK\times 1}, \mathbf{C}_y(\boldsymbol{\alpha} = \mathbf{0}, \boldsymbol{\beta}, \boldsymbol{\eta}))$$

$$\mathbf{C}_y(\boldsymbol{\alpha}, \boldsymbol{\beta}, \boldsymbol{\eta}) = [(\boldsymbol{\beta}\boldsymbol{\alpha}^H) \otimes \mathbf{C}_x]\mathbf{D}^H + \mathbf{D}[(\boldsymbol{\alpha}\boldsymbol{\beta}^H) \otimes \mathbf{C}_x] + \mathbf{D}[(\boldsymbol{\alpha}\boldsymbol{\alpha}^H) \otimes \mathbf{C}_x]\mathbf{D}^H + (\boldsymbol{\beta}\boldsymbol{\beta}^H) \otimes \mathbf{C}_x + \mathrm{diag}\{\boldsymbol{\eta}\} \otimes \mathbf{I}_M$$

- The GLRT is given by

$$\frac{\max_{\{\boldsymbol{\alpha},\boldsymbol{\beta},\boldsymbol{\eta}\}} p_1(\mathbf{y}|\boldsymbol{\alpha}, \boldsymbol{\beta}, \boldsymbol{\eta})}{\max_{\{\boldsymbol{\beta},\boldsymbol{\eta}\}} p_0(\mathbf{y}|\boldsymbol{\beta}, \boldsymbol{\eta})} \underset{\mathcal{H}_0}{\overset{\mathcal{H}_1}{\gtrless}} \zeta$$

- Again, we use the EM algorithm to develop the second GLRT detector

GLRT with Unknown Noise Power

- Test variable (GLRT_2)

$$\mathcal{L}_2 = \mathbf{y}^H \left[\mathbf{C}_y^{-1}(0, \hat{\beta}_0, \hat{\eta}_0) - \mathbf{C}_y^{-1}(\hat{\alpha}_1, \hat{\beta}_1, \hat{\eta}_1) \right] \mathbf{y} + \ln \frac{\det\left\{\mathbf{C}_y(0, \hat{\beta}_0, \hat{\eta}_0)\right\}}{\det\left\{\mathbf{C}_y(\hat{\alpha}_1, \hat{\beta}_1, \hat{\eta}_1)\right\}} \underset{\mathcal{H}_0}{\overset{\mathcal{H}_1}{\gtrless}} \kappa$$

parameter estimation under H_0

$$\hat{\beta}_k^{(l+1)} = \frac{1}{c_1^{(l)}} \left(c_{3,k}^{(l)}\right)^*$$

$$\hat{\eta}_k^{(l+1)} = \frac{1}{M} \hat{\Delta}^{(l)}\left(0, \hat{\beta}_k^{(l+1)}\right)$$

M

parameter estimation under H_1

$$\hat{\alpha}_k^{(l+1)} = \frac{\left(c_1^{(l)} c_{4,k}^{(l)} - c_{2,k}^{(l)} c_{3,k}^{(l)}\right)^*}{\left(c_1^{(l)}\right)^2 - \left|c_{2,k}^{(l)}\right|^2} \qquad \hat{\beta}_k^{(l+1)} = \frac{c_1^{(l)}\left(c_{3,k}^{(l)}\right)^* - c_{2,k}^{(l)}\left(c_{4,k}^{(l)}\right)^*}{\left(c_1^{(l)}\right)^2 - \left|c_{2,k}^{(l)}\right|^2}$$

$$\hat{\Delta}^{(l)}(\alpha_k, \beta_k) = \|\mathbf{y}_k\|^2 + \left(|\beta_k|^2 + |\alpha_k|^2\right) c_1^{(l)} + 2\Re\left\{\alpha_k \beta_k^* c_{2,k}^{(l)} - \beta_k c_{3,k}^{(l)} - \alpha_k c_{4,k}^{(l)}\right\}$$

$$\hat{\eta}_k^{(l+1)} = \frac{1}{M} \hat{\Delta}^{(l)}\left(\hat{\alpha}_k^{(l+1)}, \hat{\beta}_k^{(l+1)}\right)$$

$$c_1^{(l)} = \text{tr}\left\{\mathbf{C}_{xx|y}^{(l)}\right\}, \quad c_{2,k}^{(l)} = \text{tr}\left\{\mathcal{D}_k \mathbf{C}_{xx|y}^{(l)}\right\}, \quad c_{3,k}^{(l)} = \mathbf{y}_k^H \hat{\mathbf{x}}^{(l)}, \quad c_{4,k}^{(l)} = \mathbf{y}_k^H \mathcal{D}_k \hat{\mathbf{x}}^{(l)}$$

E

$$\hat{\mathbf{x}}^{(l)} = \mathbf{C}_{xy}^{(l)}\left(\mathbf{C}_{yy}^{(l)}\right)^{-1}\mathbf{y}, \quad \mathbf{C}_{xx|y}^{(l)} = \hat{\mathbf{x}}^{(l)}\left(\hat{\mathbf{x}}^{(l)}\right)^H + \mathbf{C}_x - \mathbf{C}_{xy}^{(l)}\left(\mathbf{C}_{yy}^{(l)}\right)^{-1}\left(\mathbf{C}_{xy}^{(l)}\right)^H$$

= 0 under H_0 = 0 under H_0

$$\mathbf{C}_{xy}^{(l)} = \left(\hat{\boldsymbol{\beta}}^{(l)}\right)^H \otimes \mathbf{C}_x + \mathbf{C}_x\left(\hat{\boldsymbol{\alpha}}^{(l)} \otimes \mathbf{I}_M\right)^H \mathbf{D}^H, \quad \mathbf{C}_{yy}^{(l)} = \mathbf{C}_y\left(\hat{\boldsymbol{\alpha}}^{(l)}, \hat{\boldsymbol{\beta}}^{(l)}, \hat{\boldsymbol{\eta}}^{(l)}\right)$$

Numerical Results

Let $\lambda_K(\cdot) \leq \lambda_{K-1}(\cdot) \leq \cdots \leq \lambda_2(\cdot) \leq \lambda_1(\cdot)$ denote the ordered eigenvalues of a K-dimensional matrix and

$$\mathbf{\Phi} = \mathbf{Y}^H \mathbf{Y}, \quad \mathbf{Y} = [\mathcal{D}_1^H \mathbf{y}_1, \mathcal{D}_2^H \mathbf{y}_2, \ldots, \mathcal{D}_K^H \mathbf{y}_K]$$

$$\mathcal{L}_{\mathsf{GCC}} = \lambda_1(\mathbf{\Phi})$$

GCC detector [Bialkowski et al. '11]

$$\mathcal{L}_{\mathsf{RLET}} = \frac{\lambda_1(\mathbf{\Phi})}{\sum_{k=1}^K \lambda_k(\mathbf{\Phi})}$$

RLET detector [Liu et al. '14]

$$\mathcal{L}_{\mathsf{ED}} = \sum_{k=1}^K \|\mathbf{y}_k\|^2$$

energy detector [Urkowitz '67]

$$\mathcal{L}_{\mathsf{GC}} = 1 - \frac{\det\{\mathbf{\Phi}\}}{\prod_{k=1}^K \|\mathbf{y}_k\|^2}$$

GC detector [Cochran et al. '95]

K. S. Bialkowski, I. V. L. Clarkson, and S. D. Howard, "Generalized canonical correlation for passive multistatic radar detection," IEEE SSP Workshop, 2011

J. Liu, H. Li, and B. Himed, "Two target detection algorithms for passive multistatic radar," *IEEE TSP*, 2014

H. Urkowitz, "Energy detection of unknown deterministic signals," *Proceedings of the IEEE*, 1967

D. Cochran, H. Gish, and D. Sinno, "A geometric approach to multichannel signal detection," *IEEE TSP*, 1995

Numerical Results

$M = 20, K = 3, \mathrm{DNR} = 0\ \mathrm{dB}, P_{FA} = 10^{-2}$

waveform with high correlation | waveform with low correlation

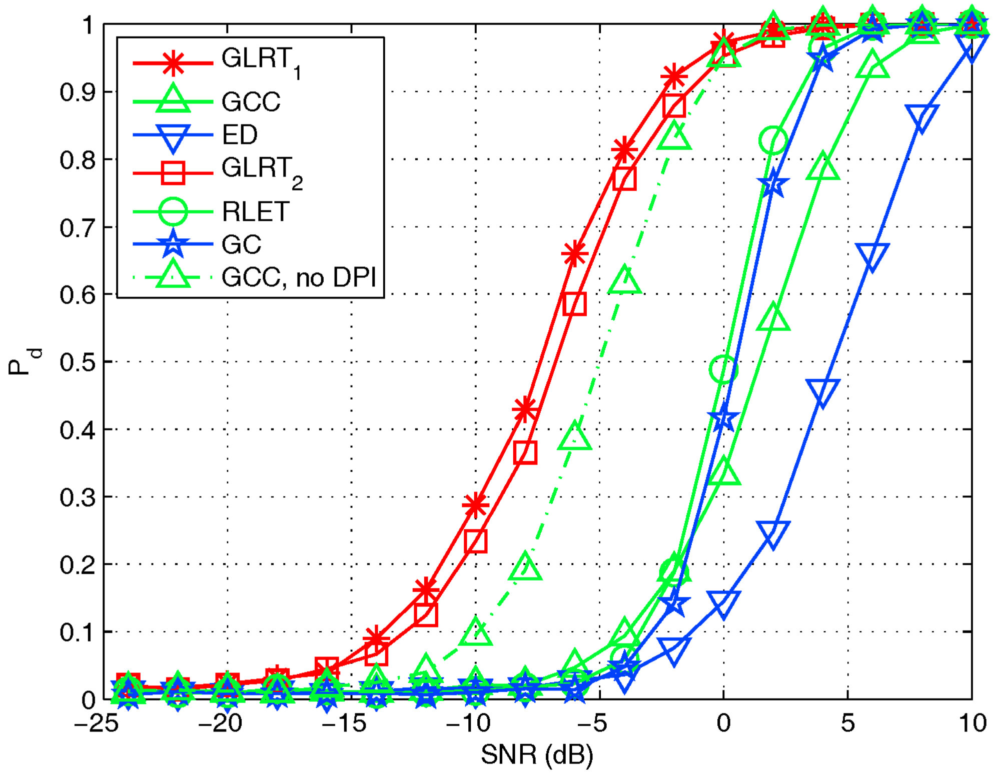

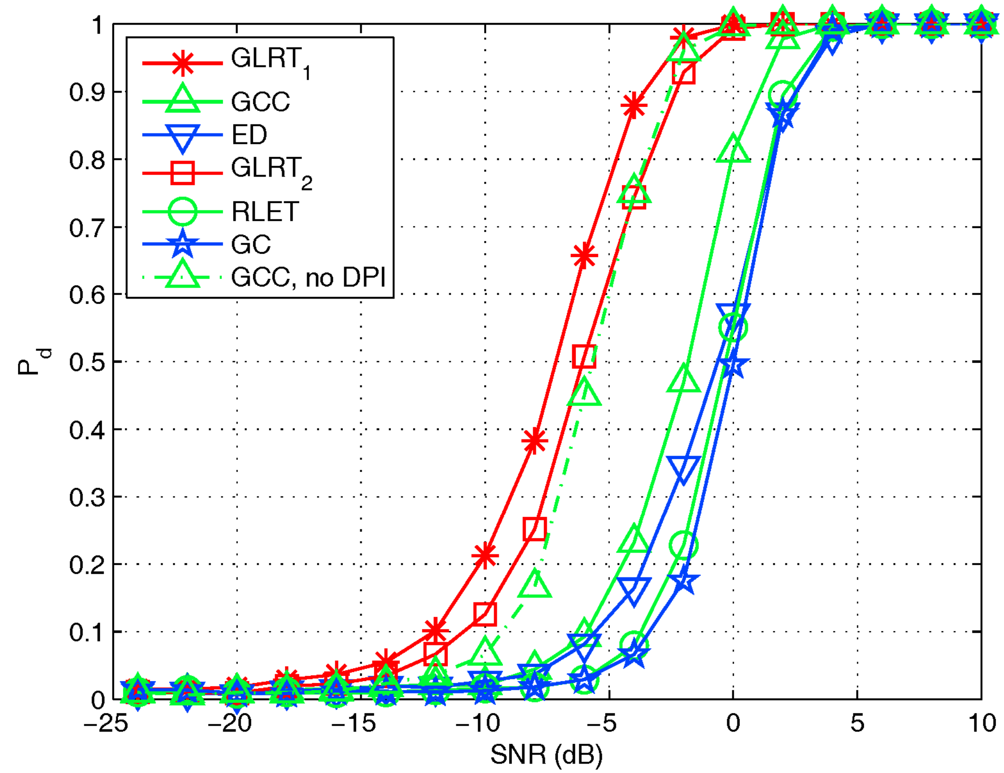

$$\mathrm{SNR} = 10 \log_{10} \frac{1}{K} \sum_{k=1}^{K} \frac{|\alpha_k|^2}{\eta_k}, \quad \mathrm{DNR} = 10 \log_{10} \frac{1}{K} \sum_{k=1}^{K} \frac{|\beta_k|^2}{\eta_k}$$

Numerical Results

$$M = 20, K = 3, P_{FA} = 10^{-2}$$
$$\text{SNR} = 0 \text{ dB}, \text{DNR} = 0 \text{ dB}$$

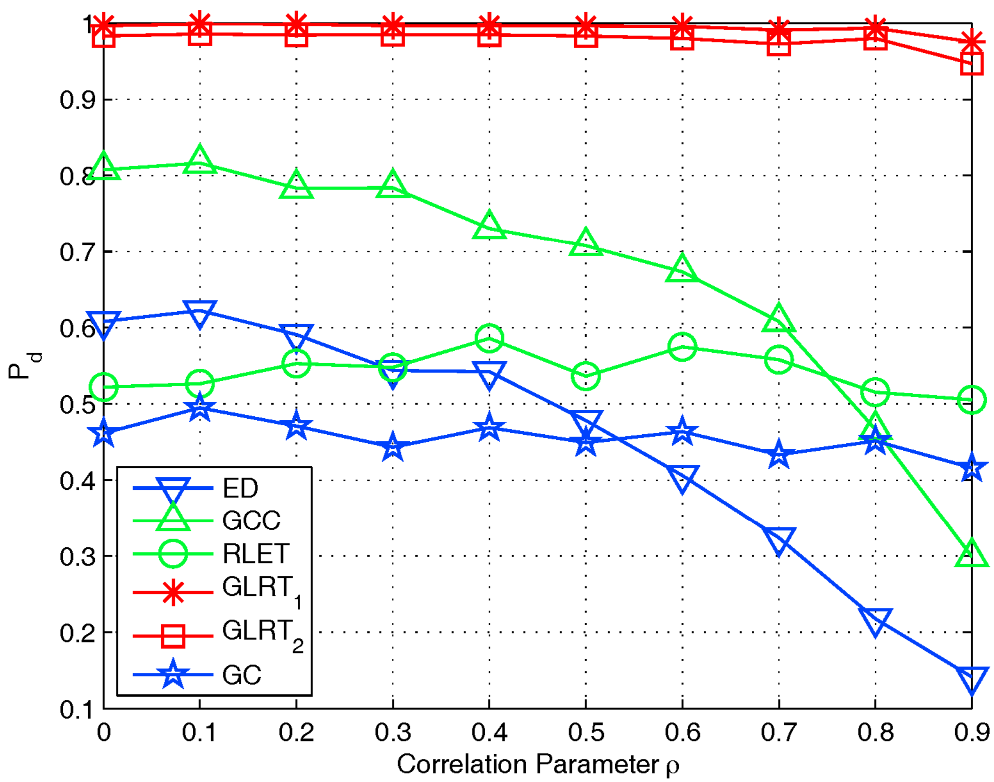

$$M = 20, K = 3, P_{FA} = 10^{-2}$$
$$\text{SNR} = 5 \text{ dB}$$

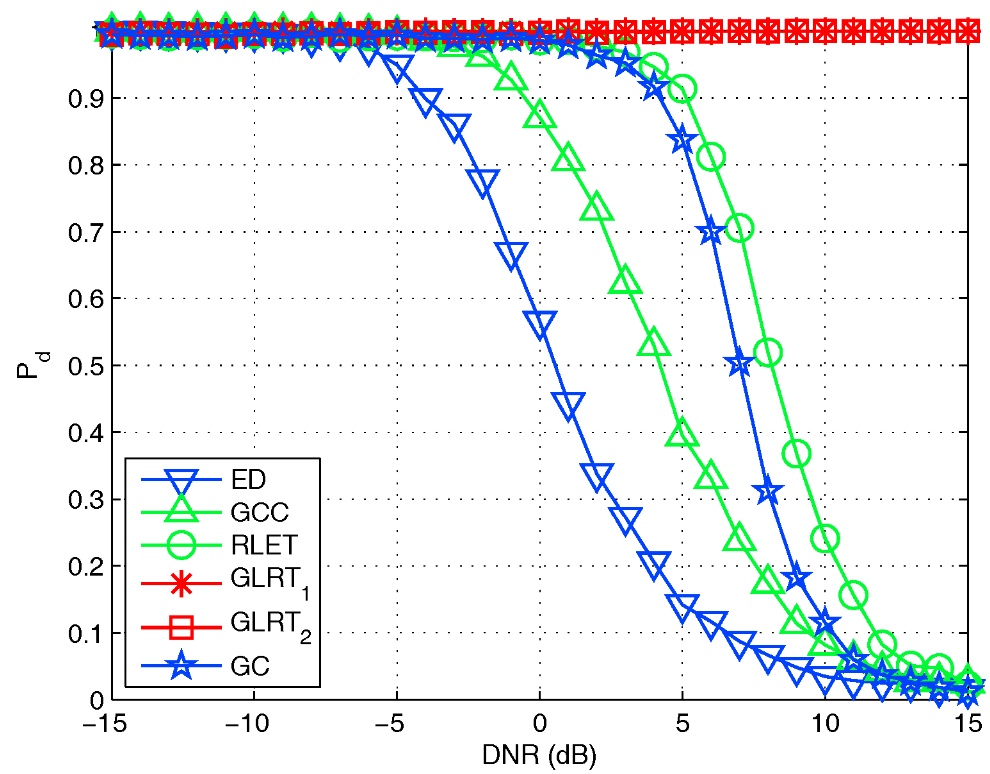

Numerical Results

$K = 3, P_{FA} = 10^{-2}$

SNR $= 5$ dB, DNR $= 0$ dB

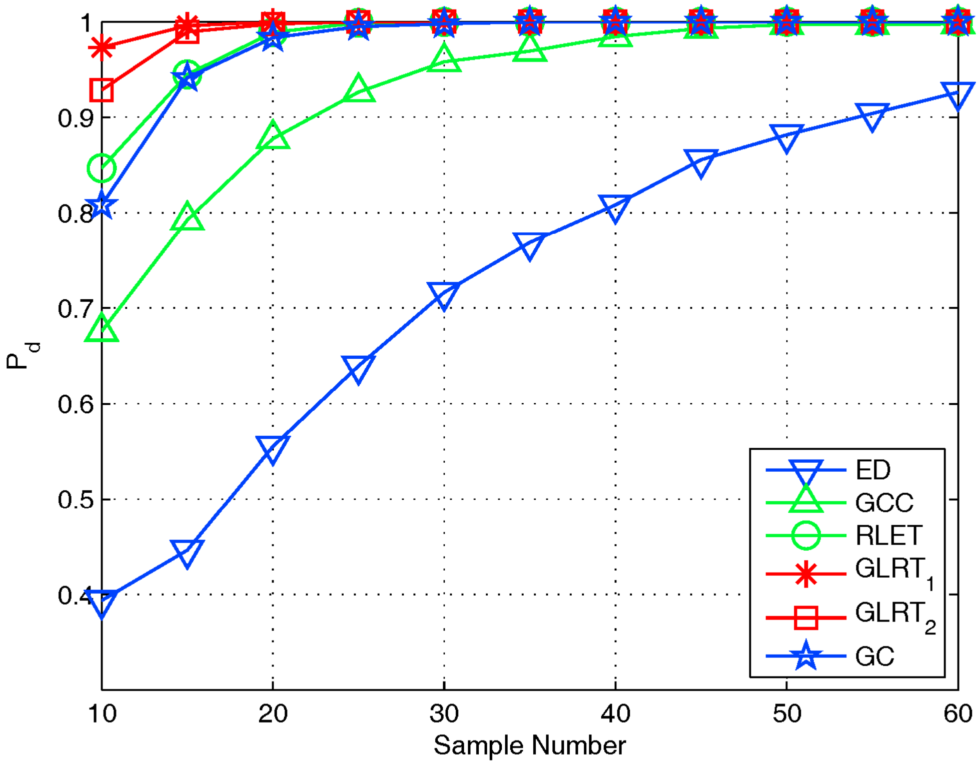

$M = 20, \quad P_{FA} = 10^{-2}$

SNR $= 5$ dB, DNR $= 0$ dB

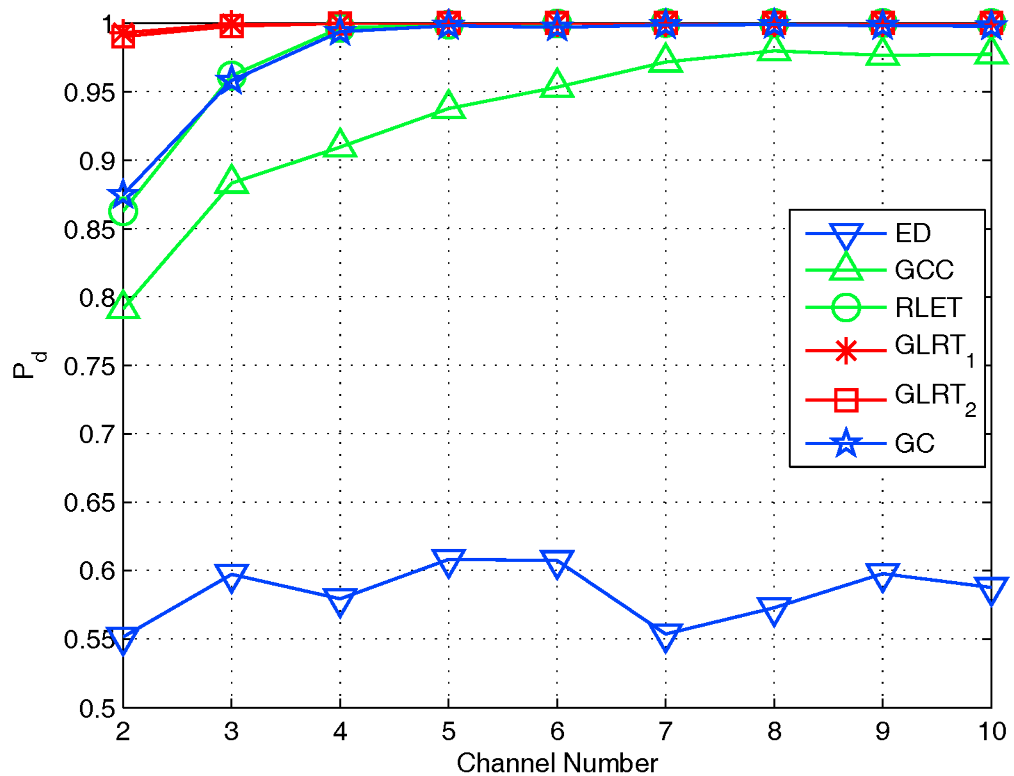

Remarks

- Examined the target detection problem for multistatic passive radar in the presence of noise and DPI
- Two GLRT detectors based on the EM algorithm are proposed for scenarios with known/unknown channel noise power
  - exploit the correlation of the IO waveform for detection
  - mitigate residual DPI
  - outperform several popular existing passive detectors
- Future directions:
  - Joint estimation of the waveform correlation and detection
  - Clutter mitigation
  - Computationally efficient detectors

Outline

- Cross-correlator in the presence of noisy reference and DPI
- Passive detection with noisy reference
- Passive detection with multiple receivers
  - Part I: No DPI
  - Part II: With DPI
- Exploit waveform correlation for passive detection and estimation
  - Part I: Joint delay-Doppler estimation
  - Part II: Multi-static detection with DPI
  - Part III: A parametric approach
- Summary

The Problem

- The composite binary hypothesis test is given by (time domain)

$$\mathbf{x} \sim \mathcal{CN}(\mathbf{0}, \mathbf{C}_x(\mathbf{a}, \sigma^2))$$

$$\mathcal{D}_k = \mathbf{W}(f_k T_s)\mathbf{T}^H \mathbf{W}(-\tau_k \Delta f)\mathbf{T}$$

$$\mathbf{n}_k \sim \mathcal{CN}(\mathbf{0}, \eta_k \mathbf{I}_M)$$

$$\begin{aligned} \mathcal{H}_1 &: \mathbf{y}_k = \beta_k \mathbf{x} + \alpha_k \mathcal{D}_k \mathbf{x} + \mathbf{n}_k \\ \mathcal{H}_0 &: \mathbf{y}_k = \beta_k \mathbf{x} + \mathbf{n}_k, \qquad k = 1, 2, \ldots, K, \end{aligned}$$

- Use a P-th order autoregressive (AR) process to fit the IO waveform $\mathbf{x}$ whose temporal correlation is parameterized by the AR coefficients $\mathbf{a} = [a(1), a(2), \ldots, a(P)]^T$ and the zero-mean driving noise variance σ^2
- For detection, we assume that delay/Doppler is known; the amplitude parameters β_k and α_k are unknown; the channel noise power is unknown

AR Modeling

- A P-th order AR process is

$$x(n) = -\sum_{p=1}^{P} a(p)x(n-p)+w(n), \quad n = 1,2,\ldots,N$$

where the zero-mean driving noise is

$$w(n) \sim \mathcal{CN}(0,\sigma^2)$$

- The covariance matrix of the IO waveform is Hermitian, Toeplitz, and fully determined by its first column, i.e., the auto-correlation function (ACF) sequence, related to $\{\mathbf{a}, \sigma^2\}$ by *Yule-Walker* equation

$$r_x(n) = \begin{cases} -\sum_{p=1}^{P} a(p)r_x(n-p) & \text{for } n \geq 1 \\ -\sum_{p=1}^{P} a(p)r_x(-p) + \sigma^2 & \text{for } n = 0 \end{cases}$$

where $r_x(n) = r_x^*(-n)$ for $n < 0$ and $r_x(0) = 1$

- Levinson-Durbin algorithm (LDA) + step-down (SD) procedure

$$\{\mathbf{a}, \sigma^2\} \Longrightarrow \mathbf{C}_x(\mathbf{a}, \sigma^2)$$

X. Zhang, H. Li, and B. Himed, "Multistatic passive detection with parametric modeling of the IO waveform," *Signal Processing*, vol.141, pp.187-198, Dec. 2017

GLRT

- In this case, the problem becomes

$$\mathcal{H}_1 : \mathbf{y} \sim \mathcal{CN}(\mathbf{0}_{MK\times 1}, \mathbf{C}_y(\boldsymbol{\alpha}, \boldsymbol{\beta}, \boldsymbol{\eta}, \mathbf{a}, \sigma^2))$$
$$\mathcal{H}_0 : \mathbf{y} \sim \mathcal{CN}(\mathbf{0}_{MK\times 1}, \mathbf{C}_y(\boldsymbol{\alpha} = \mathbf{0}, \boldsymbol{\beta}, \boldsymbol{\eta}, \mathbf{a}, \sigma^2))$$

where

$$\begin{aligned}\mathbf{C}_y(\boldsymbol{\alpha}, \boldsymbol{\beta}, \boldsymbol{\eta}, \mathbf{a}, \sigma^2) =& (\boldsymbol{\beta}\boldsymbol{\beta}^H) \otimes \mathbf{C}_x(\mathbf{a}, \sigma^2) + [(\boldsymbol{\beta}\boldsymbol{\alpha}^H) \otimes \mathbf{C}_x(\mathbf{a}, \sigma^2)]\mathbf{D}^H + \mathbf{C}_n(\boldsymbol{\eta}) \\ &+ \mathbf{D}[(\boldsymbol{\alpha}\boldsymbol{\beta}^H) \otimes \mathbf{C}_x(\mathbf{a}, \sigma^2)] + \mathbf{D}[(\boldsymbol{\alpha}\boldsymbol{\alpha}^H) \otimes \mathbf{C}_x(\mathbf{a}, \sigma^2)]\mathbf{D}^H\end{aligned}$$

- The GLRT is given by

$$\frac{\max_{\{\boldsymbol{\alpha}, \boldsymbol{\beta}, \boldsymbol{\eta}, \mathbf{a}, \sigma^2\}} p_1(\mathbf{y}|\boldsymbol{\alpha}, \boldsymbol{\beta}, \boldsymbol{\eta}, \mathbf{a}, \sigma^2)}{\max_{\{\boldsymbol{\beta}, \boldsymbol{\eta}, \mathbf{a}, \sigma^2\}} p_0(\mathbf{y}|\boldsymbol{\beta}, \boldsymbol{\eta}, \mathbf{a}, \sigma^2)} \underset{\mathcal{H}_0}{\overset{\mathcal{H}_1}{\gtrless}} \gamma$$

- Directly maximizing the likelihood functions is computationally difficult, since the covariance matrix has a complicated structure
- Resort to the EM algorithm to obtain the MLEs

GLRT

- The "complete" data is $\mathbf{z} = [\mathbf{x}^T, \mathbf{y}^T]^T$
- E-step:

$$Q\left(\boldsymbol{\theta}; \hat{\boldsymbol{\theta}}^{(l)}\right) = E_{\mathbf{x}|\mathbf{y},\hat{\boldsymbol{\theta}}^{(l)}} \{\log p(\mathbf{y}|\mathbf{x}, \boldsymbol{\theta}) p(\mathbf{x}|\boldsymbol{\theta})\}$$

$$\boxed{\mathcal{CN}(\mathbf{0}, \mathbf{C}_x(\mathbf{a}, \sigma^2)) \approx \frac{1}{(\pi\sigma^2)^{M-P}} \exp\left\{-\frac{\|\mathbf{x}_P + \mathbf{X}_P\mathbf{a}\|^2}{\sigma^2}\right\}}$$

where

$$\mathbf{x}_m = [x(m+1), x(m+2), \ldots, x(m+M-P)]^T, \quad m = 0, 1, \ldots, P$$

$$\mathbf{X}_P = [\mathbf{x}_{P-1}, \mathbf{x}_{P-2}, \ldots, \mathbf{x}_0]$$

- Here, we use the asymptotic form for the likelihood function of the IO waveform, instead of the exact likelihood function, to avoid some cumbersome mathematical operations [Kay '88, Wang et al. '13]

S. M. Kay, *Modern Spectral Estimation: Theory and Application*. Englewood Cliffs, NJ: Prentice Hall, 1988

P. Wang, H. Li, and B. Himed, A parametric moving target detector for distributed MIMO radar in non-homogeneous environment, *IEEE Trans. Signal Processing*, vol.61, no.9, pp.2282-2294, May 2013

GLRT

- Test variable

$$\mathcal{L} = \mathbf{y}^H \left[\mathbf{C}_y^{-1}(\widehat{\boldsymbol{\theta}}_0) - \mathbf{C}_y^{-1}(\widehat{\boldsymbol{\theta}}_1) \right] \mathbf{y} + \ln \frac{\det\left\{\mathbf{C}_y(\widehat{\boldsymbol{\theta}}_0)\right\}}{\det\left\{\mathbf{C}_y(\widehat{\boldsymbol{\theta}}_1)\right\}} \underset{\mathcal{H}_0}{\overset{\mathcal{H}_1}{\gtrless}} \xi$$

Final parameter estimates under H_0

$$\widehat{\alpha}_k^{(l+1)} = 0,\ \widehat{\beta}_k^{(l+1)},\ \widehat{\eta}_k^{(l+1)}$$

$$\widehat{\mathbf{a}}^{(l+1)} = -\left(\mathbf{C}_7^{(l)}\right)^{-1}\mathbf{c}_6^{(l)}$$

$$\widehat{\sigma^2}^{(l+1)} = \frac{1}{M-P}\left(c_5^{(l)} - \left(\mathbf{c}_6^{(l)}\right)^H\left(\mathbf{C}_7^{(l)}\right)^{-1}\mathbf{c}_6^{(l)}\right)$$

same as GLRT_2

Final parameter estimates under H_1

$$\widehat{\alpha}_k^{(l+1)},\ \widehat{\beta}_k^{(l+1)},\ \widehat{\eta}_k^{(l+1)}$$

$$\widehat{\mathbf{a}}^{(l+1)} = -\left(\mathbf{C}_7^{(l)}\right)^{-1}\mathbf{c}_6^{(l)}$$

$$\widehat{\sigma^2}^{(l+1)} = \frac{1}{M-P}\left(c_5^{(l)} - \left(\mathbf{c}_6^{(l)}\right)^H\left(\mathbf{C}_7^{(l)}\right)^{-1}\mathbf{c}_6^{(l)}\right)$$

$$c_1^{(l)} = \mathrm{tr}\left\{\mathbf{R}_{xx|y}^{(l)}\right\},\quad c_{2,k}^{(l)} = \mathrm{tr}\left\{\mathcal{D}_k\mathbf{R}_{xx|y}^{(l)}\right\},\quad c_5^{(l)} = \sum_{i=P+1}^{M}\left[\mathbf{R}_{xx|y}^{(l)}\right]_{i,i},\quad \left[\mathbf{c}_6^{(l)}\right]_p = \sum_{i=P+1}^{M}\left[\mathbf{R}_{xx|y}^{(l)}\right]_{i,i-p},$$

$$c_{3,k}^{(l)} = \mathbf{y}_k^H\widehat{\mathbf{x}}^{(l)},\quad c_{4,k}^{(l)} = \mathbf{y}_k^H\mathcal{D}_k\widehat{\mathbf{x}}^{(l)}\quad \left[\mathbf{C}_7^{(l)}\right]_{p,q} = \sum_{i=P+1}^{M}\left[\mathbf{R}_{xx|y}^{(l)}\right]_{i-q,i-p},\quad p,q = 1,2,\ldots,P$$

$$\widehat{\mathbf{x}}^{(l)} = \mathbf{C}_{xy}^{(l)}\left(\mathbf{C}_{yy}^{(l)}\right)^{-1}\mathbf{y},\quad \mathbf{R}_{xx|y}^{(l)} = \widehat{\mathbf{x}}^{(l)}\left(\widehat{\mathbf{x}}^{(l)}\right)^H + \mathbf{C}_{xx}^{(l)} - \mathbf{C}_{xy}^{(l)}\left(\mathbf{C}_{yy}^{(l)}\right)^{-1}\left(\mathbf{C}_{xy}^{(l)}\right)^H$$

$$\mathbf{C}_{xx}^{(l)} = \mathbf{C}_x(\widehat{\mathbf{a}}^{(l)}, \widehat{\sigma^2}^{(l)})\quad \mathbf{C}_{xy}^{(l)} = \left(\widehat{\boldsymbol{\beta}}^{(l)}\right)^H\otimes\mathbf{C}_{xx}^{(l)} + \mathbf{C}_{xx}^{(l)}\left(\underbrace{\widehat{\boldsymbol{\alpha}}^{(l)}}_{=0 \text{ under } H_0}\otimes\mathbf{I}_M\right)^H\mathbf{D}^H,\quad \mathbf{C}_{yy}^{(l)} = \mathbf{C}_y(\widehat{\boldsymbol{\theta}}^{(l)})$$

Parameter Initialization

- The EM algorithm requires an initialization of the unknown parameters
  - $\{\mathbf{a}, \sigma^2\}$ are initialized such that the covariance matrix $\mathbf{C}_{xx}^{(0)} = \mathbf{I}_M$
  - IO waveform is initialized by using a principal eigenvector (PEV) method

$$\hat{\mathbf{x}} = \mathbf{v}_1\left(\mathbf{Y}\mathbf{Y}^H\right), \text{ where } \mathbf{Y} = [\mathbf{y}_1, \mathbf{y}_2, \ldots, \mathbf{y}_K]$$

  - amplitudes and channel noise variances are initialized using least squares (LS) method

H_1:

$$\hat{\alpha}_k^{(0)} = \frac{b_2 b_{4,k} - b_{1,k} b_{3,k}^*}{b_2^2 - |b_{3,k}|^2}$$

$$\hat{\beta}_k^{(0)} = \frac{b_{1,k} b_2 - b_{3,k} b_{4,k}}{b_2^2 - |b_{3,k}|^2}$$

$$\hat{\eta}_k^{(0)} = \frac{1}{M}\left\|\mathbf{y}_k - \hat{\beta}_k^{(0)}\hat{\mathbf{x}} - \hat{\alpha}_k^{(0)}\mathcal{D}_k\hat{\mathbf{x}}\right\|^2$$

$$b_{1,k} = \hat{\mathbf{x}}^H \mathbf{y}_k, \; b_2 = \|\hat{\mathbf{x}}\|^2$$

$$b_{3,k} = \hat{\mathbf{x}}^H \mathcal{D}_k \hat{\mathbf{x}}, \; b_{4,k} = \hat{\mathbf{x}}^H \mathcal{D}_k^H \mathbf{y}_k$$

H_0:

$$\hat{\beta}_k^{(0)} = \frac{\hat{\mathbf{x}}^H \mathbf{y}_k}{\|\hat{\mathbf{x}}\|^2}$$

$$\hat{\eta}_k^{(0)} = \frac{1}{M}\left\|\mathbf{y}_k - \hat{\beta}_k^{(0)}\hat{\mathbf{x}}\right\|^2$$

Other Passive Detectors

- Provide conventional detectors with ability to handle DPI

$$\hat{\mathbf{x}} = \mathbf{v}_1\left(\mathbf{Y}\mathbf{Y}^H\right) \qquad \hat{\beta}_k = \frac{\hat{\mathbf{x}}^H \mathbf{y}_k}{\hat{\mathbf{x}}^H \hat{\mathbf{x}}} \qquad \tilde{\mathbf{y}}_k = \mathbf{y}_k - \hat{\beta}_k \hat{\mathbf{x}}$$

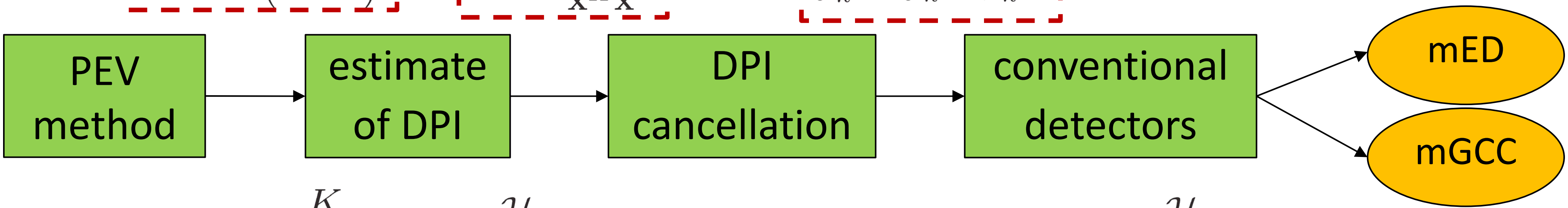

$$\mathcal{L}_{\text{mED}} = \sum_{k=1}^{K} \|\tilde{\mathbf{y}}_k\|^2 \underset{\mathcal{H}_0}{\overset{\mathcal{H}_1}{\gtrless}} \gamma_{\text{mED}}, \quad \mathcal{L}_{\text{mGCC}} = \lambda_1\left(\tilde{\mathbf{Y}}^H \tilde{\mathbf{Y}}\right) \underset{\mathcal{H}_0}{\overset{\mathcal{H}_1}{\gtrless}} \gamma_{\text{mGCC}}$$

- Clairvoyant matched filter in the presence of DPI: assumes IO waveform is known and serves as an upper bound

$$\mathcal{L}_{\text{MF}} = \prod_{k=1}^{K} \frac{\left\|\mathbf{P}_x^{\perp} \mathbf{y}_k\right\|^2}{\left\|\mathbf{P}_k^{\perp} \mathbf{y}_k\right\|^2}$$

$$\mathbf{P}_x^{\perp} = \mathbf{I}_M - \frac{1}{\|\mathbf{x}\|^2} \mathbf{x}\mathbf{x}^H$$

$$\mathbf{H}_k = [\mathcal{D}_k \mathbf{x}, \mathbf{x}]$$

$$\mathbf{P}_k^{\perp} = \mathbf{I}_M - \mathbf{H}_k \left(\mathbf{H}_k^H \mathbf{H}_k\right)^{-1} \mathbf{H}_k^H$$

Numerical Results

- Methods in the comparisons
  - pGLRT: proposed parametric GLRT detector
  - iGLRT: ideal GLRT with knowledge of covariance matrix $\mathbf{C}_x$
  - sGLRT: simple GLRT with $\mathbf{C}_x = \mathbf{I}_M$
  - Clairvoyant MF
  - mED
  - mGCC
  - mMF
- Two types of IO waveforms used to test the detectors
  I. Stochastic process with Gaussian-shaped power spectral density (PSD)
  II. Frequency modulated (FM) waveform

Numerical Results - I

$$M = 50, \quad K = 3, \quad \text{DNR} = 0 \text{ dB}$$

Highly correlated waveform

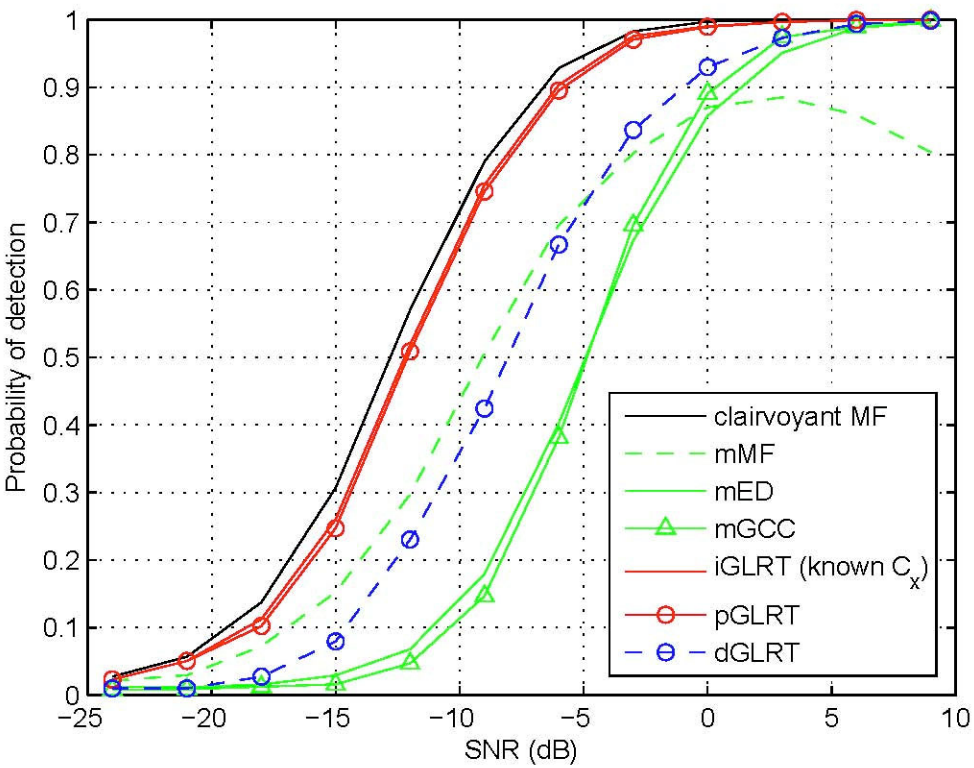

Lowly correlated waveform

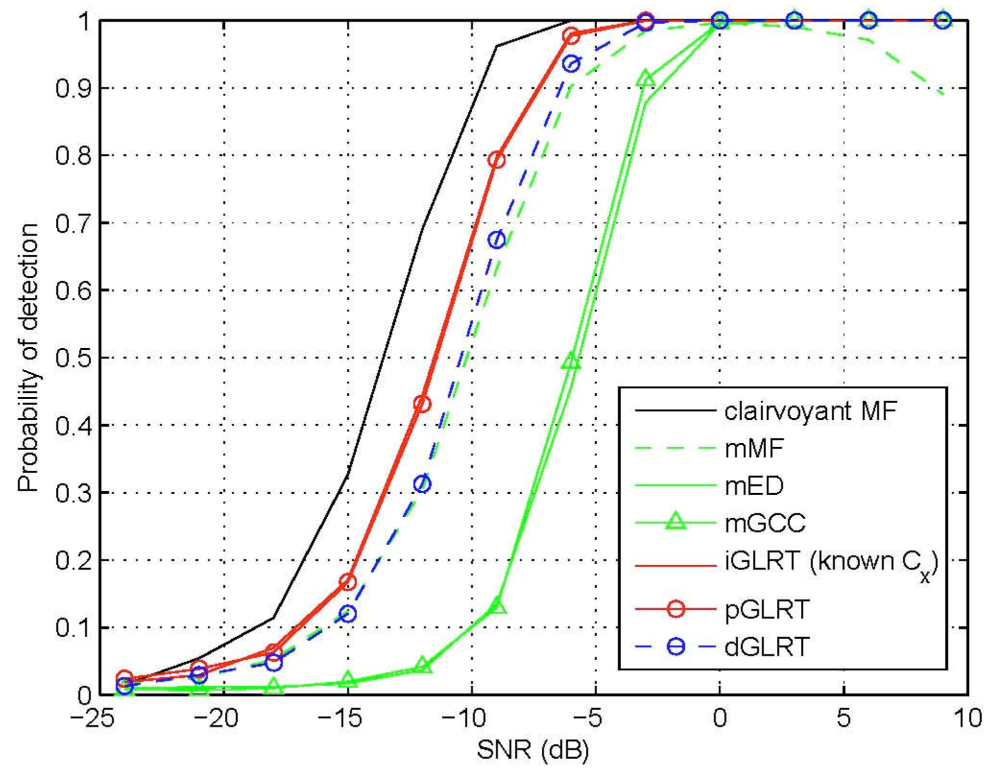

Numerical Results - I

$$M = 50, \quad K = 3, \quad \text{SNR} = -5,\ 0,\ 5\ \text{dB}$$

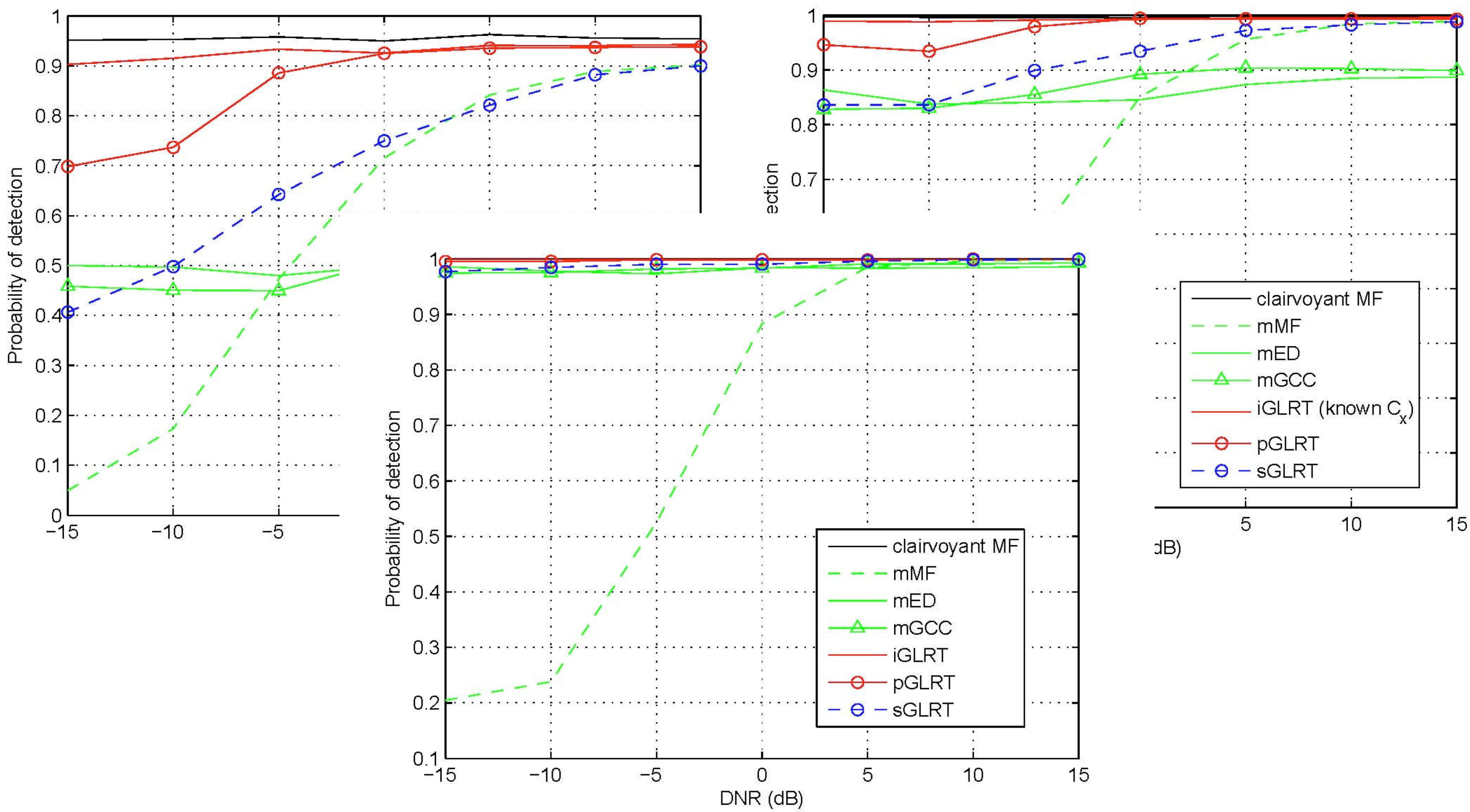

Numerical Results - I

$M = 20, \quad \text{SNR} = 0 \text{ dB}$

$\text{DNR} = 0 \text{ dB}$

$K = 3, \quad \text{SNR} = -5 \text{ dB}$

$\text{DNR} = 0 \text{ dB}$

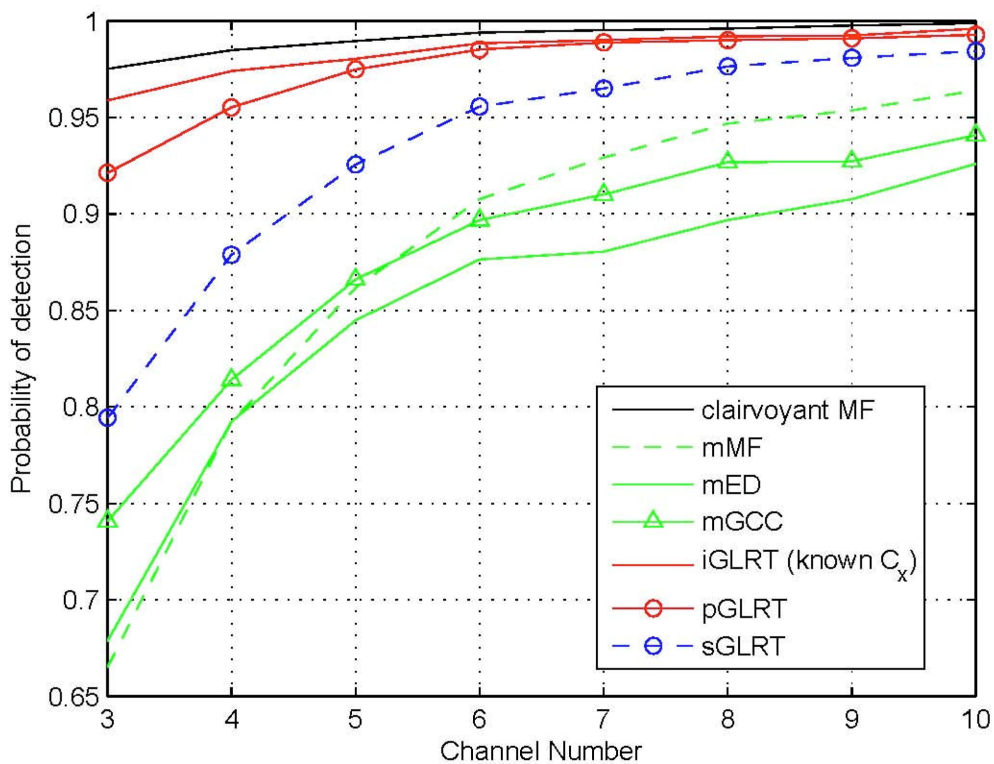

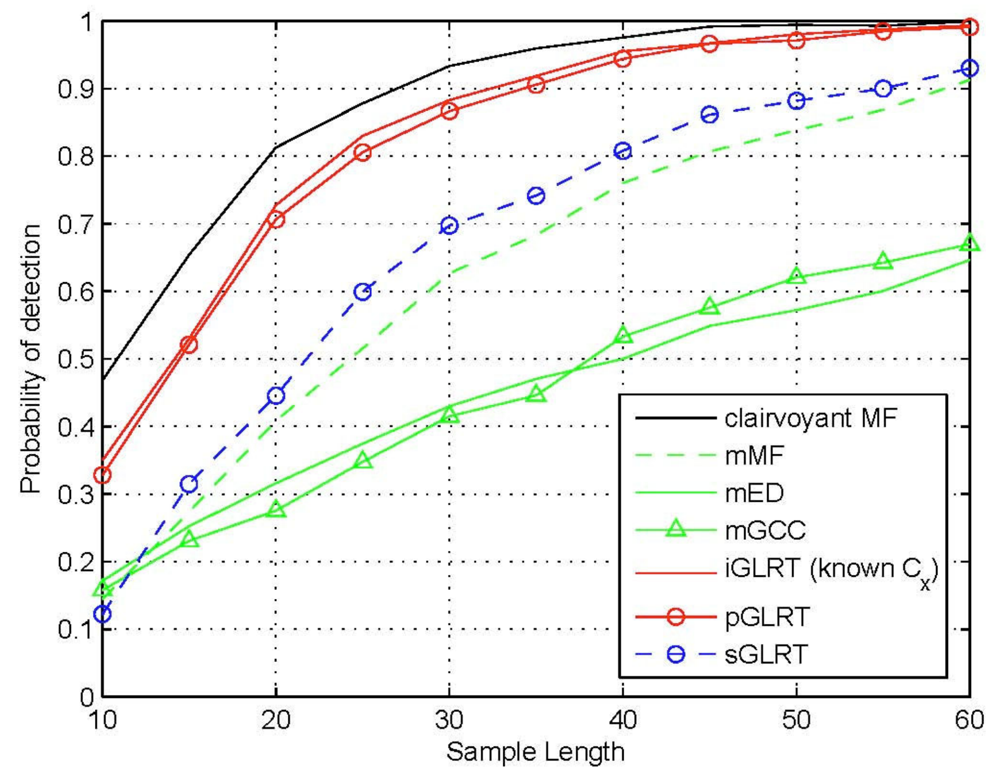

Numerical Results - II

$M = 50, \quad K = 3$

$\text{DNR} = 0 \text{ dB}$

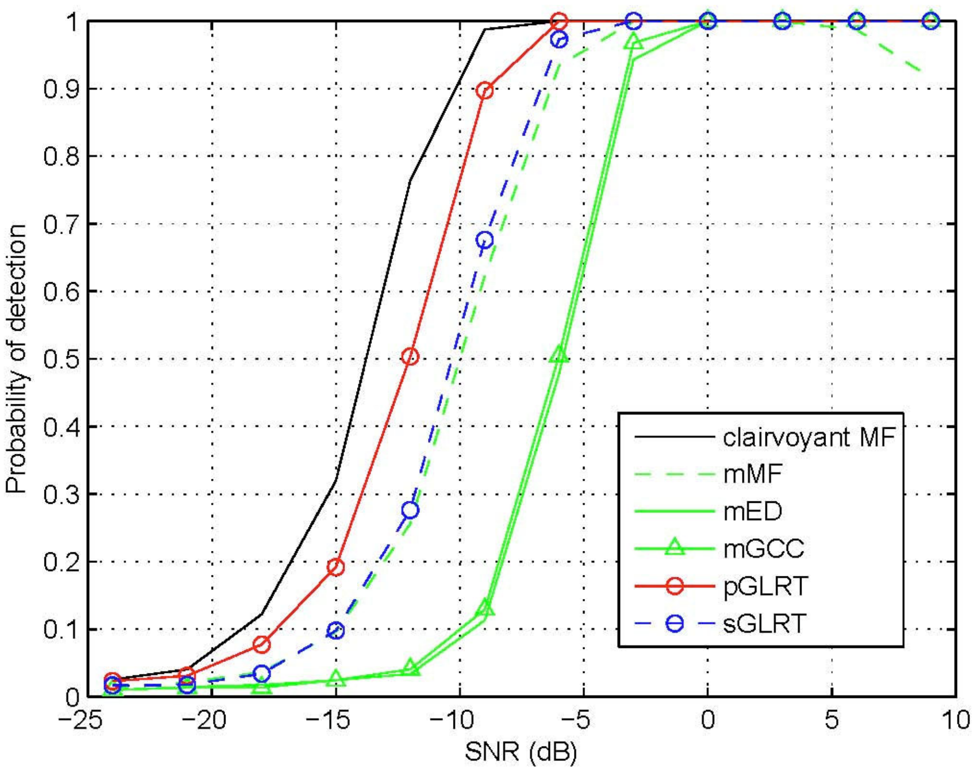

$K = 3, \quad \text{SNR} = -5 \text{ dB}$

$\text{DNR} = 0 \text{ dB}$

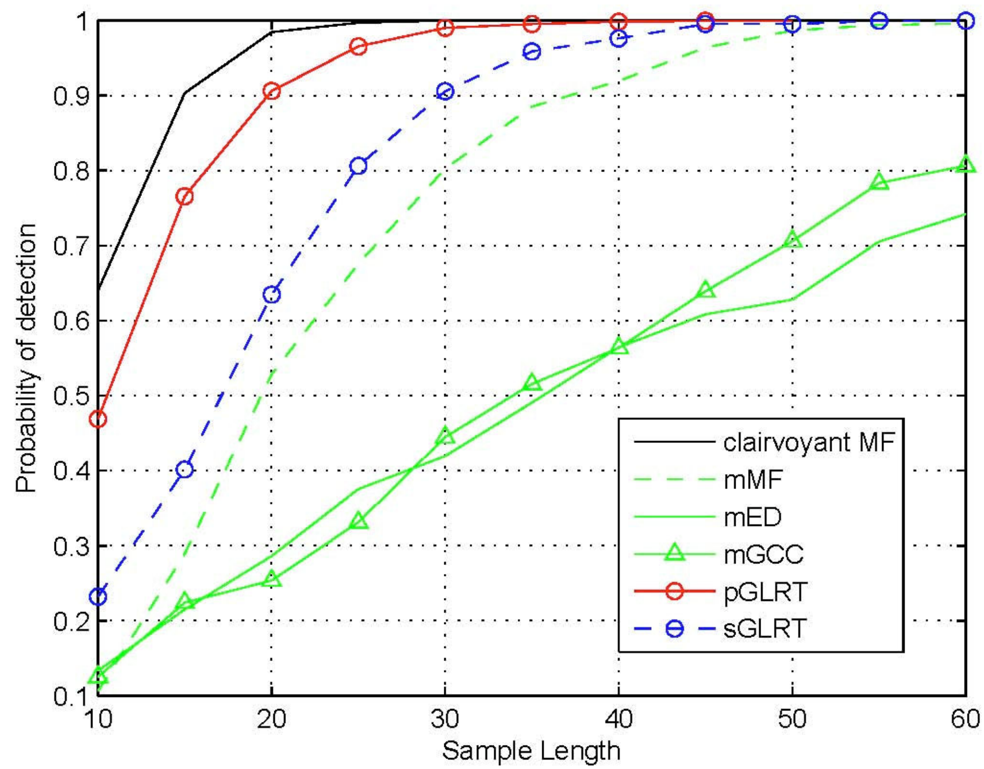

Remarks

- Examined the target detection problem in the presence of direct-path interference (DPI) for passive multistatic radar using non-cooperative illuminators of opportunity (IO)
- Proposed a parametric passive detector by modeling the unknown waveform as an auto-regressive process whose temporal correlation is jointly estimated and exploited for passive detection
- Developed an expectation-maximization (EM) based estimator for parameter estimation associated with the parametric passive detector
- Extended several conventional passive detectors, originally introduced for application in DPI-free environments, to provide them with an ability to cope with DPI

Summary on Signal Detection & Estimation

- Target detection and estimation in passive radar is much more challenging than its counterpart in active radar
  - Transmitter is non-cooperative: source waveform is unknown and not optimized for sensing
  - Strong DPI
  - Target echo, DPI, and clutter depend on the unknown IO waveform
- Analyzed the popular CC detector which uses a noisy reference for delay-Doppler processing
  - Very sensitive to noise in reference and DPI
- Presented several recently developed passive detectors and estimators by
  - Accounting for noisy reference
  - Mitigating residual DPI
  - Exploiting waveform correlation for passive detection

Part 3
SAR Imaging and STAP

Outline

- Passive multi-static SAR imaging: Challenges
- Signal sparsity and compressive sensing
- Sparsity-based high-resolution SAR imaging
  - Group sparse SAR imaging
  - Structure-aware SAR imaging
- Sparsity-based space-time adaptive processing (STAP)
- Conclusions

Passive Multi-Static SAR Imaging

Passive multi-static SAR imaging

- Bandwidth of each signal is very narrow
- Correspond to multiple illuminators and/or receivers
- Discontinuous observations in 2-D wavenumber domain
- Depend on the Tx positions, Rx observation trajectory, frequency and bandwidth
- Multi-static signals have non-coherent phases
- Conventional methods yield low image resolution and high sidelobes

Passive Multi-Static SAR Imaging

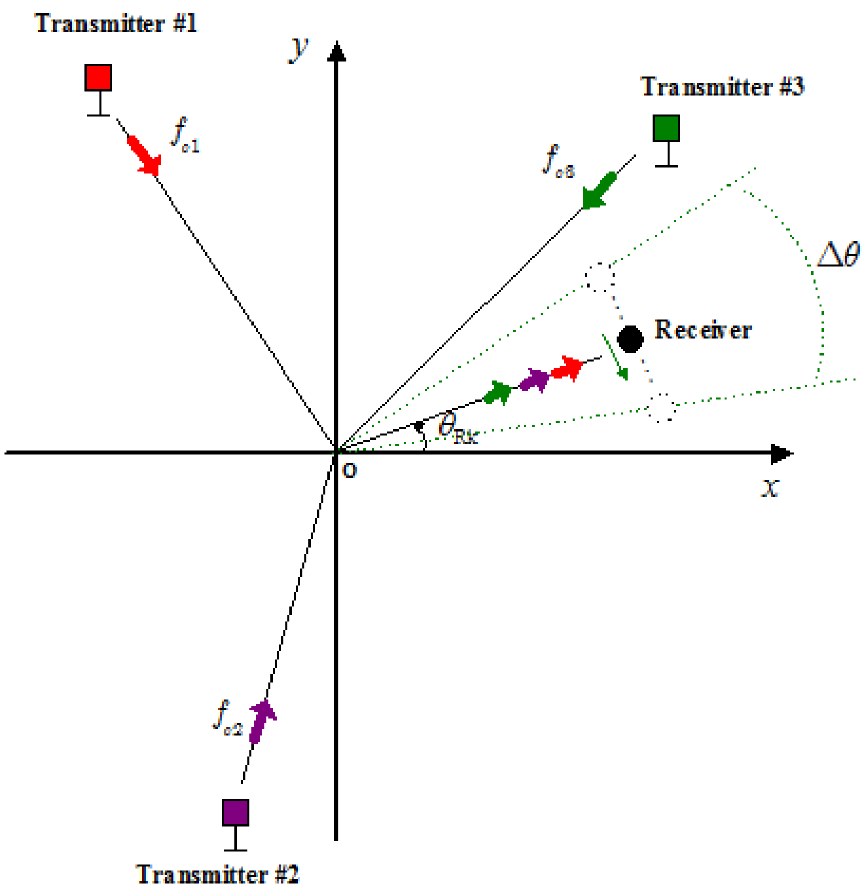

Data collection geometry

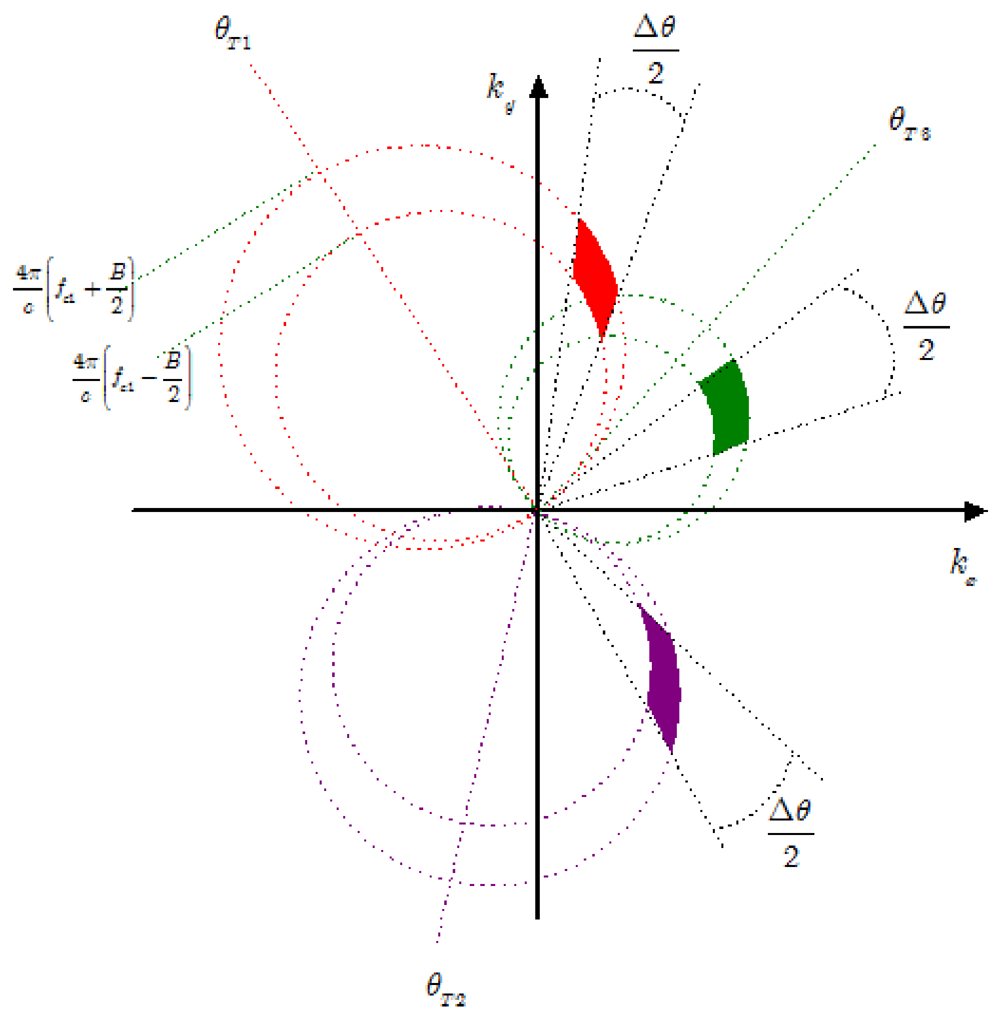

Wavenumber domain

Passive Multi-Static SAR Imaging

- Return signal corresponding to sensing sinusoid

$$\hat{r} = \sum_{x,y} \sigma(x,y)\cdot \exp\left[-j2\pi f \frac{r_{\mathrm{T}}(x,y)+r_{\mathrm{R}}(x,y)}{c}\right]$$
$$= \sum_{x,y} \sigma(x,y)\cdot \exp\left\{-j\frac{2\pi f}{c}\left[x\left(\cos\theta_{\mathrm{T}}+\cos\theta_{\mathrm{R}}\right)+y\left(\sin\theta_{\mathrm{T}}+\sin\theta_{\mathrm{R}}\right)\right]\right\}$$
$$= \sum_{x,y} \sigma(x,y)\cdot \exp\left[-j\left(xk_x+yk_y\right)\right]$$

where $k_x = \frac{2\pi f}{c}\left(\cos\theta_{\mathrm{T}}+\cos\theta_{\mathrm{R}}\right)$ and $k_y = \frac{2\pi f}{c}\left(\sin\theta_{\mathrm{T}}+\sin\theta_{\mathrm{R}}\right)$

are spatial frequency (wavenumber) in x and y directions with

$$k_r = \sqrt{k_x^2+k_y^2} = \frac{4\pi f}{c}\cos\left(\frac{\theta_T-\theta_R}{2}\right) \qquad \theta = \tan^{-1}\left(\frac{k_y}{k_x}\right) = \frac{\theta_T+\theta_R}{2}$$

- Observations for different wavenumbers are obtained by varying the frequency and the observation positions

Passive Multi-Static SAR Imaging

Example

- 8 illuminators with their locations and carrier frequencies in the following table. The bandwidth of each signal is 20 MHz.
- The receiver changes its azimuth angle from 11° to 17° during the observation period.
- The scattering coefficients vary independently for bistatic pairs associated with different illuminators

Illuminator	f_c (MHz)	Angle (°)		Illuminator	f_c (MHz)	Angle (°)
1	450	5		5	610	30
2	550	10		6	520	20
3	500	45		7	630	15
4	480	25		8	580	50

Passive Multi-Static SAR Imaging

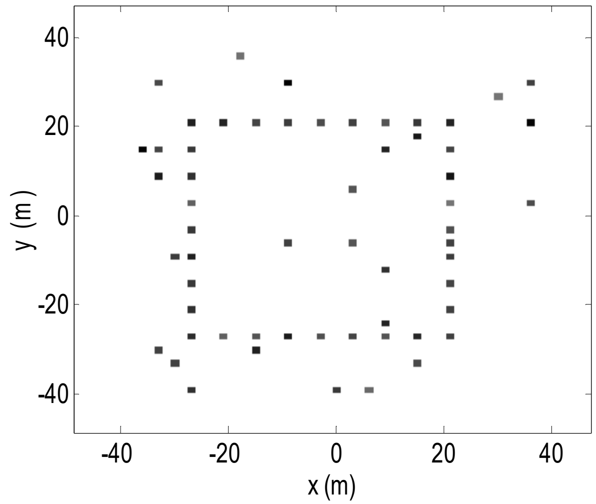

True target distribution

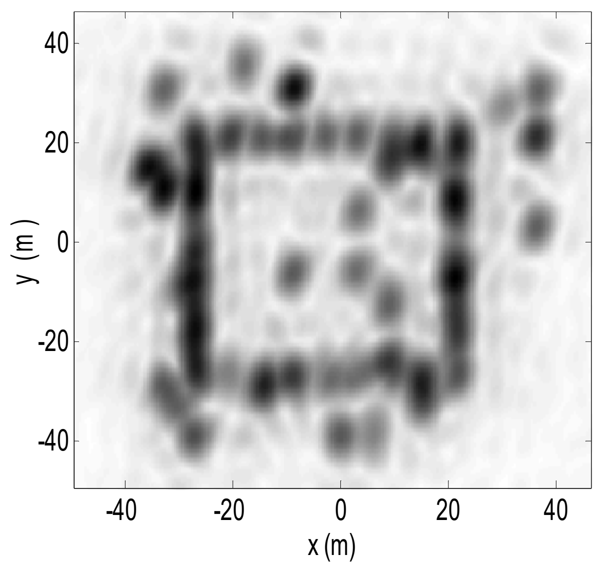

Back-projection result

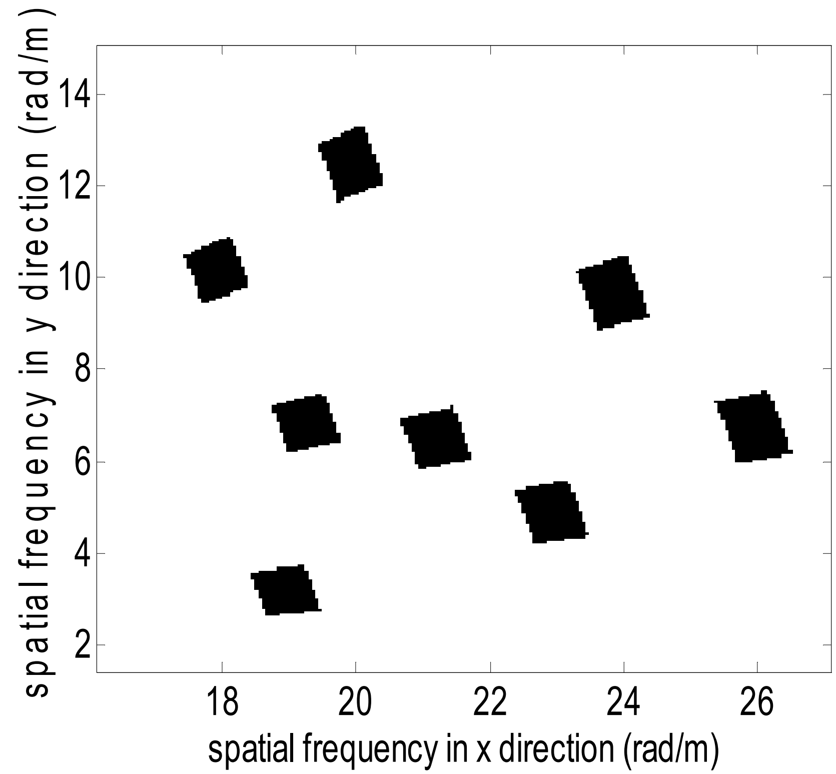

Wavenumber domain support

Approved for Public Release - PA#: 88ABW-2018-1622

Passive Multi-Static SAR Imaging

- By using the target sparsity, however, high-resolution imaging can be obtained from the same observations.

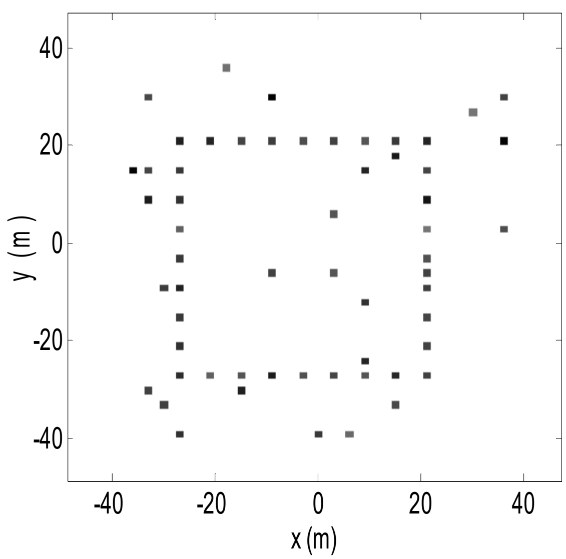

True target distribution

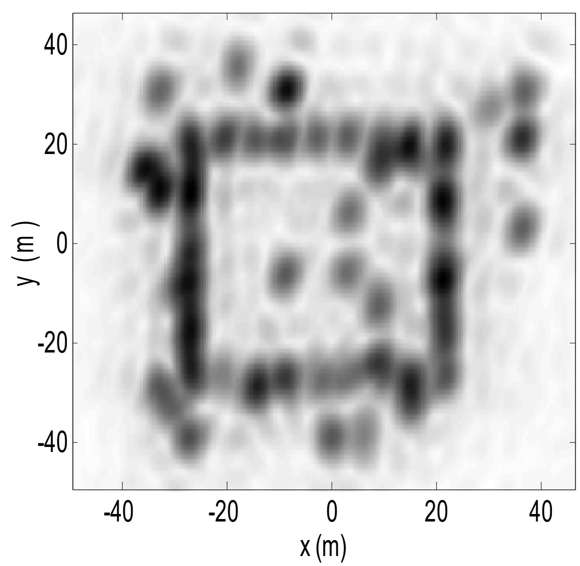

Back-projection result

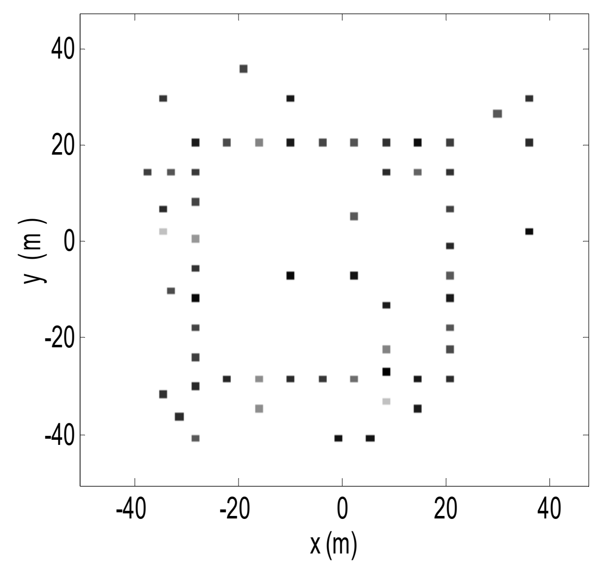

Sparse reconstruction result

X. Mao, Y. D. Zhang, and M. Amin, "Low-complexity sparse reconstruction for high-resolution multi-static passive SAR imaging," *EURASIP J. Advances Signal Processing*, 2014:104

Outline

- Passive multi-static SAR imaging: Challenges
- Signal sparsity and compressive sensing
- Sparsity-based high-resolution SAR imaging
  - Group sparse SAR imaging
  - Structure-aware SAR imaging
- Sparsity-based space-time adaptive processing (STAP)
- Conclusions

Signal Sparsity and Compressive Sensing

Original 2500 KB

Compressed 148 KB (6%)

x → sample $\xrightarrow{N}$ compress $\xrightarrow{K<<N}$ transmit/store

Can't we just directly measure the part that won't end up being thrown away?

x → **Compressive sensing** $\xrightarrow{K<<N}$ transmit/store

Signal Sparsity and Compressive Sensing

Conventional data acquisition: Sample and then compress

- Based on Nyquist sampling theorem
- Produces a huge amount of data measurements
- Challenging to sampling, storage, and processing devices

Compressive sensing: Built-in compression while sample

- Collect a reduced volume of data
- Without compromising the performance

Importance in radar applications

- Full data not accessible due to limitations in location, bandwidth, and time
- Conventional methods, e.g., back-projection, yields inferior performance
- Compressive sensing can be used to solve **sparse reconstruction** problems in order to provide high-quality signal reconstruction

Signal Sparsity and Compressive Sensing

Sparsity: Number of nonzero components is relatively small

- Signal itself is sparse
- Signal can be sparsely represented using sparsifying bases

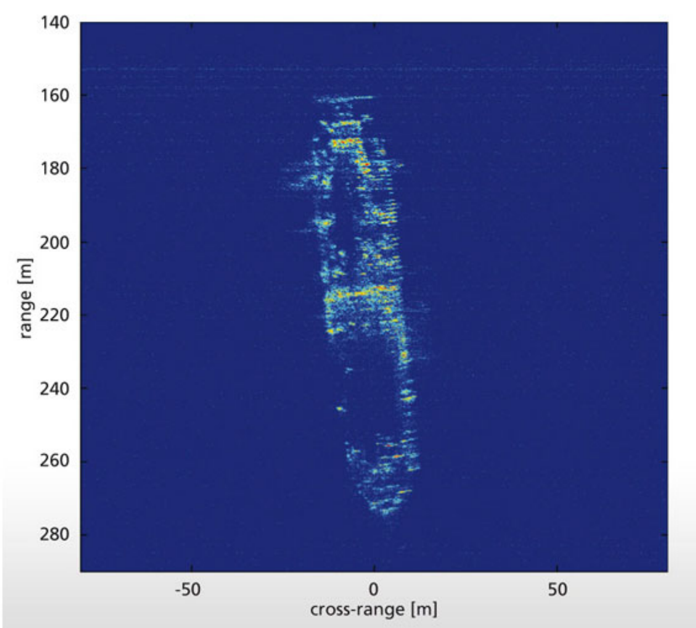

Maritime objects on high seas

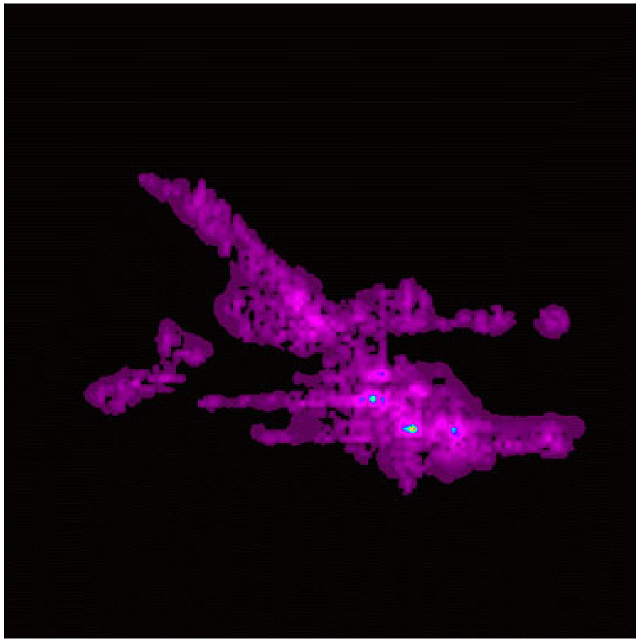

ISAR imaging of aircraft

Signal Sparsity and Compressive Sensing

Sparsity: Number of nonzero components is relatively small

- Signal itself is sparse
- Signal can be sparsely represented using sparsifying bases

Source image

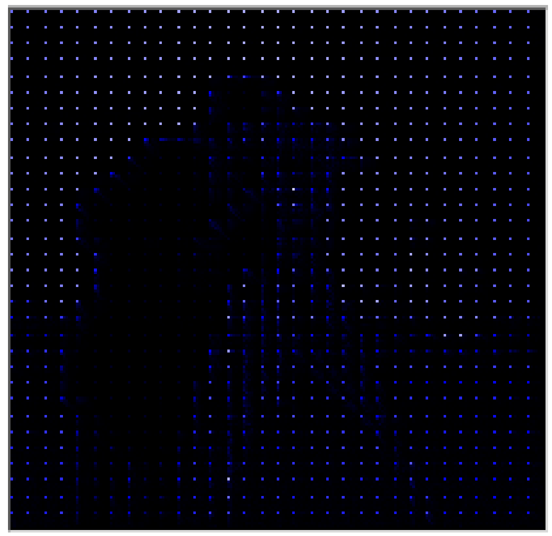

Block-based DCT (near-sparse)

Spatial gradient

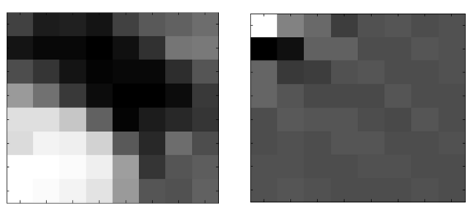

Details for 8x8 block

Signal Recovery through Compressive Sensing

Sparse signal reconstruction:

given $\mathbf{y} = \mathbf{\Phi x}$

find $\mathbf{x}$

$$\mathbf{y} \quad = \quad \mathbf{\Phi} \quad \mathbf{x}$$

M x 1
measurements

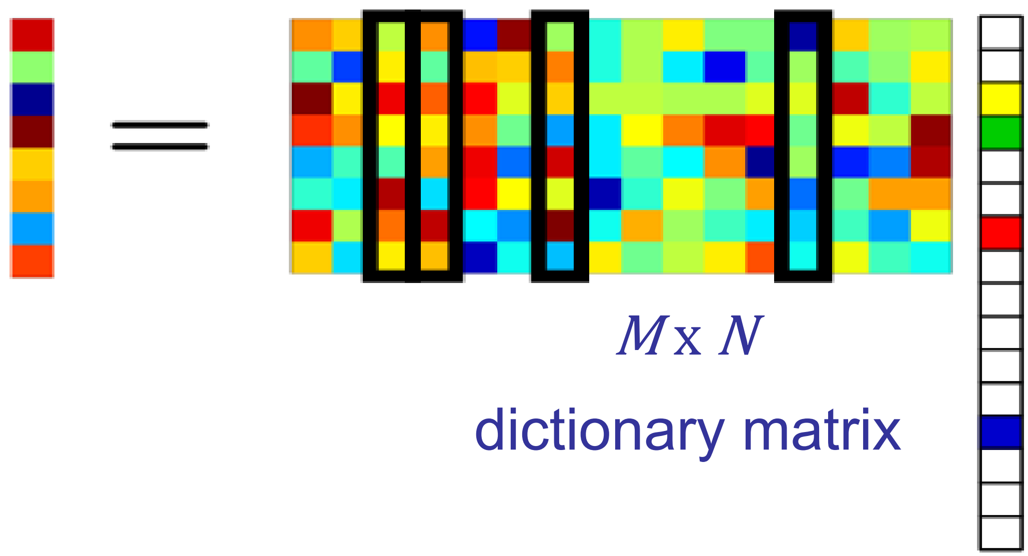

M x N
dictionary matrix

N x 1
sparse signal

K
non-zero entries

$\mathbf{x}$ may be solvable when $K < M << N$

Signal Recovery through Compressive Sensing

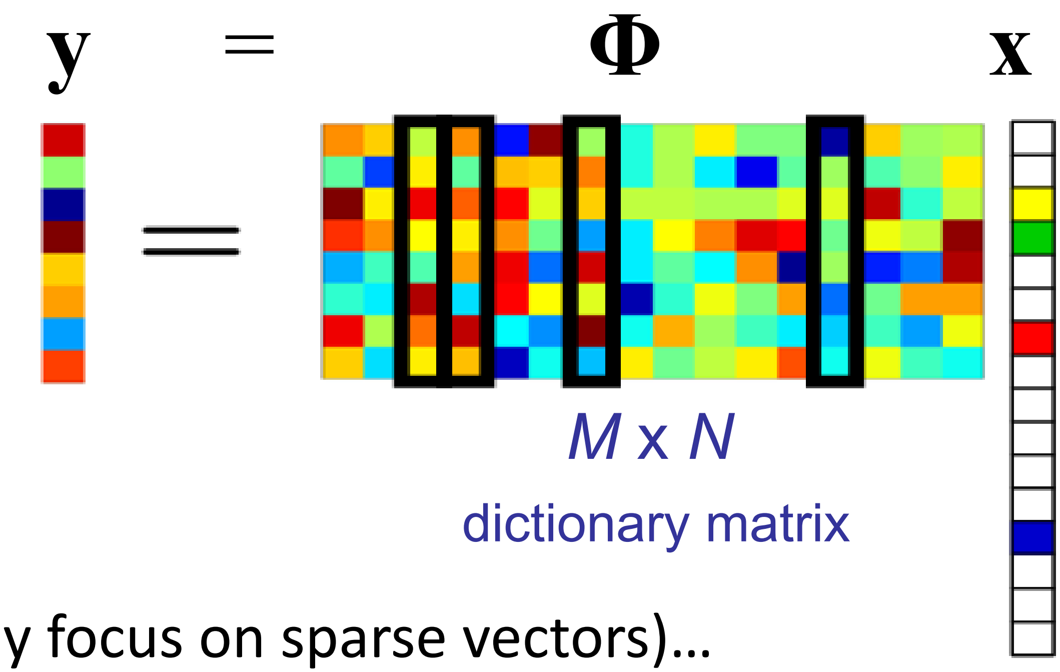

M x 1
measurements

N x 1
sparse signal

K
non-zero entries

- Effectively (if we only focus on sparse vectors)…

M x 1
measurements

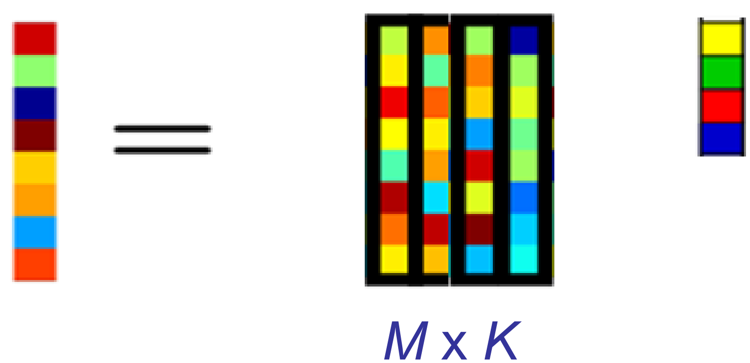

K x 1
non-zero entries

- Vector $\mathbf{x}$ may be solvable when $K < M$, provided that each of the $M \times K$ submatrices of matrix $\mathbf{\Phi}$ has a full rank

Recovery Algorithms

- Compressive sensing problems are generally expressed as

$$\text{minimize } ||\mathbf{x}||_0 \text{ subject to } \mathbf{y} = \mathbf{\Phi x}$$

- However, this problem is non-convex and NP-hard.
- **Greedy algorithms**
  - Greedy construction of "support" (=column combination) by adding one-by-one/best choice at each iteration: Orthogonal matching pursuit (OMP), iterative hard thresholding, …
- **Convex relaxation**
  - Approximation of the cost by convex functions (typically l_1-norm recovery): Basis pursuit (BP), basis pursuit denoising (BPDN), LASSO…
- **Probabilistic inference**
  - (Approximate) employment of probabilistic inference: Bayesian compressive sensing (sparse Bayesian learning) …

Greedy Algorithms

- Basic idea – Sample vector $\mathbf{y}$ stands for a linear combination of columns ϕ_i of $\mathbf{\Phi}$.

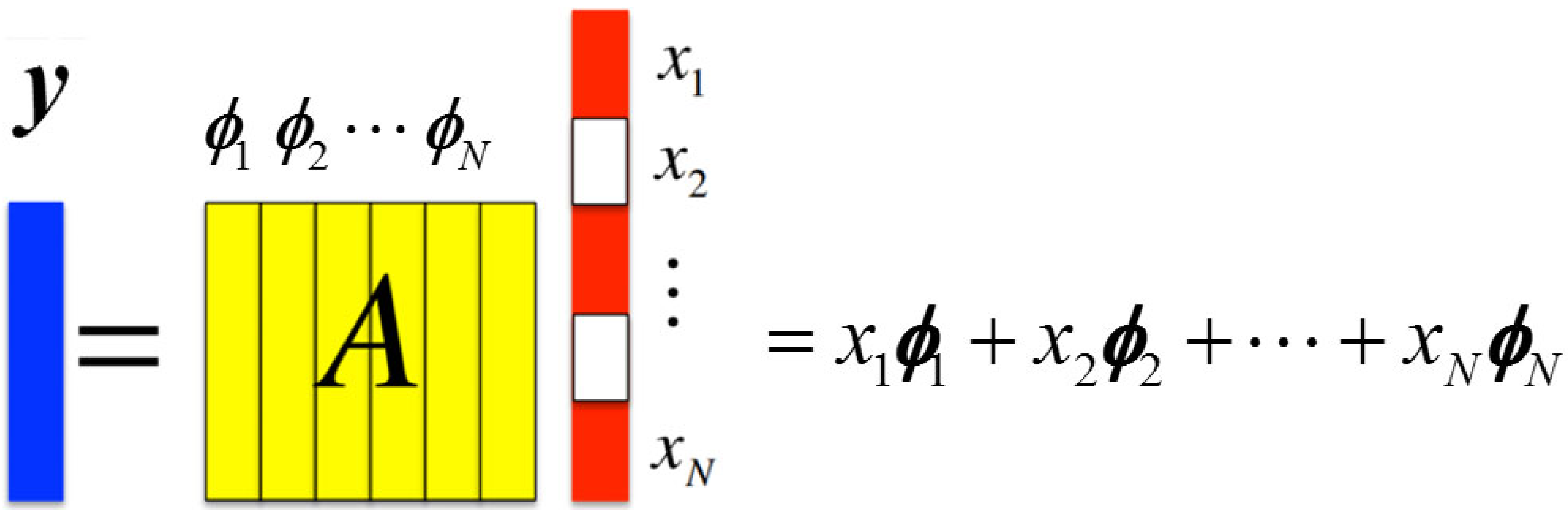

- Construct an appropriate set of columns whose coefficients are non-zero, which is termed *support*, in a greedy manner.

Orthogonal Matching Pursuit (OMP)

Initialization: Initialize $k = 0$, and set

$$\mathbf{x}^0 = 0, \mathbf{r}^0 = \mathbf{y} - \mathbf{\Phi}\mathbf{x}^0 = \mathbf{y}, S^0 = \varnothing$$

Main iteration: let $k = k + 1$, and perform the followings:

- **Rating of the columns:**

$$\varepsilon(i) = \min_{x_i} \left| x_i \boldsymbol{\phi}_i - \mathbf{r}^{k-1} \right|^2$$

- **Update support:**

$$i_0 = \arg\min_{i \notin S^{k-1}} \{\varepsilon(i)\}, S^k = S^{k-1} \cup \{i_0\}$$

- **Update provisional solution:**

$$\hat{\mathbf{x}}^k = \arg\min_{\mathbf{x}_{S^k}} \left| \mathbf{y} - \mathbf{\Phi}_{S^k} \mathbf{x}_{S^k} \right|^2$$

- **Update residual:**

$$\mathbf{r}^k = \mathbf{y} - \mathbf{\Phi}_{S^k} \hat{\mathbf{x}}^k$$

- **Stopping rule:** Stop if $\left|\mathbf{r}^k\right| < \varepsilon_0$ holds. Otherwise, apply another iteration

Convex Relaxation

- Compressive sensing problems are generally expressed as

$$\min \|\mathbf{x}\|_0 \quad \text{subject to} \quad \mathbf{y} = \mathbf{\Phi x}$$

- The non-convex l_0-norm problem is often relaxed to l_1-norm one

$$\min \|\mathbf{x}\|_1 \quad \text{subject to} \quad \mathbf{y} = \mathbf{\Phi x}$$

Consider noisy observations:

$$\min \|\mathbf{x}\|_1 \quad \text{subject to} \quad \|\mathbf{y} - \mathbf{\Phi x}\|_2 < \varepsilon_0$$

- l_1-norm
  - is convex
  - has corners (to provide sparse solutions)

$\|\mathbf{x}\|_p$

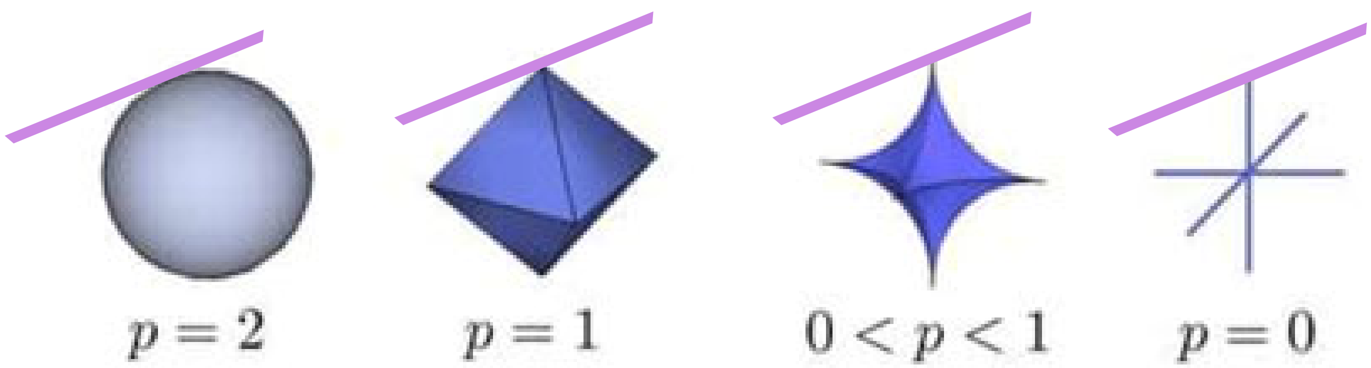

Not sparse Sparse & convex Not convex

Bayesian Compressive Sensing (Sparse Bayesian Learning)

- Obtain maximum *a posteriori* (MAP) solution of $\mathbf{x}$ from

$$\mathbf{y} = \mathbf{\Phi x} + \boldsymbol{\varepsilon}, \quad \boldsymbol{\varepsilon} \sim N(\boldsymbol{\varepsilon} \mid \mathbf{0}, \beta \mathbf{I})$$

- Sparse Bayesian learning based on relevance vector machine:

$$p(\mathbf{y} \mid \mathbf{\Phi}, \mathbf{x}) = N(\mathbf{y} \mid \mathbf{\Phi x}, \beta \mathbf{I})$$

  Place Gaussian prior on $\mathbf{x}$

$$p(\mathbf{x} \mid \boldsymbol{\gamma}) = \prod_i N(x_i \mid 0, \gamma_i)$$

- Inverse Gamma priors are placed over β and $\boldsymbol{\gamma}$
- Key advantages of Bayesian CS (BCS):
  - Close to l_0-norm sparse solution
  - Less sensitive to sensing matrix coherence
  - Convenient to consider signal structures through priors

M. E. Tipping, "Sparse Bayesian shrinkage and selection learning and the relevance vector machine," *J. Machine Learning Research*, pp. 211-244, 2001.

S. Ji, D. Dunson, and L. Carin, "Multi-task compressive sampling," *IEEE Trans. Signal Processing*, vol. 57, no. 1, pp. 92-106, Jan. 2009. [Matlab code available]

Bayesian Compressive Sensing (Sparse Bayesian Learning)

- Sparse compressive sensing uses a two-layer hierarchical prior model that involves a conditional prior pdf $p(\mathbf{x}|\boldsymbol{\gamma})$ and a hyperprior pdf $p(\boldsymbol{\gamma})$
- It constructs computationally tractable iterative algorithms that estimate both $\boldsymbol{\gamma}$ and $\mathbf{x}$, with the estimate of $\mathbf{x}$ being sparse

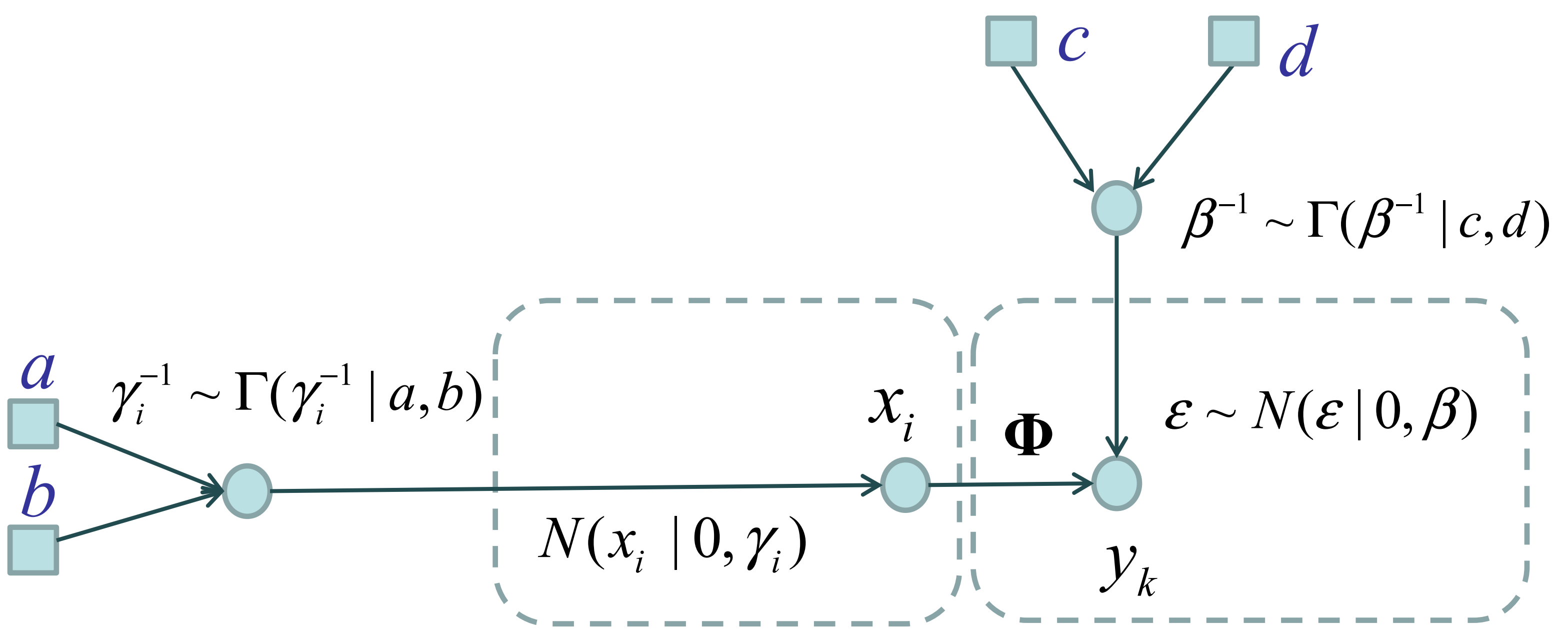

- Typically, we set $a = b = c = d = 0$ as a default choice to avoid a subjective choice and leads to simplifications of computation

Bayesian Compressive Sensing (Sparse Bayesian Learning)

- There are different ways to solve this problem
- Type-II maximum likelihood

$$p(\mathbf{x},\boldsymbol{\gamma},\beta\,|\,\mathbf{y}) = p(\mathbf{x}\,|\,\mathbf{y},\boldsymbol{\gamma},\beta)\,p(\boldsymbol{\gamma},\beta\,|\,\mathbf{y})$$

$$p(\mathbf{x}\,|\,\mathbf{y},\boldsymbol{\gamma},\beta) = N(\mathbf{x}\,|\,\mathbf{m},\boldsymbol{\Sigma}) \qquad p(\boldsymbol{\gamma},\beta\,|\,\mathbf{y}) \propto \underline{p(\mathbf{y}\,|\,\boldsymbol{\gamma},\beta)}\,p(\boldsymbol{\gamma})\,p(\beta)$$

No analytical solution
(solve numerically)

$$\mathbf{m} = \beta^{-1}\boldsymbol{\Sigma}\boldsymbol{\Phi}^T\mathbf{y}$$
$$\boldsymbol{\Sigma} = (\boldsymbol{\Gamma}^{-1} + \beta^{-1}\boldsymbol{\Phi}^T\boldsymbol{\Phi})^{-1}$$
$$\boldsymbol{\Gamma} = \mathrm{diag}(\boldsymbol{\gamma})$$

Iterate

$$\gamma_i = [m_i^2 + \Sigma_{ii}]^{-1}$$
$$\beta = \frac{\mathrm{tr}(\boldsymbol{\Sigma}\boldsymbol{\Phi}\boldsymbol{\Phi}^T) + \|\mathbf{y} - \boldsymbol{\Phi}\mathbf{m}\|^2}{K}$$

- Upon convergence, $\mathbf{m}$ is used as the estimate of $\mathbf{x}$

Mutual Incoherence Property (MIP)

- Mutual coherence of a matrix: the largest absolute normalized inner products between different columns
- For $\mathbf{\Phi} = [\boldsymbol{\phi}_1, \boldsymbol{\phi}_2, \dots, \boldsymbol{\phi}_m]$, its mutual coherence is

$$\mu(\mathbf{\Phi}) = \max_{1 \le i \ne j \le m} \frac{|\phi_i^H \phi_j|}{\|\phi_i\|_2 \cdot \|\phi_j\|_2}$$

- It characterize the dependence between columns of $\mathbf{\Phi}$
- For unitary matrices, $\mu(\mathbf{\Phi}) = 0$
- For recovery problems, we desire a small $\mu(\mathbf{\Phi})$ as it is similar to unitary matrices
- In order to achieve high-resolution signal reconstruction, however, the mutual coherence could be high

Outline

- Passive multi-static SAR imaging: Challenges
- Signal sparsity and compressive sensing
- Sparsity-based high-resolution SAR imaging
  - Group sparse SAR imaging
  - Structure-aware SAR imaging
- Sparsity-based space-time adaptive processing (STAP)
- Conclusions

Multi-illuminator SAR Imaging

- Passive SAR image resolution is highly limited by the narrow frequency bandwidth (typically a few MHz)
- Sparse observation in the 2-D wavenumber domain depends on the Tx positions, Rx observation trajectory, frequency and bandwidth

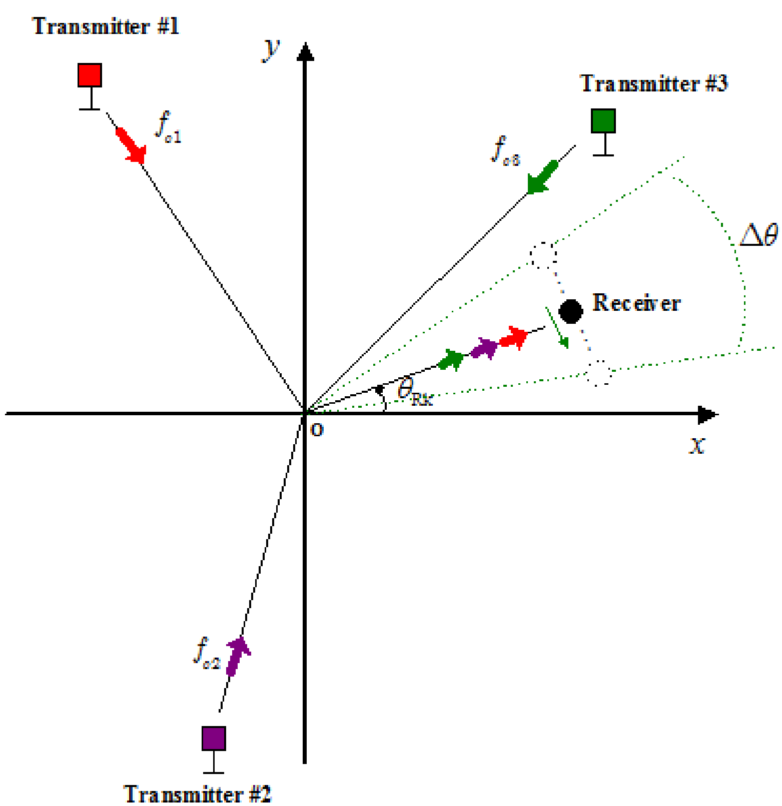

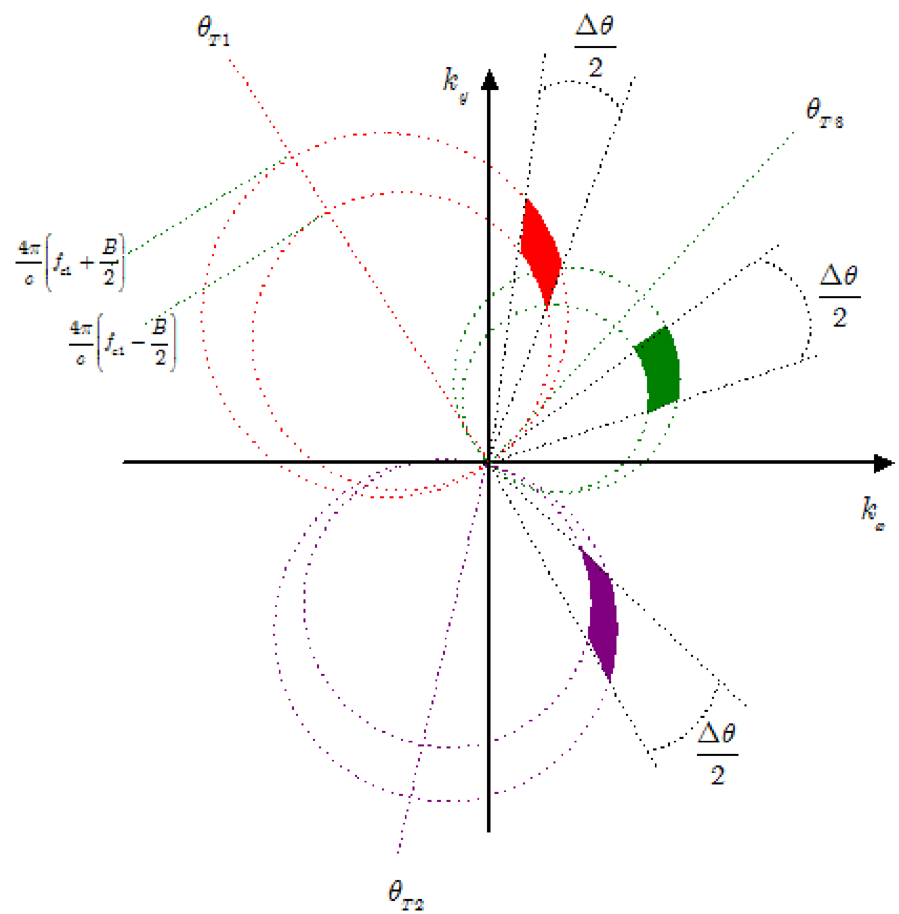

Multi-illuminator SAR Imaging

- For multi-static passive radar with multiple emitters:
  - Reflection coefficients ($\sigma^{(l)}$) depend on aspect angle (l: Tx)
  - Standard linear group CS formulation after vectorize 2-D scene

$$r^{(l)} = \sum_{x,y} \sigma^{(l)}(x,y) \cdot \exp\left[-j\left(xk_x^{(l)} + yk_y^{(l)}\right)\right]$$

x, y: coordinate in the scene

$k_x^{(l)}, k_y^{(l)}$: wavenumber (transmitter-dependent)

$\sigma^{(l)}(x,y)$: sparse reflection coefficient to be estimated

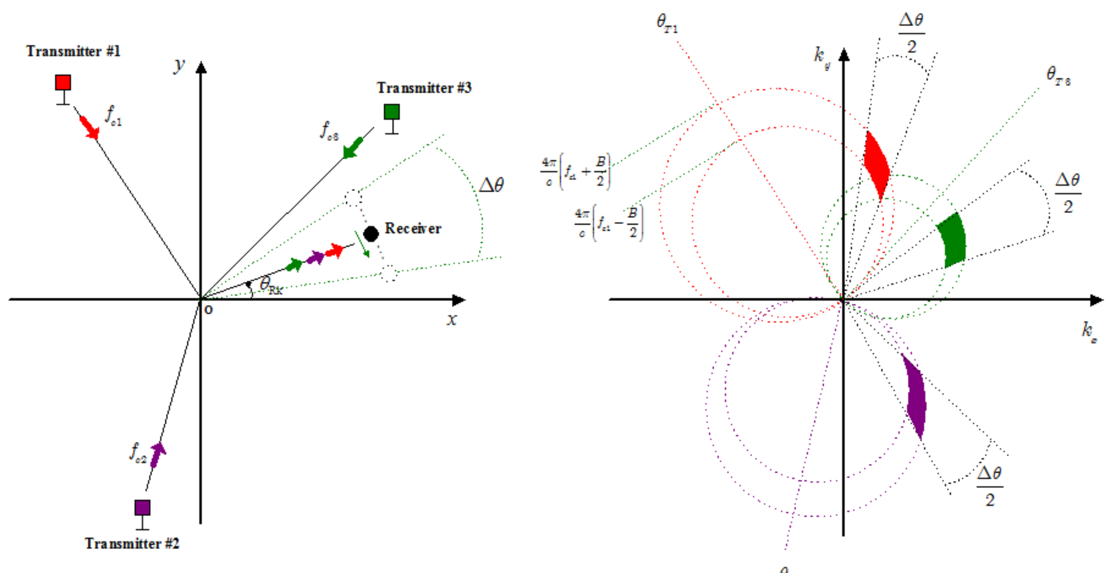

SAR Imaging

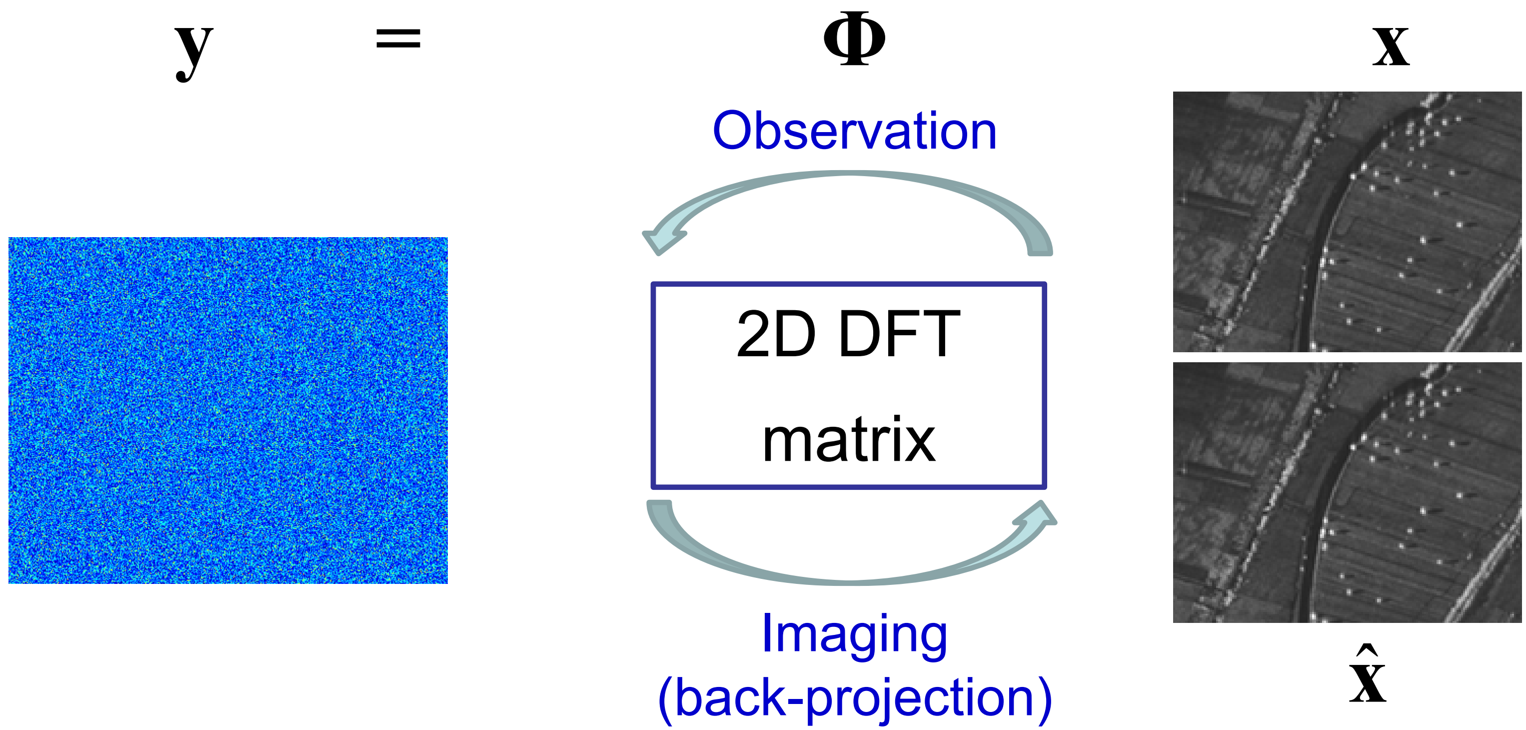

- In conventional SAR, sufficient data are observed in the wavenumber domain by exploiting a wideband sensing waveform and long azimuth time
- Image $\mathbf{x}$ can be reconstructed from observation $\mathbf{y}$ through 2-D inverse Fourier transform, typically implemented via back-projection

Sparsity in SAR Imaging

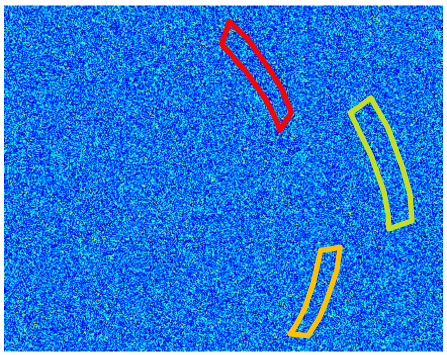

Observation

2D DFT matrix

Imaging
(compressive sensing)

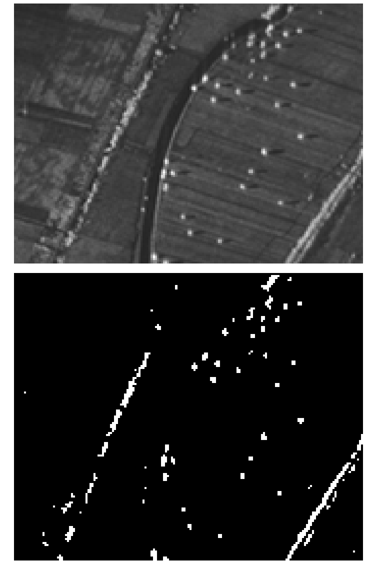

In passive radar problems, however,

- We cannot design matrix Φ (governed by DFT)
- No flexibility of choosing the observations (position, bandwidth)
- High coherence for closely spaced pixels

➔ **We need to find a solution that is robust to a dictionary matrix with high coherence**

Sparsity-based High-Resolution SAR Imaging

To achieve high-resolution images:

- Exploit wide angle and multi-static observations
  - Improves both azimuth and range resolution
  - Angle-dependence of the target reflectivity
- Using CS methods with high-resolution reconstruction capability (e.g., BCS)

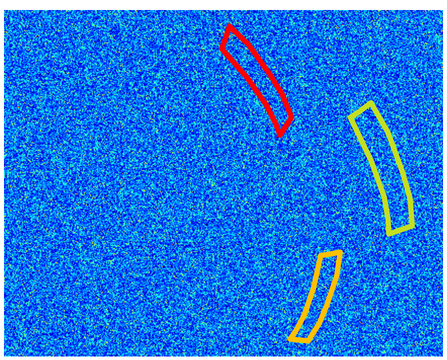

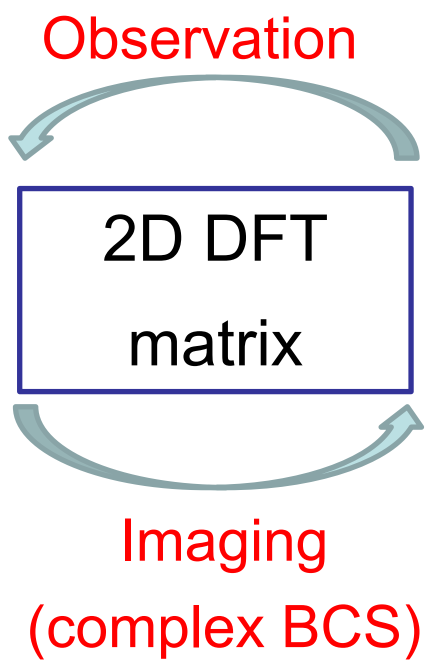

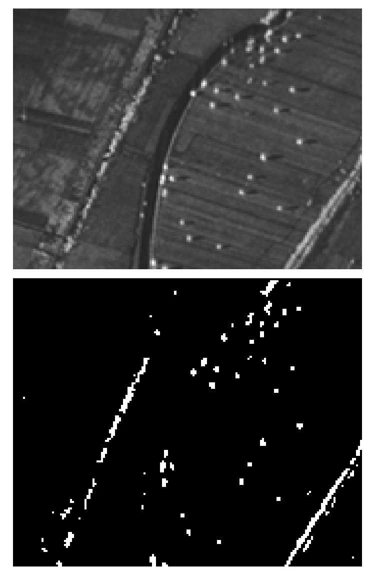

Group Sparsity

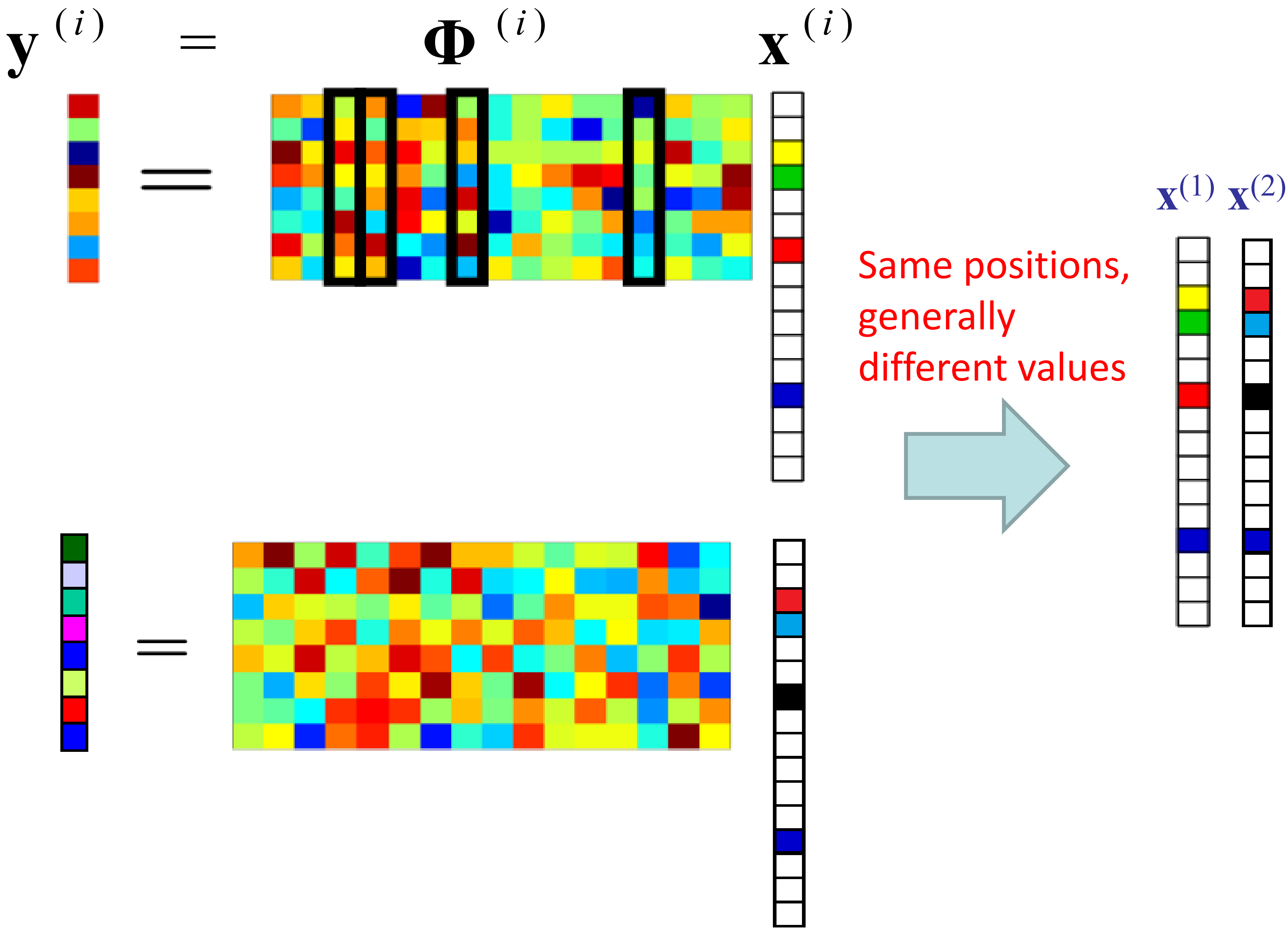

Group Sparsity in Practice

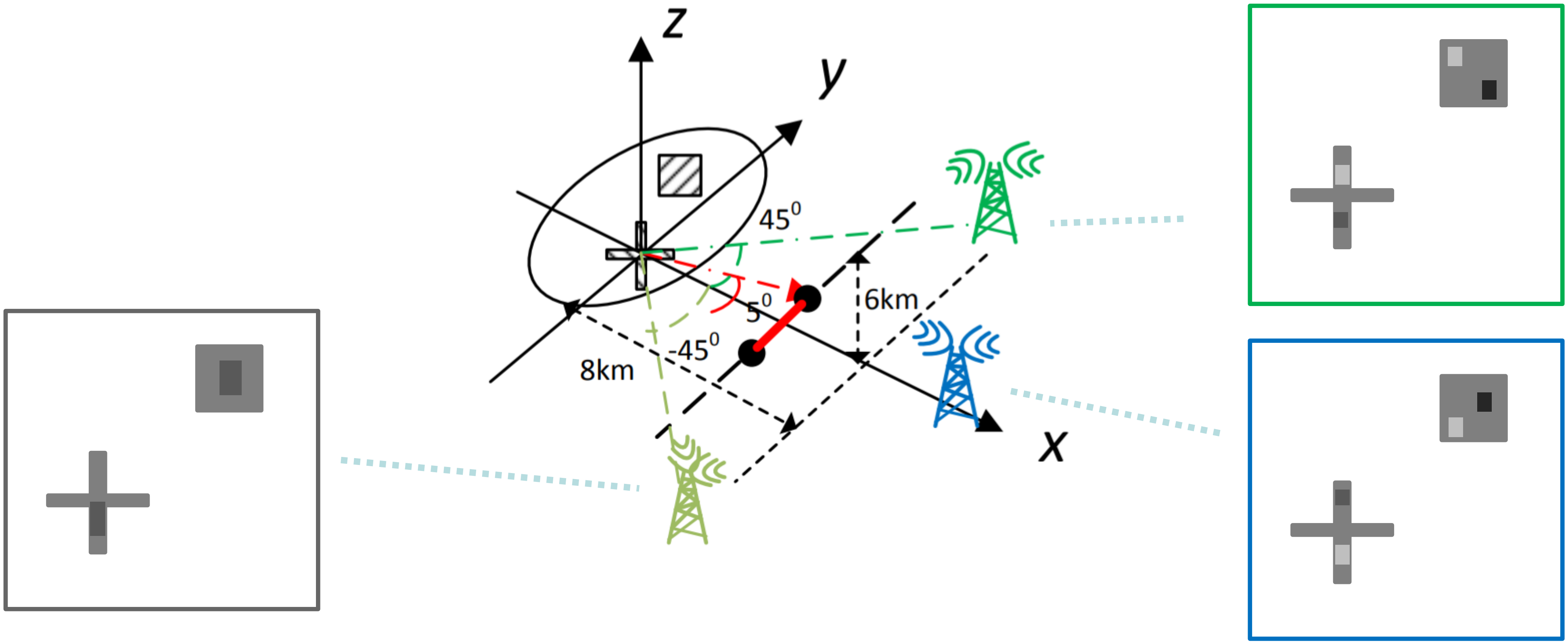

- Different aspect angles see target at the same position, but with different scattering coefficients

- Improve identification of nonzero positions

Group Sparsity Recovery

- OMP and Lasso use mixed l_2/l_1-norm (l_2-norm of the absolute values; also called l_{12}-norm) to handle signal group sparsity.

- l_1-norm relaxation ➔ mixed l_2/l_1-norm relaxation

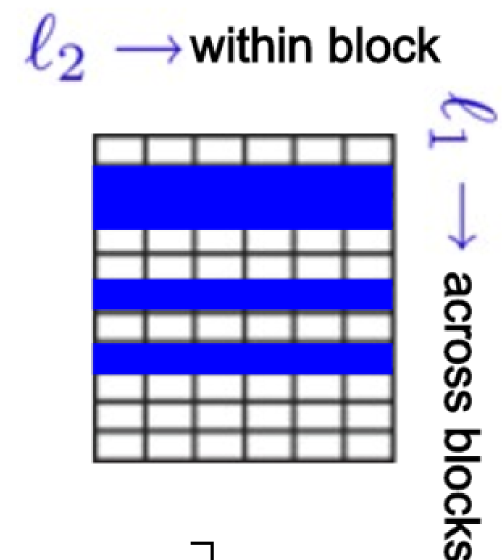

$$\min \|\mathbf{x}\|_{2,1} \quad \text{subject to } \mathbf{y} = \mathbf{\Phi x}$$

$$\min \|\mathbf{x}\|_{2,1} \quad \text{subject to } \|\mathbf{y} - \mathbf{\Phi x}\|_2 \le \varepsilon$$

where

$$\mathbf{y} = \begin{bmatrix} \mathbf{y}^{(1)} \\ \mathbf{y}^{(2)} \\ \vdots \\ \mathbf{y}^{(L)} \end{bmatrix} \qquad \mathbf{x} = \begin{bmatrix} \mathbf{x}^{(1)} \\ \mathbf{x}^{(2)} \\ \vdots \\ \mathbf{x}^{(L)} \end{bmatrix} \qquad \mathbf{\Phi} = \begin{bmatrix} \mathbf{\Phi}^{(1)} & & & \\ & \mathbf{\Phi}^{(2)} & & \\ & & \ddots & \\ & & & \mathbf{\Phi}^{(L)} \end{bmatrix}$$

Group Sparse Bayesian Learning
(Multitask Bayesian Compressive Sensing)

- In BCS, group sparse solutions can be achieved using the common prior across different groups

- Group sparse problem with $l = 1, \ldots, L$

$$\mathbf{y}_l = \mathbf{\Phi}_l \mathbf{x}_l + \boldsymbol{\varepsilon}_l, \quad \boldsymbol{\varepsilon}_l \sim N(\mathbf{0}, \beta_l \mathbf{I})$$

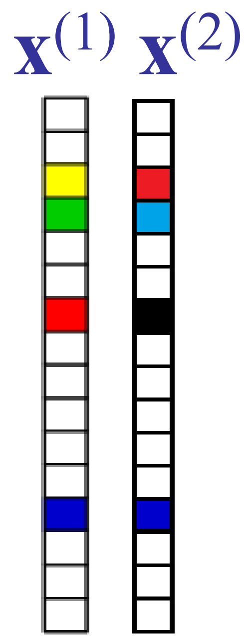

- Multitask BCS use the same prior for different groups:

$$p(\mathbf{y}_l \mid \mathbf{\Phi}_l, \mathbf{x}_l) = N(\mathbf{y}_l \mid \mathbf{\Phi}_l \mathbf{x}_l, \beta_l \mathbf{I})$$

Place Gaussian prior on $\mathbf{x}$

$$p(\mathbf{x}_l \mid \underline{\boldsymbol{\gamma}}) = \prod_i N(x_{l,i} \mid 0, \gamma_i)$$

- Notice that the **same** $\boldsymbol{\gamma}$ is used for all $\mathbf{x}_l$

Treatment of Complex Values

- BCS algorithms were developed based on real values

  S. Ji, D. Dunson, and L. Carin, "Multi-task compressive sampling," *IEEE Trans. Signal Processing*, vol. 57, no. 1, pp. 92-106, Jan. 2009

- To process complex values as required in radar sensing, many existing work decompose the signal model $\mathbf{y} = \mathbf{\Phi x}$ as

$$\begin{bmatrix} \text{real}(\mathbf{y}) \\ \text{imag}(\mathbf{y}) \end{bmatrix} = \begin{bmatrix} \text{real}(\mathbf{\Phi}) & -\text{imag}(\mathbf{\Phi}) \\ \text{imag}(\mathbf{\Phi}) & \text{real}(\mathbf{\Phi}) \end{bmatrix} \begin{bmatrix} \text{real}(\mathbf{x}) \\ \text{imag}(\mathbf{x}) \end{bmatrix}$$

  and treat $\text{real}(\mathbf{x})$ and $\text{imag}(\mathbf{x})$independently. However, this unnecessarily expands the dimension and sparse entries

- $\text{real}(\mathbf{x})$ and $\text{imag}(\mathbf{x})$ are group sparse because they are projection of the complex $\mathbf{x}$ to the real and imaginary axes

  Q. Wu, Y. D. Zhang, M. G. Amin, and B. Himed, "Complex multitask Bayesian compressive sensing," *IEEE ICASSP*, May 2014, pp. 3375-3379

- BCS based on complex Gaussian distribution is also available:

  D. Wipf and S. Nagarajan, "Beamforming using the relevance vector machine," *Int. Conf. Machine Learning*, pp. 1023–1030, 2007

Multi-static Radar SAR Imaging

Simulation example: three transmitters

- Digital Video Broadcasting–Terrestrial (DVB-T) signal (7.6 MHz bandwidth: 20 m mono-static range resolution)
- 5^o azimuth angle: same reflection coefficients corresponding to the same illuminator, but vary with different illuminators
- The proposed technique achieves 1-m resolution in both range and cross-range

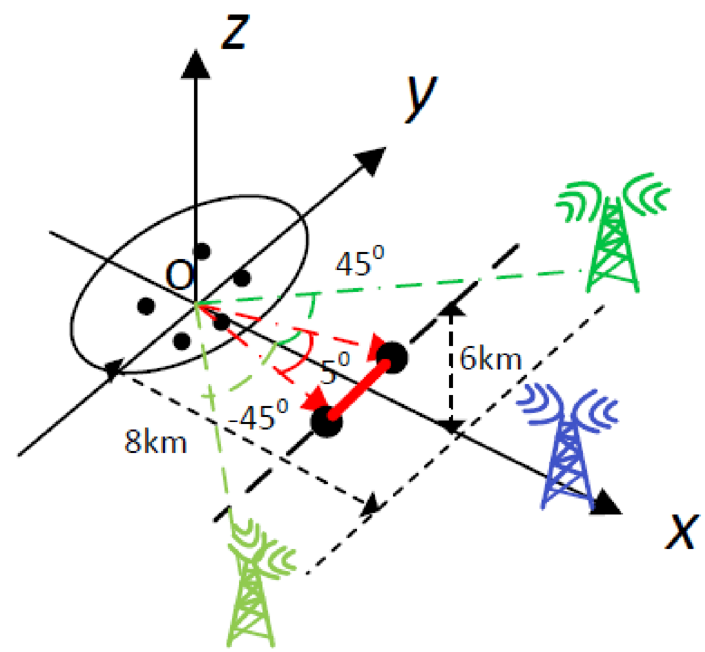

Q. Wu, Y. D. Zhang, M. G. Amin, and B. Himed, “Multi-static passive SAR imaging based on Bayesian compressive sensing,” *SPIE Compressive Sensing Conference*, May 2014

Multi-static Radar SAR Imaging

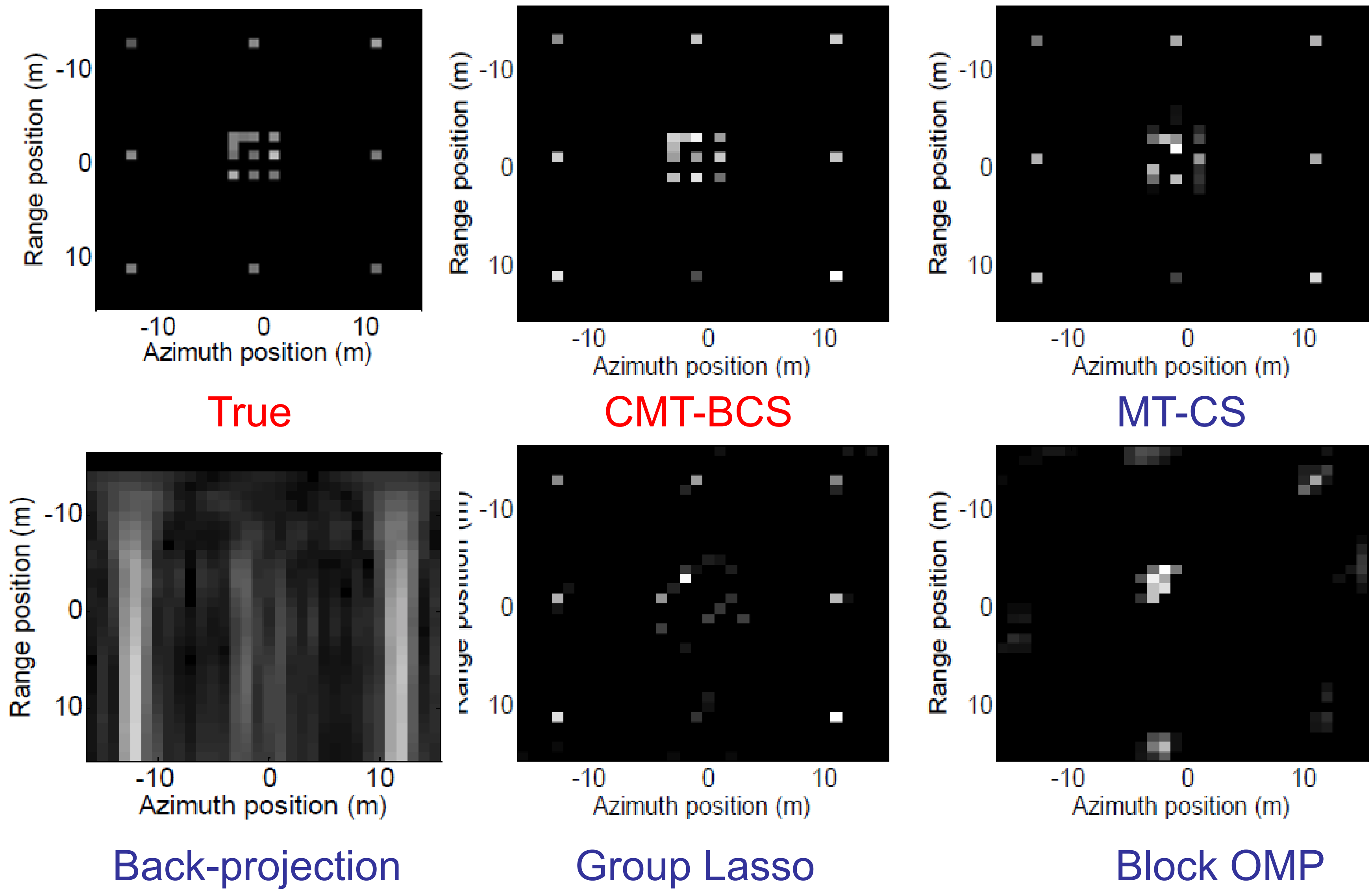

CMT-BCS: Complex multitask Bayesian compressive sensing

MT-CS: Multitask (Bayesian) compressive sensing

Outline

- Passive multi-static SAR imaging: Challenges
- Signal sparsity and compressive sensing
- Sparsity-based high-resolution SAR imaging
  - Group sparse SAR imaging
  - Structure-aware SAR imaging
- Sparsity-based space-time adaptive processing (STAP)
- Conclusions

Structure-Aware SAR Imaging

$$\mathbf{y} = \Phi\mathbf{x} + \varepsilon$$

Spike-and-slab prior for sparseness

$$p(\mathbf{x} \mid \boldsymbol{\pi}, \boldsymbol{\beta}) = \prod_{i=1}^{M} \left[(1-\pi_i)\delta(x_i) + \pi_i N(x_i \mid 0, \beta_i^{-1}) \right]$$

Increasing π_i will increase the probability of taking a non-zero value

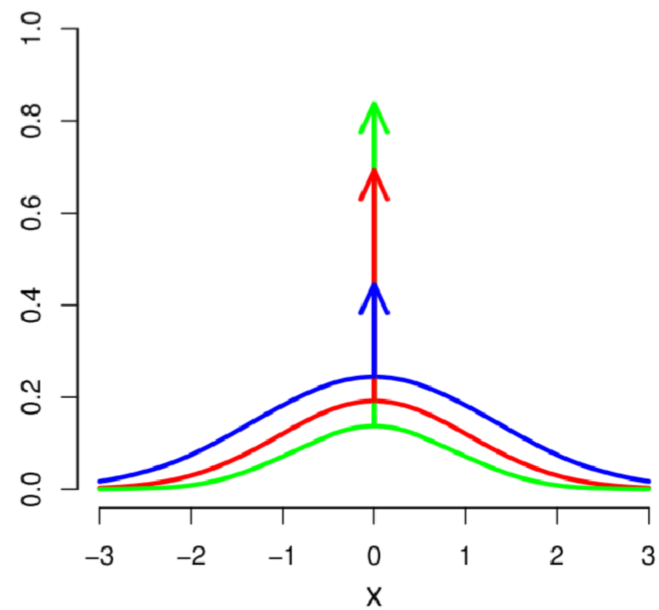

$$\mathbf{x} = \boldsymbol{\theta} \circ \mathbf{z}$$

Support $\mathbf{z}$ *is shared across* L *tasks*

$$p(\boldsymbol{\theta}) = \prod_{i=1}^{M} N(\theta_i \mid 0, \beta_i^{-1}) \qquad p(\mathbf{z}) = \prod_{i=1}^{M} \mathrm{Bern}(z_i \mid \pi_i)$$

L. Yu, H. Sun, J. P. Barbot, and G. Zheng, "Bayesian compressive sensing for cluster structured sparse signals," *Signal Processing*, vol. 92, no. 1, pp. 259-269, 2012

Structure-Aware SAR Imaging: Clustered BCS

Approach 1: Clustered BCS - Manually setting cluster prior for structure

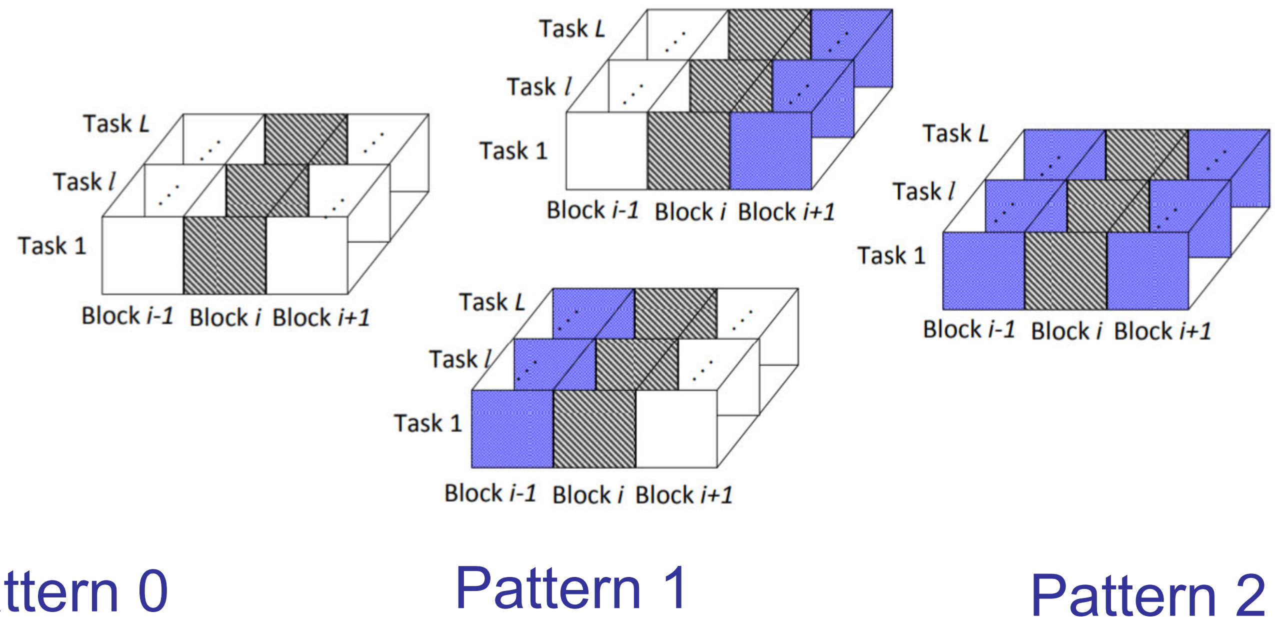

$$\pi_i = \begin{cases} \pi_i^0 \sim \mathrm{Beta}(e_0, f_0), & e_0 < f_0, \text{ if Pattern } 0 \\ \pi_i^1 \sim \mathrm{Beta}(e_1, f_1), & e_1 = f_1, \text{ if Pattern } 1 \\ \pi_i^2 \sim \mathrm{Beta}(e_2, f_2), & e_2 > f_2, \text{ if Pattern } 2 \end{cases}$$

L. Yu, H. Sun, J. P. Barbot, and G. Zheng, "Bayesian compressive sensing for cluster structured sparse signals," *Signal Processing*, vol. 92, no. 1, pp. 259-269, 2012

Q. Wu, Y. D. Zhang, M. G. Amin, and B. Himed, "Multi-task Bayesian compressive sensing exploiting intra-task correlation," *IEEE Signal Processing Letters*, vol. 22, no. 4, pp. 430-434, April 2015

Structure-Aware SAR Imaging: Kernel BCS

Approach 2: Kernel BCS - Enhance continuous structure through kernel design

$$\pi_i = \frac{1}{1 + e^{-\rho \gamma_i}}$$

$$\gamma \sim \mathcal{N}(0, \mathbf{\Sigma})$$

$$\Sigma_{ij} = \exp\left(-\frac{\|\mathbf{x}_i - \mathbf{x}_j\|^2}{2\sigma_0}\right)$$

where $\mathbf{x}_i$ and $\mathbf{x}_j$ are physical locations of the ith and jth pixels within the image, and $\sigma_0 > 0$ is a scale parameter

Closely spaced pixels are likely to have a high correlation in their support

Q. Wu, Y. D. Zhang, M. G. Amin, and B. Himed, "High-resolution passive SAR imaging exploiting structured Bayesian compressive sensing," *IEEE J. Selected Topics in Signal Processing*, vol. 9, no. 8, pp. 1484-1497, Dec. 2015

Simulation Example

Original image: TerraSAR-X SAR oil tanker imagery

- Scene size: 64×64
- Range and azimuth resolution: 1.5 m ×2 m.

Original image from: X. Xing, K. Ji, H. Zou, W. Chen, and J. Sun, "Ship classification in TerraSAR-X images with feature space based sparse representation," IEEE Geosci. Remote Sens. Lett., vol. 10, no. 6, pp. 1562–1566, 2013

Simulated Scene: For same DVB-T signals

- 2 transmitters located at -45^{o} and 0^{o} ; 1 moving receiver
- The second synthetic observation dataset is generated by randomly adding random magnitude and phase perturbations
- Full data used in Back projection: 512 azimuth x 256 range cells
- Data used for CS: 64 azimuth x 256 range cells

Q. Wu, Y. D. Zhang, M. G. Amin, and B. Himed, "High-resolution passive SAR imaging exploiting structured Bayesian compressive sensing," *IEEE J. Selected Topics in Signal Processing*, vol. 9, no. 8, pp. 1484-1497, Dec. 2015

Simulation Example

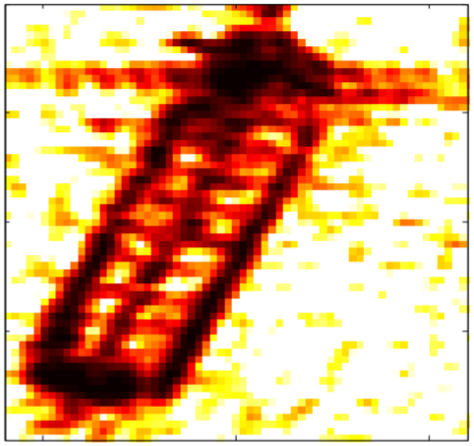

Original SAR image

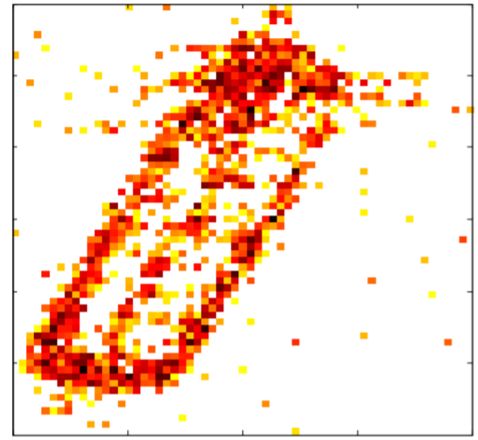

Back projection (full data)

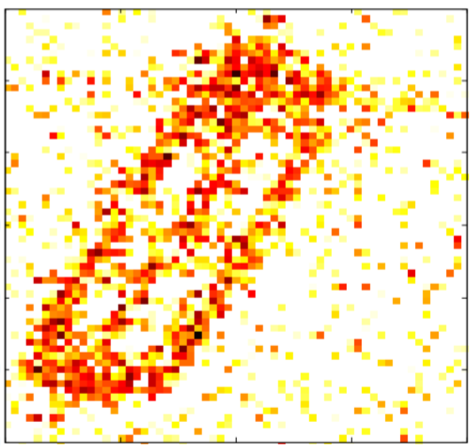

Multi-task-CS

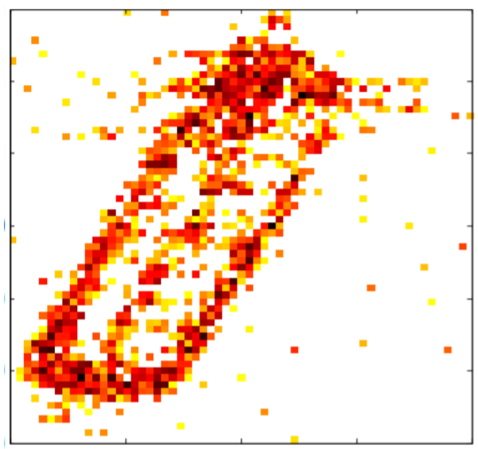

Clustered BCS

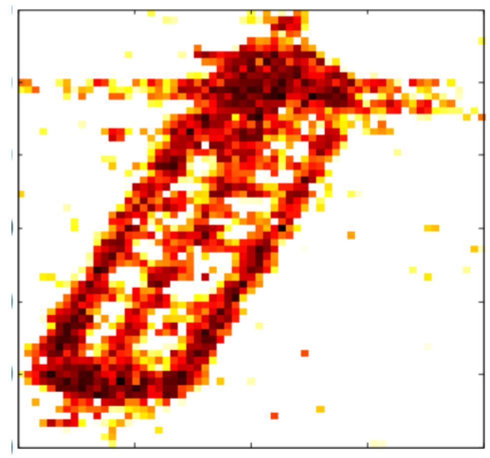

Kernel BCS

Outline

- Passive multi-static SAR imaging: Challenges
- Signal sparsity and compressive sensing
- Sparsity-based high-resolution SAR imaging
  - Group sparse SAR imaging
  - Structure-aware SAR imaging
- Sparsity-based space-time adaptive processing (STAP)
- Conclusions

Air-Borne Radar Clutter Characteristics

- Clutter Doppler frequency depends on scan direction
- Target Doppler frequency of depends on scan direction and target aspect angle

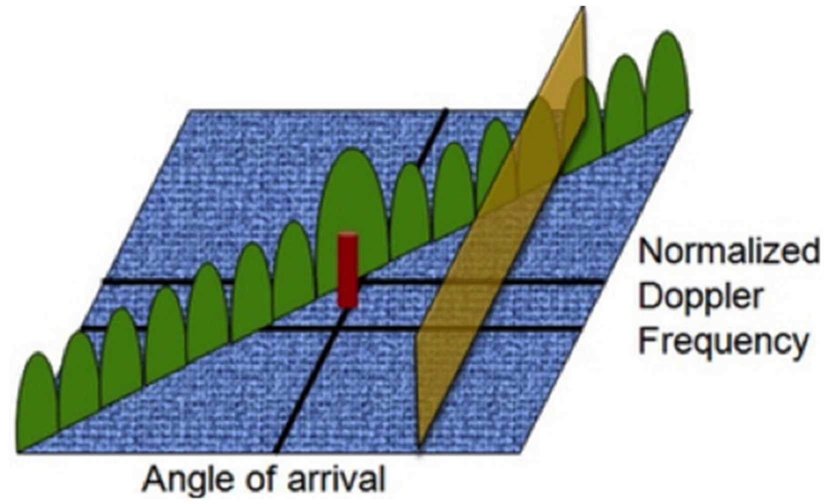

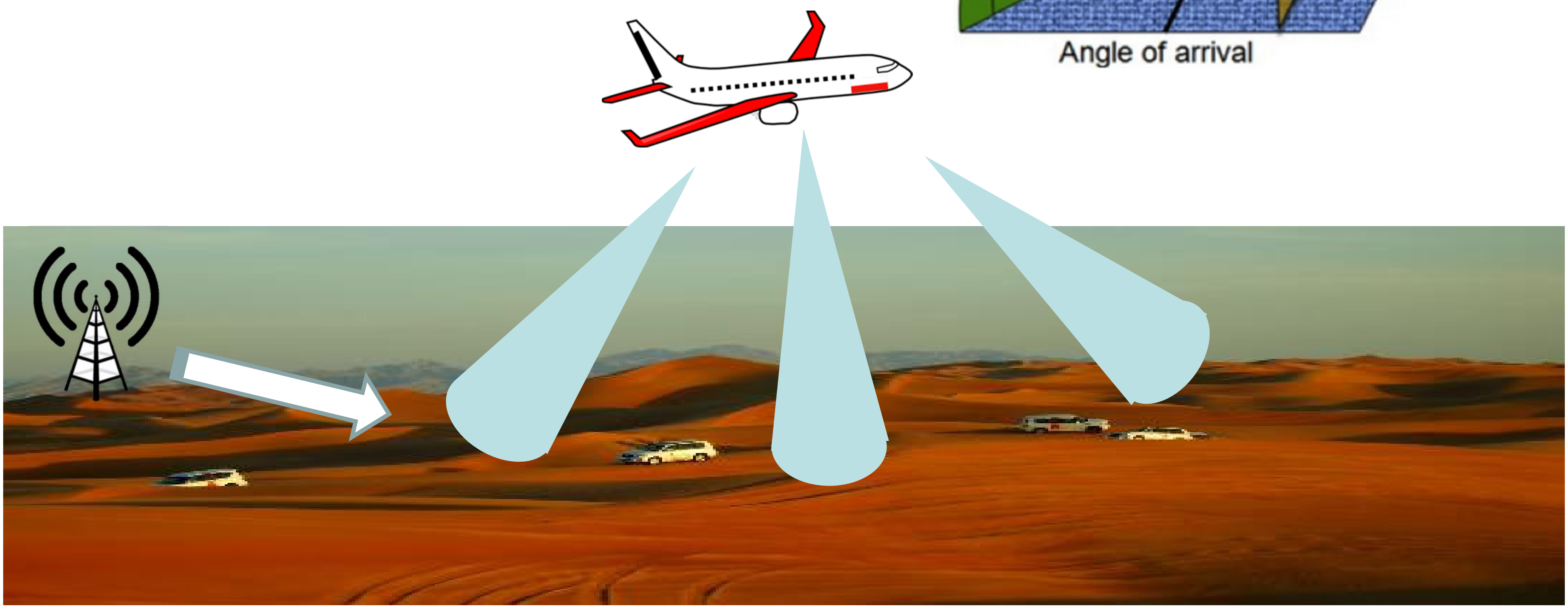

Space-Time Adaptive Processing

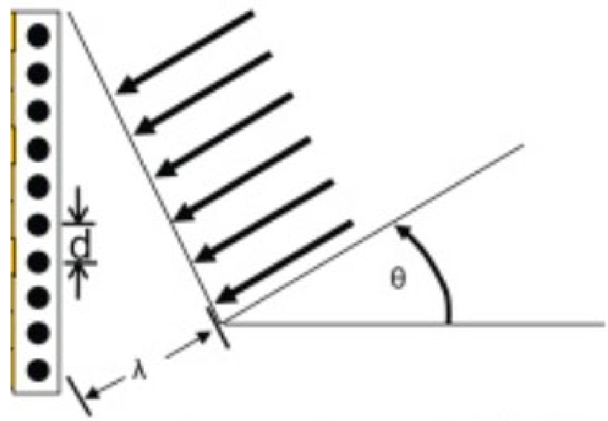

Array provides spatial dimensionality

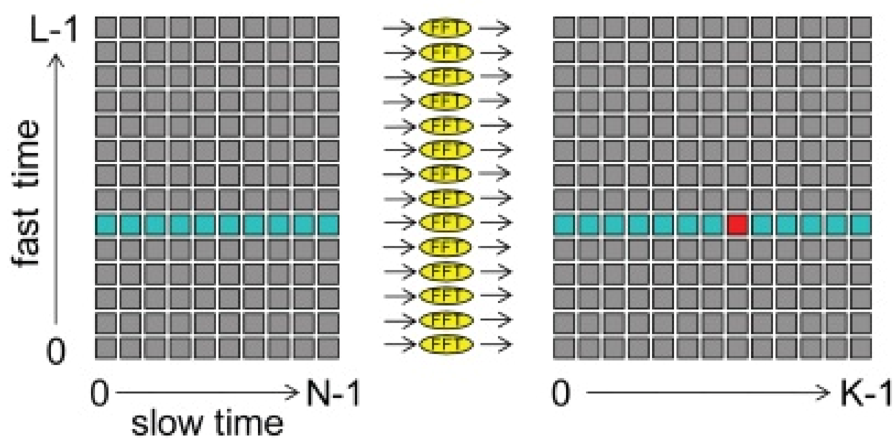

Slow time provides Doppler sensitivity

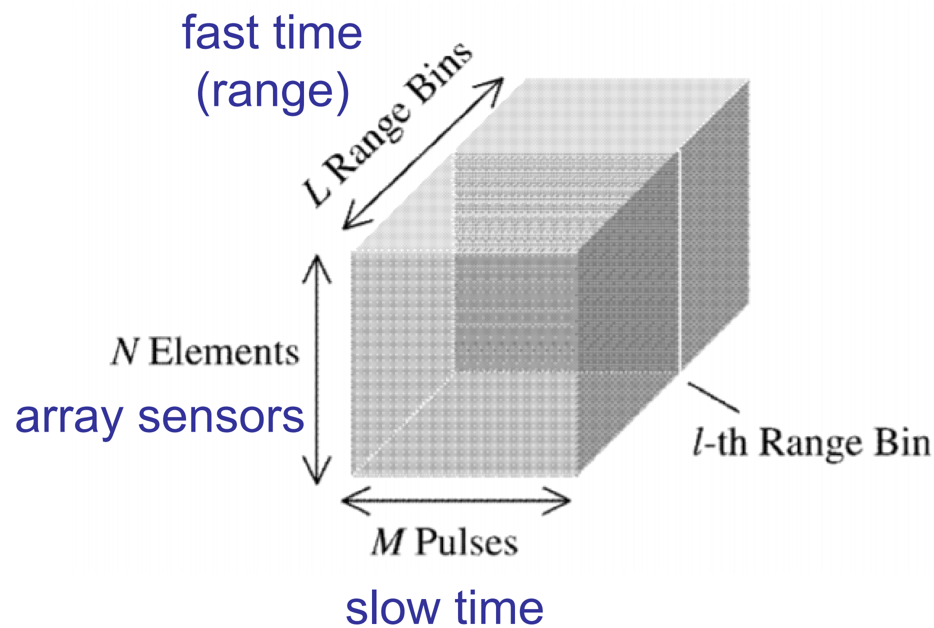

Space-Time Adaptive Processing

- In practice, the received signal is corrupted by ground clutter
- Fourier based angle-Doppler image
  - Low resolution
  - Slow targets falling within clutter region cannot be detected

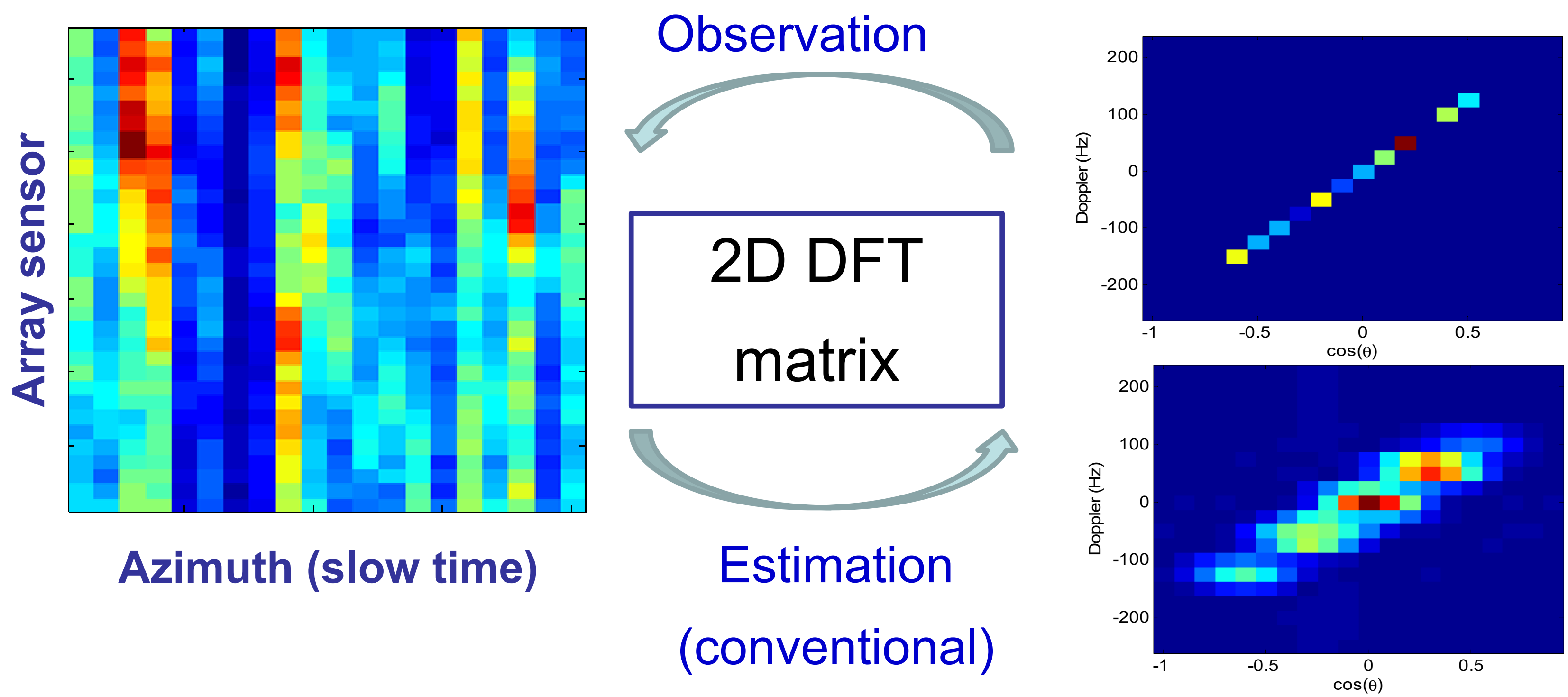

Space-Time Adaptive Processing

- Single domain processing does not provide desirable clutter suppression capability
- Space-time adaptive processing (STAP)
  - Ground clutter mitigation
  - Joint space and time domain
  - For slow-moving target detection
- Total dimension: NM from N antennas and M pulses

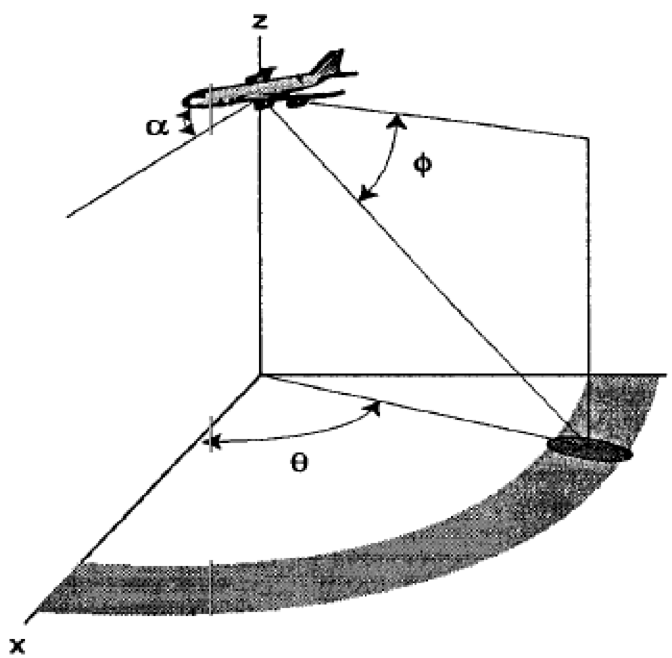

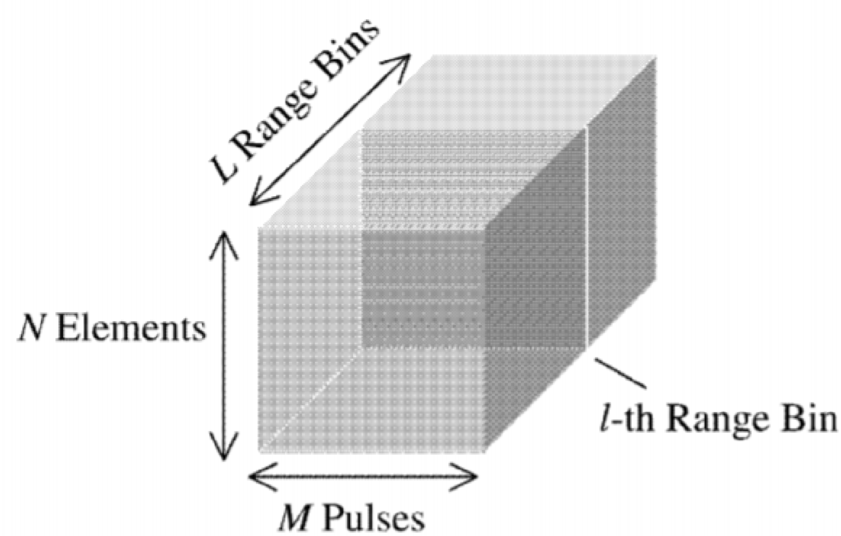

Space-Time Adaptive Processing

- STAP weight vector is determined by $\mathbf{w} = \mathbf{R}^{-1}\mathbf{y}_0$

  where $\mathbf{R}$ is the clutter covariance matrix, and $\mathbf{y}_0$ is the steering vector toward the target Doppler and angle

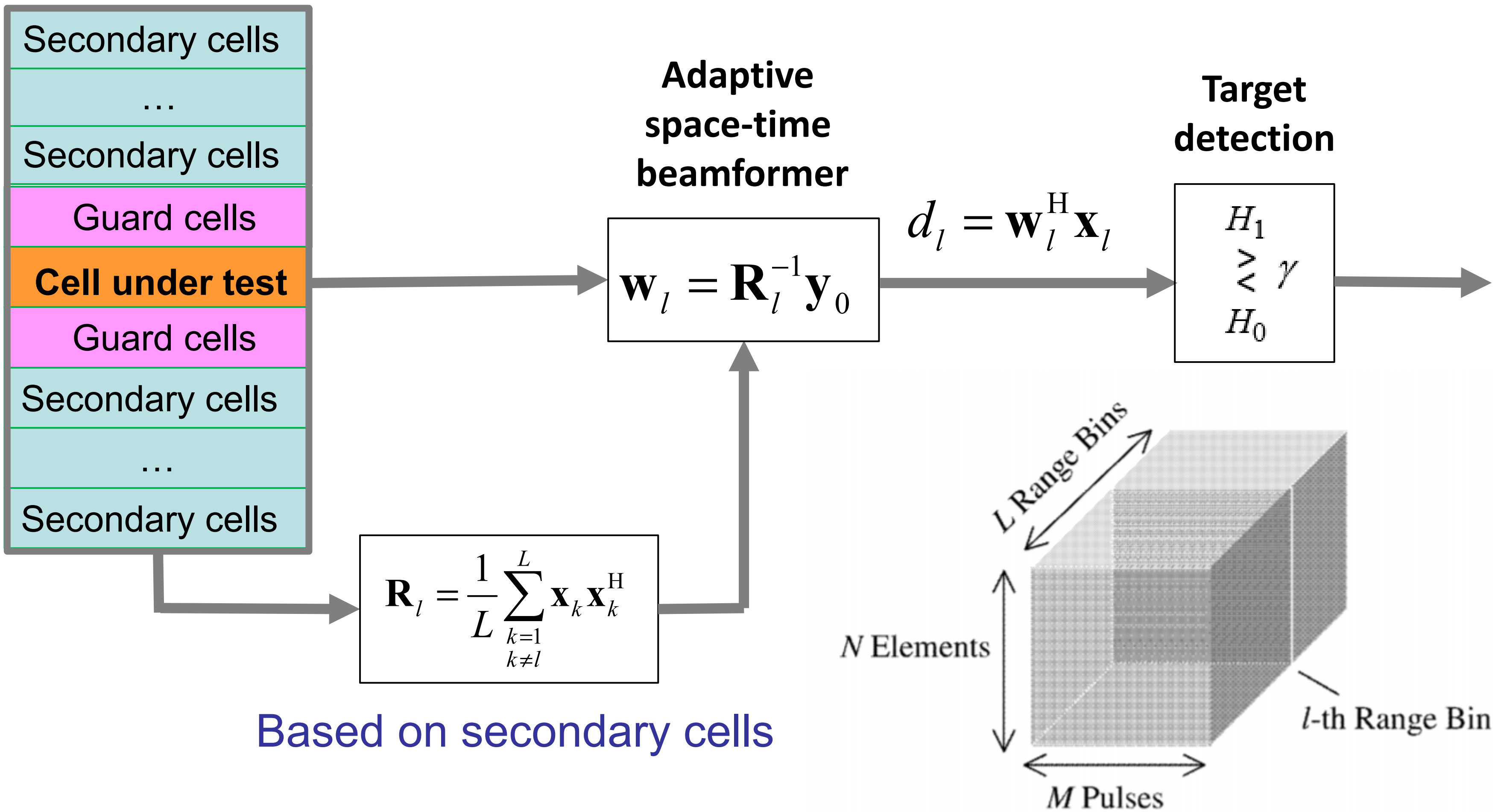

Space-Time Adaptive Processing

- When array axis coincides with the velocity vector, Doppler is
  - Range-independent and stationary in azimuth-Doppler
  - Linear to the cosine of cone angle

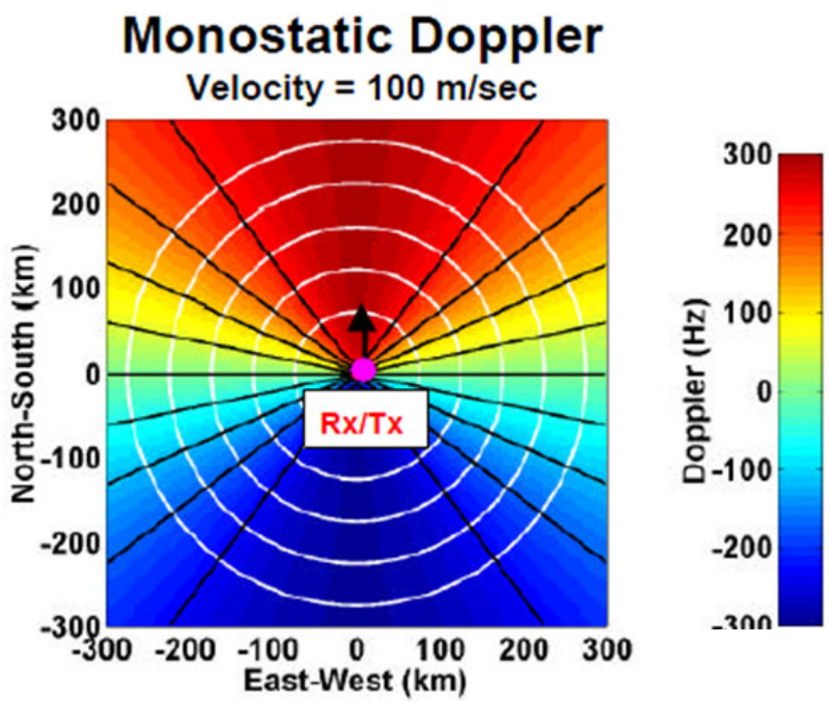

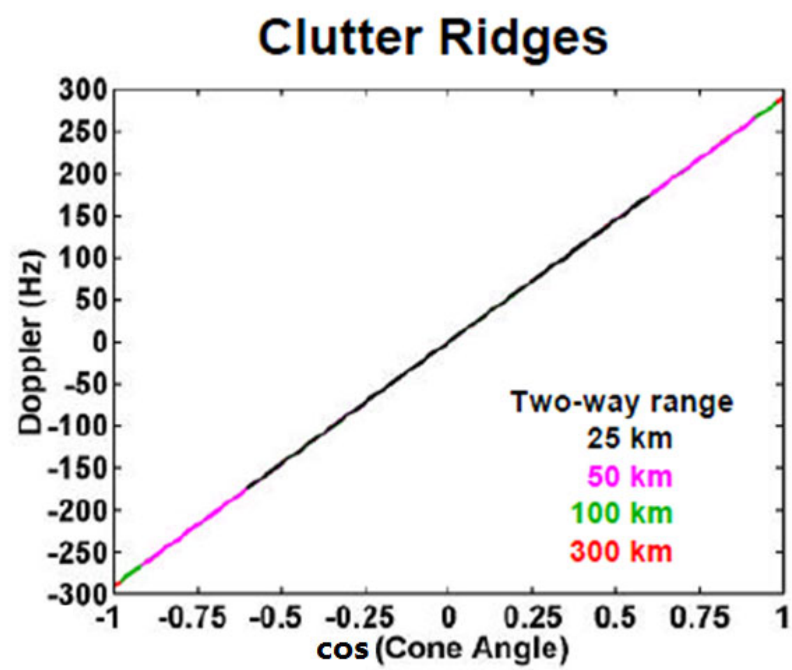

- Common reference point for Doppler and cone angles (Rx/Tx)
- Iso-Dopplers and Iso-Cones align

- Clutter ridge forms single locus in angle/Doppler
- Clutter cone angles limited by elevation angle (most noticable at near range)

Space-Time Adaptive Processing

- Key in STAP is to estimate clutter covariance matrix
- Estimation of the clutter covariance matrix requires $2MN$ i.i.d. Gaussian samples from neighboring range cells to achieve output SINR within 3 dB loss from Clairvoyant solution (RMB's rule)

  Reed, Mallett & Brennan, "Rapid convergence rate in adaptive arrays," Trans. Aerosp. Electron. Syst., vol. 10, no. 6, pp. 853-863, 1974

- Reduced-rank STAP algorithms require the number of secondary data samples to be at least twice the rank of the dominant clutter subspace

  J. Guerci, J. Goldstein, and I. Reed, "Optimal and adaptive reduced-rank STAP," IEEE Trans. Aerosp. Electron. Syst., vol. 36, no. 2, pp. 647–663, Apr. 2000

- The number of homogeneous neighboring range cells is limited in passive radar due to its low range resolution

Displacement Phase Center Antenna (DPCA)

- DPCA processing is an alternative technique for clutter suppression
- The basic concept of DPCA is to make the antenna appear stationary
- In pulse radar, when the antenna phase center displacement between two pulses equals to array antenna spacing, return from the shifted antenna is subtracted from the unshifted return
- Clutter will be cancelled whereas moving target will remain
- Because passive radar uses *continuous* broadcast or communication signals, it is more flexible to adjust the delays for better alignment

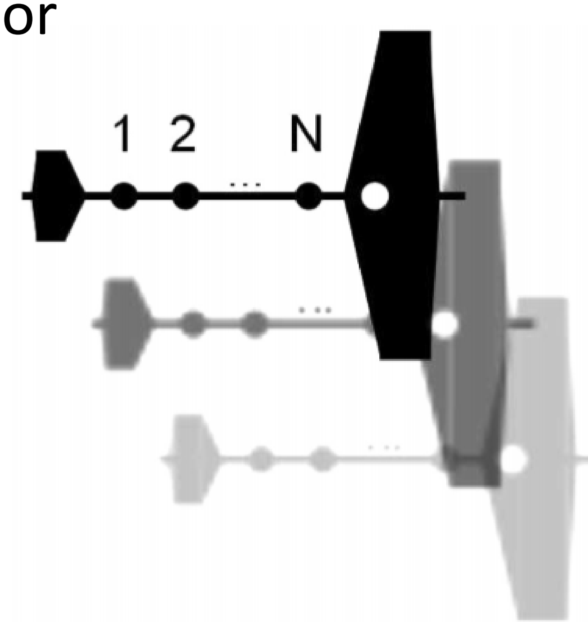

Consecutive positions of platform corresponding to displacement between antenna elements

B. Dawidowicz ; K. S. Kulpa ; M. Malanowski ; J. Misiurewicz ; P. Samczynski ; M. Smolarczyk, "DPCA detection of moving targets in airborne passive radar," IEEE Trans. Aerosp. Electron. Syst., vol. 48, no. 2, pp. 1347-1357, Apr. 2012

Displacement Phase Center Antenna (DPCA)

Experiment results: two-antenna on aircraft

B. Dawidowicz ; K. S. Kulpa ; M. Malanowski ; J. Misiurewicz ; P. Samczynski ; M. Smolarczyk, "DPCA detection of moving targets in airborne passive radar," IEEE Trans. Aerosp. Electron. Syst., vol. 48, no. 2, pp. 1347-1357, Apr. 2012

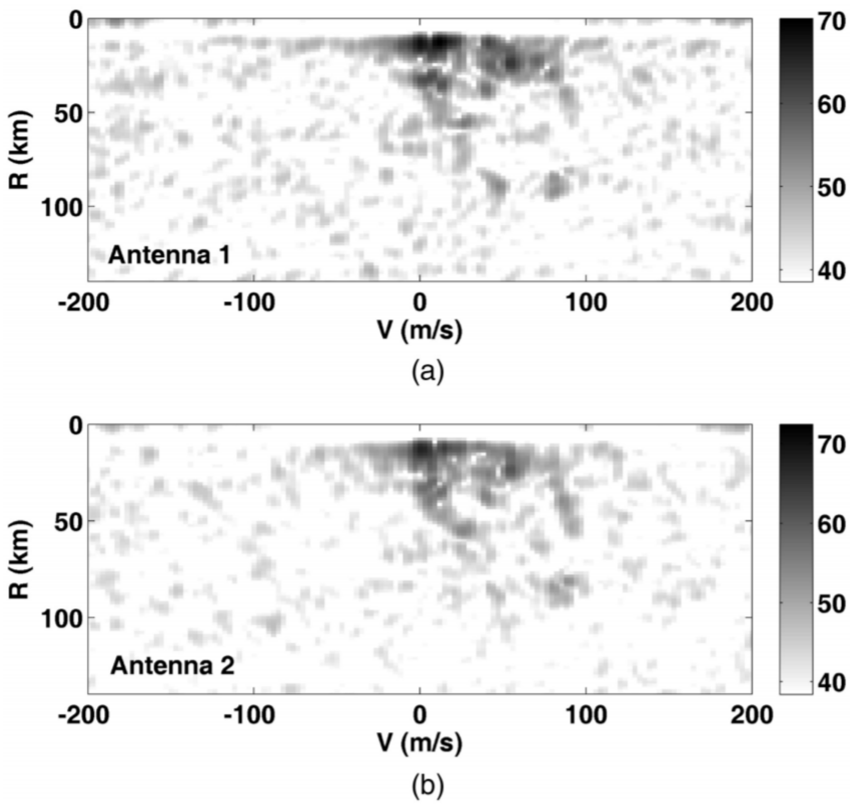

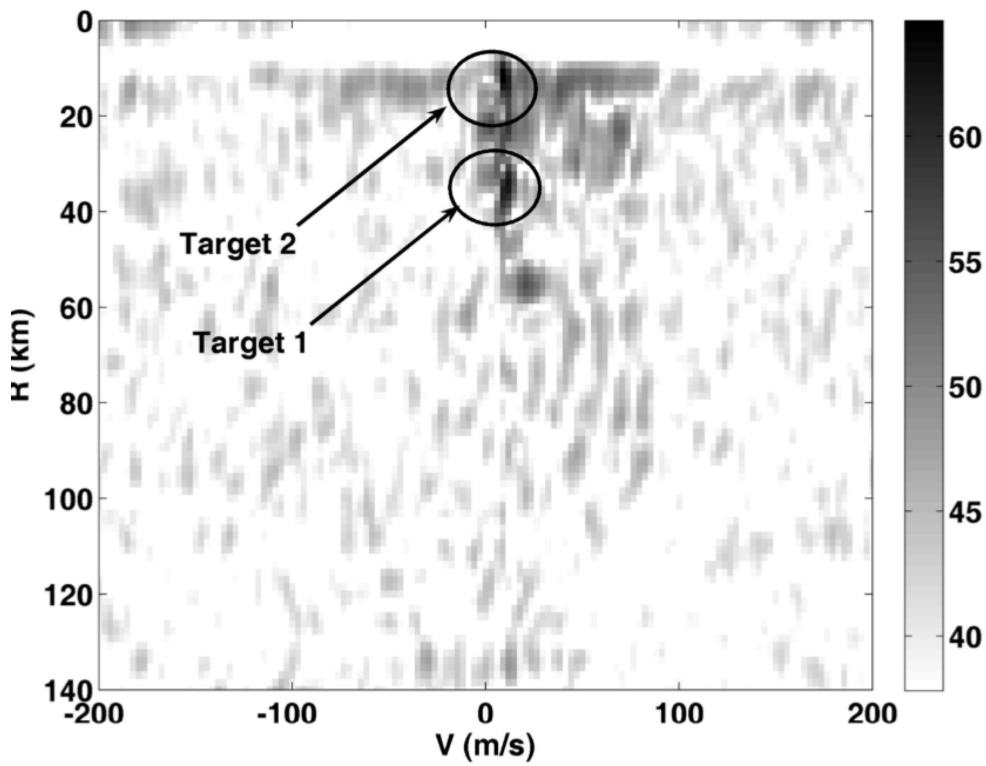

Clutter with 100 m/s spreading in bistatic velocity

DPCA suppresses clutter by approximately 30 dB

CS-based STAP

- A recent approach is to estimate the clutter covariance matrix exploiting the clutter sparsity in the angle-Doppler domain
- **Group sparsity:** Clutter components in nearby range cells are likely to share the same support
- Significantly relaxed when comparing to traditional reduced-rank STAP

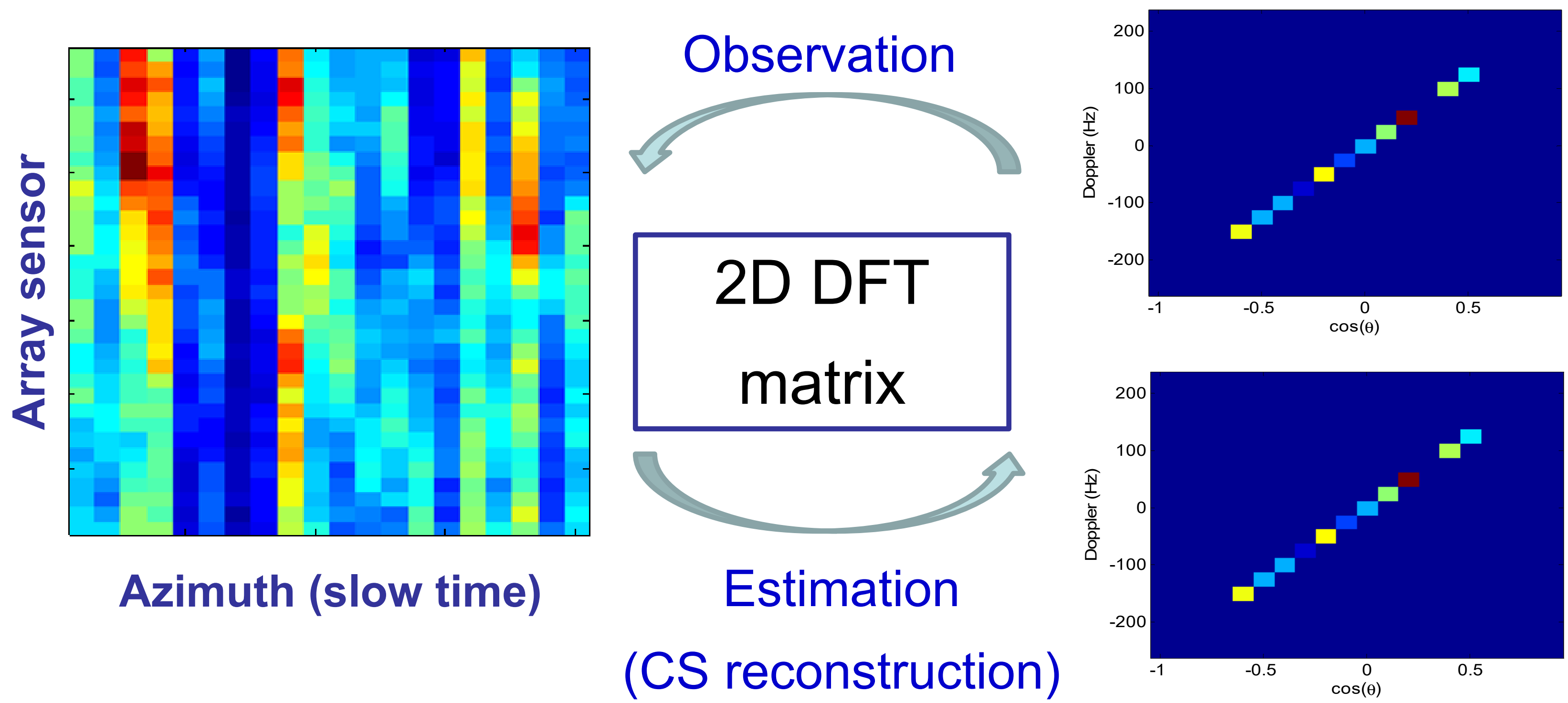

CS-based STAP

- Due to the sparsity of the clutter in angle–Doppler domain, clutter spectrum can be sparsely recovered using only one or few samples.
- Sparse clutter profile estimates used to construct the clutter covariance matrix
  - Clutter at each secondary range cell is separately estimated in the Bayesian framework

    J. T. Parker and L.C. Potter, "A Bayesian perspective on sparse regularization for STAP post-processing," IEEE Radar Conf., May 2010, pp. 1471–1475
  - Clutter profile is estimated separately at each range cell, then the maximum value is chosen for each angle–Doppler entry from all range cells being evaluated

    K. Sun, H. Meng, Y. Wang, and X. Wang, "Direct data domain STAP using sparse representation of clutter spectrum," Signal Process., vol. 91, no. 9, pp. 2222–2236, Sep. 2011.
  - Group sparsity of the clutter across range cells not used
- No guarantee to exclude target signals from the estimated clutter

Signal Model

- Target signal stacked over L azimuth samples

targets
Tx power
gain
RCS coefficient

$$\mathbf{y}_{is} = \sum_{q=1}^{Q} \frac{\sqrt{P_{T_i}}G_{iq}\sigma_{iq}}{r_{T_i q} r_{qr}} \mathbf{h}(\nu_{iq}, \phi_q)$$

Tx-target range (ith Tx)
Target-Rx range
Angle-Doppler steering vector

- Clutter stacked over L azimuth samples

$$\mathbf{y}_{ic} = \sum_{m=1}^{N_c} \frac{\sqrt{P_{T_i}}G_{im}\sigma_{im}}{r_{T_i m} r_{mr}} \mathbf{h}(\nu_{im}, \phi_m)$$

- At the range cell under test

$$\begin{aligned}\mathbf{y}_i &= \mathbf{y}_{is} + \mathbf{y}_{ic} + \mathbf{y}_{in} \\ &= \mathbf{\Phi}_i(\mathbf{x}_{is} + \mathbf{x}_{ic}) + \mathbf{y}_{in}\end{aligned}$$

- At the n_l-th secondary range cells

$$\begin{aligned}\mathbf{y}_i^{(n_l)} &= \mathbf{y}_{in}^{(n_l)} + \mathbf{y}_{in}^{(n_l)} \\ &= \mathbf{\Phi}_i \mathbf{x}_{in}^{(n_l)} + \mathbf{y}_{in}^{(n_l)}\end{aligned}$$

Single-cell Based CS Approach

- At range cell under test

$$\mathbf{y}_i = \Phi_i(\mathbf{x}_{is} + \mathbf{x}_{ic}) + \mathbf{y}_{in}$$

- Clutter angle-Doppler profile can be estimated through sparse reconstruction at the range cell under test
  - For weak target, it yields clutter angle-Doppler signature $\mathbf{x}_{ic}$
  - When target is strong, $\mathbf{x}_{is}$ may be included in the estimated clutter profile, yielding undesired target suppression
- Additional steps are required to ensure signal-free from the constructed clutter covariance matrix

CS-based STAP: Proposed

Group sparse clutter angle-Doppler profile estimation from secondary data

↓

Angle-Doppler region determination based on clutter support

↓

Clutter angle-Doppler profile estimation from cell under test data

↓

Clutter covariance matrix reconstruction

↓

STAP - clutter suppression and target detection

CS-based STAP: Proposed

- Solve the common clutter support from N_t secondary range cells

$$\mathbf{y}_i^{(n_l)} = \mathbf{\Phi}_i \mathbf{x}_{in}^{(n_l)} + \mathbf{y}_{in}^{(n_l)}$$

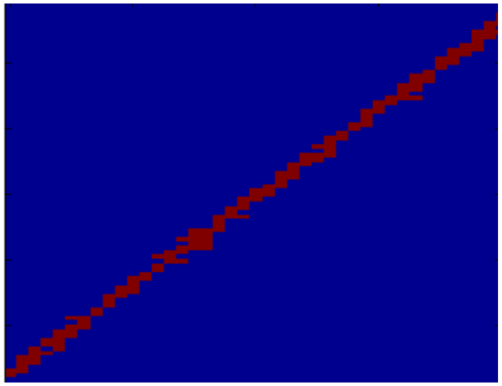

- Construct a new dictionary matrix $\mathbf{\Phi}_{i,cs}$ from $\mathbf{\Phi}_i$
  - $\mathbf{\Phi}_{i,cs}$ only includes entries corresponding to the clutter support obtained above

- Sparsely reconstruct clutter in the range under test, confined within the clutter support (through the new dictionary matrix)

$$\mathbf{y}_i^{(\mathrm{t})} = \mathbf{\Phi}_{i,cs} \mathbf{x}_{ic}^{(\mathrm{t})} + \mathbf{y}_{in}^{(\mathrm{t})}$$

- Estimate the clutter covariance matrix from the estimated $\hat{\mathbf{x}}_{ic}^{(\mathrm{t})}$

$$\hat{\mathbf{R}}^{(i)} = \sum_{m=1}^{M} |\hat{\mathbf{x}}_{ic}^{(\mathrm{t})}(\nu_{im}, \varphi_m)|^2 \mathbf{h}(\nu_{im}, \varphi_m)\mathbf{h}^H(\nu_{im}, \varphi_m) + \beta_{i,0}\mathbf{I}_{NL}$$

Q. Wu, Y. D. Zhang, M. G. Amin, and B. Himed, "Space-time adaptive processing and motion parameter estimation in multistatic passive radar using sparse Bayesian learning," IEEE Trans. Geoscience and Remote Sensing, vol. 54, no. 2, pp. 944 - 957, Feb. 2016

CS-based STAP: Proposed

- Sparse reconstruction enables accurate estimation of the clutter covariance matrix
  - from a small number of secondary samples
  - due to intrinsic sparsity of the clutter in the angle-Doppler domain
- Target exclusion in the estimated clutter profile
  - exploiting the common clutter support across nearby range cells
- Utilization of group sparsity
  - complex multi-task BCS methods provide more robust sparse reconstruction than other CS methods
- Offerings
  - does not require secondary samples to be i.i.d.
  - only require small number of secondary data samples

Simulation Example

- Carrier frequency 800 MHz with 20 MHz bandwidth
- 20-element uniform linear array with half-wavelength spacing
- Azimuth sampling frequency 600 Hz
- 30 azimuthal samples are used
- Simulation with N_t = 4 nearby secondary samples
- Clutter profile is discretized into 90 Doppler bins in −300 ~ 300 Hz and 40 angle bins in -180^o ~ 180^o
- Gaussian noise is added with clutter-to-noise ratio of 40 dB
- Insufficient samples to perform conventional sample matrix inversion based approach

Simulation Results

Clutter support obtained from four nearby secondary samples using multi-task Bayesian CS

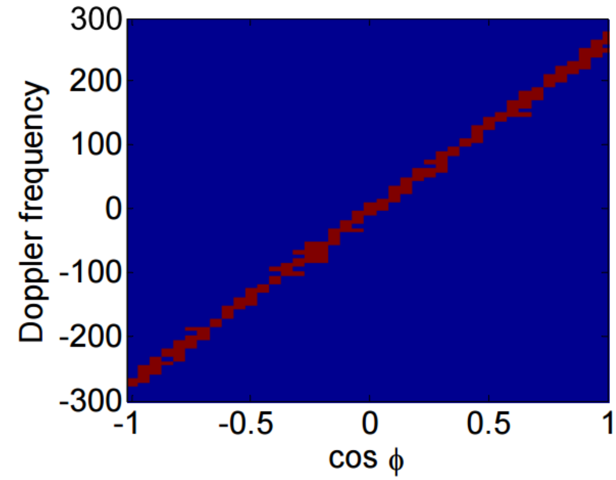

Estimated clutter profile at the range cell under test (confined within the clutter support)

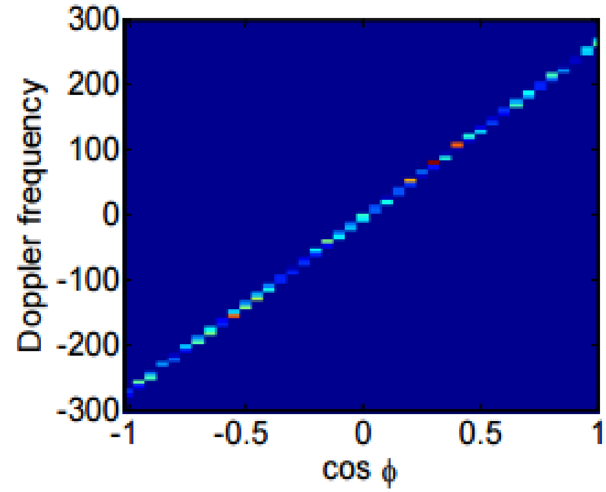

Clutter Support Estimation: Comparison with Other CS Methods

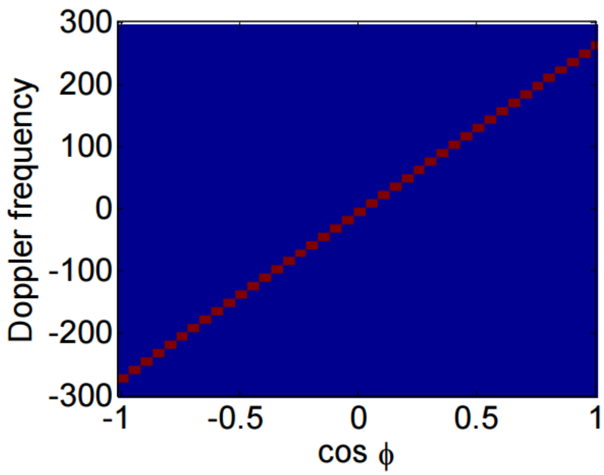

True clutter support

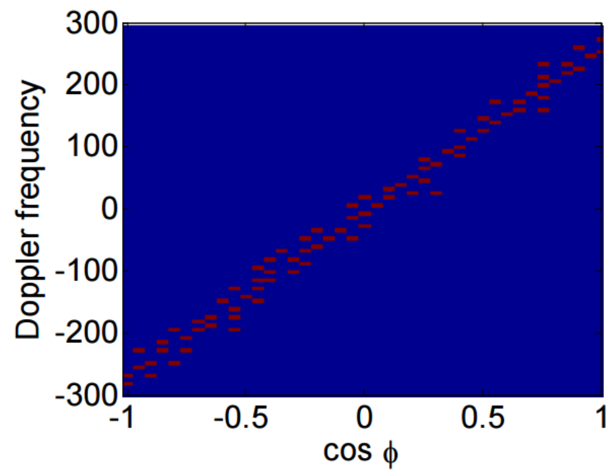

From block OMP

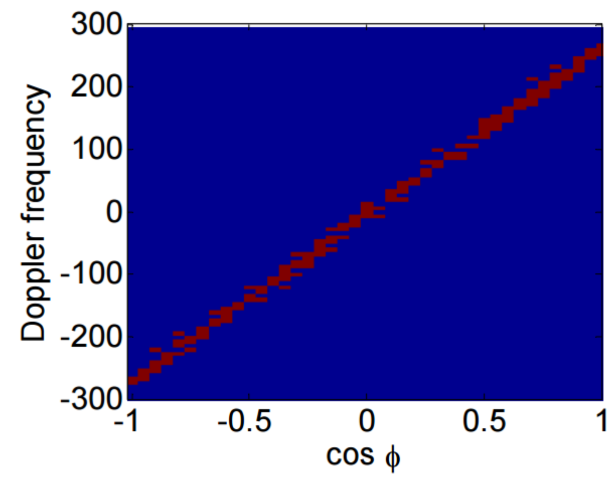

From group Lasso

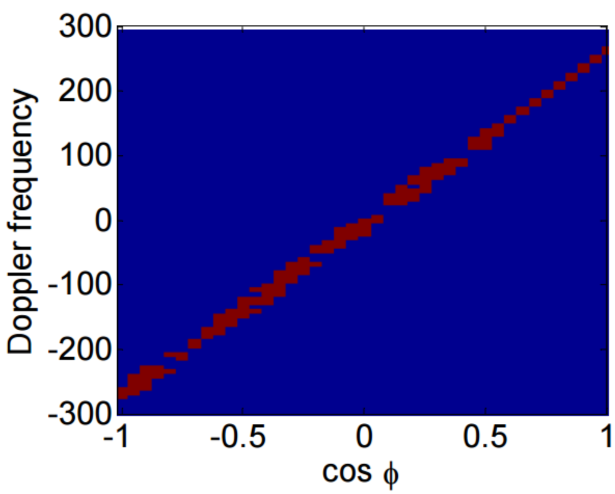

From M-FOCUSS

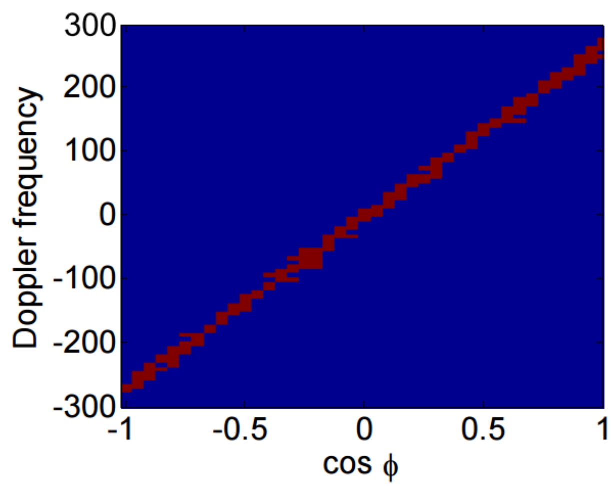

From complex multi-task Bayesian CS (proposed)

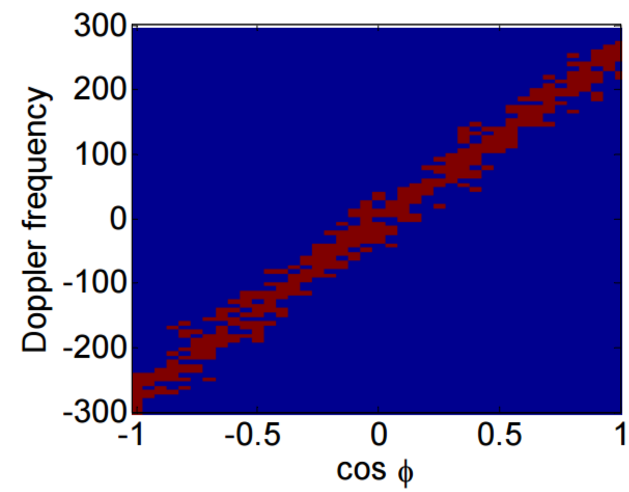

From Bayesian CS

Simulation Results

Output SINR loss

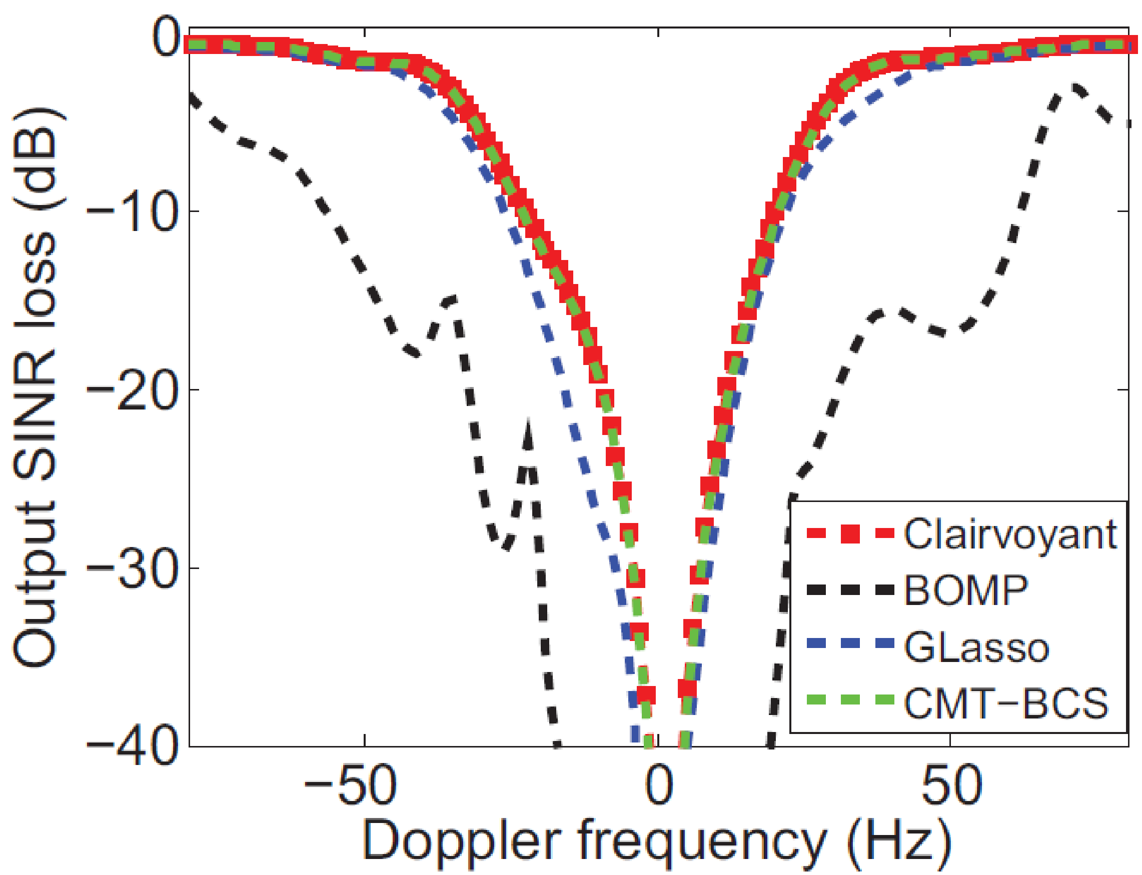

Outline

- Passive multi-static SAR imaging: Challenges
- Signal sparsity and compressive sensing
- Sparsity-based high-resolution SAR imaging
  - Group sparse SAR imaging
  - Structure-aware SAR imaging
- Sparsity-based space-time adaptive processing (STAP)
- Conclusions

Conclusions

- Passive radar may suffer from low resolution in radar imaging, and find difficult in achieving robust STAP primarily due to narrow signal bandwidth
- CS and sparse reconstruction, particularly with the use of signal group sparsity and structures, are capable tools for effective radar imaging and STAP
- Bayesian compressive sensing (BCS) techniques
  - Achieve l_0-norm solution
  - Insensitive to sensing matrix coherence
  - Flexibly use priors to exploit sparsity structures
- Group and structure-aware BCS provides powerful capabilities for passive radar applications to achieve
  - High-resolution SAR imaging
  - Effective STAP for clutter mitigation

Backup Slides
Cross-Correlator in the Presence of Noisy Reference and DPI

Performance of CC with Noisy Reference and DPI

- Define SNR in both channels and interference-to-noise ratio (INR) in SC

$$\mathrm{SNR_s} = 10\log_{10}\frac{|\alpha|^2}{\sigma_w^2}, \quad \mathrm{SNR_r} = 10\log_{10}\frac{|\beta|^2}{\sigma_v^2}, \quad \mathrm{INR_s} = 10\log_{10}\frac{|\gamma|^2}{\sigma_w^2}$$

- **Main Result:** To ensure a performance loss of no more than δ dB relative to the MF for a given $\mathrm{SNR_s}$, the $\mathrm{INR_s}$ and $\mathrm{SNR_r}$ for the CC detector must satisfy (in dB)

$$\boxed{\begin{aligned} \mathrm{INR_s} &\le 10\log_{10}\left[\frac{10^{\frac{\delta+\mathrm{SNR_r}}{10}} - 10^{\frac{\delta+\mathrm{SNR_s}}{10}} - 10^{\frac{\mathrm{SNR_r}}{10}} - 1}{1+10^{\frac{\mathrm{SNR_r}}{10}}}\right] \\ \mathrm{SNR_r} &\ge 10\log_{10}\left[\frac{10^{\frac{\mathrm{INR_s}}{10}} + 10^{\frac{\delta+\mathrm{SNR_s}}{10}} + 1}{10^{\frac{\delta}{10}} - 10^{\frac{\mathrm{INR_s}}{10}} - 1}\right] \end{aligned}}$$

J. Liu, H. Li, and B. Himed, "On the performance of the cross-correlation detector for passive radar applications," *Signal Processing*, vol.113, pp.32-37, Aug. 2015

Sketch of Proof

- Apply central limit theorem on $T_{\mathsf{CC}} \triangleq |\bar{T}|^2 = \left| \sum_{n=0}^{N-1} x_{\mathsf{s}}^*(n) x_{\mathsf{r}}(n-\tau) \exp(j\Omega_d n) \right|^2$

$$\bar{T} \sim \mathcal{CN}(\mu_i, \sigma_i^2), \quad i = 0 \text{ for } H_0 \text{ and } i = 1 \text{ for } H_1$$

$$\mu_0 = 0, \quad \sigma_0^2 = N(|\gamma|^2|\beta|^2 + |\gamma|^2\sigma_v^2 + |\beta|^2\sigma_w^2 + \sigma_v^2\sigma_w^2)$$

$$\mu_1 = N\alpha^*\beta, \quad \sigma_1^2 = N(|\gamma|^2|\beta|^2 + |\gamma|^2\sigma_v^2 + \phi|\alpha|^2|\beta|^2 + |\alpha|^2\sigma_v^2 + |\beta|^2\sigma_w^2 + \sigma_v^2\sigma_w^2)$$

- This leads to the false alarm/detection probabilities for the CC

$$P_{\mathsf{FA}} = \exp\left(-\frac{\lambda}{\sigma_0^2}\right), \quad P_{\mathsf{D}} = Q_1\left(\sqrt{\frac{2|\mu_1|^2}{\sigma_1^2}}, \sqrt{\frac{2\sigma_0^2 \ln(P_{\mathsf{FA}}^{-1})}{\sigma_1^2}}\right)$$

- Above expressions also hold for the MF by setting $\sigma_v^2 = 0$ and $\gamma = 0$
- Our result follows by setting Type equation here.

$$P_{\mathsf{D}}^{\mathsf{CC}}(\mathsf{SNR_s} + \delta) \geq P_{\mathsf{D}}^{\mathsf{MF}}(\mathsf{SNR_s})$$

and comparing the expressions

Backup Slides
Passive Detection with Noisy Reference

Summary of 4 GLRTs with Noisy Reference

- Deterministic IO waveform **s**, unknown noise power η:

$$T_1 = \frac{\widehat{\eta}_0}{\widehat{\eta}_1} = \frac{\|\mathbf{x}_t\|^2}{\|\mathbf{x}_t\|^2 + \|\mathbf{x}_r\|^2 - \sqrt{(\|\mathbf{x}_t\|^2 - \|\mathbf{x}_r\|^2)^2 + 4|\mathbf{x}_t^\dagger \mathbf{x}_r|^2}} \underset{H_0}{\overset{H_1}{\gtrless}} \gamma_1$$

- Deterministic **s**, known η:

$$T_2 = \frac{1}{\eta}\left(\|\mathbf{x}_t\|^2 - \|\mathbf{x}_r\|^2 + \sqrt{(\|\mathbf{x}_t\|^2 - \|\mathbf{x}_r\|^2)^2 + 4|\mathbf{x}_t^\dagger \mathbf{x}_r|^2}\right) \underset{H_0}{\overset{H_1}{\gtrless}} \gamma_2$$

- Stochastic **s**, known η:

$$\frac{\|\mathbf{x}_r\|^{2N}}{(\widehat{a}^2 + \widehat{b}^2 + \eta)^N} \exp\left(\frac{\|\mathbf{x}_t\|^2 \widehat{a}^2 - (\widehat{a}^2 + \eta)\|\mathbf{x}_r\|^2 + 2\widehat{a}\widehat{b}|\mathbf{x}_t^\dagger \mathbf{x}_r|}{\eta(\widehat{a}^2 + \widehat{b}^2 + \eta)}\right) \underset{H_0}{\overset{H_1}{\gtrless}} \gamma_3$$

$$a = |\alpha| \quad \text{and} \quad b = |\beta|$$

- Stochastic **s**, known η:

$$\frac{\|\mathbf{x}_r\|^{2N}\|\mathbf{x}_t\|^{2N}}{\widehat{\eta}^N(\widehat{a}^2 + \widehat{b}^2 + \widehat{\eta})^N} \exp\left(-\frac{(\widehat{b}^2 + \widehat{\eta})\|\mathbf{x}_t\|^2 + (\widehat{a}^2 + \widehat{\eta})\|\mathbf{x}_r\|^2 - 2\widehat{a}\widehat{b}|\mathbf{x}_t^\dagger \mathbf{x}_r|}{\widehat{\eta}(\widehat{a}^2 + \widehat{b}^2 + \widehat{\eta})}\right) \underset{H_0}{\overset{H_1}{\gtrless}} \gamma_4$$

Deterministic GLRT: Unknown Noise Power

- The likelihood function under hypothesis H_1 is

$$L_1 = \frac{1}{\pi^{2N}\eta^{2N}} \exp\left(-\frac{\|\mathbf{x}_r - \beta\mathbf{s}\|^2 + \|\mathbf{x}_t - \alpha\mathbf{s}\|^2}{\eta}\right)$$

- Maximum likelihood (ML) estimates of α and β: $\hat{\alpha}_1 = \frac{\mathbf{s}^\dagger\mathbf{x}_t}{\mathbf{s}^\dagger\mathbf{s}}$ and $\hat{\beta}_1 = \frac{\mathbf{s}^\dagger\mathbf{x}_r}{\mathbf{s}^\dagger\mathbf{s}}$

- Using these estimates, L_1 becomes

$$L_1 = c - 2N\ln\eta - \frac{1}{\eta}\left(\|\mathbf{x}_r\|^2 + \|\mathbf{x}_t\|^2 - \max_{\{\mathbf{s}\}}\frac{\mathbf{s}^\dagger\mathbf{F}_1\mathbf{s}}{\mathbf{s}^\dagger\mathbf{s}}\right)$$

$$\mathbf{F}_1 = \mathbf{x}_r\mathbf{x}_r^\dagger + \mathbf{x}_t\mathbf{x}_t^\dagger = \mathbf{X}\mathbf{X}^\dagger, \quad \mathbf{X} = [\mathbf{x}_r, \mathbf{x}_t]$$

$$\Longrightarrow \quad \max_{\mathbf{s}}\frac{\mathbf{s}^\dagger\mathbf{F}_1\mathbf{s}}{\mathbf{s}^\dagger\mathbf{s}} = \lambda_{\max}(\mathbf{F}_1) = \lambda_{\max}(\mathbf{\Phi}), \quad \mathbf{\Phi} = \mathbf{X}^\dagger\mathbf{X}$$

- The ML estimate of η: $\hat{\eta}_1 = \frac{1}{2N}\left[\|\mathbf{x}_r\|^2 + \|\mathbf{x}_t\|^2 - \lambda_{\max}(\mathbf{\Phi})\right]$

Deterministic GLRT: Unknown Noise Power

- The likelihood function under hypothesis H_0 is

$$L_0 = \frac{1}{\pi^{2N}\eta^{2N}} \exp\left(-\frac{\|\mathbf{x}_r - \beta\mathbf{s}\|^2 + \|\mathbf{x}_t\|^2}{\eta}\right)$$

- The ML estimate of β: $\widehat{\beta}_0 = \dfrac{\mathbf{s}^\dagger\mathbf{x}_r}{\mathbf{s}^\dagger\mathbf{s}}$
- Using above estimate, L_0 becomes

$$L_0 = c - 2N\ln\eta - \frac{1}{\eta}\left(\|\mathbf{x}_r\|^2 + \|\mathbf{x}_t\|^2 - \max_{\{\mathbf{s}\}}\frac{\mathbf{s}^\dagger\mathbf{F}_2\mathbf{s}}{\mathbf{s}^\dagger\mathbf{s}}\right)$$

$$\mathbf{F}_2 = \mathbf{x}_r\mathbf{x}_r^\dagger, \quad \Longrightarrow \quad \max_{\mathbf{s}}\frac{\mathbf{s}^\dagger\mathbf{F}_2\mathbf{s}}{\mathbf{s}^\dagger\mathbf{s}} = \lambda_{\max}(\mathbf{F}_2) = \|\mathbf{x}_r\|^2$$

- The ML estimate of η: $\widehat{\eta}_0 = \dfrac{1}{2N}\|\mathbf{x}_t\|^2$

- The GLRT detector with unknown noise power η is

$$\boxed{T_1 = \frac{\widehat{\eta}_0}{\widehat{\eta}_1} = \frac{\|\mathbf{x}_t\|^2}{\|\mathbf{x}_t\|^2 + \|\mathbf{x}_r\|^2 - \sqrt{(\|\mathbf{x}_t\|^2 - \|\mathbf{x}_r\|^2)^2 + 4|\mathbf{x}_t^\dagger\mathbf{x}_r|^2}} \underset{H_0}{\overset{H_1}{\gtrless}} \gamma_1}$$

Deterministic GLRT: Known Noise Power

- The GLRT with known noise power η can be obtained in a similar way

$$\boxed{T_2 = \frac{1}{\eta}\left(\|\mathbf{x}_t\|^2 - \|\mathbf{x}_r\|^2 + \sqrt{(\|\mathbf{x}_t\|^2 - \|\mathbf{x}_r\|^2)^2 + 4|\mathbf{x}_t^\dagger \mathbf{x}_r|^2}\right) \underset{H_0}{\overset{H_1}{\gtrless}} \gamma_2}$$

- Equivalently, the test variable can be written in terms of eigenvalues

$$\boxed{T_2 = \frac{1}{\eta}\left[\lambda_{\max}(\mathbf{\Phi}) - \lambda_{\max}(\mathbf{\Psi})\right] \underset{H_0}{\overset{H_1}{\gtrless}} \gamma_2}$$

$$\mathbf{\Phi} = \begin{bmatrix} \|\mathbf{x}_r\|^2 & \mathbf{x}_r^\dagger \mathbf{x}_t \\ \mathbf{x}_t^\dagger \mathbf{x}_r & \|\mathbf{x}_t\|^2 \end{bmatrix}$$

$$\mathbf{\Psi} = \mathbf{x}_r \mathbf{x}_r^\dagger$$

Stochastic GLRTs

- **Stochastic model:**
  - IO signal $s(n)$ are modeled as *i.i.d.* complex Gaussian with zero-mean and unit variance
  - Justified for sources with multiplexing techniques (e.g., DVB-T signal)
- With known noise power, the GLRT is

$$\boxed{\frac{\|\mathbf{x}_r\|^{2N}}{(\hat{a}^2+\hat{b}^2+\eta)^N} \exp\left(\frac{\|\mathbf{x}_t\|^2\hat{a}^2-(\hat{a}^2+\eta)\|\mathbf{x}_r\|^2+2\hat{a}\hat{b}|\mathbf{x}_t^\dagger\mathbf{x}_r|}{\eta(\hat{a}^2+\hat{b}^2+\eta)}\right) \underset{H_0}{\overset{H_1}{\gtrless}} \gamma_3}$$

$$a=|\alpha| \quad \text{and} \quad b=|\beta|$$

- With unknown noise power, the GLRT is

$$\boxed{\frac{\|\mathbf{x}_r\|^{2N}\|\mathbf{x}_t\|^{2N}}{\hat{\eta}^N(\hat{a}^2+\hat{b}^2+\hat{\eta})^N} \exp\left(-\frac{(\hat{b}^2+\hat{\eta})\|\mathbf{x}_t\|^2+(\hat{a}^2+\hat{\eta})\|\mathbf{x}_r\|^2-2\hat{a}\hat{b}|\mathbf{x}_t^\dagger\mathbf{x}_r|}{\hat{\eta}(\hat{a}^2+\hat{b}^2+\hat{\eta})}\right) \underset{H_0}{\overset{H_1}{\gtrless}} \gamma_4}$$

- Above two detectors are also referred to as B-GLRTs

Stochastic GLRTs

- As an example, consider B-GLRT with known noise power η
- Estimates of a and b can be obtained by numerically solving the following equations:

$$\boxed{\begin{cases} p(a|b) = 0 \\ q(b|a) = 0 \end{cases}}$$

where

$$a = |\alpha|, \text{ and } b = |\beta|$$

$$\begin{aligned} p(a|b) = {} & N\eta a^3 + b|\mathbf{x}_t^\dagger \mathbf{x}_r|a^2 - b|\mathbf{x}_t^\dagger \mathbf{x}_r|(b^2+\eta) \\ & + \left[(N\eta + \|\mathbf{x}_r\|^2 - \|\mathbf{x}_t\|^2)(b^2+\eta) - \eta\|\mathbf{x}_r\|^2\right] a \end{aligned}$$

$$\begin{aligned} q(b|a) = {} & N\eta b^3 + a|\mathbf{x}_t^\dagger \mathbf{x}_r|b^2 - a|\mathbf{x}_t^\dagger \mathbf{x}_r|(a^2+\eta) \\ & + \left[(N\eta + \|\mathbf{x}_t\|^2 - \|\mathbf{x}_r\|^2)(a^2+\eta) - \eta\|\mathbf{x}_t\|^2\right] b \end{aligned}$$

- Use the Newton-Raphson iterative method to solve the equations, and obtain the estimates of a and b

Backup Slides
Passive Detection with Multiple Receivers
Part I: No DPI

GCC with Known σ^2

- Under H_1: $\mathbf{\Phi} = \mathbf{X}^H\mathbf{X}$ has a non-central Wishart distribution. Using the result in [Kang-Alouini'03], the probability of detection can be written as

$$\boxed{P_{\mathrm{D}} = 1 - \frac{\exp\left(-\frac{\theta}{\sigma^2}\right)\det\{\mathbf{\Omega}(\delta)\}}{\sigma^{2(KN-2K+2)}\theta^{K-1}\Gamma(N-K-1)\prod_{k=1}^{K-1}\left[\Gamma(N-k)\Gamma(K-k)\right]}}$$

- θ is the non-zero eigenvalue of rank-1 matrix $\|\mathbf{s}\|^2\boldsymbol{\alpha}\boldsymbol{\alpha}^H$, and the $K \times K$ matrix $\mathbf{\Omega}(\delta)$ is given by

confluent hypergeometric function

$$\mathbf{\Omega}_{i,j}(\delta) = \sigma^{2(N+K-i-j+1)}\gamma\left(N+K-i-j+1, \frac{\delta}{\sigma^2}\right), \quad \text{for} \quad j \neq 1$$

Nuttall Q-function

$$\mathbf{\Omega}_{i,1}(\delta) = \sigma^{2(N-i+1)}\Gamma(N-i+1)\,{}_1F_1\left(N-i+1; N-K+1; \frac{\theta}{\sigma^2}\right) - \frac{\Gamma(N-K+1)}{2^{K-i}a^{N-K}}\exp\left(\frac{\theta}{\sigma^2}\right)Q_{N-K+2(K-i)+1,N-K}(a,b)$$

$$a \triangleq \sqrt{\frac{2\theta}{\sigma^2}}$$

- The Nuttall Q-function can be recursively computed by generalized Marcum Q-function and modified Bessel functions

$$b \triangleq \sqrt{\frac{2\delta}{\sigma^2}}$$

M. Kang and M.-S. Alouini, "Largest eigenvalue of complex Wishart matrices and performance analysis of MIMO MRC systems," *IEEE J. Sel. Areas Commun.*, vol. 21, no. 3, pp. 418–426, Apr. 2003

GLRT with Unknown σ^2

- GCC is quite sensitive to the accuracy of the noise variance
- With unknown σ^2, the GLRT is given by

$$\frac{\max_{\{\alpha_k,\mathbf{s},\sigma^2\}} f(\mathbf{X}|H_1)}{\max_{\{\sigma^2\}} f(\mathbf{X}|H_0)} \underset{H_0}{\overset{H_1}{\gtrless}} \xi$$

$$f(\mathbf{X}|H_i) = \frac{1}{\pi^{KN}\sigma^{2KN}} \exp\left(-\frac{1}{\sigma^2}\sum_{k=1}^{K} \|\mathbf{x}_k - \alpha_k b_i \mathbf{s}\|^2\right), \quad b_0 = 0 \quad \text{and} \quad b_1 = 1$$

- Under H_1, the maximum likelihood estimates (MLEs) are

$$\hat{\alpha}_k = \frac{\mathbf{s}^H \mathbf{x}_k}{\mathbf{s}^H \mathbf{s}}, \qquad \mathbf{\Phi} = \mathbf{X}^H \mathbf{X} \quad (\text{Gram matrix})$$

$$\hat{\sigma}^2 = \frac{1}{KN}\left(\sum_{k=1}^{K} \|\mathbf{x}_k\|^2 - \lambda_1(\mathbf{\Phi})\right) = \frac{1}{KN}\sum_{k=2}^{K} \lambda_k(\mathbf{\Phi})$$

and $\mathbf{s}$ is the eigenvector corresponding to the largest eigenvalue of $\mathbf{X}\mathbf{X}^H$

- Under H_0, the MLE of the noise variance is $\hat{\sigma}^2 = \frac{1}{KN}\sum_{k=1}^{K} \|\mathbf{x}_k\|^2$

J. Liu, H. Li, and B. Himed, “Two target detection algorithms for passive multistatic radar," *IEEE Trans. Signal Process.*, vol.62, no.22, pp.5930-5939, Nov. 2014

GLRT with Unknown σ^2

- Substituting the MLEs into the likelihood ratio yields the GLRT statistic

$$\boxed{\Xi = \frac{\lambda_1(\Phi)}{\sum_{k=1}^{K} \lambda_k(\Phi)} \underset{H_0}{\overset{H_1}{\gtrless}} \xi}$$

- By a simple transformation, above test statistic can be equivalently written as

$$\frac{\lambda_1(\Phi)}{\hat{\sigma}^2} \underset{H_0}{\overset{H_1}{\gtrless}} \xi', \quad \text{where } \hat{\sigma}^2 \triangleq \frac{1}{KN} \sum_{k=2}^{K} \lambda_k(\Phi)$$

that is, the largest eigenvalue normalized by the MLE of noise variance under H_1

- Interestingly, the above test takes the same form as the following developed for a different application:

P. Wang, J. Fang, N. Han, and H. Li, "Multiantenna-assisted spectrum sensing for cognitive radio," *IEEE Trans. Vehicular Technology*, vol.59, no.4, pp.1791-1800, May 2010

GLRT with Unknown σ^2

- It can be shown the false alarm probability is given by

$$\boxed{\begin{aligned} P_{\mathrm{FA}} =& 1 - \frac{\Gamma(KN)}{M_0} \sum_{k=1}^{K} \sum_{j=N-K}^{(N+K-2k)k} \sum_{i=0}^{KN-j-2} \frac{\beta_{k,j} \binom{KN-j-2}{i} (-k)^i}{\Gamma(KN-j-1)} \\ & \times \left\{ g_1(\xi, j, i) \left[u\left(\xi - \frac{1}{K}\right) - u\left(\xi - \frac{1}{k}\right) \right] + g_2(k, j, i) u\left(\xi - \frac{1}{k}\right) \right\} \end{aligned}}$$

$$M_0 = \prod_{k=1}^{K} [(K-k)!(N-k)!],$$

$$g_1(\xi, j, i) = \frac{1}{j+i+1} \left[\xi^{j+i+1} - K^{-(j+i+1)} \right]$$

$$g_2(k, j, i) = \frac{1}{j+i+1} \left[k^{-(j+i+1)} - K^{-(j+i+1)} \right]$$

step function

$\beta_{k,j}$ can be computed symbolically (shown next)

- The above result indicates GLRT is a CFAR detector

GLRT with Unknown σ^2

- Coefficients $\beta_{k,j}$ are defined implicitly by

$$\frac{\mathrm{d}}{\mathrm{d}\xi}\det\{\Theta(\xi)\} = \sum_{k=1}^{K}\sum_{j=N-K}^{(N+K-2k)k}\beta_{k,j}\xi^j e^{-k\xi}$$

$$\Theta_{n,m}(\xi) = \gamma(N-K+n+m-1,\xi), \quad \gamma(n,y) = \int_0^y t^{n-1}e^{-t}\mathrm{d}t$$

which can be computed by using a symbolic software [Maaref-Aissa'05]

- Specifically, by exploiting the different decaying rates of the summands, the coefficients $\beta_{k,j}$ can be recursively computed, starting from $\beta_{1,N+K-2}$ which has the slowest decaying rate

$$\beta_{1,N+K-2} = \lim_{\xi\to\infty}\frac{\mathrm{d}}{\mathrm{d}\xi}\det\{\Theta(\xi)\}\Big/\left[\xi^{N+K-2}e^{-\xi}\right]$$

Then the contribution $\beta_{1,N+K-2}\xi^{N+K-2}e^{-\xi}$ is removed from the derivative, and the remainder is used to compute the 2nd slowest decaying term, so on and so forth.

A. Maaref and S. Aissa, "Closed-form expression for the outage and ergodic Shannon capacity of MIMO MRC systems," *IEEE Trans. Commun.*, vol. 53, no. 7, Jul. 2005

GCC with Known σ^2

- This case was considered in [Bialkowski et al.'11; Vankayalapati-Kay'12]. The detector is called generalized canonical correlation (GCC) detector

$$\Delta = \lambda_1(\mathbf{\Phi}) \underset{H_0}{\overset{H_1}{\gtrless}} \delta, \quad \text{equivalently,} \quad \Delta_1 = \frac{1}{\sigma^2}\lambda_1(\mathbf{\Phi}) \underset{H_0}{\overset{H_1}{\gtrless}} \delta_1$$

- Its detection performance was not analyzed. Under H_0: $\mathbf{\Phi} = \mathbf{X}^H\mathbf{X}$ has a complex Wishart distribution. Using the result in [Khatri'64], the probability of false alarm can be obtained as

$$\boxed{P_{\mathrm{FA}} = 1 - \frac{\det\{\mathbf{\Psi}(\delta)\}}{\sigma^{2KN}\prod_{k=1}^{K}[\Gamma(N-k+1)\Gamma(K-k+1)]}}$$

- The $K \times K$ matrix $\mathbf{\Psi}$ is given by

$$\Psi_{i,j}(\delta) = \sigma^{2(N-K+i+j-1)}\gamma\left(N-K+i+j-1, \frac{\delta}{\sigma^2}\right).$$

K.S. Bialkowski, I.V.L. Clarkson, and S.D. Howard, "Generalized canonical correlation for passive multistatic radar detection," in *Proc. IEEE Statist. Signal Process. Workshop*, Jun. 2011

N.Vankayalapati and S.Kay, "Asymptotically optimal detection of low probability of intercept signals using distributed sensors," *IEEE Trans. Aerosp. Electron. Syst*, vol. 48, no. 1, Jan. 2012.

C. G. Khatri, "Distribution of the largest or the smallest characteristic root under null hypothesis concerning complex multivariate normal populations," *Ann. Math. Statist.*, vol. 35, Dec. 1964

Backup Slides
Passive Detection with Multiple Receivers
Part II: with DPI

GLRT

- Consider the GLRT for the detection problem:

$$\frac{\max_{\{\boldsymbol{\alpha},\boldsymbol{\beta},\mathbf{x},\eta\}} p(\mathbf{Y}|\boldsymbol{\alpha},\boldsymbol{\beta},\mathbf{x},\eta)}{\max_{\{\boldsymbol{\beta},\mathbf{x},\eta\}} p(\mathbf{Y}|\boldsymbol{\beta},\mathbf{x},\eta)} \underset{\mathcal{H}_0}{\overset{\mathcal{H}_1}{\gtrless}} \zeta$$

- GLRT requires the maximum likelihood estimates (MLEs) of the unknown parameters
- There is a multiplicative ambiguity among the amplitudes parameters $\{\boldsymbol{\alpha},\boldsymbol{\beta}\}$ and the IO waveform $\mathbf{x}$. To resolve the ambiguity, we impose a constraint $\|\mathbf{x}\| = 1$, which does not affect the GLRT
- Under $\mathcal{H}_1$, the likelihood function is given by

$$p(\mathbf{Y}|\boldsymbol{\alpha},\boldsymbol{\beta},\mathbf{x},\eta) = \frac{1}{(\pi\eta)^{KM}} \exp\left\{ -\frac{1}{\eta}\sum_{k=1}^{K} \|\mathbf{y}_k - \beta_k\mathbf{x} - \alpha_k\mathcal{D}_k\mathbf{x}\|^2 \right\}$$

MLE

- The MLEs of $\{\boldsymbol{\alpha}, \boldsymbol{\beta}\}$, conditioned on the IO waveform $\mathbf{x}$, are given by

$$\left[\widehat{\alpha}_k, \widehat{\beta}_k\right]^T = \left(\mathbf{H}_k^H \mathbf{H}_k\right)^{-1} \mathbf{H}_k^H \mathbf{y}_k, \qquad \text{where} \quad \mathbf{H}_k \triangleq [\mathcal{D}_k \mathbf{x}, \mathbf{x}]$$

- Substituting above estimates back into the likelihood function yields

$$\widehat{\mathbf{x}} = \arg \min_{\|\mathbf{x}\|=1} \sum_{k=1}^{K} \left\|\mathbf{P}_k^{\perp} \mathbf{y}_k\right\|^2 = \arg \max_{\|\mathbf{x}\|=1} \sum_{k=1}^{K} \mathbf{y}_k^H \mathbf{P}_k \mathbf{y}_k$$

$$\mathbf{P}_k = \mathbf{H}_k \left(\mathbf{H}_k^H \mathbf{H}_k\right)^{-1} \mathbf{H}_k^H, \qquad \mathbf{P}_k^{\perp} = \mathbf{I} - \mathbf{P}_k$$

- Expanding the cost function

$$\begin{aligned}\sum_{k=1}^{K} \mathbf{y}_k^H \mathbf{P}_k \mathbf{y}_k &= \sum_{k=1}^{K} \mathbf{y}_k^H \mathbf{H}_k \left(\mathbf{H}_k^H \mathbf{H}_k\right)^{-1} \mathbf{H}_k^H \mathbf{y}_k \\ &= \sum_{k=1}^{K} \left[\mathbf{y}_k^H \mathcal{D}_k \mathbf{x}, \mathbf{y}_k^H \mathbf{x}\right] \begin{bmatrix} \|\mathbf{x}\|^2 & \mathbf{x}^H \mathcal{D}_k^H \mathbf{x} \\ \mathbf{x}^H \mathcal{D}_k \mathbf{x} & \|\mathbf{x}\|^2 \end{bmatrix}^{-1} \begin{bmatrix} \mathbf{x}^H \mathcal{D}_k^H \mathbf{y}_k \\ \mathbf{x}^H \mathbf{y}_k \end{bmatrix}\end{aligned}$$

MLE

$$
\begin{aligned}
\sum_{k=1}^{K} \mathbf{y}_k^H \mathbf{P}_k \mathbf{y}_k &= \sum_{k=1}^{K} \frac{1}{\|\mathbf{x}\|^4 - |\mathbf{x}^H \mathcal{D}_k \mathbf{x}|^2} \Big(\|\mathbf{x}\|^2 \mathbf{x}^H \mathcal{D}_k^H \mathbf{y}_k \mathbf{y}_k^H \mathcal{D}_k \mathbf{x} \\
&+ \|\mathbf{x}\|^2 \mathbf{x}^H \mathbf{y}_k \mathbf{y}_k^H \mathbf{x} - \mathbf{x}^H \mathcal{D}_k \mathbf{x} \mathbf{x}^H \mathcal{D}_k^H \mathbf{y}_k \mathbf{y}_k^H \mathbf{x} \\
&- \mathbf{x}^H \mathcal{D}_k^H \mathbf{x} \mathbf{x}^H \mathbf{y}_k \mathbf{y}_k^H \mathcal{D}_k \mathbf{x} \Big) \\
&\triangleq \mathbf{x}^H \boldsymbol{\Theta}(\mathbf{x}) \mathbf{x}
\end{aligned}
$$

$$
\begin{aligned}
\boldsymbol{\Theta}(\mathbf{x}) = \sum_{k=1}^{K} \Big(& \omega_{1,k}(\mathbf{x}) \mathcal{D}_k^H \mathbf{y}_k \mathbf{y}_k^H \mathcal{D}_k + \omega_{1,k}(\mathbf{x}) \mathbf{y}_k \mathbf{y}_k^H \\
& + \omega_{2,k}^*(\mathbf{x}) \mathcal{D}_k^H \mathbf{y}_k \mathbf{y}_k^H + \omega_{2,k}(\mathbf{x}) \mathbf{y}_k \mathbf{y}_k^H \mathcal{D}_k \Big)
\end{aligned}
$$

$$
\omega_{1,k}(\mathbf{x}) \triangleq \frac{\|\mathbf{x}\|^2}{\|\mathbf{x}\|^4 - |\mathbf{x}^H \mathcal{D}_k \mathbf{x}|^2} = \frac{1}{1 - |\mathbf{x}^H \mathcal{D}_k \mathbf{x}|^2}
$$

$$
\omega_{2,k}(\mathbf{x}) = \frac{-\mathbf{x}^H \mathcal{D}_k^H \mathbf{x}}{\|\mathbf{x}\|^4 - |\mathbf{x}^H \mathcal{D}_k \mathbf{x}|^2} = \frac{-\mathbf{x}^H \mathcal{D}_k^H \mathbf{x}}{1 - |\mathbf{x}^H \mathcal{D}_k \mathbf{x}|^2}
$$

Iterative Algorithm for IO Waveform Estimation

- Hence, we have

$$\hat{\mathrm{x}} = \arg \max_{\|\mathrm{x}\|=1} \mathrm{x}^H \Theta(\mathrm{x})\mathrm{x}$$

- If the dependence of $\boldsymbol{\Theta}(\mathbf{x})$ on x is neglected, the cost function is maximized by the principal eigenvector. This leads to an iterative algorithm for estimating the IO waveform:

Algorithm 1 Proposed Approach

Initialization: $l = 0$ and $\mathbf{x}^{(0)} = \sum_{k=1}^{K} \mathbf{y}_k / \| \sum_{k=1}^{K} \mathbf{y}_k \|$.

for $l = 0, 1, 2, \ldots$ **do**

1) Compute $\boldsymbol{\Theta}^{(l)}$ by substituting $\mathbf{x}^{(l)}$ into $\boldsymbol{\Theta}(\mathbf{x})$.
2) $\mathbf{x}^{(l+1)} = \arg\max_{\|\mathbf{x}\|=1} \mathbf{x}^H \boldsymbol{\Theta}^{(l)} \mathbf{x}$, i.e., the principal eigenvector of $\boldsymbol{\Theta}^{(l)}$, and $\gamma^{(l+1)}$ is the corresponding principal eigenvalue.
3) Check convergence.

end for

MLE

- Let γ denote the final update of the principal eigenvector. The noise power can be estimated as

$$\widehat{\eta}_1 = \frac{\sum_{k=1}^{K} \|\mathbf{y}_k\|^2 - \gamma}{MK}$$

- Under $\mathcal{H}_0$, the target signal is absent with $\boldsymbol{\alpha} = \mathbf{0}$. The MLE of the direct-path's amplitude is given by

$$\widehat{\beta}_k = \left(\mathbf{x}^H \mathbf{x}\right)^{-1} \mathbf{x}^H \mathbf{y}_k$$

- Using above amplitude estimate in the likelihood function leads to

$$\widehat{\mathbf{x}} = \arg \max_{\|\mathbf{x}\|=1} \mathbf{x}^H \mathbf{Y}\mathbf{Y}^H \mathbf{x} = \text{princpal e-vector}\{\mathbf{Y}\mathbf{Y}^H\}$$

- Finally, the MLE of noise power is

$$\widehat{\eta}_0 = \frac{\sum_{k=1}^{K} \|\mathbf{y}_k\|^2 - \lambda_1}{MK}$$

GLRT

- Using the MLEs in the likelihood ratio followed by simplification, the test variable the GLRT is given by the ratio of noise power estimates under $\mathcal{H}_1$ and $\mathcal{H}_0$, respectively

$$\frac{\sum_{k=1}^{K} \|\mathbf{y}_k\|^2 - \lambda_1}{\sum_{k=1}^{K} \|\mathbf{y}_k\|^2 - \gamma} \underset{\mathcal{H}_0}{\overset{\mathcal{H}_1}{\gtrless}} \xi$$

- Denote $\lambda_1 \geq \lambda_2 \geq \cdots \geq \lambda_K$ as the ordered eigenvalues of the $K \times K$ matrix $\mathbf{\Phi} = \mathbf{Y}^{\mathrm{H}}\mathbf{Y}$. The GLRT can be written as

$$\frac{1}{\frac{1}{MK}\sum_{k=2}^{K} \lambda_k}(\gamma - \lambda_1) \underset{\mathcal{H}_0}{\overset{\mathcal{H}_1}{\gtrless}} \bar{\xi}$$

  - Denominator is the MLE of the noise power under $\mathcal{H}_0$
  - Numerator is the difference of two principal eigenvalues obtained under $\mathcal{H}_1$ and $\mathcal{H}_0$, respectively

Backup Slides
Exploit Waveform Correlation
Part I: Joint Delay-Doppler Estimation

EM Estimator: E-Step

- The LLF can be written as

$$\log p(\mathbf{z}|\boldsymbol{\theta}) = \log p(\mathbf{y}|\mathbf{x},\boldsymbol{\theta})p(\mathbf{x}|\boldsymbol{\theta}) = s_1(\mathbf{x}) - s_2(\mathbf{x},\boldsymbol{\theta})$$

Bayes' rule

- Only the second term involves the parameters to be estimated

$$Q\left(\boldsymbol{\theta};\widehat{\boldsymbol{\theta}}^{(l)}\right) = E_{\mathbf{x}|\mathbf{y},\widehat{\boldsymbol{\theta}}^{(l)}}\{s_1(\mathbf{x})\} - E_{\mathbf{x}|\mathbf{y},\widehat{\boldsymbol{\theta}}^{(l)}}\{s_2(\mathbf{x},\boldsymbol{\theta})\}$$

constant

$$\begin{aligned} s_2(\mathbf{x},\boldsymbol{\theta}) =& |\beta|^2 \operatorname{tr}\{\mathbf{C}_{ns}^{-1}\mathbf{x}\mathbf{x}^H\} + |\alpha|^2 \operatorname{tr}\{\mathbf{W}^H\mathbf{A}^H\mathbf{C}_{ns}^{-1}\mathbf{A}\mathbf{W}\mathbf{x}\mathbf{x}^H\} \\ &+ 2\Re\left\{\alpha\beta^* \operatorname{tr}\{\mathbf{C}_{ns}^{-1}\mathbf{A}\mathbf{W}\mathbf{x}\mathbf{x}^H\} - \beta\mathbf{y}_s^H\mathbf{C}_{ns}^{-1}\mathbf{x} - \alpha\mathbf{y}_s^H\mathbf{C}_{ns}^{-1}\mathbf{A}\mathbf{W}\mathbf{x}\right\} \end{aligned}$$

- In E-step, we need to compute

$$\begin{aligned} \widehat{\mathbf{x}}^{(l)} &= E_{\mathbf{x}|\mathbf{y},\widehat{\boldsymbol{\theta}}^{(l)}}\{\mathbf{x}\} \\ \mathbf{C}_{xx|y}^{(l)} &= E_{\mathbf{x}|\mathbf{y},\widehat{\boldsymbol{\theta}}^{(l)}}\left\{\mathbf{x}\mathbf{x}^H\right\} \end{aligned}$$

MMSE estimate

EM Estimator: E-Step

- By using the results of MMSE estimation and the block matrix inversion formula

$$\hat{\mathbf{x}}^{(l)} = \mathbf{C}_{nr}\mathbf{G}^{-1}\mathbf{B}^{(l)}\mathbf{S}_G^{-1}\mathbf{y}_s + \mathbf{y}_r - \mathbf{C}_{nr}\mathbf{S}_D^{-1}\mathbf{y}_r$$

$$\mathbf{C}_{xx|y}^{(l)} = \hat{\mathbf{x}}^{(l)}\left(\hat{\mathbf{x}}^{(l)}\right)^H + \mathbf{C}_{nr} - \mathbf{C}_{nr}\mathbf{S}_D^{-1}\mathbf{C}_{nr}$$

  where the *Schur complements* are defined as

$$\mathbf{S}_G = \mathbf{D}^{(l)} - \left(\mathbf{B}^{(l)}\right)^H \mathbf{G}^{-1}\mathbf{B}^{(l)}$$

$$\mathbf{S}_D = \mathbf{G} - \mathbf{B}^{(l)}\left(\mathbf{D}^{(l)}\right)^{-1}\left(\mathbf{B}^{(l)}\right)^H$$

- The cost function related to the unknown parameters is

$$Q_1\left(\boldsymbol{\theta};\hat{\boldsymbol{\theta}}^{(l)}\right) = |\beta|^2 c_1^{(l)} + |\alpha|^2 c_2^{(l)}(\tau, f_d) + 2\Re\left\{\alpha\beta^* c_3^{(l)}(\tau, f_d) - \beta c_4^{(l)} - \alpha c_5^{(l)}(\tau, f_d)\right\}$$

  where

$$c_1^{(l)} = \mathrm{tr}\left\{\mathbf{C}_{ns}^{-1}\mathbf{C}_{xx|y}^{(l)}\right\},\quad c_2^{(l)}(\tau, f_d) = \mathrm{tr}\left\{\mathbf{W}\mathbf{C}_{xx|y}^{(l)}\mathbf{W}^H\mathbf{A}^H\mathbf{C}_{ns}^{-1}\mathbf{A}\right\}$$

$$c_3^{(l)}(\tau, f_d) = \mathrm{tr}\left\{\mathbf{C}_{ns}^{-1}\mathbf{A}\mathbf{W}\mathbf{C}_{xx|y}^{(l)}\right\},\quad c_4^{(l)} = \mathbf{y}_s^H\mathbf{C}_{ns}^{-1}\hat{\mathbf{x}}^{(l)},\quad c_5^{(l)}(\tau, f_d) = \mathbf{y}_s^H\mathbf{C}_{ns}^{-1}\mathbf{A}\mathbf{W}\hat{\mathbf{x}}^{(l)}$$

S. M. Kay, *Fundamentals of Statistical Signal Processing: Estimation Theory*. Upper Saddle River, NJ: Prentice Hall, 1993

EM Estimator: M-Step

- In M-step, we need to solve the following optimization problem

$$\widehat{\boldsymbol{\theta}}^{(l+1)} = \arg\min_{\boldsymbol{\theta}} Q_1\left(\boldsymbol{\theta}; \widehat{\boldsymbol{\theta}}^{(l)}\right)$$

- Using person-by-person optimization, we partition the unknown parameters into three subsets: $\{\tau\}$, $\{f_d\}$, and $\{\alpha, \beta\}$, and minimize the cost function sequentially over these subsets [a.k.a. expectation conditional maximization (ECM)]

$$\widehat{\tau}^{(l+1)} = \arg\min_{\tau} Q_1\left(\tau, \widehat{f}_d^{(l)}, \widehat{\alpha}^{(l)}, \widehat{\beta}^{(l)}; \widehat{\boldsymbol{\theta}}^{(l)}\right),$$

$$\widehat{f}_d^{(l+1)} = \arg\min_{f_d} Q_1\left(\widehat{\tau}^{(l+1)}, f_d, \widehat{\alpha}^{(l)}, \widehat{\beta}^{(l)}; \widehat{\boldsymbol{\theta}}^{(l)}\right),$$

$$\left\{\widehat{\alpha}^{(l+1)}, \widehat{\beta}^{(l+1)}\right\} = \arg\min_{\alpha,\beta} Q_1\left(\widehat{\tau}^{(l+1)}, \widehat{f}_d^{(l+1)}, \alpha, \beta; \widehat{\boldsymbol{\theta}}^{(l)}\right).$$

- For the first two problems, the estimates can be obtained by using Newton's method; there is a closed-form result for the third problem

EM Estimator: M-Step

- Take τ as an example, a coarse one-dimensional search is conducted to find an initial estimate. Then, the solution is refined by exploiting the following necessary condition of optimality

$$g\left(\widehat{\tau}^{(l+1)}\right) = 0, \quad g(\tau) = \frac{\partial Q_1\left(\tau, \widehat{f}_d^{(l)}, \widehat{\alpha}^{(l)}, \widehat{\beta}^{(l)}; \widehat{\boldsymbol{\theta}}^{(l)}\right)}{\partial \tau}$$

- Newton's method is used to find the root of the first derivative $g(\tau)$ in the neighborhood of the initial estimate. At the m-th iteration of Newton's method, we compute

$$\tau_m = \tau_{m-1} - \frac{g\left(\tau_{m-1}\right)}{g'\left(\tau_{m-1}\right)}, \quad g'(\tau) = \frac{\partial^2 Q_1\left(\tau, \widehat{f}_d^{(l)}, \widehat{\alpha}^{(l)}, \widehat{\beta}^{(l)}; \widehat{\boldsymbol{\theta}}^{(l)}\right)}{\partial \tau^2}$$

- This process is repeated until convergence

EM Estimator: M-Step

- For the third sub-problem, the cost function is a quadratic function with respect to α and β. Taking partial derivatives of the cost function with respect to the conjugates of $\{\alpha, \beta\}$ and setting them equal to zero, we have

$$\widehat{\alpha}^{(l+1)} = \frac{\left(\left(c_1^{(l)}\right)^* c_5^{(l)} - c_3^{(l)} c_4^{(l)}\right)^*}{c_1^{(l)} c_2^{(l)} - \left|c_3^{(l)}\right|^2}, \quad \widehat{\beta}^{(l+1)} = \frac{c_2^{(l)} \left(c_4^{(l)}\right)^* - c_3^{(l)} \left(c_5^{(l)}\right)^*}{c_1^{(l)} c_2^{(l)} - \left|c_3^{(l)}\right|^2}$$

where

$$\begin{aligned} c_2^{(l)} &= c_2^{(l)}\left(\widehat{\tau}^{(l+1)}, \widehat{f}_d^{(l+1)}\right) \\ c_3^{(l)} &= c_3^{(l)}\left(\widehat{\tau}^{(l+1)}, \widehat{f}_d^{(l+1)}\right) \\ c_5^{(l)} &= c_5^{(l)}\left(\widehat{\tau}^{(l+1)}, \widehat{f}_d^{(l+1)}\right) \end{aligned}$$